

**ASPECTS OF PERTURBATIVE CORRECTIONS
IN QUANTUM CHROMODYNAMICS**

by
Stavros Papadopoulos

Department of Physics
McGill University, Montreal
December 1989

A Thesis submitted to the Faculty of Graduate Studies and Research in partial fulfillment of the requirements for the degree of Doctor of Philosophy.

© Stavros Papadopoulos 1989

ABSTRACT

The perturbative regime of Quantum Chromodynamics (QCD) is considered and certain aspects related with higher order corrections (HOC) are studied. Certain large correction terms in the perturbative expansion are determined, in particular for large transverse momentum (p_T) direct photon production. The origin of these terms is specified and simple forms, called K -factors, are provided (soft gluon approach).

Furthermore, for processes initiated by $2 \rightarrow 2$ particle subprocesses the structure of the complete HOC is analyzed. It is shown that when structure functions and/or fragmentation functions are involved, there is a gauge invariant part that dominates HOC over a sizable kinematic range. Simple and general expressions are derived allowing an easy calculation of this part. Also, it is shown that, under certain approximations, this part reduces to the form of the simple K -factors.

Other aspects of HOC, in particular the dependence on the choice of scales, are considered. Using complete HOC, detailed analysis of recent and old data on large- p_T direct photon production is carried out. The dependence of the form of the gluon distribution on the choice of the scales (physical versus optimal scales) is discussed and it is concluded that appreciable ambiguity in this distribution still remains.

RÉSUMÉ

On considère le régime perturbatif de Chromodynamique Quantique (CDQ) et on étudie quelques aspects des corrections de l'ordre supérieur (COS). On détermine quelques grands termes des corrections de l'expansion perturbative, en particulier pour la production des photons directs de grand moment d'impulsion (p_T). On précise la source des grands termes et on fournit des formes simples, ce qu'on appelle facteurs K (méthode des gluons mous).

En plus, pour des processus qui sont initiés par des sous-processus du type particules $2 \rightarrow 2$, on analyse la structure des COS complets. On montre que, pour des réactions avec des fonctions de structure ou des fonctions de fragmentation, une partie existe qui reste invariante sous des transformations de jauge et qui domine les COS dans un domaine cinématique appréciable. On obtient des expressions simples et générales qui permettent le calcul facile de cette partie. On montre aussi que, avec quelques approximations, cette partie reproduit la forme simple des facteurs K .

On considère aussi quelques autres aspects des COS, surtout la dépendance sur le choix des échelles. On fait en détail et avec des COS complets une analyse des résultats d'expériences récentes et anciennes sur la production des photons directs de grand p_T . On considère la dépendance de la forme de la distribution des gluons sur le choix des échelles (échelles physiques contre optimales) et on conclut qu'une ambiguïté appréciable sur cette distribution demeure.

ACKNOWLEDGEMENTS

I wish to express my thanks to my Research Director and Thesis Supervisor, Professor A.P. Contogouris, for his continued guidance, active collaboration and constant encouragement, as well as for his suggestions during the preparation of this Thesis.

My thanks are also due to the Physics Department of McGill University for the knowledge I acquired in pursuing the program of graduate studies.

Also, I would like to thank Drs. J. Ralston and N. Mebarki for collaboration and helpful discussions, and D. Atwood for collaboration and help in the computer calculations.

I am grateful to Lynda Corkum for her careful typing of the manuscript.

It is also a pleasure for me to acknowledge the encouragement I received from my wife throughout all this work; without her patience the task could not have been accomplished.

TABLE OF CONTENTS

Title Page	1
Abstract	2
Résumé	3
Acknowledgements	4
Table of Contents	5
PREFACE	8
CHAPTER 1: INTRODUCTION	9
1.1 The QCD Lagrangian and its Main Features	11
1.2 Asymptotic Freedom	14
1.3 QCD Improved Parton Model	16
PART I	22
CHAPTER 2: DIRECT PHOTON PRODUCTION AND THE SOFT GLUON APPROACH	23
2.1 Born Contributions and Photon Brems	25
2.1.1 Basic Formalism and Computational Details	25
2.1.2 Results and Discussion	27
2.1.3 Photon Brems	28
2.2 HOC in the Soft Gluon Limit	31
2.2.1 The Soft Gluon Technique	31
2.2.2 The Differential Cross Section	35
2.2.3 Phenomenological Implications	39
2.3 Other Large Correction Terms	39
PART II	41
THE DOMINANT PART OF HIGHER ORDER CORRECTIONS	42
CHAPTER 3: STRUCTURE OF HOC AND THE EXISTENCE OF A DOMINANT PART	43
3.1 The Structure of HOC	43
3.2 The Dominant Part of HOC	45
3.3 Remarks	49

CHAPTER 4: DETERMINATION OF THE DOMINANT PART.....	53
4.1 Brems from Initial Partons.....	53
4.2 Brems from Final Partons.....	57
4.2.1 Evaluation of Matrix Elements.....	58
4.2.2 Total Contributions and General Expressions.....	64
4.3 The Virtual Contribution.....	66
4.4 Factorization of Mass Singularities.....	67
4.5 The Dominant Part.....	70
4.6 Concluding Remarks.....	72
 CHAPTER 5: APPLICATION OF THE APPROACH OF CH. 4.....	 73
5.1 Generalization of the Results of Ch. 4.....	73
5.2 Brems Contributions to the Dominant Part of $qg \rightarrow \gamma q$	75
5.3 Virtual Contributions and Factorization of Mass Singularities.....	77
5.4 The Dominant Part ($qg \rightarrow \gamma q$).....	79
5.5 Conclusions and Remarks.....	80
 PART III.....	 83
ADDITIONAL CONTRIBUTIONS AND APPLICATION.....	84
 CHAPTER 6: VIRTUAL CONTRIBUTIONS AND CHECK OF THE DOMINANT PART.....	 85
6.1 HOC to $d\sigma/d\hat{t}(q\bar{q} \rightarrow \gamma g)$ from Loop Graphs.....	85
6.2 Gluon Brems Contributions to the HOC.....	88
6.3 Verification of the Dominant Part.....	91
 CHAPTER 7: NONDOMINANT CONTRIBUTIONS AND PHOTON BREMS.....	 94
7.1 Nondominant Contributions.....	94
7.2 Classification of the Remaining Nonsinglet Contributions.....	96
7.3 Collinear Photon Brems and its Separation.....	98
7.4 Leftover Contributions from Photon Brems.....	101

CHAPTER 8: THE GLUON DISTRIBUTION AND PHYSICAL VERSUS OPTIMAL SCALES IN DIRECT PHOTON PRODUCTION	103
8.1 Problems of Optimal Scales	103
8.2 Higher Order Corrections	106
8.3 Photon Brems, Related and Other Uncertainties	108
8.4 Results and Discussion	110
8.5 Conclusions	113
OVERALL CONCLUSIONS	114
APPENDICES	
A	116
B	118
C	120
D	125
E	128
F	131
TABLES	
I	132
II	133
III	134
IV	135
V	136
VI	137
FOOTNOTES	138
REFERENCES	140
FIGURE CAPTIONS	147
FIGURES	153

PREFACE

The first Part of the research in this Thesis was carried during 1979-82. After having completed, in 1979, my M.Sc. Thesis on large- p_T hadron production in the framework of Quantum Chromodynamics (QCD),⁽¹⁾ I continued working on other problems of perturbative QCD, in particular large- p_T direct photon production⁽²⁾ as well as lepton-pair production.⁽³⁾ At that time it was becoming evident that large correction terms were present in the higher orders of the QCD perturbation expansion. Part I is an effort to understand the origin and the sources of certain such terms, particularly in relation with large- p_T direct photons.⁽⁴⁾⁻⁽⁶⁾ It is based on or makes some use of, Refs. (2)-(10).

At the beginning of 1983, because of personal reasons, I was obliged to interrupt my research work, and I resumed research in 1988. During this period complete higher order calculations had been carried for several processes. Still, in many cases the resulting inclusive cross sections were very similar to those of Part I, especially when physical renormalization and factorization scales (see Ch. 3) were chosen. Then we set up to analyse certain of these complete calculations and to understand the structure of higher order corrections (HOC). We realized that in a very wide class of processes (those involving parton distribution and/or fragmentation functions) there is a part that dominates the HOC (dominant part).^{(11),(12)} We have shown that this part is much easier to calculate than the complete HOC, and we have provided simple and general expressions explicitly determining what is perhaps the most difficult portion (the gluon Bremsstrahlung contributions) to this part. Finally, we have shown that with a certain approximation, this dominant part reduces to the forms we have derived in Part I. This research forms the Part II of the Thesis.

Part III is also very recent work, but stems from a different motivation, which we explain at the beginning of Ch. 8. Nevertheless, we make use of all the results derived in Part II. Also, we indicate briefly the relation and relevance of certain results and comparisons of Part I to the analysis of more recent experimental data presented in Ch. 8.

CHAPTER 1

INTRODUCTION

Quantum Chromodynamics (QCD) is a theory of strong interactions. It is the final outcome of two decades of continuous work and developments, both experimental and theoretical, in many areas of particle physics. QCD represents a remarkable synthesis of ideas and concepts developed about hadronic physics, like quarks, gluons, color and asymptotic freedom. It emerges as a gauge theory of quarks and gluons much as Quantum Electrodynamics (QED), the theory of electromagnetic interactions, is a gauge theory of leptons and photons.

QCD has many common features with, as well as important differences from QED. The common features arise from the fact that both theories are renormalizable gauge theories. Their differences arise from the fact that QCD is a non-Abelian gauge theory, in contrast to QED which is an Abelian one. In fact, all the complexity, subtleties and distinct properties of QCD arise either directly or indirectly from its non-Abelian character. This somehow includes the fact that only hadrons composed of colored quarks and gluons are observed in nature and not their constituents. Indeed, QCD implies that gluons can couple directly to other gluons, whereas photons cannot couple directly to photons. Thus the strong forces transmitted by gluons differ significantly from the electromagnetic forces transmitted by photons. The most striking consequence is that the strength of the force between constituents increases (decreases) as the distance increases (decreases).

This distinct feature of QCD suggests that only colorless states are allowed as isolated particles, i.e. the observed hadrons. Neither quarks nor gluons can appear in isolation; they can only exist within (color-neutral) composites, the hadrons. Then the strong forces between these hadrons are like the residual Van der Waals forces between electrically neutral atoms, which are suppressed at large distances. However, at shorter distances, they are strong enough to bind protons and neutrons to form nuclei.

The properties of hadrons and the dynamics of their constituents can be better studied in high energy collisions, involving at least one hadron in the initial or final state. In these collisions quarks and gluons can interact with themselves or other particles, at very short distances. The strength of the force is described by an effective coupling α_s , which becomes small at short distances. Otherwise stated, with Q an energy scale characteristic of the collision, α_s is a function of Q^2 , (running coupling) such that $\alpha_s(Q^2) \rightarrow 0$ for $Q^2 \rightarrow \infty$. This property of QCD has been called asymptotic freedom; quarks and gluons appear as free when prompted at very small distances or by large values of Q^2 .

The smallness of $\alpha_s(Q^2)$ at sufficiently large Q^2 offers the possibility of using perturbation expansion in $\alpha_s(Q^2)$ to calculate physical quantities relevant to strong interactions. Because of this possibility, much effort has been devoted by theorists to determine corrections due to higher orders of the perturbation expansion, i.e. to calculate inclusive cross sections beyond the leading order in the running coupling $\alpha_s(Q^2)$. Of course, because of asymptotic freedom, for very large values of the scale Q , such higher order corrections (HOC) are expected to be unimportant. However, for many of the presently available experimental data, $\alpha_s(Q^2)$ is not very small and in many cases the next to leading order corrections are large, i.e. comparable to the leading order (Born term). This situation arises in numerous processes, including cases of paramount importance for testing QCD.

Thus calculations of QCD HOC were and remain an essential part of the theoretical effort to understand the physics of hadrons. These calculations, in particular when the leading term is of $O(\alpha_s)$ or higher, are very involved and the resulting expressions very complicated. Yet, in most of the cases, for a wide range of the kinematic variables, the result is very simple: an overall cross section differing from the Born by a slowly varying factor.

This fact suggests that perhaps there is a relatively simple part of the HOC which dominates over a wide kinematic domain. Then it would be of interest to look for such a part (dominant part), identify its origin and, if possible, determine general procedures by which it can be calculated easily. Such a program could be

useful in various directions. One direction is determining HOC for QCD subprocesses of the type $a + b \rightarrow c + d + e$, where a, b, c, d, e stand for quarks, gluons or photons; for such subprocesses, due to their complexity, HOC are hitherto completely unknown. Another direction is going beyond the next to leading order in $\alpha_s(Q^2)$, where HOC remain almost completely undetermined. Still another use of determining the dominant part can be to check the results of existing calculations of HOC; as we stated, these results are in general very complicated.

In the rest of this chapter we present in more technical terms some of the basic features of Quantum Chromodynamics and in particular certain aspects of its perturbative regime. We restrict our presentation to concepts and formulas which may form a short framework for the work that follows. More details on these topics and QCD in general can be found in several review articles⁽¹³⁾⁻⁽²¹⁾ and textbooks as e.g. of Refs. 22-25.

1.1 The QCD Lagrangian and its Main Features

The main idea leading to QCD has been the postulate that the symmetry $SU(N_c)$ ($N_c = \text{number of colors} = 3$) is a local rather than merely a global one. In this way QCD emerges as a non-Abelian gauge theory.

The requirement of local $SU(3)$ invariance is implemented by introducing vector gauge fields A_μ^a ($a = 1, \dots, 8$) which correspond to the gluons, together with the colored quark fermion fields q_i^α (color index $\alpha = 1, 2, 3$ and flavor index $i = 1, 2, \dots, N_f$ with $N_f = \text{number of flavors}$); the fields q_i^α and A_μ^a transform according to the defining (triplet) and adjoint (octet) representation of the $SU(3)$ group. With these fields one obtains the unrenormalized Lagrangian density

$$\mathcal{L} = \bar{q}_k^\alpha (i\gamma_\mu D_{\alpha\beta}^\mu - m_k \delta_{\alpha\beta}) q_k^\beta - \frac{1}{4} F_{\mu\nu}^a F^{a\mu\nu}. \quad (1.1.1)$$

Here, and in the following, summation is understood over any type of repeated indices (no matter whether they are Lorentz, quark flavor, quark or gluon color). The constant m_k stands for the bare mass of the quark with flavor k .

In (1.1.1), the first term arises from the free fermion Lagrangian (without gluons) by applying the principle of minimal coupling, according to which the ordinary derivative, acting on the quark fields, is replaced by the covariant derivative:

$$D_{\alpha\beta}^{\mu} = \delta_{\alpha\beta}\partial^{\mu} + ig(t^a)_{\alpha\beta}A^{a\mu}; \quad (1.1.2)$$

the second term corresponds to the “kinetic energy” of the gauge fields, with the gluon field tensor

$$F_{\mu\nu}^a = \partial_{\mu}A_{\nu}^a - \partial_{\nu}A_{\mu}^a - gf_{abc}A_{\mu}^bA_{\nu}^c. \quad (1.1.3)$$

Both terms in (1.1.1) are invariant under local gauge transformations; their infinitesimal form is:

$$q_i^{\alpha} \rightarrow q_i'^{\alpha} = [\delta^{\alpha\beta} - ig\epsilon_a(t^a)_{\alpha\beta}]q_i^{\beta} \quad (1.1.4a)$$

$$A_a^{\mu} \rightarrow A_a'^{\mu} = A_a^{\mu} + \partial^{\mu}\epsilon_a + gf_{abc}\epsilon_bA_c^{\mu}, \quad (1.1.4b)$$

where ϵ_a are arbitrary infinitesimal functions of the space-time point x .

In (1.1.2)–(1.1.4) the matrices $(t^a)_{\alpha\beta}$ form the 3-dimensional representation (defining) of the generators of the $SU(3)$ group, and f_{abc} are the structure constants of the associated algebra. The generators t^a , satisfy the commutation relations

$$[t^a, t^b] = i f_{abc} t^c, \quad (1.1.5)$$

and the matrices $(t^a)_{\alpha\beta}$ are normalized in the defining representation R by:

$$Tr[t^a t^b] = T(R)\delta^{ab}, \quad T(R) = \frac{1}{2}. \quad (1.1.6)$$

This trace appears in contributions of colored fermion loops.

Note that in Eqs. (1.1.2)–(1.1.4) there exists only one parameter g , owing to gauge invariance. This is called the bare (unrenormalized) strong coupling constant.

Finally, in terms of \mathcal{L} , the unrenormalized QCD Lagrangian density is:

$$\mathcal{L}_{QCD} = \mathcal{L} + \mathcal{L}_{gf} + \mathcal{L}_{ghost}. \quad (1.1.7)$$

\mathcal{L}_{gf} stands for the gauge fixing term, which is required to insure a proper quantization procedure. \mathcal{L}_{ghost} stands for the Faddeev-Popov ghost term, which is required

to preserve unitarity (by completely eliminating the unphysical degrees of polarization of the gluon field).

For the class of covariant gauges, the gluon field is constrained by the Lorentz condition $\partial^\mu A_\mu^a = 0$, or alternatively by the term

$$\mathcal{L}_{gf} = -\frac{1}{2\xi}(\partial^\mu A_\mu^a)^2 \quad (1.1.8)$$

where $1/\xi$ acts as a Lagrange multiplier. The parameter ξ is called the gauge parameter and can take any value. Particular important cases are $\xi = 1$ (Feynman gauge) and $\xi = 0$ (Landau gauge). In the class of covariant gauges the ghost term has the form

$$\mathcal{L}_{ghost} = \bar{\eta}^c(\partial_\mu \partial^\mu \delta_{ac} + g f_{abc} A_\mu^b \partial^\mu) \eta^a \quad (1.1.9)$$

where η^a ($a = 1, \dots, 8$) denotes a set of fictitious (unphysical) fields, called (Faddeev-Popov) ghosts. They are scalar but anticommuting fields.

The necessity of introducing the above ghost fields and the associated term in the Lagrangian is closely related to the non-Abelian character of the theory. E.g. for an Abelian theory, $f_{abc} = 0$ and thus Eq. (1.1.9) is independent of the gauge fields; it simply describes free ghost propagation totally decoupled from the rest of the theory. This means that in such theories, as e.g. in QED, the gauge fixing term suffices to eliminate the unphysical degrees of freedom of the gauge boson. A similar situation occurs also for non-Abelian theories, but for the class of physical gauges which includes the important cases of axial and temporal ones. However, calculations in these ghost free gauges are less straightforward than in the covariant ones.

Unlike QED, where photons can interact with themselves only via electron (charged fermion) loops, the QCD Lagrangian density gives rise to triple and quartic gluon couplings. These gluon self-interactions are due to the presence of the coupling constant g already at the level of the gluon field strength $F_{\mu\nu}^a$ in Eq. (1.1.3) and they are due to the non-Abelian nature of the theory.

Starting from the total Lagrangian density, \mathcal{L}_{QCD} , the Feynman rules can be derived using standard techniques.^{(15),(17),(22)} The calculations of Feynman graphs

in QCD is very similar to those in QED apart from certain more elaborate treatments due to color ($SU(3)$ group) factors and to the presence of new fields (ghosts) and of new vertices (gluon self-interactions and gluon-ghost coupling).

Finally, we notice that the complete QCD Lagrangian density Eq. (1.1.7) although not invariant under the transformations (1.1.4), is invariant under the generalized gauge transformations, or BRS (Becci-Rouet-Stora)⁽²²⁾ transformations, in which the ghost fields are also transformed. This symmetry leads to the generalized Ward-Takahashi or Slavnov-Taylor identities, which provide a powerful tool for the demonstration of the renormalizability (to all orders) of QCD.^{(22),(23)}

1.2 Asymptotic Freedom

As we stated, the QCD Lagrangian (1.1.7) describes a renormalizable field theory. The renormalized coupling $g(\mu)$ is a function of the renormalization scale μ , at which ultraviolet (UV) singularities appearing in loop contributions, are subtracted and absorbed in the bare coupling g present in the Lagrangian.

We introduce the running coupling $\alpha_s(\mu^2) = g^2(\mu^2)/4\pi$; its dependence on μ is described by a renormalization group equation (RGE). This equation attains a simpler form when expressed in terms of the couplant $\alpha' = \alpha_s/\pi$ (the expansion parameter in perturbation theory). It is:

$$\mu \frac{\partial \alpha'}{\partial \mu} = \beta(\alpha') = -b\alpha'^2(1 + 0(\alpha')) \quad (1.2.1)$$

where the Callan-Symanzik beta function $\beta(\alpha')$ is perturbatively calculable. A one loop calculation determines the coefficient b :

$$b = \frac{1}{6}[11C_2(A) - 4T(R)N_f] \quad (1.2.2)$$

with $T(R)$ as in Eq. (1.1.6). The other Casimir factor of the adjoint representation of $SU(N_c)$ arises from gluon loops:

$$C_2(A)\delta_{ab} \equiv f_{acd}f_{bcd} \Rightarrow C_2(A) = N_c \quad (1.2.3)$$

so that

$$b = \frac{1}{6}(11N_c - 2N_f) \quad (1.2.4)$$

The solution of Eq. (1.2.1) is

$$\alpha_s(\mu^2) = \frac{\alpha_s(\mu_0^2)}{1 + \frac{b}{2\pi}\alpha_s(\mu_0^2)\ell n \frac{\mu^2}{\mu_0^2}} \quad (1.2.5)$$

From (1.2.4) it is evident that for $N_f = 16$, b is positive and hence $\alpha_s(\mu^2)$ decreases with μ^2 . In particular $\alpha_s(\mu^2) \rightarrow 0$ as $\mu^2 \rightarrow \infty$. This is the property of asymptotic freedom.⁽²⁶⁾

Eq. (1.2.5) can be further simplified by introducing the parameter Λ :

$$\Lambda = \mu_0 \exp\left(-\frac{\pi}{b\alpha_s(\mu_0^2)}\right) \quad (1.2.6)$$

and setting $\mu^2 = Q^2$ where Q is a large momentum transfer. Then,

$$\alpha_s(Q^2) = \frac{2\pi}{b\ell n \frac{Q^2}{\Lambda^2}} \quad (1.2.7)$$

Λ is the fundamental scale of the theory and it is called the QCD parameter. The value of Λ is a measure of the energy scale at which the running coupling becomes large and the nonperturbative regime of QCD is entered. Since the strong interactions must be strong enough to bind quarks inside the hadrons, Λ is expected to be of the order of a typical hadron mass, i.e. between that of the pion and the proton. Indeed experimental measurements give values in the range 0.15–0.5 GeV, depending on the process, the renormalization scheme, and the order of the perturbation expansion used in fitting data.⁽²⁷⁾ For momentum transfers much greater than Λ , asymptotic freedom guarantees that perturbation theory applies. This in turn justifies the expansion in Eq. (1.2.1) we started with

It should be noted that among all renormalizable field theories asymptotic freedom is a unique property of the non-Abelian gauge theories. For example in the familiar gauge theory of QED the effective coupling $\alpha(\mu^2)$ increases with μ^2 . To make this explicit, we consider Eq. (1.2.2) and for QED we take $C_2(A) = 0$

(no analogue of gluon loops) and $T(R)N_f \rightarrow \sum_i e_i^2$ where summation runs over all charged fermions (e_i in units of electron charge) with $(2m_i)^2 \leq \mu^2$. Then

$$b_{QED} = -\frac{2}{3} \sum_i e_i^2 < 0 \quad (1.2.8)$$

in clear contradistinction with QCD and asymptotic freedom.

Now we present the solution of Eq. (1.2.1) with $\beta(\alpha)$ evaluated at two loops. Thus with $\beta(\alpha') = -ba'^2(1 + ca')$ where

$$c = \frac{17N_c^2 - (5N_c + 3C_F)N_f}{12b} \quad (1.2.9)$$

with $C_F = (N_c^2 - 1)/2N_c$, the solution is

$$\alpha_s(\mu^2) = \frac{\pi}{b \ln \frac{\mu}{\Lambda}} \left(1 - \frac{c \ln \ln(\mu^2/\Lambda^2)}{b \ln(\mu/\Lambda)} \right) \quad (1.2.10)$$

Here, Λ has been chosen so that there are no terms of $O(\ln \ln(\mu^2/\Lambda^2)/\ln^3(\mu/\Lambda))$; it is:

$$\Lambda = \mu_0 \left(1 + \frac{\pi}{c \alpha_s(\mu_0^2)} \right)^{c/b} \exp \left[-\frac{\pi}{b \alpha_s(\mu_0^2)} \right]. \quad (1.2.11)$$

Again Λ replaces the unknown $\alpha_s(\mu_0^2)$ and is determined from experiment. We notice that the coefficients b and c in the expansion of $\beta(\alpha)$ are renormalization scheme (and gauge) independent. In fact, this is only true for these two coefficients; higher order terms in the expansion of $\beta(\alpha)$ do not share this property.

1.3 QCD Improved Parton Model

Asymptotic freedom provides a plausible justification for the successes of the parton model (PM) and in particular for the approximate scaling observed in ep deep inelastic scattering (DIS) and other experiments. In addition, perturbative QCD predicts scale violations which have been observed in accurate DIS data over a large domain of the kinematic variables. Also it modifies the original PM in such a way that the resulting improved PM constitutes a self-consistent framework for making definite predictions based on perturbative QCD.

According to the PM, at high energy, collisions involving hadrons can be viewed as due to incoherent elastic scattering of pointlike constituents, the partons, with other partons (or elementary fields); in these collisions the partons are treated as free particles.⁽²⁸⁾

This picture is best illustrated by considering electron nucleon DIS. Here an energetic virtual photon γ^* , with large momentum transfer squared Q^2 , interacts with one of the quarks of the nucleon (Fig. 1(a)); this quark is considered as non interacting with other constituents of the hadron. This behaviour is justified as follows (impulse approximation): In the C.M. frame of the colliding particles, time dilation slows down processes in the hadron, so that they typically occur on a rather long time scale of $0(Q/m_N^2)$ where m_N is the nucleon mass. However, the scattering takes place on a much shorter time scale of $0(1/Q)$. This implies that the hadron may be regarded as an assembly of non interacting point like constituents.

Since the hadron in the C.M. frame is ultrarelativistic, partons are regarded as massless and moving parallel to the hadron, each with a certain fraction x of its momentum. Then it follows that the structure function of the hadron is obtained by the structure function of the parton and by summing over all parton types weighted by their density.

Denote by $f_{i/H}(x)$ the probability density to find within a hadron H a parton of type i , carrying a fraction x of hadron's momentum (parton distribution function). Then one obtains

$$d\sigma^H(P) = \sum_i \int_0^1 dx f_{i/H}(x) d\sigma^i(xP) \quad (1.3.1)$$

where $d\sigma^H$ ($d\sigma^i$) denotes the γ^* -hadron (i type parton) differential cross section.

PM ideas as above are generalized and applied to other hard scattering processes involving hadrons.⁽²⁸⁾ The corresponding differential cross section is expressed in a factorized form as in Eq. (1.3.1). E.g. for the inclusive process of Fig. 2(a)

$$H_1(P_1) + H_2(P_2) \rightarrow H(P) + X \quad (1.3.2)$$

one writes:

$$d\sigma_H^{H_1, H_2}(P_1, P_2, P) = \sum_{i, j, k} \int_0^1 dx_1 dx_2 dz f_{i/H_1}(x_1) f_{j/H_2}(x_2) d\hat{\sigma}_k^{ij}(p_1, p_2, p) D_{H/k}(z) \quad (1.3.3)$$

where $d\hat{\sigma}_k^{ij}$ is the differential cross section for the subprocess $i + j \rightarrow k + x$, with partons i, j , and k carrying momenta $p_1 = x_1 P_1, p_2 = x_2 P_2$ and $p = P/z$ respectively. Here, $D_{H/k}(z)$ denotes the probability density for the scattered parton k to fragment into a hadron H carrying a fraction z of parton's momentum (parton fragmentation function).

In the PM, distribution and fragmentation functions were assumed to scale (independent of any energy scale Q). Also, partons were originally identified with quarks.

Now, one identifies partons with quarks and gluons, and computes $d\hat{\sigma}_k^{ij}$ of Eq. (1.3.3) perturbatively in QCD. The simplest procedure is to take the QCD lowest order parton-parton subprocesses (Born terms). Then in general, contributions will arise corresponding to one or more of i, j, k being gluons (Fig 2(b)). This is the first QCD modification to the original PM. Next, one may calculate HOC of $d\hat{\sigma}_k^{ij}$ in terms of the appropriate Feynman graphs (cf Figs. 1(b) and 2(c)).

However, the perturbative expansion of $d\hat{\sigma}$, in the running coupling constant $\alpha_s(Q^2)$, contains terms proportional to $\alpha_s(Q^2) \ln(Q^2/\mu^2)$ at the next to leading order, and terms $\sim \alpha_s^n(Q^2) \ln^m(Q^2/\mu^2)$ with $n \leq m \leq 1$ at order n ; here μ is a regularization mass scale. These terms, in the limit of interest, $Q^2/\mu^2 \gg 1$ (or $\mu \rightarrow 0$), spoil the naive use of perturbation theory.

The key point in handling these terms was the observation that they arise from kinematic configurations corresponding to collinear production of a parton from another parton. Such configurations do not correspond to hard scattering, and, in position space, lead to propagation of partons over long times and distances. Therefore, the divergent pieces may be taken as parts of the distribution and/or fragmentation functions describing long distance effects.

To this end, the following procedure, called factorization of mass singularities,

is applied in QCD at any order of perturbation theory.⁽²⁹⁾⁻⁽³¹⁾

First, consider a subprocess with only one incoming parton leg (Eq. 1.3.1). Then the corresponding parton cross section $d\hat{\sigma}^i$ calculated at any order in $\alpha_s(Q^2)$ is written in the form:

$$d\hat{\sigma}^i(p) = \sum_{i'} \int_0^1 d\beta \Gamma_{i'/i}(\beta, \frac{Q^2}{\mu^2}) d\sigma^{i'}(\beta p) \quad (1.3.4)$$

where $\Gamma_{i'/i}$ includes all the leading and subleading logarithms of Q^2/μ^2 ; the coefficients of the corresponding divergent terms are process independent functions of β . Then the cross section $d\sigma^{i'}$ is finite in the limit of massless partons ($\mu \rightarrow 0$).

Thus the parton cross section factorizes into a finite piece times an infrared divergent factor, which can be absorbed in the parton distribution function. Indeed, using (1.3.4) the hadronic cross section, Eq. (1.3.1), is written

$$d\sigma^H(P) = \sum_i \int_0^1 dx f_{i/H}(x, Q^2) d\sigma^i(xP) \quad (1.3.5)$$

where

$$f_{i/H}(x, Q^2) \equiv \sum_{i'} \int_x^1 \frac{d\beta}{\beta} \Gamma_{i'/i}(\beta, \frac{Q^2}{\mu^2}) f_{i'/H}(\frac{x}{\beta}) \quad (1.3.6)$$

In this way the singularities disappear into renormalized (i.e. physically measurable and finite) quantities which are the redefined distribution functions $f(x, Q^2)$. This procedure has also introduced a Q^2 -dependence (scale breaking) into these functions, and shows how scaling is violated in QCD.

A similar procedure is applied for a subprocess with an outgoing parton leg, leading to a redefinition of the fragmentation function:

$$D_{H/k}(z, Q^2) = \sum_{k'} \int_x^1 \frac{d\beta}{\beta} D_{H/k'}(\frac{z}{\beta}) G_{k'/k}(\beta, \frac{Q^2}{\mu^2}) \quad (1.3.7)$$

where the singular part of $G_{k'/k}(\beta, \frac{Q^2}{\mu^2})$ is again process independent.

The above procedures are applied to each incoming or outgoing parton leg, associated with observed hadrons, in any process for which HOC are taken into account. After factorization of the mass singularities, the final hadronic cross section

is given by an expression similar to the PM one, but with now obvious modifications. E.g. referring to the process (1.3.2), the final result is given by Eq. (1.3.3) with distribution and fragmentation functions replaced by the corresponding scale violating ones and with $d\hat{\sigma}_k^{ij}$ replaced by the finite $d\hat{\sigma}_k^{ij}$.⁽¹⁾ (Compare also (1.3.5) to (1.3.1)). This last cross section admits a well behaved series expansion in $\alpha_s(Q^2)$ and can be extracted, at any order, from the corresponding $d\hat{\sigma}$ in accord with the above procedures.

At lowest order $d\hat{\sigma}' = d\hat{\sigma}$, and this is uniquely defined. At higher orders, however, $d\hat{\sigma}'$ involves some arbitrariness since a priori there is no way of defining completely the non-divergent part of the infinite factors $\Gamma_{i,j'}$ and/or $G_{k',k}$ extracted from $d\hat{\sigma}$ (cf. Eq. (1.3.4)). This part may also be regularization prescription dependent, reflecting a similar dependence in $d\hat{\sigma}'$.

To be more specific we consider the singular functions $\Gamma_{i,j}$. At next to leading order they have the form:

$$\Gamma_{i,j}(x, \frac{Q^2}{\mu^2}) = \delta_{i,j} \delta(1-x) - \frac{\alpha_s(Q^2)}{2\pi} [P_{i,j}(x) \ell n \frac{Q^2}{\mu^2} + u_{i,j}(x)] \quad (1.3.8)$$

where the coefficients $P_{i,j}(x)$ of the singular terms are process and regularization prescription independent. These are the Altarelli-Parisi split functions.⁽³²⁾ The non-diverging piece $u_{i,j}(x)$ is arbitrary and, in general, regularization prescription dependent. One way to fix it, is to define the HOC in $d\hat{\sigma}'$ to be zero in some reference process used to extract the parton distribution $f_{i/H}(x, Q^2)$. Then, predictions made with the same conventions, for any other process, are prescription independent. The same procedure can be applied for fragmentation functions and/or higher order terms.

Finally, we notice that in the leading logarithm approximation (and all orders in $\alpha_s(Q^2)$), the renormalized parton distributions satisfy the Altarelli-Parisi evolution equations:⁽³²⁾

$$\frac{df_{i/H}(x, Q^2)}{d \ln Q^2} = \frac{\alpha_s(Q^2)}{2\pi} \sum_j \int_x^1 \frac{dy}{y} P_{i,j}(y) f_{j/H}(\frac{x}{y}, Q^2) \quad (1.3.9)$$

where i denotes a quark or antiquark (of any flavor) or a gluon, and the summation runs over all parton types. Notice that in this summation, terms corresponding to i, j being a q, \bar{q} pair, or a pair of quarks (or antiquarks) with different flavor, give vanishing contributions; for such terms $P_{i,j} = 0$. The same is true for (1.3.8). However, beyond the next to leading order, such terms also contribute⁽⁹⁾.

Similar equations are valid for the evolution of the fragmentation functions.

PART I

CHAPTER 2

DIRECT PHOTON PRODUCTION AND THE SOFT GLUON APPROACH

In this Part we present a survey of some of our earlier work. This work is related with our effort to understand some of the sources (origins), of large corrections in higher orders of perturbative QCD; large in the sense that the overall next to leading logarithm contribution is comparable to the leading logarithm one.

In various considerations we focus on the hadroproduction of large p_T direct photons. We often use this reaction as a pilot process in our effort to identify, isolate and calculate HOC.

The above process presents much theoretical and experimental interest, because it provides a place where important predictions of perturbative QCD can be tested, and helps to complete our overall picture about the structure of hadrons.⁽³³⁾⁻⁽⁴⁰⁾ Experiments first carried at ISR have brilliantly verified the predictions, and this has substantially enhanced our confidence in QCD.

The interest in direct photon production^{(41),(42)} originally stemmed from the fact that, on a qualitative level, a substantial yield of photons at large transverse momentum, would suggest the presence of pointlike charged constituents within the hadrons.

Moreover, in perturbative QCD, direct photons at large p_T can arise via hard scattering subprocesses and to leading order in α_s , through the QCD Compton subprocess

$$q + g \rightarrow \gamma + q \quad (2.1a)$$

(Fig. 3(a)), and the annihilation subprocess

$$q + \bar{q} \rightarrow \gamma + g \quad (2.1b)$$

(Fig. 3(b)). In view of the small number of subprocesses and the well understood electromagnetic coupling of a photon to a quark, direct photon production helps to

unfold the underlying quark-gluon dynamics and hadron structure. In particular, from Figs. 3(a), (b) we see that, to leading order, when a photon is produced, there is a gluon either in the initial or in the final state. Therefore, if the contribution of these subprocesses is isolated (by properly selecting certain physical processes), direct γ production can be used to extract information on both the gluon distribution within hadrons and the gluon fragmentation function to hadrons.

Above all, as we stated, large p_T direct photon production is known to provide an important test of QCD. To briefly review a basic reason, consider the ratio of the inclusive cross sections

$$\left(\frac{\gamma}{\pi^0}\right) \equiv \frac{Ed\sigma/d^3p(A+B \rightarrow \gamma + X)}{Ed\sigma/d^3p(A+B \rightarrow \pi^0 + X)} \quad (2.2)$$

where A and B denote hadrons. Notice that $A+B \rightarrow \pi^0 + X$ is a purely hadronic process. In this, the observed π^0 carries only a fraction of the momentum of its parent parton; $Ed\sigma/d^3p(A+B \rightarrow \pi^0 + X)$ involves a fragmentation function $D_{\pi^0/c}(z)$ which behaves as $(1-z)^m$ with $m > 1$, and significantly suppresses this cross section at large z (or p_T). In contrast, in $A+B \rightarrow \gamma + X$ the photon carries away the entire p_T of the elementary collision. As a result, QCD predicts fairly large γ/π^0 ratio (20-50%); moreover it predicts that, at fixed s , γ/π^0 increases rapidly with p_T .

In addition, from the point of view of HOC and their structure, $A+B \rightarrow \gamma + X$ is less complex than e.g. $A+B \rightarrow \pi^0 + X$ at large- p_T , and therefore easier to analyze.

In this early part of the research, our work proceeded through certain steps which can be summarized as follows: First, in the leading logarithm approximation (Born terms) we considered large p_T $pp \rightarrow \gamma + X$ and studied the effects of scale violations. At that time the available data were too scanty to allow a meaningful comparison (Figs. 4(a),(b)) Next, we considered the effect of photon Bremsstrahlung (Brems) as well as effects due to parton's intrinsic transverse momentum (k_T effects). Then data of good quality became available, and detailed comparisons (Figs. 9 and 10 dashed lines) indicated a significant discrepancy. This suggested that we search for large correction terms in the next to leading order.

Thus we were led to the soft gluon approach and the related π^2 -terms arising from loop graphs in the soft gluon limit and from collinear and soft gluon Brems.

The essential parts of this research, in particular our work on the soft gluon technique, are presented in some detail in the present chapter.

2.1 Born Contributions and Photon Brems

2.1.1 Basic Formalism and Computational Details.

We consider the inclusive cross section for $A + B \rightarrow \gamma + X$ where A, B are hadrons and the photon γ is produced at 90° in the C.M. of A and B , with (large) transverse momentum p_T . We are interested in the contribution of the subprocesses (2.1) which are of the type

$$a + b \rightarrow c + \gamma \quad (2.1.1)$$

Then the inclusive cross section for $A + B \rightarrow \gamma + X$ is written (App. A)

$$E \frac{d\sigma}{d^3p}(p_T, s) = \frac{4}{\pi} \sum_{\substack{a,b \\ a \neq b}} \int_{x_1}^1 \frac{dx_a}{2x_a - x_T} F_{a/A}(x_a, Q^2) F_{b/B}(x_b, Q^2) \frac{d\sigma_{ab}}{d\hat{t}} \quad (2.1.2)$$

where

$$x_T = \frac{2p_T}{\sqrt{s}}, \quad x_b = x_T \frac{x_a}{2x_a - x_T}, \quad x_1 \equiv x_{a,\min} = \frac{x_T}{2 - x_T} \quad (2.1.3)$$

and the summation runs over quarks, antiquarks and gluons.

The differential cross sections $d\sigma_{ab}/d\hat{t}$ for the contributing subprocesses (2.1.1) are given by^{(41),(42),(2),(10)}

$$\frac{d\sigma_{qg}}{d\hat{t}} = e_q^2 \frac{2\pi\alpha_s}{\hat{s}^2} \frac{1}{2N_c} \frac{\hat{s}^2 + \hat{u}^2}{-\hat{s}\hat{u}} \quad (2.1.4)$$

$$\frac{d\sigma_{q\bar{q}}}{d\hat{t}} = e_q^2 \frac{2\pi\alpha_s}{\hat{s}^2} \frac{C_F}{N_c} \frac{\hat{t}^2 + \hat{u}^2}{\hat{t}\hat{u}} \quad (2.1.5)$$

where e_q is the quark charge, α is the fine-structure constant, α_s is the QCD running coupling,

$$\alpha_s = \alpha_s(Q^2) = \frac{12\pi}{25\ln(Q^2/\Lambda^2)} \quad (2.1.6)$$

(4 flavors), and the color factors are:

$$C_F = \frac{N_c^2 - 1}{2N_c}, \quad N_c = 3 \text{ for color } SU(3). \quad (2.1.7)$$

With momenta as in Figs. 3(a),(b) the subprocess invariants are

$$\hat{s} = (p_1 + p_2)^2, \quad \hat{t} = (q - p_1)^2, \quad \hat{u} = (q - p_2)^2 \quad (2.1.8a)$$

and neglecting quark masses

$$\hat{s} = x_a x_b s, \quad \hat{t} = -\frac{1}{2} x_a x_T s, \quad \hat{u} = -\frac{1}{2} x_b x_T s \quad (2.1.8b)$$

In (2.1.2) $F_{a/A}(x_a, Q^2)$ and $F_{b/B}(x_b, Q^2)$ denote parton momentum distributions inside the hadrons A and B respectively.⁽⁴³⁾⁻⁽⁴⁶⁾

In our early work^{(2),(10)} we carried calculations for $pp \rightarrow \gamma + X$ using two different sets I and II of parton distributions, both satisfying exact QCD requirements for their Q^2 evolution. The purpose of using two sets is to have a measure of the sensitivity of our results regarding the input forms which, as always, involve some arbitrariness.

Set I is taken from Ref. 44. The input forms $F(x, Q_0^2)$ are in accord with counting rules and their Q^2 dependence is provided by simple forms based on improved parametrizations of the type presented in Ref. 45. Set II is taken from Ref. 46.

We present below the input gluon distribution $F_{g/p}(x, Q_0^2)$, the reference point $Q = Q_0$ and the QCD momentum scale Λ of each set.

$$\text{SET I: } F_{g/p}(x, Q_0^2) = 2.4(1 - x)^5 \quad (\text{weak or soft}) \quad (2.1.9a)$$

$$Q_0^2 = 1.8 \text{ Gev}^2, \quad \Lambda = 0.5 \text{ Gev}.$$

$$\text{SET II: } F_{g/p}(x, Q_0^2) = 0.866(1 + 9x)(1 - x)^4 \quad (\text{strong or hard}) \quad (2.1.9b)$$

$$Q_0^2 = 4 \text{ Gev}^2, \quad \Lambda = 0.4 \text{ Gev}.$$

Finally, regarding the choice of the variable Q^2 , that enters the running coupling constant $\alpha_s(Q^2)$ and the functions $F(x, Q^2)$, we notice that it is not uniquely determined. Usual choices are:

$$(a) \quad Q^2 = -\hat{t} \qquad (b) \quad Q^2 = 2(\hat{s} + \hat{t}^2 + \hat{u}^2)$$

and even simpler:

$$(c) \quad Q^2 = p_T^2 \quad \text{or} \quad Q^2 = 2p_T^2 \qquad (2.1.10)$$

Notice that away from kinematic endpoints, roughly speaking, at fixed x_T , most of the contribution to the integral (2.1.2) comes from the region $x_a \simeq x_b \simeq x_T$. In this region, in view of Eq. (2.1.8b), all these choices amount to $Q^2 = \alpha p_T^2$ with α of $O(1)$. We call:

$$Q^2 = p_T^2 \qquad \text{physical scale}$$

$$Q^2 = \alpha p_T^2 \quad \alpha = O(1) \quad \text{near - physical scale.} \qquad (2.1.11)$$

2.1.2 Results and Discussion.

Now we present our results for the inclusive cross-section $Ed\sigma/d^3p(pp \rightarrow \gamma + X)$ and the ratio γ/π^0 of inclusive cross sections of γ to π^0 production in pp collisions. We present calculations at $\sqrt{s} = 53$ and 19.4 GeV with $Q^2 = 2p_T^2$.^{(2),(10)}

Our results using the QCD distributions of set I are presented in Fig. 4(a) and of set II in Fig. 4(b). The upper parts of these figures present separately contributions from the $q+g \rightarrow q+\gamma$ (denoted by qg) and the $q+\bar{q} \rightarrow g+\gamma$ (denoted by $q\bar{q}$) subprocesses. The lower parts present the ratio γ/π^0 . At each energy in calculating γ/π^0 we have used the experimental $Ed\sigma/d^3p(pp \rightarrow \pi^0 + X)$, which is also presented in Figs. 4(a), (b) (dash-dotted lines, denoted by $\pi^0(\text{expt})$).^(f0)

Our first remark is that, as expected, direct γ production in pp collisions is dominated by the qg subprocess; the $q\bar{q}$ contribution is typically one order of magnitude smaller (upper parts of Figs. 4(a), (b)). It is also clear that set II (strong gluon), of the QCD evolved parton distributions, predicts higher cross sections than set I (soft gluon).

Our second remark concerns the scale violating effects in the parton distributions. We notice that

- a) at relatively low p_T ($\lesssim 4$ Gev) these effects are naturally not very important, and
- b) at high p_T , inclusion of scale violations reduces the predicted γ (and γ/π^0) cross section by almost one order of magnitude.

The effects of scale violations are easy to understand. At low p_T ($\lesssim 4$ Gev), $x_T \lesssim 0.15$ for $\sqrt{s} = 53$ Gev, and $Q^2 \sim p_T^2$ is not much greater than Q_0^2 ; in this range of x and Q^2 the parton distributions do not appreciably differ from their input values. At high p_T (and fixed s), on the other hand, x_T is large and both the quark and the gluon distributions decrease with Q^2 and hence with p_T .

In addition we notice, that the Q^2 dependence is stronger in the gluon than in the quark distributions. In view of the fact that the gluon initiated subprocess dominates the cross section, we conclude that the fact that the presence of scale violations decreases the cross section (relative to that corresponding to scaling distributions^{(41),(42)}) is essentially due to the gluon distribution.^{(2),(10)}

2.1.3 Photon Brems.

Large p_T photons also arise via Brems from hard parton scattering subprocesses of the type^{(8),(10),(47)}

$$a + b \rightarrow c + d + \gamma \quad (2.1.12)$$

There are eight distinct quark and gluon initiated subprocesses of this form.

A typical case is

$$q + q \rightarrow q + q + \gamma \quad (2.1.13)$$

Fig. 3(c), which has been calculated completely to $O(\alpha_s^2)$. It was found^{(8),(10)} that its dominant part arises from kinematic configurations in which the real photon is produced collinearly with one of the final quarks. This part factorizes to the cross section for $qq \rightarrow qq$ scattering and the fragmentation function $q \rightarrow \gamma$;^{(48),(49)} notice that this is proportional to $\ln Q^2$ (see Eq. (2.1.17) below). The remaining

part ("constant piece"), depends on the definition (beyond the leading logarithm approximation) of the gluon density inside the quark⁽⁹⁾ and it is very small through the entire kinematic range.^{(8),(10)}

Anticipating a similar situation for all Brems type subprocesses, and in view of the fact that the factorized result corresponding to collinear photon configurations is of general validity (factorization theorem), we write for the contribution of (2.1.12) to $A + B \rightarrow \gamma + X$, at $\theta = 90^\circ$ (see also App. A),

$$E \frac{d\sigma}{d^3p}(p_T, s) = \frac{1}{\pi} \int_{x_1}^1 \frac{dx_a}{x_a} \int_{x_2}^1 \frac{dx_b}{x_b} F_{a/A}(x_a, Q^2) F_{b/B}(x_b, Q^2) \frac{d\sigma^{(ab \rightarrow cd)}}{d\hat{t}}(\hat{s}, \hat{t})$$

$$\frac{1}{z^2} D_{\gamma/c}(z, Q^2) + (A \leftrightarrow B) \quad (2.1.14)$$

where $d\sigma^{(ab \rightarrow cd)}/d\hat{t}$ is the Born differential cross section for the $2 \rightarrow 2$ subprocess

$$a + b \rightarrow c + d, \quad (2.1.15)$$

and for $\theta = 90^\circ$, x_1 is given by (2.1.3) while x_2 and z are:

$$x_2 = x_T \frac{x_a}{2 - x_T}, \quad z = \frac{x_T}{2} \left(\frac{1}{x_a} + \frac{1}{x_b} \right) \quad (2.1.16)$$

In (2.1.14), $D_{\gamma/c}$ is the fragmentation function of the parton c to the photon γ , which is of the form

$$D_{\gamma/c}(z, Q^2) = \frac{\alpha}{2\pi} d_{\gamma/c}(z) \ell n \frac{Q^2}{\tilde{\Lambda}^2} \quad (2.1.17)$$

where $\tilde{\Lambda}$ is some momentum scale (to be specified later). To the lowest nontrivial order^{(8),(10),(48),(51)}

$$\frac{1}{z} d_{\gamma/q}(z) = e_q^2 \frac{1 + (1 - z)^2}{z} = e_q^2 P_{\gamma q}(z) \quad (2.1.18)$$

and

$$d_{\gamma/g}(z) = 0; \quad (2.1.19)$$

$P_{\gamma q}(z)$ is the Altarelli-Parisi split function for $q \rightarrow \gamma$. There has been much work regarding $D_{\gamma/c}(z, Q^2)$ by summing leading logarithm contributions. The result

is still proportional to $\ell n Q^2$, Eq. (2.1.17). For $d_{\gamma/q}(z)$ one obtains the simple approximate form⁽⁴⁸⁾

$$d_{\gamma/q}(z) = \frac{1.124z}{1 - 0.72\ell n(1 - z)}; \quad (2.1.20)$$

this has the right behaviour at $z \sim 1$, but for smaller z it significantly deviates from the exact result. A better parametrization is provided by the forms⁽⁴⁹⁾

$$d_{\gamma/c}(z) = 2z^{-0.6} \sum_{n=0}^4 a_n^c z^n \quad (2.1.21)$$

where the constants a_n^c , $n = 0, 1 \dots 4$ depend on the type of the fragmenting parton c and are given in Ref. 49.

We note that in next to leading and higher orders in α_s , a gluon can also fragment into a photon as a result of the intermediate transition $g \rightarrow q\bar{q}$. Hence leading logarithm summations lead to $d_{\gamma/g}(z) \neq 0$, in contrast to the lowest order result (2.1.19). In fact, the parametric form (2.1.21) determines also $d_{\gamma/g}$. However, contributions of this type are now known to be very small.^{(50),(51)}

In our early work,^{(8),(10)} in order to study the significance of the Brems subprocesses (2.1.12) we evaluated the complete contribution arising from the typical subprocess (2.1.13). As we stated, we concluded that most of the contribution is due to collinear photon emission.

We carried calculations for $pp \rightarrow \gamma + X$ ^{(8),(10)} (as well as for other reactions)⁽¹⁰⁾ using the parton distributions of Subsect. 2.1.1 (Eqs. (2.1.9)), and taking again $Q^2 = 2p_T^2$ and $\Lambda = 0.5$ GeV. In Eq. (2.1.17) we used $\tilde{\Lambda} = \Lambda$ and the simple form (2.1.18) which arises from the lowest order perturbative calculation; this form leads to somewhat higher Brems contributions than the form (2.1.21).⁽⁵¹⁾

We also included effects due to partons' intrinsic transverse momentum k_T . For this, as in previous work,^{(1),(3)} we used for the parton distributions in (2.1.2) and (2.1.14) the replacement $F(x, Q^2) \rightarrow F(x, \vec{k}_T, Q^2)$ and the factorized form

$$F(x, \vec{k}_T, Q^2) = F(x, Q^2) D(\vec{k}_T) \quad , \quad \int d^2 k_T D(\vec{k}_T) = 1 \quad (2.1.22)$$

with a Gaussian distribution function

$$D(\vec{k}_T) = \frac{b^2}{\pi} \exp(-b^2 k_T^2) \quad , \quad \langle k_T \rangle = \frac{\sqrt{\pi}}{2b} \quad (2.1.23)$$

and a moderate $\langle k_T \rangle = 0.5 \text{ GeV}$.^{(1),(8),(10)}

In proton-proton collisions, the contribution of the subprocess (2.1.13) may be comparable to the leading contribution in some kinematic range. The reason is that (2.1.13) involves valence quark distributions $F_{q/p}$, whereas the leading Born term (2.1a) involves a gluon distribution $F_{g/p}$. Indeed, Fig. 5(a) shows that, with a soft distribution (Eq. (2.1.9a)), Brems gives an important contribution at large x_T (Fig. 5(a) in particular for $\sqrt{s} = 31 \text{ GeV}$). However, with a stronger gluon distribution (Eq. (2.1.9b)), the subprocess (2.1.13) gives a small contribution.

Fig. 5(b) shows the effect of partons' k_T , where $\sigma(k_T)$ denotes $E d\sigma/d^3p$ with $\langle k_T \rangle = 0.5 \text{ GeV}$ and $\sigma(0)$ the same with $\langle k_T \rangle = 0$. As in $pp \rightarrow \pi^0 + X$,⁽¹⁾ k_T effects are important only at low p_T , where the cross section is steeper.

At the end of the next section (Subsect. 2.2.3) we compare with data our predictions based on the Born and photon Brems contributions (with k_T effects included). In what follows we examine whether there are important contributions from HOC terms to the leading subprocess (2.1a). The motivation is that, as it will become clear, without significant HOC, the theoretical predictions lie below the data.

2.2 Large Correction Terms in the Soft Gluon Limit

Here we look for large corrections from higher orders in the perturbation expansion. One class of such corrections are certain constant pieces, usually called π^2 -terms, which were first observed in Drell-Yan dilepton production⁽⁵²⁾ We study corrections of this nature and we show that they occur in large- p_T direct photon and dilepton production.⁽⁴⁾⁻⁽⁶⁾ Our results are well supported by all available data.

2.2.1 The Soft Gluon Technique.

We present in this section the main results of our soft gluon technique,⁽⁴⁾⁻⁽⁶⁾ and try to make clear the origin of the resulting large corrections.

We begin by considering for $qg \rightarrow \gamma q$ the $0(\alpha_s^2)$ graphs which are infrared (IR) singular; these are presented in Figs. 6(a)-(1). They are formed by attaching a

gluon to on-shell colored lines of the Born graphs shown in Figs. 6(A) and (B); such graphs are referred to as A or B type graphs respectively. The attached gluon with momentum k_μ , polarization ρ and color index c is denoted by a dotted line.

The amplitude for the subprocess (2.1a), contributing to the cross section at order α_s^ℓ ($\ell = 1, 2$) is denoted by $M_{\alpha\mu}^{(\ell)}(P)$ for loop graphs, and by $M_{\alpha\mu\rho}^{(\ell)}(P, k)$ for Brems graphs. Here P stands for the set $\{p_1, p_2, q\}$ of 4-momenta of the incoming partons and of the outgoing photon. The indices α and μ stand for the polarization of the incoming gluon and the photon. The color indices are suppressed.

The soft gluon technique consists of the following procedures:⁽⁴⁾⁻⁽⁶⁾

- (a) setting $k_\mu \rightarrow 0$ and permuting the Dirac matrices in the numerator,
- (b) setting $k_\mu \rightarrow 0$ in hard propagators only, leaving unchanged all other factors in the denominator.

It follows from the procedure (a) that:

- (i) a soft gluon attached to fermion lines does not change the Dirac structure of the Born amplitude, and
- (ii) the same is true for three-gluon attachments, provided a summation over graphs is performed.

The above statement (i) can be easily derived and is known from soft photon techniques in QED. To illustrate the statement (ii) we refer to Fig. 6(a) and in the expression of the amplitude $M_{(a)}^{(2)}(P)^{\alpha\mu}$ we make the replacement

$$\begin{aligned} & \bar{u}(r)\gamma_\lambda(\not{p}_2 + \not{k} - \not{q})\gamma^\mu(\not{p}_2 + \not{k})\gamma_\rho u(p_2)V^{\lambda\rho\alpha}(k, p_1) \\ & \rightarrow \bar{u}(r)\gamma_\lambda(\not{p}_2 - \not{q})\gamma^\mu u(p_2)2p_{2\rho}V^{\lambda\rho\alpha}(0, p_1) \end{aligned} \quad (2.2.1)$$

where the limit $k_\mu \rightarrow 0$ was taken and the permutation

$$\not{p}_2\gamma_\rho u(p_2) = (2p_{2\rho} - \gamma_\rho\not{p}_2)u(p_2) = u(p_2)2p_{2\rho} \quad (2.2.2)$$

was used. The tensor $V^{\lambda\rho\alpha}$ is associated with the three-gluon vertex which in the limit $k_\mu \rightarrow 0$ becomes:

$$V^{\lambda\rho\alpha}(0, p_1) = 2p_1^\rho g^{\alpha\lambda} - p_1^\lambda g^{\alpha\rho} - p_1^\alpha g^{\lambda\rho}. \quad (2.2.3)$$

The first term in Eq. (2.2.3) replaced in (2.2.1) gives immediately a factorized result with the Born Dirac structure. The last two terms in (2.2.3) give contributions which cancel each other because of the Ward identity. We have explicitly verified this cancellation for the set of graphs in Fig. 6. To simplify the calculation, from now on we drop the last terms in Eq. (2.2.3). The result is that for either three-gluon or QED-like graphs the soft gluon polarization is proportional to the momentum of the line to which the gluon is attached.

Procedure (b) is crucial in preserving exactly the singularities and analytic structure of the amplitude as $k_\mu \rightarrow 0$. In hard propagators the limit $k_\mu \rightarrow 0$ can be safely taken. To illustrate this, we refer again to Fig. 6(a) and write

$$\frac{1}{(p_2 - q - k)^2} = \frac{1}{(p_2 - q)^2} - \frac{k^2 + 2k_1 \cdot (p_2 - q)}{(p_2 - q)^2(p_2 - q + k)^2} \rightarrow \frac{1}{(p_2 - q)^2} \quad (2.2.4)$$

Notice that the second term, which is of $0(k)$ compared to the first, can be dropped as $k_\mu \rightarrow 0$. However, all other denominators of the form $(p_J \pm k)^2$ with $p_J^2 = 0$ are left unchanged because there are regions of integration where $|k^2| > |2p_J \cdot k|$, even as $k_\mu \rightarrow 0$. (For example, when \vec{k} is perpendicular to \vec{p}_J).

Applying procedures (a) and (b) we find factorized expressions for the amplitudes of either loop or Brems graphs. In these limiting expressions the analyticity properties and singularity structure is preserved. We present our results in the following.

2.2.1a Loop amplitudes and π^2 -terms.

Returning to Fig. 6(a) we obtain the factorized contribution to the amplitude

$$M_{(a)}^{(2)}(P)^{\alpha\mu} = g^2 \frac{N_c}{2} 4p_1 \cdot p_2 iL(p_1, -p_2) M_A^{(1)}(P)^{\alpha\mu} \quad (2.2.5)$$

where the integral

$$L(p_1, p_2) \equiv \mu^{2\epsilon} \int \frac{d^n k}{(2\pi)^n} \frac{1}{(k^2 + i\eta)((p_1 - k)^2 + i\eta)((p_2 - k)^2 + i\eta)} ; p_1^2 = p_2^2 = 0 \quad (2.2.6)$$

is characteristic of loop contributions.

Performing the integration (App. B) we obtain:

$$iL(p_1, -p_2) = \frac{1}{(4\pi)^2} \frac{1}{\epsilon^2} \frac{1}{(-2p_1 \cdot p_2)} \left(\frac{-2p_1 \cdot p_2 - i\eta}{4\pi\mu^2} \right)^{-\epsilon} \frac{\Gamma(1+\epsilon)\Gamma^2(1-\epsilon)}{\Gamma(1-2\epsilon)} \quad (2.2.7)$$

so that

$$M_{(a)}^{(2)}(P)^{\alpha\mu} = \frac{\alpha_s N_c}{4\pi} \frac{-2}{2} \frac{1}{\epsilon^2} \left(\frac{-\hat{s} - i\eta}{4\pi\mu^2} \right)^{-\epsilon} \Gamma_L(\epsilon) M_A^{(1)}(P)^{\alpha\mu} \quad (2.2.8)$$

with $\hat{s} = (p_1 + p_2)^2$ and

$$\Gamma_L(\epsilon) \equiv \frac{\Gamma(1+\epsilon)\Gamma^2(1-\epsilon)}{\Gamma(1-2\epsilon)}. \quad (2.2.9)$$

At this point we can already see the origin of a large correction, or π^2 term: Eq. (2.2.8) has a threshold for $s = 0$ and must be analytically continued. Thus,

$$ReM_{(a)}^{(2)}(P)^{\alpha\mu} = \frac{\alpha_s N_c}{4\pi} \frac{1}{2} \Gamma_L(\epsilon) \left(\frac{\hat{s}}{4\pi\mu^2} \right)^{-\epsilon} \left(\frac{-2}{\epsilon^2} + \pi^2 \right) M_A^{(1)}(P)^{\alpha\mu} \quad (2.2.10)$$

The other loop contributions from Fig. 6, including the B type graphs, are evaluated in the same way. After restoring color matrices, the factors composing each amplitude $M^{(2)}(P)^{\alpha\mu}$ are summarized in Table I (upper part).

In the cross section, the $1/\epsilon^2$ singularity of Eq. (2.2.10) is cancelled by a similar singularity in the Brems contribution. This is clearly shown in Subsect. 2.2.1b below.

As a final remark, concerning loop contributions, notice that the graphs (u) and (v) of Fig. 6 are not infrared singular. For example, the amplitude of graph (u) involves the integral

$$I = \int \frac{d^n k}{(2\pi)^n} \frac{(k + \not{p}_2 - \not{q})\gamma_\mu(k + \not{p}_2)}{k^2(k + p_2 - q)^2(k + p_2)^2}, \quad (2.2.11)$$

which in the soft gluon limit becomes:

$$I \rightarrow \frac{(\not{p}_2 - \not{q})\gamma_\mu \not{p}_2}{(p_2 - q)^2} \int \frac{d^n k}{(2\pi)^n} \frac{1}{k^2(p_2 + k)^2}. \quad (2.2.12)$$

It is well known that the last integral does not introduce a $1/\epsilon^2$ singularity. As a result, no π^2 -term of the soft gluon type is generated.

Similarly, in the Feynman gauge, self energy contributions are not $1/\epsilon^2$ divergent; the corresponding graphs are not presented.

2.2.1b Gluon Brems amplitudes.

Now we consider Brems graphs, Figs. 6(d)–(f) and 6(j)–(l), and apply procedures (a) and (b) of the soft gluon limit.^{(4)–(6)} Referring to Fig. 6(d) we obtain for the corresponding amplitude

$$M_{(d)}^{(2)}(P, k)^{\alpha\mu\rho} = g \frac{2p_1^\rho}{2p_1 \cdot k} [t_c, M_A^{(1)}(P)^{\alpha\mu}] \quad (2.2.13)$$

Thus, the amplitude factorizes into a vector and a color matrix and has the Dirac structure of the lowest order graph. Notice that Brems amplitudes are real and consequently no analytic continuation is required; no π^2 term of the above type is generated.

Similar results are obtained for each of the other Brems graphs of Fig. 6, either of type A or B. Again, after restoring color matrices, the factors composing each amplitude $M^{(2)}(P, k)^{\alpha\mu\rho}$ are listed in Table I (lower part).

2.2.2 The Differential Cross Section.

We are now ready to calculate the subprocess differential cross section. We denote it by $q_0 d\sigma^{(\ell)}/d^3q$ where $\ell(= 1, 2)$ means that it is evaluated at order α_s^ℓ .

We remarked the proportionality between the next to leading and the corresponding leading order amplitude. Such a relationship shall also be valid between the corresponding interference terms (unitarity graphs).^{(4)–(6)}

Figs. 7(a)–(d) show the four Born unitarity graphs arising from interference of the graphs of Figs. 6(A) and 6(B). We denote by $q^0 d\sigma_i^{(1)}/d^3q$ the contribution to the cross section of the (i) graph, with $i = a, b, c, d$. The interference terms of Figs. 7(b) and 7(d) are of $O(q^2)$ and consequently vanish for real photons. However we keep them in our calculation so that our final result, Eq (2.2.22), can also be used for lepton pair production with the replacement: $q^0 d\sigma/d^3q \rightarrow q^2 d\sigma/d^4q$.

The other unitarity graphs in Fig. 7 show pairs of associated loop (primed) and Brems (unprimed) graphs. They are associated in the following sense: they

arise from the same Born graph by attaching a virtual or real gluon between two on-shell parton legs. In this way, the resulting contributions to the cross section are proportional to the same Born cross section with the same color factor; this permits a pair-wise cancellation of the $1/\epsilon^2$ infrared divergencies. We present only those graphs which introduce a large correction either directly or through their crossed counterparts (see below).

To illustrate the pattern of cancellation of $1/\epsilon^2$ singularities, we consider in detail the effect of adding a particular Brems [Fig. 7(C)] and loop [Fig. 7(C')] combination of contributions.

Referring to Table I and taking into account a factor of 2 for the Hermitian conjugate graph, the contribution of Fig. 7(C) is written as

$$q^0 \frac{d\sigma_{(C)}^{(2)}}{d^3q} = 2g^2 \frac{N_c}{2} 4p_1 \cdot p_2 B(p_1, p_2) \frac{q_0 d\sigma_c^{(1)}}{d^3q} \quad (2.2.14)$$

where

$$B(p_1, p_2) = \mu^{2\epsilon} \int \frac{d^n k}{(2\pi)^{n-1}} \frac{\delta(k^2) \theta(k_0)}{2p_1 \cdot k 2p_2 \cdot k} \quad (2.2.15)$$

The integration in (2.2.15) is performed according to standard methods and gives (see also App. B):

$$B(p_1, p_2) = \frac{1}{(4\pi)^2} \frac{1}{\epsilon^2} \frac{1}{2p_1 \cdot p_2} \Gamma_B(\epsilon) \left(\frac{4k_{max}}{4\pi\mu^2} \right)^{-\epsilon} \quad (2.2.16)$$

with

$$\Gamma_B(\epsilon) = \frac{\Gamma(1-\epsilon)}{\Gamma(1-2\epsilon)} \quad (2.2.17)$$

In (2.2.16) k_{max} is determined from the kinematics of the subprocess; for direct photon production $4k_{max}^2 \sim \hat{s}$, so that:

$$q^0 \frac{d\sigma_{(C)}^{(2)}}{d^3q} = \frac{\alpha_s N_c}{2\pi} \frac{1}{2} \left(\frac{\hat{s}}{4\pi\mu^2} \right)^{-\epsilon} \Gamma_B(\epsilon) \frac{2}{\epsilon^2} q^0 \frac{d\sigma_c^{(1)}}{d^3q} \quad (2.2.18)$$

Twice the real part of the loop contribution from Fig. 7(C') (accounting also for the contribution of the Hermitian conjugate graph), gives with the help of Table I:

$$q^0 \frac{d\sigma_{(C')}^{(2)}}{d^3q} = \frac{\alpha_s N_c}{2\pi} \frac{1}{2} \left(\frac{\hat{s}}{4\pi\mu^2} \right)^{-\epsilon} \Gamma_L(\epsilon) \left[-\frac{2}{\epsilon^2} + \pi^2 \right] q^0 \frac{d\sigma_c^{(1)}}{d^3q}. \quad (2.2.19)$$

Addition of Eqs. (2.2.18) and (2.2.19) cancels the $1/\epsilon^2$ terms; the remainder contains the large correction $\sim (N_c/2)\pi^2$. This pattern of cancellation of $1/\epsilon^2$ terms between primed (loop) and unprimed (Brems) graphs in Fig. 7 is as expected from general properties of IR divergences.⁽⁴⁾⁻⁽⁶⁾

Table II lists the factors composing the equation corresponding to (2.2.18) or (2.2.19) for each unitarity graph. Notice that graphs in the same row of Fig. 7 have identical factors multiplying the Born term (at the top of each column).

Although IR singularities cancel in the sum of loop and Brems contributions, there remain subleading $1/\epsilon$ (collinear or mass) singularities which are process independent; they only depend on the type of partons initiating the leading and the next to leading order subprocess. However, the remaining non singular piece depends on the regularization procedure (here dimensional regularization). For example, Eqs. (2.2.18) and (2.2.19) contain $1/\epsilon$ terms and $0(1)$ regularization dependent pieces. To properly specify a correction one must remove both the singular and the regularization dependent terms by absorbing them into the parton distribution functions. This is done by a consistent definition of parton distributions through another process using the same regularization procedure.

It is convenient, as emphasized by Altarelli et al,^(52a) to fix the definition of parton distributions at a given order of α_s , by defining corrections to a related deep inelastic scattering (DIS) subprocess to be zero. This means that the expression giving the DIS physical quantity in terms of parton distributions and the parton scattering cross section, should retain at the given order of α_s exactly the form it has at the lowest order.

The quark distributions defined in Ref. 52(a), as measured in inclusive DIS, have no large corrections to one loop order. For the gluon distribution, a DIS subprocess must be chosen so that the gluon distribution is as directly involved as possible and so that the soft gluon approximation is applicable. For example, the inclusive (flavor singlet channel) DIS quantity $F_L(x, Q^2)$ lacks a large momentum transfer scale, because it involves integrations over final state momenta;⁽⁵⁾ then the soft gluon approximation, Eq. (2.2.4), is not directly applicable.

Motivated by Ref. 52(a) we adopt the following definition of the correction: we consider electroproduction of a large p_T jet through the subprocess

$$\gamma^* + g \rightarrow q + \bar{q}; \quad (2.2.20)$$

then we require that the correction to (2.2.20) at $0(\alpha_s^2)$ be zero. This means that all the next to leading order perturbative contributions are absorbed in the gluon distribution function. Notice that (2.2.20) is related to (2.1a) by crossing. The Born unitarity graph and the subprocess momenta assigned to (2.2.20) are shown in Fig. 8(a). Defining the z axis parallel to \vec{q} in the γ^*p C.M. frame and \hat{j} the jet axis, contributions to $d\sigma/d^3p$ can be obtained by crossing $|M(p_1, p_2, q)|^2$ of (2.1a) with $p_2 \rightarrow -p_2 = p$ and $q \rightarrow -q$, followed by an analytic continuation $q^2 > 0 \rightarrow q^2 < 0$. For large $p_T^2 \sim 0(|q^2|)$ the soft gluon approximation applies in both cases; typical $0(\alpha_s^2)$ unitarity graphs are shown in Figs. 8(b)–8(c'). Defining (soft) gluon corrections to (2.2.20) to be zero, we find corrections to (2.1a) by subtracting terms at $0(\alpha_s^2)$ via

$$|M(p_1, p_2, q)|^2 \rightarrow |M(p_1, p_2, q; q^2 > 0)|^2 - |M(p_1, -p_2, -q; q^2 < 0)|^2. \quad (2.2.21)$$

This means that from the contribution of each unitarity graph we subtract the corresponding contribution of its crossed counterpart. In the difference, collinear singularities associated with the incoming gluon p_1 cancel as well as the regularization dependent pieces.

In Table II we have summarized the contributions giving a π^2 -term in accord with the above definition of corrections. Adding these terms to the Born contribution, we finally obtain

$$q^0 \frac{d\sigma}{d^3q} = [1 + \frac{\alpha_s}{2\pi}(N_c - C_F)\pi^2] q^0 \frac{d\sigma^{(1)}}{d^3q}. \quad (2.2.22)$$

Clearly in Eq. (2.2.22) we have neglected terms of $0(\ln^2(q_T^2/s))$ in the limit $q_T^2 \sim s$ (or $x_T \sim 1$); these terms, however, are easily available from Table II. Such terms would be important only in the small q_T (or x_T) region.

Finally we remark that Eq. (2.2.22), corresponding to a nonuniversal definition of corrections, can be easily transformed to that of Refs. 53 (universal definition).

2.2.3 Phenomenological Implications.

We close this section by briefly presenting certain phenomenological implications of the large $0(\alpha_s^2)$ correction of Eq. (2.2.22).

Fig. 9 presents all the ISR data on the inclusive cross section $q^0 d\sigma/d^3q$ (usually denoted by $E d\sigma/d^3p$) available at the time of our calculation.⁽⁴⁾⁻⁽⁶⁾ Whenever a Collaboration gives only the ratio γ/π^0 (Eq. (2.2)) we have multiplied by π^0 data of the same collaboration. Fig. 10 presents data of the A^2BC Collab. on the ratio γ/π^0 .

Figs. 9 and 10, dashed lines, show the results of the calculations of Sect. 2.1 (Born terms and photon Brems) with a strong gluon distribution Eq. (2.1.9b) and $\langle k_T \rangle = 0.5$ Gev. Clearly a large correction is required.

Next, Figs. 9 and 10, solid lines, present predictions based on Eq. (2.2.22) which includes the $0(\alpha_s^2)$ correction of this section. Clearly, inclusion of this correction significantly improves the agreement with the A^2BC and the rest of the data.

On the whole, the situation for large- p_T direct photon production is very similar to that for the Drell-Yan $d\sigma/dq^2$ for dilepton production (see also Ch. 8, Sect. 8.4); it is well known that data require that the Drell-Yan cross section be multiplied by a K -factor of magnitude $K \simeq 2$.

2.3 Other Large Correction Terms

The soft gluon approach, which we presented and developed in the last section, pinpointed a large correction term to the contribution of the subprocess $qg \rightarrow \gamma g$. As we stated, this subprocess dominates $pp \rightarrow \gamma + X$ at large p_T . The available data were well accounted for by the HOC of Eq. (2.2.22).

However, one can see that there must be other sources of large corrections, as well. For example, consider the difference of the inclusive cross sections for large- p_T

$\ell^+\ell^-$ production in π^-p and π^+p collisions. This is dominated by the subprocess $q\bar{q} \rightarrow \gamma^*y$; and for this a complete calculation of next-to-leading order corrections gives a large HOC (comparable to Born).⁽⁵⁴⁾ This is in accord with experimental data. Now for $q\bar{q} \rightarrow \gamma^*g$, the soft gluon limit technique of Sect. 2.2. does not give a large correction; therefore one should look elsewhere.

An additional source of large correction terms was identified in Ref. 55, where it was shown that such terms arise also from collinear and soft gluon Brems. In fact, it was shown that addition of the large corrections from loops in the soft gluon limit (Sect. 2.2) and from collinear and soft gluon Brems, leads to HOC in good accord with most complete calculations⁽⁵⁶⁾ and with experiments.^{(38),(39),(12),(57)}

These two sources of HOC lead to an approximate K -factor of the form:

$$K \simeq 1 + \frac{\alpha_s(Q^2)}{2\pi} C \pi^2 \quad (2.3.1)$$

where

$$C = \sum_{\text{loops}} C_l + \sum_{\text{Brems}} C_B \quad (2.3.2)$$

C_l are essentially color factors determined from graphs involving loops in the soft gluon limit (soft gluon technique of Subsect. 2.2.1) and C_b are determined from graphs contributing to collinear and soft gluon Brems.^{(55),(56)}

As an example of the effectiveness of the approximate K -factors, Eq. (2.3.1), we present Fig. 11 (taken from Ref. 56). This compares predictions for $\bar{p}p \rightarrow \gamma + X$ based on Eq. (2.3.1) (solid lines)⁽⁵⁶⁾ to the results of a complete calculation (dash-dotted lines).^(65b) The two calculations use the same input distributions.⁽⁵⁶⁾ Clearly the difference between them is small, much smaller than changing the gluon distribution (dashed-lines).

PART II

THE DOMINANT PART OF HIGHER ORDER CORRECTIONS

In our earlier work (Ch. 2), the procedure we followed can be briefly described as follows: Working always at physical (or near-physical) scales we pinpointed certain large terms in the perturbative expansion, specified their origin and provided simple ways to determine their contribution. This resulted in the simple K -factors of Eq. (2.3.1). Comparison with the then available data led to considerable success.

In our recent work (this and the next chapter) we follow a different procedure: We start from the complete HOC, we analyse its structure, we show that there is a part that dominates and we give reasons explaining the dominance. This part, to be called dominant, is considerably simpler than the complete HOC; as a result, we show that we can determine it more easily (Ch. 4).

The dominant part amounts to a correction of a much more complicated form than that of the simple K -factors of Ch. 2. Nevertheless, we shall show (end of Ch. 5) that, with certain approximations, the form of the simple K -factors does arise, thus offering some insight into the reason of their success. We should note, however, that the main motivation of the following work is to establish as much as possible the existence of a dominant part and to explicitly demonstrate that it is calculable with relative ease.

CHAPTER 3

STRUCTURE OF HOC AND THE EXISTENCE OF A DOMINANT PART

We proceed to analyze the structure of HOC and show with specific examples that there is a relatively simple part that dominates the HOC. Also we discuss the origin of this part, its gauge invariance and certain other aspects, as e.g. its stability against changes of the scales.

3.1 The Structure of HOC

We consider the structure of HOC for a physical single inclusive process involving distribution and/or fragmentation functions, and initiated by $2 \rightarrow 2$ particle hard scattering subprocesses.

To begin with and to be more specific, we consider large p_T direct photon production in hadronic collisions (our pilot reaction); in fact two of the examples presented at the next section refer to this process, and are extensively studied in the following chapters. We emphasize, however, results and statements of general validity.

The contribution of the subprocess

$$a + b \rightarrow \gamma + x, \quad (3.1.1)$$

including HOC of order α_s^2 , to the inclusive cross section for $A + B \rightarrow \gamma + X$ can be written:

$$E \frac{d\sigma}{d^3p}(p_T, s, \eta) = \frac{\alpha_s(\mu)}{\pi} \int dx_a dx_b \{ F_{a/A}(x_a, M) F_{b/B}(x_b, M) [\hat{\sigma}_B \delta(1 + \frac{\hat{t} + \hat{u}}{\hat{s}}) + \frac{\alpha_s(\mu)}{\pi} f\theta(1 + \frac{\hat{t} + \hat{u}}{\hat{s}})] + F_{b/A}(x_a, M) F_{a/B}(x_b, M) [\hat{t} \leftrightarrow \hat{u}] \} \quad (3.1.2)$$

where $E(p)$ denotes the energy (momentum) of the observed photon with transverse momentum p_T and (pseudo-) rapidity η . In (3.1.2), $\alpha_s(\mu)$ is the QCD running coupling, and $F_{a/A}(x_a, M)$, $F_{b/B}(x_b, M)$ are parton momentum distributions; $\mu(M)$

stands for the renormalization (factorization) scale. $\hat{\sigma}_B$ denotes the Born contribution and f the HOC. Both $\hat{\sigma}_B$ and f are functions of the subprocess invariants \hat{s} , \hat{t} , and \hat{u} introduced in Eq. (2.1.8a). In addition, f depends on the scales μ and M ; however, to simplify the notation, we suppress this dependence.

We introduce the following dimensionless variables

$$v = 1 + \frac{\hat{t}}{\hat{s}}, \quad w = -\frac{\hat{u}}{\hat{t} + \hat{s}} \quad (3.1.3)$$

so that

$$\hat{t} = -\hat{s}(1 - v), \quad \hat{u} = -\hat{s}vw \quad (3.1.4)$$

and

$$\hat{s} + \hat{t} + \hat{u} = \hat{s}v(1 - w) \quad (3.1.5)$$

Thus regarding the x_a, x_b integration in (3.1.2) the boundary corresponds to $w = 1$, the rest to $w < 1$. Clearly, the HOC arises by integrating over the whole hatched region indicated in Fig. 12(a) for $\eta = 0$ and Figs. 12(b) and (c) for $\eta \neq 0$.

Now, it follows from a number of complete calculations, and will become clear in the next chapter, that the general structure of HOC is as follows:^{(58)-(61),(11),(12)}

$$f(v, w) = f_s(v, w) + \tilde{f}(v, w) \quad (3.1.6)$$

where the first part of the r.h.s. of (3.1.6) contains distributions in the variable w and has the form

$$\begin{aligned} f_s(v, w) \equiv & a_1(v)\delta(1 - w) + b_1(v)\frac{1}{(1 - w)_+} + c(v)\left(\frac{\ell n(1 - w)}{1 - w}\right)_+ \\ & + (a_2(v)\delta(1 - w) + b_2(v)\frac{1}{(1 - w)_+})\ell n\frac{\hat{s}}{M^2}, \end{aligned} \quad (3.1.7)$$

while the function $\tilde{f}(v, w)$ contains the remaining terms of the HOC (no distributions) and, in general, is very complicated; it is the most complicated part of HOC⁽⁵⁸⁾⁻⁽⁶¹⁾ (See also Sect. 7.1 of this Thesis).

In the following section we demonstrate with specific examples that the contribution of $f_s(v, w)$ dominates the HOC, and we present reasons explaining this fact. Also, as we discuss in Sect. 3.3, $f_s(v, w)$ is a gauge invariant part.

3.2 The Dominant Part of HOC

We denote by σ_B and σ_{HO} the contributions of the Born term and of the complete HOC f to the inclusive cross section σ ; $\sigma = \sigma_B + \sigma_{HO}$. Also, we denote by σ_s the contribution of f_s ; thus $\sigma_{HO} - \sigma_s$ is the contribution of \tilde{f} . We consider the ratio

$$\tilde{R}_T = \frac{\sigma_{HO} - \sigma_s}{\sigma_B + \sigma_{HO}} \quad (3.2.1)$$

which determines the relative contribution of \tilde{f} to the total inclusive cross section of the physical process.

We present results for this ratio as a function of p_T at fixed s and for simplicity at $\eta = 0$. Our results correspond to the choice of physical scales $\mu = M = p_T$.

We consider the subprocess $q\bar{q} \rightarrow \gamma g$, which dominates the difference of the inclusive cross sections for $\bar{A}+B \rightarrow \gamma+X$ and $A+B \rightarrow \gamma+X$. Take $A = B = \text{proton}$ and let σ in (3.1.2) to denote the nonsinglet cross section:

$$\sigma \equiv E \frac{d\sigma}{d^3p}(\bar{p}p \rightarrow \gamma X) - E \frac{d\sigma}{d^3p}(pp \rightarrow \gamma X) \quad (3.2.2)$$

then the structure function $F_{a/A}(x_a, p_T)$ ($F_{b/B}(x_b, p_T)$), entering Eq. (3.1.2), refers only to valence quarks in p (antiquarks in \bar{p}).

We carried calculations using set I of Ref. 62 for these distributions, and the results of Ref. 59, for the terms in f (see also Ch. 7 and related discussion).

Fig. 13(a) presents, with solid line (corresponding to $n = n_{QCD}(p_T)$), the ratio \tilde{R}_T as function of p_T at $\sqrt{s} = 63$ GeV. We see that, this ratio is small, and decreases rather fast with p_T [e.g. for $p_T = 4$ GeV ($x_T \simeq 0.13$) this ratio is $\simeq 16\%$ and for $p_T = 16$ GeV ($x_T \simeq 0.5$) it is only $\simeq 3.5\%$].

To understand the reason, we refer to Eq. (3.1.2) and consider fixed s and rapidity η . With $x_T = 2p_T/\sqrt{s}$ and in view of App. A we have:

$$\hat{s} + \hat{t} + \hat{u} = s(x_a x_b - \frac{1}{2}x_a x_T e^{-\eta} - \frac{1}{2}x_b x_T e^{\eta}) \quad (3.2.3)$$

In (3.1.2), in view of the δ and θ functions, the integration region is determined from $\hat{s} + \hat{t} + \hat{u} \geq 0$ together with the conditions $x_a \leq 1$, $x_b \leq 1$; we obtain:

$$\frac{e^{\eta}}{x_a} + \frac{e^{-\eta}}{x_b} \leq \frac{2}{x_T} \quad (3.2.4)$$

where the sign of equality determines the (curved) boundary of the region.

To simplify matters we first consider $\eta = 0$. For this case the corresponding region is indicated in Fig. 12(a). As we stated, the boundary of the region corresponds to $w = 1$; the rest to $w < 1$. Clearly the Born contribution arises by integrating over the boundary, while the HOC over the whole hatched region.

Now, a crucial observation is that in Eq. (3.1.2), with the choice of the physical scale $\mu = M = p_T$, $F_{a/A}(x_a, p_T)$ behaves like $(1 - x_a)^{n(p_T)}$; with $A = \text{proton}$, n is quite large ($n = 3 \sim 4$ if $a = \text{valence quark}$, $n \simeq 5$ if $a = \text{gluon}$, $n \simeq 7$ if $a = \text{sea quark}$). Notice also that the scale violations further enhance n as p_T increases. The same holds for $F_{b/B}(x_b, p_T)$. Then, referring to Fig. 12(a), contributions arising from the region away from $w = 1$ (large x_a and/or x_b), are suppressed by high powers of $1 - x_a$ and/or $1 - x_b$.

The terms $f_s(v, w)$, Eq. (3.1.7), give their main contribution near $w = 1$ (cross hatched region of Fig. 12(a)); while the multitude of terms of $\tilde{f}(v, w)$ do not mainly contribute at $w \sim 1$ (we further substantiate these statements at the end of this section). As a result, in the presence of the structure functions, $\tilde{f}(v, w)$ is suppressed.

Now notice that as p_T increases for fixed s , (or as x_T increases) the boundary of integration moves towards the point $x_a = x_b = 1$ and the region shrinks; thus the suppression of contributions from \tilde{f} increases with p_T , and it is further enhanced by the scale violations. Hence as p_T increases for fixed s (or as x_T increases) the terms comprising f_s , dominate more and more the HOC.

Notice also that in $\tilde{f}(v, w)$ the multitude of terms contribute with almost random signs; some of them are positive, others are negative, without any concrete pattern (e.g. regarding the nonsinglet cross section $(\bar{p}p - pp) \rightarrow \gamma X$, which is dominated by the subprocess $q\bar{q} \rightarrow \gamma g$, see the Appendix of Ref. 59(a) and Ch. 7 of this Thesis). This reduces even more the overall contribution of these terms. This point has been remarked long ago.^{(5),(55),(56)}

As a further test of the above ideas we have carried calculations in the following manner. We write the structure functions (in the present case, valence momentum

distributions) in the form:

$$F_{a/A}(x, p_T) = F_{b/B}(x, p_T) = (1 - x)^n \quad (3.2.5)$$

and determine the ratio (3.2.1) for the fictitious values $n = 20$ (extremely soft distribution) and $n = 0.01$ (extremely hard). As expected, in the first case (dashed line in Fig. 13(a)) the ratio is significantly smaller than for $n = n_{QCD}(p_T)$; in the second case (long dashed line) it is significantly larger.

Clearly, the softness of the distribution plays a very important role in suppressing the part $\tilde{f}(v, w)$ of HOC.

In addition to the ratio (3.2.1) we have also determined the ratio

$$\tilde{R}_{HO} = \frac{\sigma_{HO} - \sigma_s}{\sigma_{HO}} \quad (3.2.6)$$

which gives the relative contribution of \tilde{f} to that of the complete HOC f . Fig. 13(b) shows that this ratio is somewhat greater than (3.2.1) but shows the same features for each of the cases considered ($n = n_{QCD}(p_T)$ and the fictitious values $n = 20$ and $n = 0.01$). Perhaps, it should be noted that the ratio \tilde{R}_T is a quantity more important than \tilde{R}_{HO} , since it is $\sigma_B + \sigma_{HO}$ that corresponds to the measurable cross section.

Now we consider other values of the rapidity η . In Figs. 12(b), (c) we indicate the integration region for $|\eta| \neq 0$ ($\simeq 0.7$) and for the same x_T as in Fig. 12(a) ($\eta = 0$). Notice that as $|\eta|$ increases, one of the asymptotes of the boundary moves toward the point $x_a = x_b = 1$, while the other moves away from it; the integration region shrinks on one side, and expands on the other. These two compensating effects lead to an overall suppression of $\tilde{f}(v, w)$ comparable to that discussed before ($\eta = 0$). Hence, as long as x_T is not too small, the terms of $f_s(v, w)$ dominate the HOC in a wide range of the rapidity η .

Now, we consider the subprocess $qg \rightarrow \gamma q$. As we have seen in Part I, this subprocess dominates the inclusive cross section for $pp \rightarrow \gamma$ (large p_T) + X. For this subprocess results very similar to those for $q\bar{q} \rightarrow \gamma g$ (Fig. 13(a), $\sqrt{s} = 63$ GeV, $\eta = 0$) have been obtained^{(11),(12)}. Again, the corresponding ratio \tilde{R}_T for

$n = n_{QCD}(p_T)$ is small and decreases with p_T . Similar results have been obtained for the corresponding ratio \tilde{R}_{HO} .

Again, writing the parton (here quark and gluon) momentum distributions in the form (3.2.5) and using the fictitious values $n = 20$ and $n = 0.01$ as in the previous case, the ratio \tilde{R}_T is for the first value significantly smaller, and for the second significantly larger than that for $n = n_{QCD}(p_T)$.^{(11),(12)}

For $qg \rightarrow \gamma q$, at fixed s and η and not too small x_T , the ratio \tilde{R}_T is expected to decrease with p_T somewhat faster than the corresponding ratio for $q\bar{q} \rightarrow \gamma q$. This, because n_g is larger than n_{q_v} and consequently the suppression of the terms \tilde{f} should be stronger for $qg \rightarrow \gamma q$ than for $q\bar{q} \rightarrow \gamma q$. This was indeed found to be the case in detailed calculations.^{(11),(12)}

Similar results we have obtained for the contribution of the subprocess $\gamma q \rightarrow \gamma q$, which dominates the cross section for the inclusive deep QED Compton process ($\gamma p \rightarrow \gamma$ (large p_T) + X); this we have also analyzed in detail using the results of Ref. 63. Figs. 14(a) and (b) present the ratios \tilde{R}_T and \tilde{R}_{HO} respectively, as functions of p_T at incoming photon lab energy $E_\gamma = 100 \text{ GeV}^{(64)}$; again for simplicity we work at rapidity $\eta = 0$.

Finally, essentially similar results have been obtained for the contribution of the subprocess $\gamma\gamma \rightarrow q\bar{q}$ to the inclusive cross section for $\gamma\gamma \rightarrow$ hadron (large p_T) + X ; this involves the fragmentation function for $q \rightarrow$ hadron.⁽¹²⁾

In the remaining part of this section we examine the contributions to $f_s(v, w)$ from a different point of view. We believe that this will further elucidate the importance of this part relative to the rest of the HOC. Moreover, it will help to establish later (Sect. 5.5.) a connection between this Part of the Thesis and the simple K-factor approach of Ch. 2, and thus, as we stated, to offer some insight into the reasons of the success of that approach.

To this end we introduce the k^{th} moment $M(k)$ (Mellin transform) of the function $\phi(w)$

$$M(k) = \int_0^1 w^{k-1} \phi(w) dw \quad (3.2.7)$$

The moments of some of the functions appearing in the complete HOC are given in Table III; $\psi(x)$ is the Euler function

$$\psi(x) = \frac{\Gamma'(x)}{\Gamma(x)} ; \psi(k) = -\gamma + \sum_{j=1}^{k-1} \frac{1}{j} \quad (3.2.8)$$

$\psi'(x)$ its derivative, and γ the Euler constant. In the last column of the Table we give the asymptotic behaviour of $M(k)$ as $k \rightarrow \infty$.

Now the point to remark is that, as $k \rightarrow \infty$, for the three distributions determining $f_s(v, w)$, $|M(k)|$ either equals a constant ($= 1$) or it increases with k . In contrast, for all the functions contributing to $\tilde{f}(v, w)$, $|M(k)|$ decreases with k . From Eq. (3.2.7) it is evident that the large moments control the behaviour of $\phi(w)$ near $w = 1$ and the small moments control the behaviour away from $w = 1$. Conversely, if in absolute value the moments of a function increase with k , the function is particularly prominent near $w = 1$, and if they decrease the function is not particularly important near $w = 1$. As a result, due to the presence of the structure functions $F_{a/A}(x)$ and $F_{b/B}(x)$, the part $\tilde{f}(v, w)$ is suppressed.

Concluding this section we may make the following general statement: For processes involving structure functions and/or fragmentation functions, as x_T increases, the relative contribution of the part $f_s(v, w)$ dominates more and more the HOC; and the dominance increases with the softness of the structure and/or fragmentation functions.

3.3 Remarks

We conclude this chapter with some remarks regarding the origin of the contributions to the dominant part $f_s(v, w)$, as well as certain of its features.

The terms in $f_s(v, w)$ originate as follows:

- (a) From loop graphs, i.e. $2 \rightarrow 2$ subprocesses involving virtual partons. Clearly, these contribute part of the coefficient $a_1(v)$ of $\delta(1 - w)$.
- (b) From kinematic configurations of $2 \rightarrow 3$ subprocesses corresponding to soft and collinear gluon emission. Also, in the case of $q\bar{q} \rightarrow \gamma g$ additional contributions

arise from similar configurations of the subprocess $q\bar{q} \rightarrow \gamma q\bar{q}$. Such contributions determine $b_1(v)$, $c(v)$ and the remaining part of $a_1(v)$. These points become more clear in Ch. 4 as well as in Ch. 5.

(c) From leftover contributions after the factorization of mass singularities and absorption in the parton distributions at scale M . Such contributions determine $a_2(v)$ and $b_2(v)$ (see Chs. 4 & 5).

Thus the nondominant part $\tilde{f}(v, w)$ receives contributions from kinematic configurations corresponding to hard and noncollinear gluon Brems and more generally such configurations of $2 \rightarrow 3$ subprocesses.

As a second remark, the fact that terms of the form (3.1.7) dominate the HOC has been noted in Ref. 55 (see its Eq. (3.17) and the related discussion). Later it was verified in Ref. 65, and was further stressed in Ref. 56. However, no explanation or justification was provided. To our knowledge, only recently such an explanation was advanced^{(11),(12)} and this has essentially formed the first part of Sect. 3.2.

As a third point, we wish to state that the dominant part is a gauge invariant part of the HOC. To show this we proceed as follows:

We denote by $M(v; k)$ the Mellin transform of the complete HOC $f(v, w)$. Clearly, to one loop order, $M(v; k)$ contains terms which for $k \rightarrow \infty$ diverge at most like $\sim \ln^2 k$. With $\psi(k)$ as in Eq. (3.2.8) the following limits are well defined:

$$\lim_{k \rightarrow \infty} \frac{M(v; k)}{\psi^2(k)} \equiv F_2(v) \quad (3.3.1a)$$

$$\lim_{k \rightarrow \infty} \frac{M(v; k) - F_2(v)\psi^2(k)}{\psi(k)} \equiv F_1(v) \quad (3.3.1b)$$

$$\lim_{k \rightarrow \infty} \{M(v; k) - F_2(v)\psi^2(k) - F_1(v)\psi(k)\} \equiv F_0(v), \quad (3.3.1c)$$

Thus we can write:

$$M(v; k) = F_0(v) + F_1(v)\psi(k) + F_2(v)\psi^2(k) + M'(v; k) \quad (3.3.2)$$

where $M'(v; k)$ satisfies

$$\lim_{k \rightarrow \infty} M'(v; k) = 0; \quad (3.3.3)$$

thus $M'(v; k)$ contains terms decreasing in absolute value with k .

We notice that each of the functions $F_0(v)$, $F_1(v)$ and $F_2(v)$ is gauge invariant, because it is determined in a gauge independent way, by Eqs. (3.3.1a), (3.3.1b) and (3.3.1c) respectively.

Now we consider the inverse Mellin transform of (3.3.2). Using Table III we obtain

$$f(v, w) = A(v)\delta(1-w) + B(v)\frac{1}{(1-w)_+} + C(v)\left(\frac{\ell n(1-w)}{1-w}\right)_+ + \tilde{f}(v, w) \quad (3.3.4)$$

where $A(v)$, $B(v)$, $C(v)$ and $\tilde{f}(v, w)$ are uniquely determined in terms of the functions in (3.3.2):

$$A(v) = F_0(v) - \gamma F_1(v) + \left(\gamma^2 - \frac{\pi^2}{6}\right) F_2(v) \quad (3.3.5a)$$

$$B(v) = -F_1(v) + 2\gamma F_2(v) \quad (3.3.5b)$$

$$C(v) = 2F_2(v) \quad (3.3.5c)$$

and

$$\tilde{f}(v, w) = -F_2(v)\frac{\ell n w}{1-w} + f'(v, w) \quad (3.3.6)$$

where $f'(v, w)$ is the inverse Mellin transform of $M'(v; k)$. Thus, each of $A(v)$, $B(v)$, $C(v)$ and the function $\tilde{f}(v, w)$ is gauge invariant.

A fourth point should be made in relation with possible changes of the renormalization and factorization scales μ and M . As we stated, the calculations of Sect. 3.2 were carried with the choice of the physical scales $\mu = M = p_T$. One may ask whether $f_s(v, w)$ still gives the dominant contribution for a different choice of μ and M .

The answer to this question is affirmative. The key point is the presence of certain terms^{(66),(67)} proportional to $\ell n(\hat{s}/M^2)$ and to $b\ell n(\hat{s}/\mu^2)$, where b is the coefficient of the Callan-Symanzik beta function

$$b = \frac{11}{6}N_c - \frac{1}{3}N_f \quad (3.3.7)$$

where N_f is the number of flavors and $N_c = 3$ in color $SU(3)$. The terms proportional to $\ell n(\hat{s}/M^2)$ comprise the functions $a_2(v)$ and $b_2(v)$ of $f_s(v, w)$, Eq. (3.1.7).

The term proportional to $b\ell n(\hat{s}/\mu^2)$ will also be included in the expression of $a_1(v)$ [see Eq. (4.5.7), end of Ch. 4]. Now we know that for $\mu = M = p_T$ the part $f_s(v, w)$ dominates the HOC. Then the work of Ref. 67 immediately implies that it will still dominate for wide variations of μ and M away from p_T .

The same also holds regarding optimization procedures, like the application of the Principle of Minimal Sensitivity (PMS)⁽⁶⁸⁾ or of Fastest Apparent Convergence.⁽⁶⁹⁾ Again Ref. 67 implies that, due to the presence of the above terms, the dominant part $f_s(v, w)$ will give results similar to those of the complete HOC. This means the same structure of the two-dimensional surface $\sigma = Ed\sigma/d^3p(\mu, M)$ considered as function of μ and M , including fine details like the presence of a saddle point related with the application of PMS.^{(66),(67)} It also implies the same degree of stability of $Ed\sigma/d^3p(\mu, M)$ against changes of μ and M . Finally, it is not difficult to see⁽⁶⁷⁾ that changes in the renormalization scheme (e.g. $\overline{MS} \rightarrow MS$) can be carried for $f_s(v, w)$ with very similar results as for the complete HOC.

A final remark is that all our conclusions apply also to supersymmetric QCD at ultrahigh energies and large transverse momenta (so that the partons can be treated as massless).⁽¹¹⁾ Very probably, they also apply to heavy quark production (in conventional or supersymmetric QCD) provided that we consider subprocesses initiated by massless partons. We have not studied, however, this case in any detail.

Now it is natural to ask the following question: Can one determine any significant part of $f_s(v, w)$ without recourse to the full calculation of the complete HOC? The purpose of the next chapter is to show that this is indeed possible, and to provide simple and general expressions determining the contributions of $2 \rightarrow 3$ subprocesses to the dominant part.

CHAPTER 4

DETERMINATION OF THE DOMINANT PART

In this chapter we explicitly determine the dominant part of HOC for the subprocess $q\bar{q} \rightarrow \gamma g$.

We show that the collinear and soft gluon Brems contribution to this part can be determined with relative ease. In addition, this contribution and more generally the contribution to the dominant part of HOC from $2 \rightarrow 3$ parton subprocesses, is shown to arise from expressions remarkably simple and general.^{(60),(61)}

As in Part I, we work in the Feynman gauge, and to regulate the singularities (infrared and collinear) we use dimensional regularization with $n = 4 - 2\epsilon$ dimensions ($\epsilon < 0$). Our results refer to the modified minimal subtraction (\overline{MS}) renormalization (and factorization) scheme, and to the universal definition of corrections.⁽⁵³⁾

Our procedure for treating gluon Brems (here $q\bar{q} \rightarrow \gamma gg$) is as follows: For unitarity graphs involving emission only from the initial partons (here q and \bar{q}) we use Sudakov variables. For unitarity graphs in which one or both amplitudes involve gluon emission from the final parton (here g) we use the center of momentum frame of the two final partons (here gg). This frame is also used for unitarity graphs involving the split of a final gluon into a $q\bar{q}$ pair.

4.1 Brems from Initial Partons

We consider gluon Brems from initial partons. We use Sudakov variables to parametrize the momentum k of the emitted gluon. In this way we make manifest the collinear as well as the soft gluon configurations.^{(11),(61)}

We write

$$k = \alpha p_1 + \beta p_2 + \ell \tag{4.1.1}$$

with

$$p_1 \cdot \ell = p_2 \cdot \ell = 0 \quad \ell = (0; \vec{\ell}) \tag{4.1.2}$$

where p_1 and p_2 denote the initial parton momenta (Fig. 15(a)), and $\vec{\ell}$ the components of k perpendicular to \vec{p}_1 and \vec{p}_2 . In view of (4.1.1) and (4.1.2), the on-shell condition $k^2 = 0$ implies

$$|\vec{\ell}|^2 = \alpha\beta\hat{s} \quad (4.1.3)$$

where $\hat{s} = (p_1 + p_2)^2$.

With the other subprocess invariants \hat{t} and \hat{u} defined by (2.1.8a), we introduce the dimensionless variables v and w as in Eq. (3.1.3). We are interested in the leading contribution of the Brems graphs to the differential cross section, as $w \rightarrow 1$. Then in App. D, we show the following statement:⁽⁶¹⁾

For $w \rightarrow 1$, the condition $r^2 = 0$ (on-shellness of the final parton) requires both $\alpha \rightarrow 0$ and $\beta \rightarrow 0$. In view of (4.1.1)–(4.1.3) this implies that the emitted gluon becomes soft ($k \rightarrow 0$).

As it becomes clear below, the only unitarity graphs providing contributions to the dominant part are those shown in Figs. 15(a) and 15(a').

Consider the unitarity graph of Fig. 15(a) arising from the interference of the Brems amplitudes M_1 and M_2 . With $\bar{\Sigma}$ denoting summation over final and average over initial spins and colors we find:

$$\bar{\Sigma} M_1 M_2^+ = -C_{12} \frac{S(p_1, p_2; k)}{(q - p_2)^2 (p_1 - k)^2 (p_2 - k)^2 (q - p_2 + k)^2} \quad (4.1.4)$$

where

$$C_{12} = \frac{1}{4} e^2 g^4 \mu^{4\epsilon} \frac{C_F}{N_c} \left(C_F - \frac{N_c}{2} \right) \quad (4.1.5)$$

and the numerator in (4.1.4) is the trace:

$$S(p_1, p_2; k) = \text{Tr}[\not{p}_2 \gamma_\lambda (\not{q} - \not{p}_2) \gamma_\mu (\not{p}_1 - \not{k}) \gamma_\nu \not{p}_1 \gamma^\mu (\not{q} - \not{p}_2 + \not{k}) \gamma^\lambda (\not{k} - \not{p}_2) \gamma^\nu]. \quad (4.1.6)$$

As it is well known, the parameter μ appearing in (4.1.5) is a mass scale introduced via

$$g_{d,m} = g \mu^{2\epsilon} \quad (4.1.7)$$

To calculate $S(p_1, p_2; k)$ we first take $\alpha \rightarrow 0$ (i.e. $k \simeq \beta p_2$) and obtain

$$S(p_1, p_2; k) \rightarrow -2\hat{s} S_B(p_1, (1 - \beta)p_2) \quad (4.1.8)$$

where $S_B(p_1, p_2)$ is the trace of the corresponding Born term, given by

$$S_B(p_1, p_2) = \text{Tr}[\not{p}_2 \gamma_\lambda (\not{q} - \not{p}_2) \gamma_\mu \not{p}_1 \gamma^\mu (\not{q} - \not{p}_2) \gamma^\lambda] \quad (4.1.9)$$

Also, in view of (4.1.1) and (4.1.2):

$$(p_1 - k)^2 = -\beta \hat{s}, \quad (p_2 - k)^2 = -\alpha \hat{s} \quad (4.1.10)$$

Then, using expression (D.12) of App. D for the phase space integral, we find for the contribution of $\bar{\Sigma}(M_1 M_2^+ + M_2 M_1^+)$ to the cross section $d\sigma/dv dw$:

$$\begin{aligned} \frac{d\sigma_{12}^{(a)}}{dv dw} = g^2 (C_F - \frac{N_c}{2}) N \frac{\Gamma(1-2\epsilon)}{\pi^{1-\epsilon} \Gamma(1-\epsilon)} w^{-\epsilon} \int_0^1 d\beta \beta^{-1-\epsilon} (1-\beta) T_B(p_1, (1-\beta)p_2) \\ \int_0^{1-\beta} d\alpha \alpha^{-1-\epsilon} \int d\Omega_T \delta_+(r^2) \end{aligned} \quad (4.1.11)$$

where

$$N \equiv \frac{v}{(4\pi)^3 \Gamma(1-2\epsilon)} \left(\frac{4\pi\mu^2}{\hat{s}} \right)^{2\epsilon} [v(1-v)]^{-\epsilon} \quad (4.1.12)$$

and

$$\begin{aligned} T_B(p_1, p_2) &= \frac{1}{4} e^2 g^2 \frac{C_F}{N_c} \frac{S_B(p_1, p_2)}{[(q-p_2)^2]^2} \\ &= 2e^2 g^2 \frac{C_F}{N_c} (1-\epsilon)^2 \frac{\hat{t}}{\hat{u}} \end{aligned} \quad (4.1.13)$$

corresponds to the squared Born amplitude summed over final and averaged over initial spins and colors. Notice that in (4.1.11) T_B appears with argument $[p_1, (1-\beta)p_2]$ as it is pertinent to the emission of a gluon with $k \simeq \beta p_2$.

Now, App. D shows that for $w \rightarrow 1$ the limiting behaviour of the integrals in (4.1.11) leads to the following result:

$$\frac{d\sigma_{12}^{(a)}}{dv dw} = g^2 (C_F - \frac{N_c}{2}) N \frac{2}{\hat{s}} \left(\frac{v}{1-v} \right)^{-\epsilon} (1-w)^{-1-2\epsilon} \left(-\frac{1}{\epsilon} \right) \left(1 + \epsilon^2 \frac{\pi^2}{6} \right) T_B(p_1, p_2) \quad (4.1.14)$$

Of course, an identical contribution is obtained by taking first $\beta = 0$ (i.e. $k \simeq \alpha p_1$) and then repeating the above procedure.

Adding the contribution of the graph Fig. 15 (a') and of the $\hat{t} \leftrightarrow \hat{u}$ crossed graphs, the overall contribution of Figs. 15(a) and 15(a') to the differential cross section $d\sigma/dv dw$ is:

$$\frac{d\sigma^{in}}{dv dw} = FT_0(v, \epsilon) \left(C_F - \frac{N_c}{2} \right) \left(-\frac{4}{\epsilon} \right) \left(\frac{v}{1-v} \right)^{-\epsilon} (1-w)^{-1-2\epsilon} \left(1 + \epsilon^2 \frac{\pi^2}{6} \right) \quad (4.1.15)$$

where

$$F \equiv \frac{2\pi\alpha C_F \alpha_s^2(\mu)}{\hat{s} N_c 2\pi} \left(\frac{4\pi\mu^2}{\hat{s}} \right)^{2\epsilon} \frac{[v(1-v)]^{-\epsilon}}{\Gamma(1-2\epsilon)} \quad (4.1.16)$$

and

$$T_0(v, \epsilon) \equiv (1-\epsilon) \left[(1-\epsilon) \frac{v^2 + (1-v)^2}{v(1-v)} - 2\epsilon \right] \quad (4.1.17)$$

corresponds to the total squared Born amplitude. The superscript in $d\sigma^{in}$ denotes Brems from initial partons.

Eq. (4.1.15) is the key formula of this section.^{(60),(61)} It is remarkable that it depends on the particular subprocess only through the Born term and color factors.

Now we expand in powers of ϵ to make transparent the various terms contributing to the coefficient functions of the dominant part $f_s(v, w)$. We use

$$\left(\frac{v}{1-v} \right)^{-\epsilon} = 1 - \epsilon \ell n \left(\frac{v}{1-v} \right) + \frac{\epsilon^2}{2} \ell n^2 \left(\frac{v}{1-v} \right) + 0(\epsilon^3) \quad (4.1.18)$$

and

$$(1-w)^{-1-2\epsilon} = -\frac{1}{2\epsilon} \delta(1-w) + \frac{1}{(1-w)_+} - 2\epsilon \left(\frac{\ell n(1-w)}{1-w} \right)_+ + 0(\epsilon^2), \quad (4.1.19)$$

and obtain:

$$\begin{aligned} \frac{d\sigma^{in}}{dv dw} = F \left(C_F - \frac{N_c}{2} \right) & \left\{ T_0(v, \epsilon) \left[\frac{2}{\epsilon^2} \delta(1-w) - \frac{1}{\epsilon} \left(\frac{4}{(1-w)_+} + 2\ell n \frac{v}{1-v} \delta(1-w) \right) \right] \right. \\ & \left. + \tilde{T}_0(v) \left[\left(\frac{\pi^2}{3} + \ell n^2 \frac{v}{1-v} \right) \delta(1-w) + \ell n \frac{v}{1-v} \frac{4}{(1-w)_+} + 8 \left(\frac{\ell n(1-w)}{1-w} \right)_+ \right] \right\}; \end{aligned} \quad (4.1.20)$$

we have introduced

$$\tilde{T}_0(v) \equiv T_0(v, 0) = \frac{v^2 + (1-v)^2}{v(1-v)}. \quad (4.1.21)$$

The term $\frac{2}{\epsilon}\delta(1-w)$ is an infrared singularity and is cancelled by a similar term in the virtual gluon (loop) contribution (Sect. 4.3). Regarding the term $\sim 1/\epsilon$, the part proportional to C_F is absorbed in the bare parton distributions (factorization procedure, Sect. 4.4) and the part proportional to N_c is cancelled by Brems contributions from a final parton (Sect. 4.2) and loop contributions (Sect. 4.3).

The rest of (4.1.20), the finite piece at $\epsilon = 0$, is clearly a contribution to the dominant part $f_s(v, w)$; as it can be seen (Eq. (4.5.7)), the last two terms exactly determine parts of $b_1(v)$ and $c(v)$. Of course, the term $\sim \delta(1-w)$ contributes to $a_1(v)$.

It is important to note that in $n = 4$ dimensions the contribution (4.1.15) amounts to a pole at $w = 1$. This pole arises because $\Sigma M_1 M_2^+ \sim 1/\beta$ (see (4.1.10)) and, in view of (D.15), $\beta \sim 1-w$. The residue of this pole is calculated in the soft gluon limit ($\alpha \rightarrow 0$, $k \sim \beta p_2 \sim (1-w)p_2$), e.g. the trace $S(p_1, p_2, k)$ is taken at $k = 0$. Thus the above procedure leads to the following statement: The initial Brems contributions to the coefficients $a_1(v)$, $b_1(v)$ etc. of the dominant part correspond to collinear gluon emissions and are determined by the residue of the pole at $w = 1$; this residue is calculated in the soft gluon limit.

Within the Sudakov procedure it can be seen that between QED-like graphs (involving no 3-gluon couplings), Figs. 15(a) and 15(a') are the only Brems unitarity graphs contributing to the dominant terms. E.g. with $k \simeq \beta p_2 (\alpha \rightarrow 0)$ the contribution of Fig. 15(b) is not proportional to $1/\beta$ and introduces no pole at $w = 1$. On the other hand, Fig. 15(c) gives a contribution $\sim 1/\beta$, but the gluon is not emitted by the parton p_2 in either of the amplitudes, so that $k \simeq \beta p_2$ implies no collinear gluon emission.

Aside from this argument, we have found by detailed calculation and working in the C.M. frame of the two final partons (App. C) that the graphs Figs. 15(b), (c) introduce no terms $\sim (1-w)^{-1-2\epsilon}$ or $\sim (1-w)^{-1-\epsilon}$.

4.2 Brems from Final Partons

Now, we consider unitarity graphs in which one or both the amplitudes repre-

sent gluon Brems from a final parton (Figs. 16(a)–(g)). We also consider contributions from the subprocess $q\bar{q} \rightarrow \gamma q\bar{q}$ (Figs. 16(a'),(b')). Since in these cases an intermediate transition of the form $g \rightarrow gg$ or $g \rightarrow q\bar{q}$ occurs, it is convenient to work in the C.M. frame of the two final partons.^{(58),(61)} Some of the kinematics are given in App. C and summarized in a compact form in Table IV.

Again to isolate and evaluate the contributions to the dominant part we determine the residue of the pole in the squared matrix elements at $w = 1$. Denoting by k and r the momenta of the two outgoing partons (Fig. 16(a)) we introduce

$$s_2 \equiv (k + r)^2 = \hat{s}v(1 - w). \quad (4.2.1)$$

4.2.1 Evaluation of Matrix Elements.

Below we give in some detail our calculational procedures with the hope that they can be extended to more complicated cases, as e.g. to determine the dominant corrections for processes initiated by $2 \rightarrow 3$ parton subprocesses, for which HOC are hitherto completely unknown.

The squared matrix element of the subprocess

$$a(p_1) + b(p_2) \rightarrow \gamma(q) + c(r) + d(k)$$

is, in general, a function of five independent variables.

In the rest frame of the two outgoing partons it is convenient to choose the invariants $\hat{s}, \hat{t}, \hat{u}$ (or \hat{s}, v, w) and the two angular variables θ_1 (or y) and θ_2 used to parametrize the vectors k and r (App. C, and Fig. 17). The scalar products of p_1, p_2, q with each of k and r are presented in Table V (upper part).

We distinguish unitarity graphs according to whether their contribution to $|M|^2$ involves terms:⁽⁶¹⁾

- (i) proportional to $1/s_2$ (simple pole at $w = 1$)
- (ii) proportional to $1/s_2^2$ (double pole at $w = 1$).

Case (i) [respectively (ii)] occurs in graphs where only one [resp. both] of the amplitudes represents [resp. represent] the splitting of an off-shell parton into two

final on-shell partons Figs. 16(a)–(c) [resp. Figs. 16(d)–(g) and 16(a'), (b')]; such graphs provide a $1/s_2$ [resp. $1/s_2^2$] factor due to the propagator of the parton which splits. We proceed as follows:

case (i)

In this case we have to evaluate the residue of the pole as $w \rightarrow 1$, and we consider the scalar products in Table V. For $w \rightarrow 1$ their expressions become much simpler and θ_2 independent. Thus, e.g. in system S_1 :

$$2p_1 \cdot r = -\hat{u}y, \quad 2p_2 \cdot r = -\hat{t}y, \quad 2q \cdot r = \hat{s}y$$

$$2p_1 \cdot k = -\hat{u}(1-y), \quad 2p_2 \cdot k = -\hat{t}(1-y), \quad 2q \cdot k = \hat{s}(1-y) \quad (4.2.2)$$

It is remarkable that

$$\frac{p_1 \cdot k}{p_1 \cdot r} = \frac{p_2 \cdot k}{p_2 \cdot r} = \frac{q \cdot k}{q \cdot r} = \frac{1-y}{y} \quad (4.2.3)$$

This relation suggests that the traces of the relevant unitarity graphs can be calculated with the replacement:

$$k \rightarrow \frac{1-y}{y} r; \quad (4.2.4)$$

this much reduces the number of terms.

In view of (4.2.1) and (C.3), $w \rightarrow 1$ implies $k \rightarrow 0$ (and $r \rightarrow 0$), i.e. that the emitted gluon becomes soft. The replacement $k \rightarrow \frac{1-y}{y} r$ is to be understood as a soft gluon relation. We have checked in detail that for $w \rightarrow 1$ this replacement gives the correct result.^(f1)

To demonstrate the efficiency of the simplified kinematics, Eq. (4.2.4), we evaluate as example the contribution of the graph shown in Fig. 16(a) arising from the amplitudes M_1 , and M_3 . It gives

$$t_a \equiv \bar{\Sigma}(M_1 M_3^+ + M_3 M_1^+) = C_g \frac{T^{\lambda\sigma\rho}(k, r) V_{\lambda\sigma\rho}(k+r, -r, -k)}{s_2 \hat{u}^2 (p_1 - k)^2} \quad (4.2.5)$$

where

$$C_g \equiv \frac{1}{2} e^2 g^4 \mu^{4\epsilon} N_c \frac{C_F}{N_c} \quad (4.2.6)$$

The tensor $T^{\lambda\rho\sigma}$ is the trace associated with the incoming fermions and $V_{\lambda\sigma\rho}$ the tensor assigned to the three gluon vertex. They are given by

$$T^{\lambda\rho\sigma} = \text{Tr}[\not{p}_2 \gamma^\mu (\not{q} - \not{p}_2) \gamma^\lambda \not{p}_1 \gamma^\rho (\not{p}_1 - \not{k}) \gamma^\sigma (\not{q} - \not{p}_2) \gamma_\mu] \quad (4.2.7)$$

and

$$V_{\lambda\sigma\rho} = (2r + k)_\rho g_{\lambda\sigma} - (2k + r)_\sigma g_{\lambda\rho} + (k - r)_\lambda g_{\sigma\rho}. \quad (4.2.8)$$

Using the replacement (4.2.4) these tensors are rewritten as follows:

$$T^{\lambda\rho\sigma} \rightarrow -2(1 - \epsilon) \hat{u} \text{Tr}[\gamma^\lambda \not{p}_1 \gamma^\rho (\not{p}_1 - \frac{1-y}{y} \not{f}) \gamma^\sigma \not{q}] \quad (4.2.9)$$

and

$$V_{\lambda\sigma\rho} \rightarrow \frac{1}{y} [(1 + y) r_\rho g_{\lambda\sigma} - (2 - y) r_\sigma g_{\lambda\rho} + (1 - 2y) r_\lambda g_{\sigma\rho}] \quad (4.2.10)$$

Consider the first term in (4.2.10). Its contribution to (4.2.5) is easily evaluated to be

$$t_a(y) = 2A_g(1 - \epsilon) \frac{1 + y}{1 - y} \frac{\hat{t}}{\hat{u}} \quad (4.2.11)$$

where we have introduced

$$A_g \equiv 2e^2 g^4 \mu^{4\epsilon} N_c \frac{C_F(1 - \epsilon)}{N_c s_2} \quad (4.2.12)$$

Now, in view of Eq. (C.18) of App. C, we can symmetrize this result with respect to y and $1 - y$. Hence setting

$$\bar{t}_a \equiv \frac{1}{2} [t_a(y) + t_a(1 - y)] \quad (4.2.13)$$

we find

$$\bar{t}_a = 2A_g(1 - \epsilon) \left(\frac{1}{Y} - 1 \right) \frac{\hat{t}}{\hat{u}} \quad (4.2.14)$$

where

$$Y \equiv y(1 - y) \quad (4.2.15)$$

Eq. (4.2.14) gives the total contribution of Fig. 16(a) to the matrix element. Indeed, the second term in (4.2.10), when contracted with $T^{\lambda\rho\sigma}$, is readily seen to give a vanishing contribution. We also find that the last term of (4.2.10) gives

a vanishing contribution to the symmetrized result (4.2.13). Hence only the first term of the vertex tensor contributes, and its contribution is given by (4.2.14).

Finally adding to (4.2.14) the contribution arising from the same graph with $p_1 \leftrightarrow p_2$ (or equivalently $\hat{t} \leftrightarrow \hat{u}$) we obtain the overall contribution of Fig. 16(a).

$$T_a \equiv \bar{t}_a + (\hat{t} \leftrightarrow \hat{u}) = 2A_g(1 - \epsilon)\left(\frac{1}{Y} - 1\right)\frac{\hat{t}^2 + \hat{u}^2}{\hat{t}\hat{u}} \quad (4.2.16)$$

case (ii)

In this case, in view of the presence of the overall $1/s_2^2$ factor, the traces of the contributing unitarity graphs must be calculated up to terms proportional to s_2 . It turns out, as we shall see, that these are precisely the terms of interest.

Since in this case the limit $w \rightarrow 1$ cannot be directly taken in the traces, to determine the $0(1)$ and $0(s_2)$ terms we proceed as follows. We first notice that graphs belonging to this class are necessarily symmetric with respect to k and r (Figs. 16(d)-(g) and 16(a'), (b')). In addition we notice that, apart from $1/s_2$, no other propagator depends on k and/or r . We conclude that the traces must be symmetric under $k \leftrightarrow r$ and that they must carry all the possible dependence on the angular variables (θ_1 and θ_2). Consequently the traces of the unitarity graphs can be expressed in terms of symmetric (under $k \leftrightarrow r$) combinations of scalar products. Such combinations, evaluated in the proper system of axes, become θ_2 independent and have a particularly simple form. This much simplifies the calculations.

We present symmetric combinations of scalar products in a summary form in Table V (lower part). They are expressed in terms of the subprocess invariants and the symmetric (in $y \leftrightarrow (1 - y)$) forms Y (Eq. (4.2.15)) and

$$Y_s \equiv y^2 + (1 - y)^2 \quad (4.2.17)$$

We employ these combinations in the calculations referred to the graphs of this class.

To be more specific we consider as example the contribution to the squared matrix element of the unitarity graph shown in Fig. 16(a'). We write

$$\bar{t}_{a'} = \frac{-C_g}{\hat{u}^2 s_2^2} T^{\rho\lambda}(k, r) T'_{\rho\lambda}(k, r) \quad (4.2.18)$$

where

$$C_q \equiv \frac{1}{8} e^2 g^4 \mu^{4\epsilon} \frac{C_F}{N_c} N_f \quad (4.2.19)$$

In (4.2.18), the first tensor is the trace associated with the incoming fermions

$$T^{\rho\lambda} = \text{Tr}[\not{p}_2 \gamma^\mu (\not{p}_2 - \not{q}) \gamma^\rho \gamma^\lambda (\not{p}_2 - \not{q}) \gamma_\mu] \quad (4.2.20)$$

and the second tensor is the trace associated with the outgoing fermions

$$T'_{\rho\lambda} = \text{Tr}[\not{k} \gamma_\rho \not{k} \gamma_\lambda] = 4[r_\rho k_\lambda + r_\lambda k_\rho - \frac{s_2}{2} g_{\rho\lambda}]. \quad (4.2.21)$$

Then (4.2.18) gives

$$\bar{t}_{a'} = \frac{-16(1-\epsilon)C_q}{s_2^2 \hat{u}} [2p_1 \cdot r \ 2q \cdot k + 2p_1 \cdot k \ 2q \cdot r + \epsilon \hat{t} s_2] \quad (4.2.22)$$

Notice the symmetry in $k \leftrightarrow r$. In view of Table V,

$$2p_1 \cdot r \ 2q \cdot k + 2p_1 \cdot k \ 2q \cdot r = -\hat{t} s_2 Y_s - 2\hat{s} \hat{u} Y \quad (4.2.23)$$

where Y and Y_s are given by (4.2.15) and (4.2.17). Clearly expression (4.2.23) is independent of θ_2 . Now, Eq. (4.2.22) immediately implies:

$$\bar{t}_{a'} = A_q (1-\epsilon) [(Y_s - \epsilon) \frac{\hat{t}}{\hat{u}} + \frac{2\hat{s}}{s_2} Y] \quad (4.2.24)$$

where

$$A_q \equiv 16 C_q \frac{1}{s_2} \quad (4.2.25)$$

Adding the contribution of the graph with $\hat{t} \leftrightarrow \hat{u}$, we obtain for the overall contribution of Fig. 16(a')

$$T_{a'} = A_q (1-\epsilon) [(Y_s - \epsilon) \frac{\hat{t}^2 + \hat{u}^2}{\hat{t}\hat{u}} + \frac{4\hat{s}}{s_2} Y] \quad (4.2.26)$$

The first term in (4.2.26) comes from the terms $\sim s_2$ in the numerator of (4.2.18) arising from the evaluation of the traces. In view of the $1/s_2$ factor included in A_q , this term is the residue of the pole at $w = 1$. The second term in (4.2.26) gives a

contribution $\sim 1/s_2^2$ (a double pole at $w = 1$). This contribution is cancelled by a similar contribution of the graph Fig. 16(b'). Indeed, this graph gives

$$T_{b'} = A_q[-2\epsilon Y_s - (1 - \epsilon)\frac{4\hat{s}}{s_2}Y] + \{(A_q s_2)\frac{2\hat{s}}{\hat{t}\hat{u}}Y_s\}; \quad (4.2.27)$$

the terms $\sim A_q/s_2 \sim 1/s_2^2$ cancel in the sum $T_{a'} + T_{b'}$.

A point to remark here is that cancellation of such terms ($\sim 1/s_2^2$) is a general feature of the graphs of this class. In fact, as it can be seen from Table VI, contributions of this type cancel likewise in pairs of graphs; i.e. between Figs. 16(d) and (e) or between 16(f) and (g).

Finally, we notice that the term in the curly bracket of (4.2.27) is a contribution to the nondominant part \tilde{f} (a term regular for $w \rightarrow 1$); we will consider again this term in Ch. 7, and for this reason we have chosen to keep it.

Now we present the contributions of the graphs of Fig. 16. Only terms contributing to the dominant part have been kept.

The graph Fig. 16(a) gives (see Eq. (4.2.16)):

$$T_a = 2A_g(1 - \epsilon)(\frac{1}{Y} - 1)\tilde{T}_0(v) \quad (4.2.28)$$

where A_g , Y and $\tilde{T}_0(v)$ are given by (4.2.12), (4.2.15) and (4.1.21) respectively. Likewise, the graphs 16(b) and (c) belong to case (i) and give:

$$T_b = A_g\left\{\left[\frac{3}{Y} - 2\epsilon\left(\frac{1}{Y} - 1\right)\right]\tilde{T}_0(v) + 2\left[\frac{1}{Y} + 2 - 2\epsilon\left(\frac{1}{Y} - 1\right)\right]\right\} \quad (4.2.29)$$

and

$$T_c = A_g\left\{-\left(\frac{1}{Y} + 2\right)\tilde{T}_0(v) - 2\left[\frac{1}{Y} + 2 + 2\epsilon\left(\frac{1}{Y} - 1\right)\right]\right\} \quad (4.2.30)$$

The rest of the graphs of Fig. 16 belong to case (ii). Thus, we find that the graphs 16(d) and (e) give:

$$T_d = A_g\left\{(5Y - 4 + 4\epsilon(1 - Y))\tilde{T}_0(v) - 2[5Y + 1 - \epsilon(4Y - 1)]\frac{\hat{s}}{s_2}\right\} \quad (4.2.31)$$

$$T_e = A_g\left\{2\epsilon(4 - 5Y) + 2[5Y + 1 - \epsilon(4Y - 1)]\frac{\hat{s}}{s_2}\right\} \quad (4.2.32)$$

Notice the cancellation between the last terms (contributions $\sim A_g/s_2 \sim 1/s_2^2$) of these equations. Likewise the graphs 16(f) and (g), involving ghost contributions, give:

$$T_f = A_g \left\{ -Y \tilde{T}_0(v) + 2 \left(Y - \frac{1}{4} \right) \frac{\hat{s}}{s_2} \right\} \quad (4.2.33)$$

$$T_g = A_g \left\{ 2\epsilon Y - 2 \left(Y - \frac{1}{4} \right) \frac{\hat{s}}{s_2} \right\}. \quad (4.2.34)$$

Again, contributions with double pole at $w = 1$ ($s_2 = 0$, last terms) cancel. Finally regarding graphs 16(a') and (b'), their contributions are obtained from (4.2.26) and (4.2.27) respectively.

4.2.2 Total Contributions and General Expressions

Now we evaluate the total contribution to the squared amplitude and to the differential cross section $d\sigma/dv dw$.

Regarding gluon Brems contributions we sum the results given in Eqs. (4.2.28)–(4.2.34) (see also Table VI). Denoting the sum $T_a + T_b + \dots + T_g$ by T_{a-g} we obtain:

$$T_{a-g} = C N_c \frac{1}{s_2} P_{gg}(y) T_0(v, \epsilon) \quad (4.2.35)$$

where

$$P_{gg}(y) = \frac{1}{y} + \frac{1}{1-y} - 2 + y(1-y) \quad (4.2.36)$$

and

$$C = 8e^2 g^4 \mu^{4\epsilon} \frac{C_F}{N_c}. \quad (4.2.37)$$

The expression (4.2.35) is remarkably simple. $P_{gg}(y)$ is essentially the Altarelli-Parisi split function for $g \rightarrow gg$ at $y < 1$. Thus the residue of the pole at $s_2 = 0$ (or $w = 1$) is proportional to $P_{gg}(y)$ times the Born term. This result may be anticipated.

We now introduce

$$\tilde{P}_{gg}(\epsilon) \equiv \frac{\Gamma(1-2\epsilon)}{\Gamma^2(1-\epsilon)} \int_0^1 y^{-\epsilon} (1-y)^{-\epsilon} P_{gg}(y) dy \quad (4.2.38)$$

Then, in view of Eq. (C.18), the contribution of (4.2.35) to the differential cross-section becomes:

$$\frac{d\sigma^{f^{in}}}{dvdw} = FT_0(v, \epsilon) N_c v^{-\epsilon} (1-w)^{-1-\epsilon} \tilde{P}_{gg}(\epsilon) \quad (4.2.39)$$

where F is given by (4.1.16) and the superscript in $d\sigma^{f^{in}}$ is to denote Brems from final partons. Calculating (4.2.38), and expanding the result in powers of ϵ we obtain:

$$\tilde{P}_{gg}(\epsilon) = -\frac{2}{\epsilon} - \frac{11}{6} - \frac{67}{18}\epsilon. \quad (4.2.40)$$

Using (4.2.40) and expanding $v^{-\epsilon}$ and $(1-w)^{-1-\epsilon}$ in powers of ϵ we rewrite Eq. (4.2.39) in the form:

$$\begin{aligned} \frac{d\sigma^{f^{in}}}{dvdw} = FN_c \{ & T_0(v, \epsilon) \left[\frac{2}{\epsilon^2} \delta(1-w) + \frac{1}{\epsilon} \left(\left(\frac{11}{6} - 2\ell n v \right) \delta(1-w) - \frac{2}{(1-w)_+} \right) \right] \\ & + \tilde{T}_0(v) \left[\left(\frac{67}{18} - \frac{11}{6} \ell n v + \ell n^2 v \right) \delta(1-w) + \left(2\ell n v - \frac{11}{6} \right) \frac{1}{(1-w)_+} + 2 \left(\frac{\ell n(1-w)}{1-w} \right)_+ \right] \} \end{aligned} \quad (4.2.41)$$

Here, the infrared singularity $\sim 1/\epsilon^2$ is cancelled by a virtual gluon contribution (Eq. (4.3.1)). The term $\sim (1/\epsilon)(2/(1-w)_+)$ is cancelled by a similar term in (4.1.15). The remaining part $\sim 1/\epsilon$ is cancelled by contributions of (4.1.15) and (4.3.1). As expected, no collinear singularities associated with (final state and) unobserved partons remain.

The rest of (4.2.41), which is finite for $\epsilon = 0$, contributes to the dominant part $f_s(v, w)$; as it can be seen, the last two terms $\sim 1/(1-w)_+$ and $(\ell n(1-w)/(1-w))_+$ exactly determine parts of $b_1(v)$ and $c(v)$ respectively (Eq. (4.5.7)).

Now we consider the subprocess $q\bar{q} \rightarrow \gamma q\bar{q}$. We sum the (dominant) contributions in (4.2.26) and (4.2.27) and obtain:

$$T_{a'} + T_{b'} = C \frac{N_f}{2} \frac{1}{s_2} P_{qg}(y, \epsilon) T_0(v, \epsilon) \quad (4.2.42)$$

where

$$P_{qg}(y, \epsilon) \equiv \frac{y^2 + (1-y)^2 - \epsilon}{2(1-\epsilon)} \quad (4.2.43)$$

and C is given by (4.2.37).

We remark that $P_{gg}(y, \epsilon = 0)$ is the split function $P_{gg}(y)$; the expression (4.2.43) is its generalization in $n = 4 - 2\epsilon$ dimensions. Note that the form of $P_{gg}(y)$ remains unaltered in n dimensions. Both these results are in accord with Ref. 70; and since that work refers to a completely different process ($e^+e^- \rightarrow 3$ jets) the results establish the universality of the functions $P_{gg}(y, \epsilon)$ and $P_{gg}(y)$.

In view of this we note the similarity of Eqs. (4.2.35) and (4.2.42).

As in (4.2.38) we introduce

$$\tilde{P}_{gg}(\epsilon) \equiv \frac{\Gamma(1-2\epsilon)}{\Gamma^2(1-\epsilon)} \int_0^1 y^{-\epsilon}(1-y)^{-\epsilon} P_{gg}(y, \epsilon) dy. \quad (4.2.44)$$

Then, in view of Eq. (C.18), the contribution of (4.2.42) to the differential cross-section becomes:

$$\frac{d\sigma^{fin'}}{dvdw} = FT_0(v, \epsilon) N_f v^{-\epsilon} (1-w)^{-1-\epsilon} \tilde{P}_{gg}(\epsilon). \quad (4.2.45)$$

Calculating (4.2.44) and expanding the result in powers of ϵ we obtain

$$\tilde{P}_{gg}(\epsilon) = \frac{1}{2} \left(\frac{2}{3} + \frac{10}{9} \epsilon \right) \quad (4.2.46)$$

so that:

$$\begin{aligned} \frac{d\sigma^{fin'}}{dvdw} = F \frac{N_f}{2} \{ T_0(v, \epsilon) \left(-\frac{1}{\epsilon} \right) \frac{2}{3} \delta(1-w) + \\ + \tilde{T}_0(v) \left[\left(-\frac{10}{9} + \frac{2}{3} \ell n v \right) \delta(1-w) + \frac{2}{3} \frac{1}{(1-w)_+} \right] \} \end{aligned} \quad (4.2.47)$$

Here, the term $\sim 1/\epsilon$ is cancelled by a similar term of the loop contributions (Eq. (4.3.1)).

The rest of (4.2.47) exactly determines parts of $a_1(v)$ and $b_1(v)$; namely the parts of these coefficients which are $\sim N_f$. (Eq. (4.5.7)).

Finally, notice the similarity of Eqs. (4.2.39) and (4.2.45). These two equations are the key formulas of this section.^{(60),(61)}

4.3 The Virtual Contribution

In this section we present the contribution of virtual partons (loop graphs) to the HOC of $q\bar{q} \rightarrow \gamma g$. The differential cross section $d\sigma^{vir}/d\hat{t}$ is determined in Ch.

6; it is presented in Eq. (6.1.13) as a function of the subprocess invariants \hat{s} , \hat{t} and \hat{u} . Using $\hat{t} = -\hat{s}(1-v)$ and $\hat{u} = -\hat{s}v$ we easily transform Eq. (6.1.13) into the following form:⁽⁶¹⁾

$$\begin{aligned}
\frac{d\sigma^{vir}}{dv} = & F\{T_0(v, \epsilon)\left[-\frac{2C_F + N_c}{\epsilon^2} - \frac{1}{\epsilon}(3C_F + b - N_c \ln(v(1-v)))\right] + b\tilde{T}_0(v)\ln\frac{\mu^2}{\hat{s}} \\
& + \frac{1}{v(1-v)}\left\{C_F\left[\left(\frac{2}{3}\pi^2 - 7\right)B(v) + (v^2 - 4v + 3)\ln v + (v^2 + 2v)\ln(1-v)\right.\right. \\
& \quad \left.\left.+ (1+v^2)\ln^2 v + (v^2 - 2v + 2)\ln^2(1-v)\right]\right. \\
& \quad \left.- N_c\left[\frac{\pi^2}{6}B(v) + v(1-v)\ln v + v(1-v)\ln(1-v) + \ln v \ln(1-v)B(v)\right.\right. \\
& \quad \left.\left.+ \frac{1}{2}(1+v^2)\ln^2 v + \frac{1}{2}(v^2 - 2v + 2)\ln^2(1-v)\right]\right\}. \quad (4.3.1)
\end{aligned}$$

Here F , $T_0(v, \epsilon)$ and $\tilde{T}_0(v)$ are given by (4.1.16), (4.1.17) and (4.1.21) respectively. b is the coefficient of the Callan-Symanzik beta function, Eq. (1.2.4), and

$$B(v) \equiv v(1-v)\tilde{T}_0(v) = v^2 + (1-v)^2 \quad (4.3.2)$$

is related to the squared Born amplitude.

4.4 Factorization of Mass Singularities

The perturbative differential cross section

$$\frac{d\sigma}{dvdw} = \frac{d\sigma^{vir}}{dv}\delta(1-w) + \frac{d\sigma^{real}}{dvdw}, \quad (4.4.1)$$

where $d\sigma^{real}/dvdw$ is the sum of (4.1.20), (4.2.41) and (4.2.47), and $d\sigma^{vir}/dv$ is given by (4.3.1), contains uncanceled terms $\sim 1/\epsilon$. As we stated in the introduction, these terms are associated in a process independent way with the external (here incoming) partons. Together with accompanying logarithms of a large scale M , they are factored out of the parton cross section and absorbed in the bare parton distributions. This (factorization) procedure redefines the parton densities and introduces their M dependence. At the same time leftover terms depending on M remain in the finite part $d\sigma'$ (Sect. 1.3) of the cross section.

We denote by $-d\sigma^{fact}/dvdw$ the part extracted from $d\sigma/dv dw$. This is given by:

$$\begin{aligned} \frac{1}{\hat{s}v} \frac{d\sigma^{fact}}{dvdw} = & -\frac{\alpha_s}{2\pi} \left[\int dx_1 H_{qq}(x_1, M^2) \frac{d\sigma_B}{dv}(x_1 \hat{s}, v) \delta(x_1(\hat{s} + \hat{t}) + \hat{u}) \right. \\ & \left. + \int dx_2 H_{qq}(x_2, M^2) \frac{d\sigma_B}{dv}(x_2 \hat{s}, v) \delta(x_2(\hat{s} + \hat{u}) + \hat{t}) \right]. \end{aligned} \quad (4.4.2)$$

Then, the remaining part of the cross section is denoted by $d\sigma'/dvdw$ and is related to $d\sigma/dv dw$ by

$$\frac{d\sigma'}{dvdw} = \frac{d\sigma^{fact}}{dvdw} + \frac{d\sigma}{dvdw}. \quad (4.4.3)$$

In (4.4.2) $H_{qq}(x, M^2)$ is:

$$H_{qq}(x, M^2) = -\frac{1}{\epsilon} C_F P_{qq}(x) \frac{\Gamma(1-\epsilon)}{\Gamma(1-2\epsilon)} \left(\frac{4\pi\mu^2}{M^2} \right)^\epsilon + u_{qq}(x) \quad (4.4.4)$$

Here $P_{qq}(x)$ is the Altarelli-Parisi split function⁽³²⁾ (the color factor C_F has been factored out)

$$P_{qq}(x) = \frac{1+x^2}{(1-x)_+} + \frac{3}{2} \delta(1-x), \quad (4.4.5)$$

and the finite term $u_{qq}(x)$ specifies the definition of corrections. In Eq. (4.4.2) $d\sigma_B/dv(\hat{s}, v)$ denotes the Born differential cross section which, for $q\bar{q} \rightarrow \gamma g$, is given by:

$$\frac{d\sigma_B}{dv}(\hat{s}, v) = k(\hat{s}) T_0(v, \epsilon). \quad (4.4.6)$$

$T_0(v, \epsilon)$ is given by Eq. (4.1.17) and the factor $k(\hat{s})$ is:

$$k(\hat{s}) = \frac{1}{\hat{s}} \frac{2\pi\alpha}{\Gamma(1-\epsilon)} \frac{C_F}{N_c} \left(\frac{4\pi\mu^2}{\hat{s}} \right)^\epsilon [v(1-v)]^{-\epsilon}. \quad (4.4.7)$$

Performing the trivial integrations in (4.4.2) we obtain:

$$\frac{d\sigma^{fact}}{dvdw} = -\frac{\alpha_s}{2\pi} \left[H(x_1, M^2) x_1^{-1-\epsilon} + \frac{v}{1-vw} H(x_2, M^2) x_2^{-1-\epsilon} \right] \frac{d\sigma_B}{dv}(\hat{s}, v) \quad (4.4.8)$$

with

$$x_1 = w \quad x_2 = \frac{1-v}{1-vw} \quad (4.4.9)$$

We are interested in the leading terms as $w \rightarrow 1$. In this limit, $x_1 \rightarrow 1$ and $x_2 \rightarrow 1$. Then, using the universal definition of corrections⁽⁵³⁾ ($u_{qq}(x) = 0$), Eqs. (4.4.8) and (4.4.4) imply:

$$\frac{d\sigma^{fact}}{dvdw} = FT_0(v, \epsilon) C_F \frac{1}{\epsilon} \left[P_{qq}(w) + \frac{v}{1-v} P_{qq}\left(\frac{1-v}{1-vw}\right) \right] \left(\frac{\hat{s}}{M^2} \right)^\epsilon \quad (4.4.10)$$

For $w \rightarrow 1$, the split function (4.4.5) yields,

$$P_{qq}(w) \rightarrow \frac{2}{(1-w)_+} + \frac{3}{2}\delta(1-w) \quad (4.4.11a)$$

and using Eqs. (E.6a, b) of App. E,

$$\frac{v}{1-v} P_{qq}\left(\frac{1-v}{1-vw}\right) \rightarrow \frac{2}{(1-w)_+} + \left(\frac{3}{2} + 2\ell n\left(\frac{v}{1-v}\right)\right)\delta(1-w). \quad (4.4.11b)$$

Then, expanding the factor $(\hat{s}/M^2)^\epsilon$ in powers of ϵ , we find:⁽⁶¹⁾

$$\begin{aligned} \frac{d\sigma^{fact}}{dvdw} = FC_F \{ T_0(v, \epsilon) \frac{1}{\epsilon} [(3 + 2\ell n \frac{v}{1-v}) \delta(1-w) + \frac{4}{(1-w)_+}] \\ + \tilde{T}_0(v) [(3 + 2\ell n \frac{v}{1-v}) \delta(1-w) + \frac{4}{(1-w)_+}] \ell n \frac{\hat{s}}{M^2} \} \end{aligned} \quad (4.4.12)$$

This cross section must be added to the sum of real and virtual contributions, to give a finite result in accord with (4.4.3). Indeed, the singular part ($\sim 1/\epsilon$) of (4.4.12) exactly cancels corresponding terms in $d\sigma/dv dw$ (Eq. (4.4.1)). As we stated, this cancellation represents the factorization and absorption of mass (collinear) singularities in the bare parton distributions

The finite part of Eq. (4.4.12) completely determines the coefficient functions $a_2(v)$ and $b_2(v)$. This part contains leftover terms from Brems contributions, of which only a part is absorbed in the distribution functions, introducing an arbitrary factorization scale M . To be more specific we consider the singular term $-\frac{1}{\epsilon} F(C_F - \frac{N_c}{2}) T_0(v, \epsilon) \frac{4}{(1-w)_+}$ present in Eq. (4.1.20). The part proportional to N_c is cancelled by a similar term in Eq. (4.2.41). The remaining singular part $\sim C_F$ is not cancelled by any other contribution either real or virtual; it is an uncancelled mass singularity and has to be absorbed in the quark distribution. Notice that this term is proportional to:

$$-\frac{1}{\epsilon} \left(\frac{4\pi\mu^2}{\hat{s}} \right)^\epsilon \frac{4}{(1-w)_+} = -\frac{1}{\epsilon} \left(\frac{4\pi\mu^2}{M^2} \right)^\epsilon \frac{4}{(1-w)_+} + \frac{4}{(1-w)_+} \ell n \frac{\hat{s}}{M^2}. \quad (4.4.13)$$

In the factorization procedure (corresponding to \overline{MS}), only the first term of the r.h.s. of (4.4.13) is absorbed in the bare distribution function. The leftover term $\sim \ell n(\hat{s}/M^2)$ remains as part of the HOC (here it determines $a_2(v)$).

4.5 The Dominant Part

To determine the dominant part we simply sum the contributions determined in the previous sections. We consider the cross section

$$\frac{d\sigma'}{dvdw} = \frac{d\sigma}{dv}\delta(1-w) + \frac{d\sigma^{real}}{dvdw} + \frac{d\sigma^{fact}}{dvdw} \quad (4.5.1)$$

where $(d\sigma/dv)\delta(1-w)$ and $d\sigma^{fact}/dvdw$ as in (4.3.1) and (4.4.12), and $d\sigma^{real}/dvdw$ denotes the sum of (4.1.20), (4.2.41) and (4.2.47). $d\sigma'/dvdw$ is finite; all singular terms $\sim 1/\epsilon^2$ and $\sim 1/\epsilon$ cancel. This cross section is related to the dominant part $f_s(v, w)$ by

$$f_s(v, w) = \Xi \frac{d\sigma'}{dvdw} ; \quad \Xi \equiv \frac{\pi s}{\alpha_s^2(\mu) \hat{s}^2 v} \quad (4.5.2)$$

Finally we introduce:

$$f_s(v, w) = H \bar{f}_s(v, w) ; \quad H = \frac{\Xi F}{v(1-v)} \quad (4.5.3)$$

To express the inclusive cross section σ of Eq. (3.1.2) in terms of $\bar{f}(v, w)$ we change integration variables from x_a, x_b to v, w ; the relations are:

$$x_a = \frac{w_1}{w} \quad x_b = \frac{1-v_2}{1-v}$$

and

$$w_1 = \frac{v_1}{v} \quad v_1 = \frac{x_T}{2} e^\eta \quad v_2 = 1 - \frac{x_T}{2} e^{-\eta}. \quad (4.5.4)$$

Then the contribution σ_s^{HOC} of the dominant part f_s is:

$$\sigma_s^{HOC} = \frac{\pi \alpha}{p_T^4} \left(\frac{\alpha_s(\mu)}{\pi} \right)^2 \frac{C_F}{N_c} \int_{v_1}^{v_2} dv \int_{w_1}^1 dw \bar{f}_s(v, w) F_{a/A}(x_a, M) F_{b/B}(x_b, M) \quad (4.5.5)$$

Writing $\bar{f}_s(v, w)$ in the form (3.1.7):

$$\begin{aligned} \bar{f}_s(v, w) = & \bar{a}_1(v)\delta(1-w) + \bar{b}_1(v) \frac{1}{(1-w)_+} + \bar{c}(v) \left(\frac{\ell n(1-w)}{1-w} \right)_+ \\ & [\bar{a}_2(v)\delta(1-w) + \bar{b}_2(v) \frac{1}{(1-w)_+}] \ell n \frac{\hat{s}}{M^2} \end{aligned} \quad (4.5.6)$$

and collecting the finite terms in Eqs. (4.1.20), (4.2.41) and (4.2.47) which contribute to $d\sigma'/dvdw$ we easily determine the coefficient functions:⁽⁶¹⁾

$$\begin{aligned}
\bar{a}_1(v) &= C_F \{ \pi^2 B(v) + (v^2 - 4v + 3)\ell n v + v(v+2)\ell n(1-v) + (3v^2 - 2v + 2)\ell n^2 v \\
&\quad + (3v^2 - 4v + 3)\ell n^2(1-v) - (2\ell n v \ell n(1-v) + 7)B(v) \} \\
&+ N_c \{ (\frac{67}{18} - \frac{\pi^2}{3})B(v) - (\frac{11}{6}B(v) + v(1-v))\ell n v - v(1-v)\ell n(1-v) \\
&\quad + N_f (-\frac{5}{9} + \frac{1}{3}\ell n v)B(v) + bB(v)\ell n \frac{\mu^2}{\hat{s}} \}. \\
\bar{b}_1(v) &= [4C_F(\ell n v - \ell n(1-v)) + N_c(-\frac{11}{6} + 2\ell n(1-v)) + \frac{N_f}{3}]B(v) \\
\bar{c}(v) &= 2(4C_F - N_c)B(v) \\
\bar{a}_2(v) &= C_F(3 + 2\ell n v - 2\ell n(1-v))B(v) \\
\bar{b}_2(v) &= 4C_F B(v). \tag{4.5.7}
\end{aligned}$$

Now we compare our expressions with results of other related work.⁽⁵⁹⁾

First, expressions (4.5.7) are in agreement with computer outputs provided by the authors of Ref. 59(b).^(f2)

Now, we compare with the results published in Ref. 59(a) (Appendix). As they state, the authors leave out the contributions from $q\bar{q} \rightarrow \gamma q\bar{q}$, so the terms $N_f(-\frac{5}{9} + \frac{1}{3}\ell n v)B(v)$ in $\bar{a}_1(v)$ and $\frac{1}{3}N_f B(v)$ in $\bar{b}_1(v)$ do not appear in their expressions. Also in their expression of $\bar{a}_1(v)$ a term $\frac{2}{3}N_f(v(1-v) - 1)$ is present, which is cancelled in the final result.

We note that our expression of $\bar{b}_1(v)$ contains the term $(-\frac{11}{6}N_c + \frac{1}{3}N_f)B(v) = -bB(v)$ where b is the coefficient of the Callan-Symanzik beta function, Eq. (3.3.7); and the presence of such a term is related with the term $bB(v)\ell n(\mu^2/\hat{s})$ in the expression $\bar{a}_1(v)$. The same holds for the sum of terms $-\frac{11}{6}N_c B(v)\ell n v + \frac{1}{3}N_f B(v)\ell n v = -bB(v)\ell n v$ appearing in $\bar{a}_1(v)$.

4.6 Concluding Remarks

Our first remark concerns the origin of the dominant part of HOC. The analysis and the detailed calculations presented in this chapter make clear that this part arises from soft and collinear gluon Brems as well as from virtual gluons. Hard and non-collinear gluon Brems does not contribute.

Our second remark is that, as we have seen, the Brems contributions to the dominant part can be calculated with relative ease. Clearly, the determination of the dominant part is accomplished more easily than of the complete HOC.

As a third remark, we stress the simplicity of our final expressions, Eqs. (4.1.15) and (4.2.39), which determine practically all the Brems contributions to the dominant part $f_s(v, w)$. The same holds for Eq. (4.2.45) which determines contributions from $q\bar{q} \rightarrow \gamma q\bar{q}$. The efficiency and usefulness of these expressions is further demonstrated in the next chapter, in which we employ them and determine easily the dominant part for the subprocess $qg \rightarrow \gamma q$.

A final point to remark is that the dominant part determined in this chapter, includes all the dominant contributions to the nonsinglet cross section; such contributions do not arise from the subprocess $qq \rightarrow \gamma qq$.

CHAPTER 5

APPLICATION OF THE APPROACH OF CH. 4

In Ch. 4 it was shown that the Brems contributions to the dominant part of HOC are determined from expressions remarkably simple and general, and we presented in detail the determination of this part for the subprocess $q\bar{q} \rightarrow \gamma g$.^{(60),(61)}

Here, we employ the expressions derived in Ch. 4 and determine the dominant part of the subprocess $qg \rightarrow \gamma q$.⁽⁷¹⁾ These two subprocesses, as we have seen, control large- p_T direct photon production in hadronic collisions. Thus this chapter complements Ch. 4. Nevertheless, it also offers a good example of the efficiency and usefulness of the general expressions. We also discuss certain additional points like an estimate of the accuracy of keeping only the dominant part.

As before, we work in the Feynman gauge, and use dimensional regularization with $n = 4 - 2\epsilon$. We also use the universal definition of corrections,⁽⁵³⁾ and our results refer to the \overline{MS} renormalization (and factorization) scheme.

5.1 Generalization of the Results of Ch. 4

We consider the simple expressions of the previous chapter, which determine the gluon Brems contributions, and more generally contributions from $2 \rightarrow 3$ subprocesses, to the dominant part.

The Brems contributions from initial partons were determined from the expression (4.1.15). We noticed that this expression depends on the particular subprocess only through the Born term and color factors. Hence it can be written in general as:

$$\frac{d\sigma^{in}}{dvdw} = F^{(ab)} T_0^{(ab)}(v, \epsilon) C_{in}^{(ab)} \left(-\frac{4}{\epsilon}\right) \left(\frac{v}{1-v}\right)^{-\epsilon} (1-w)^{-1-2\epsilon} \left(1 + \epsilon^2 \frac{\pi^2}{6}\right) \quad (5.1.1)$$

where

$$F^{(ab)} = \frac{2\pi\alpha}{\hat{s}} C^{(ab)} \frac{\alpha_s^2(\mu)}{2\pi} \left(\frac{4\pi\mu^2}{\hat{s}}\right)^{2\epsilon} \frac{[v(1-v)]^{-\epsilon}}{\Gamma(1-2\epsilon)} \quad (5.1.2)$$

and $T_0^{(ab)}(v, \epsilon)$ is essentially the Born cross section for $a + b \rightarrow \gamma + c$ in $n = 4 - 2\epsilon$ dimensions with its color factor $C^{(ab)}$ included in (5.1.2). In (5.1.1) the color factor

$C_{in}^{(ab)}$ is determined from a single unitarity graph, the one in which the radiated gluon connects the legs of the two different initial partons (i.e. of the type of Figs. 15(a) and 18).

The contribution from unitarity graphs in which one or both amplitudes contain gluon Brems from a final parton (or the split of such a parton to two on-shell partons) were determined from expressions (4.2.39) and (4.2.45). As we remarked, these expressions are similar and have the same structure. They depend on the particular subprocess through the Born term, color factors, and the final parton split function. Thus their sum can be written in general as:

$$\frac{d\sigma^{fin}}{dvdw} = F^{(ab)} T_0^{(ab)}(v, \epsilon) v^{-\epsilon} (1-w)^{-1-\epsilon} \sum_d C_{dc} \tilde{P}_{dc}(\epsilon) \quad (5.1.3)$$

where

$$\tilde{P}_{dc}(\epsilon) = \frac{\Gamma(1-2\epsilon)}{\Gamma^2(1-\epsilon)} \int_0^1 y^{-\epsilon} (1-y)^{-\epsilon} P_{dc}(y, \epsilon) dy \quad (5.1.4)$$

and $P_{dc}(y, \epsilon)$ is the generalization in $n = 4 - 2\epsilon$ dimensions of the split function $P_{dc}(y)$ at $y < 1$ for $c \rightarrow d$. As usual, we have separated the Casimir factor C_{dc} from the split function for convenience; it helps to keep track of color factors in specific subprocesses. In (5.1.3), $F^{(ab)}$ and $T_0^{(ab)}(v, \epsilon)$ are as in (5.1.1).

Finally we consider the factorization procedure. It was implemented by introducing Eq. (4.4.10), which depends on the particular subprocess only through the Born term and the split functions associated with initial partons. Clearly it can be written in general as:

$$\frac{d\sigma^{fact}}{dvdw} = F^{(ab)} T_0^{(ab)}(v, \epsilon) \frac{1}{\epsilon} \left\{ C_{aa} P_{aa}(w) + \frac{v}{1-v} C_{bb} P_{bb}\left(\frac{1-v}{1-vw}\right) \right\} \left(\frac{\hat{s}}{M^2}\right)^\epsilon \quad (5.1.5)$$

where again $F^{(ab)}$ and $T_0^{(ab)}(v, \epsilon)$ as in (5.1.1). Notice that only the diagonal elements of the matrix P_i , of split functions⁽³²⁾ enter in Eq. (5.1.5). This because only these elements (P_{qq} and/or P_{gg}) contain distributions $\delta(1-w)$ and $1/(1-w)_+$ resulting in contributions to the dominant part. The other split functions introduce contributions to the nondominant part \tilde{f} of the HOC; hence they are neglected.

Now we proceed to evaluate the Brems contributions to the dominant part for $qg \rightarrow \gamma q$.

5.2 Brems Contributions to the Dominant Part of $qg \rightarrow \gamma q$

We turn to the subprocess $qg \rightarrow \gamma q$ and make use of the above results.⁽⁷¹⁾ This subprocess is a special case of $a + b \rightarrow \gamma + c$; we take $a \equiv g$ which corresponds to the gluon carrying momentum p_1 (originating from the hadron A). Then the Born cross section equivalent to (4.1.17) is

$$T_0^{(qg)}(v, \epsilon) = (1 - \epsilon) \left[(1 - \epsilon) \frac{1 + v^2}{v} + 2\epsilon \right] \quad (5.2.1)$$

Note that, in contrast to $q\bar{q} \rightarrow \gamma g$, for $qg \rightarrow \gamma q$ the Born cross section is not symmetric in \hat{t} and \hat{u} (or v and $1 - v$) as can be seen by comparing (5.2.1) to (4.1.17) (or (2.1.4) to (2.1.5)); and the same is true for the HOC. Our final expression (Eq. (5.4.1)) takes care of this.

The contribution to $f_s(v, w)$ from initial parton Brems is determined by employing Eq. (5.1.1). The Born color factor is $C^{(qg)} = 1/2N_c$ (see Eq. (2.1.4)), and the color factor $C_{in}^{(qg)} = N_c/2$ is determined from the unitarity graph Fig. 18. Then Eqs. (5.1.1) and (5.1.2) imply:⁽⁷¹⁾

$$\frac{d\sigma^{in}}{dvdw} = \Phi T_0^{(qg)}(v, \epsilon) N_c \left(-\frac{2}{\epsilon}\right) \left(\frac{v}{1-v}\right)^{-\epsilon} (1-w)^{-1-2\epsilon} \left(1 + \epsilon^2 \frac{\pi^2}{6}\right) \quad (5.2.2)$$

where

$$\Phi \equiv F^{(qg)} = \frac{2\pi a}{\hat{s}} \frac{1}{2N_c} \frac{\alpha_s^2(\mu)}{2\pi} \left(\frac{4\pi\mu^2}{\hat{s}}\right)^{2\epsilon} \frac{[v(1-v)]^{-\epsilon}}{\Gamma(1-2\epsilon)} \quad (5.2.3)$$

and $T_0^{(qg)}(v, \epsilon)$ is given by (5.2.1).

Now, using the expansions (4.1.18) and (4.1.19), we obtain:

$$\begin{aligned} \frac{d\sigma^{in}}{dvdw} = & \Phi N_c \left\{ T_0^{(qg)}(v, \epsilon) \left[\frac{1}{\epsilon^2} \delta(1-w) - \frac{1}{\epsilon} \left(\frac{2}{(1-w)_+} + \ell n \frac{v}{1-v} \delta(1-w) \right) \right] \right. \\ & \left. + \tilde{T}_0^{(qg)}(v) \left[\frac{1}{2} \left(\frac{\pi^2}{3} + \ell n^2 \frac{v}{1-v} \right) \delta(1-w) + \ell n \frac{v}{1-v} \frac{2}{(1-w)_+} + 4 \left(\frac{\ell n(1-w)}{1-w} \right)_+ \right] \right\} \quad (5.2.4) \end{aligned}$$

where

$$\tilde{T}_0^{(qg)}(v) \equiv T_0^{(qg)}(v, 0) = \frac{1 + v^2}{v}. \quad (5.2.5)$$

The contribution to $f_s(v, w)$ from unitarity graphs in which one or both amplitudes involve the split of a final parton is determined by employing Eq. (5.1.3). We notice that, in this case, the split $c \rightarrow d + d'$ occurs only in one mode, namely $q \rightarrow q + g$ (gluon Brems). Then to apply Eq. (5.1.3) we introduce^(f3)

$$P_{qq}(y, \epsilon) = \frac{2}{1-y} - 1 - y - \epsilon(1-y) \quad (5.2.6)$$

which for $y < 1$ is the generalization in n dimensions of the split function $P_{qq}(y)$ ⁽⁷⁰⁾ (apart from the color factor $C_F = C_{qq}$ present in (5.2.7) below). Thus we obtain⁽⁷¹⁾

$$\frac{d\sigma^{f_1 n}}{dvdw} = \Phi T_0^{(qq)}(v, \epsilon) C_F v^{-\epsilon} (1-w)^{-1-\epsilon} \tilde{P}_{qq}(\epsilon) \quad (5.2.7)$$

where

$$\tilde{P}_{qq}(\epsilon) \equiv \frac{\Gamma(1-2\epsilon)}{\Gamma^2(1-\epsilon)} \int_0^1 y^{-\epsilon} (1-y)^{-\epsilon} P_{qq}(y, \epsilon). \quad (5.2.8)$$

Integrating (5.2.8) and expanding in powers of ϵ we find:

$$\tilde{P}_{qq}(\epsilon) = -\frac{2}{\epsilon} - \frac{3}{2} - \frac{7}{2}\epsilon \quad (5.2.9)$$

so that Eq. (5.2.7) becomes

$$\begin{aligned} \frac{d\sigma^{f_1 n}}{dvdw} = & \Phi C_F \{ T_0^{(qq)}(v, \epsilon) [\frac{2}{\epsilon^2} \delta(1-w) + \frac{1}{\epsilon} ((\frac{3}{2} - 2\ell n v) \delta(1-w) - \frac{2}{(1-w)_+})] \\ & + \tilde{T}_0(v) [(\frac{7}{2} - \frac{3}{2} \ell n v + \ell n^2 v) \delta(1-w) + (2\ell n v - \frac{3}{2}) \frac{1}{(1-w)_+} + 2(\frac{\ell n(1-w)}{1-w})_+] \}. \end{aligned} \quad (5.2.10)$$

Finally, adding Eqs. (5.2.4) and (5.2.10) we find for the total Brems contribution to $d\sigma/dv dw$:

$$\begin{aligned} \frac{d\sigma^{Brems}}{dvdw} = & \Phi \{ T_0^{(qq)}(v, \epsilon) [[\frac{2C_F + N_c}{\epsilon^2} + \frac{1}{\epsilon} (C_F (\frac{3}{2} - 2\ell n v) - N_c \ell n \frac{v}{1-v})] \delta(1-w) + \\ & - \frac{1}{\epsilon} (C_F + N_c) \frac{2}{(1-w)_+}] \\ & + C_F \tilde{T}_0^{(qq)}(v) [(\frac{7}{2} - \frac{3}{2} \ell n v + \ell n^2 v) \delta(1-w) + (2\ell n v - \frac{3}{2}) \frac{1}{(1-w)_+} + 2(\frac{\ell n(1-w)}{1-w})_+] \} \end{aligned}$$

$$+N_c \tilde{T}_0^{(gg)}(v) \left[\frac{1}{2} \left(\frac{\pi^2}{3} + \ell n^2 \frac{v}{1-v} \right) \delta(1-w) + \ell n \frac{v}{1-v} \frac{2}{(1-w)_+} + 4 \left(\frac{\ell n(1-w)}{1-w} \right)_+ \right]. \quad (5.2.11)$$

The elimination of the singular terms $\sim 1/\epsilon^2$ and $\sim 1/\epsilon$ in (5.2.11) is discussed in the next section.

5.3 Virtual Contributions and Factorization of Mass Singularities

We first present the contribution of virtual partons (loop graphs) to the HOC of $qg \rightarrow \gamma q$. For this subprocess the differential cross section $d\sigma^{vir}/d\hat{t}$ can be obtained from the corresponding result for the subprocess $q\bar{q} \rightarrow \gamma g$ (Eq. (6.1.13), Ch. 6). This is done by $\hat{s} \leftrightarrow \hat{t}$ crossing (including a factor (-1) for crossing a fermion), and division by $2C_F$ in order to transform the average over colors of an initial quark to that of a gluon. After a straightforward but lengthy calculation and using $\hat{t} = -\hat{s}(1-v)$, $\hat{u} = -\hat{s}v$ we find:⁽⁷¹⁾

$$\begin{aligned} \frac{d\sigma^{vir}}{dv} = & \Phi \{ T_0^{(gg)}(v, \epsilon) \left[-\frac{2C_F + N_c}{\epsilon^2} - \frac{1}{\epsilon} (3C_F + b - 2C_F \ell n(1-v) + N_c \ell n \frac{1-v}{v}) \right] \right. \\ & + \frac{1}{v(1-v)} \{ C_F \left[\left(\frac{2}{3} \pi^2 - 7 \right) B_g(v) - \pi^2 v(1-v)(2-v) + (1-v) \left[(3-2v) \ell n v + 4v \ell n(1-v) \right. \right. \\ & \quad \left. \left. + (1-2v+2v^2) \ell n^2 \frac{v}{1-v} - (2v-1) \ell n^2(1-v) \right] \right. \\ & \quad \left. + \frac{N_c}{2} \left[\left(-\frac{\pi^2}{3} \right) B_g(v) + \pi^2 v(1-v)(2-v) + (1-v) \left[2v \ell n v - 4v \ell n(1-v) \right. \right. \right. \\ & \quad \left. \left. \left. - (1-2v+2v^2) \ell n^2 \frac{v}{1-v} + (2v-1) \ell n^2(1-v) \right] \right] - B_g(v) b \ell n \frac{\hat{s}}{\mu^2} \} \right. \quad (5.3.1) \end{aligned}$$

where b is given by (1.2.4) and

$$B_g(v) \equiv v(1-v) \tilde{T}_0^{(gg)}(v) = (1-v)(1+v^2) \quad (5.3.2)$$

We have checked that the same expression is obtained from Eq. (2.28) of Ref. 66.

One can immediately observe that in the sum of $d\sigma^{Brems}/dvdw$ and $(d\sigma^{vir}/dv)$ $\delta(1-w)$ the infrared singular terms $\sim 1/\epsilon^2$ cancel.

The singular terms $\sim 1/\epsilon$ are eliminated via the factorization procedure. We implement this by employing Eq. (5.1.5) with $a \equiv g$, $b \equiv q$ and hence introducing the term⁽⁷¹⁾:

$$\frac{d\sigma^{fact}}{dvdw} = \Phi T_0^{(qq)}(v, \epsilon) \frac{1}{\epsilon} \left\{ 2N_c P_{gg}(w) + \frac{v}{1-v} C_F P_{qq}\left(\frac{1-w}{1-vw}\right) \right\} \left(\frac{\hat{s}}{M^2}\right)^\epsilon \quad (5.3.3)$$

As we have explained in Ch. 4, this term must be added to the sum $d\sigma^{Brems}/dvdw + (d\sigma^{virt}/dv)\delta(1-w)$ to yield a finite cross section. In (5.3.3), $P_{gg}(w)$ and $P_{qq}(w)$ are the complete split functions ($0 \leq w \leq 1$);

$$P_{gg}(w) = \frac{w}{(1-w)_+} + \frac{1-w}{w} + w(1-w) + \frac{b}{2N_c} \delta(1-w) \quad (5.3.4)$$

and $P_{qq}(x)$ is given in Eq. (4.4.5). For $w \rightarrow 1$ (contributions to the dominant part) we use

$$P_{gg}(w) \rightarrow \frac{1}{(1-w)_+} + \frac{b}{2N_c} \delta(1-w) \quad (5.3.5)$$

and Eq. (4.4.11b) for $\frac{v}{1-v} P_{qq}\left(\frac{1-v}{1-vw}\right)$. Then, expanding the factor $(\hat{s}/M^2)^\epsilon$ in powers of ϵ , we obtain:

$$\begin{aligned} \frac{d\sigma^{fact}}{dvdw} = & \Phi \left\{ T_0^{(qq)}(v, \epsilon) \frac{1}{\epsilon} \left[(b + C_F \left(\frac{3}{2} + 2\ell n \frac{v}{1-v} \right)) \delta(1-w) + (C_F + N_c) \frac{2}{(1-w)_+} \right] \right. \\ & + \tilde{T}_0^{(qq)}(v) \left\{ C_F \left[\left(\frac{3}{2} + 2\ell n \frac{v}{1-v} \right) \delta(1-w) + \frac{2}{(1-w)_+} \right] \right. \\ & \left. \left. + N_c \frac{2}{(1-w)_+} + b\delta(1-w) \right\} \right\}. \end{aligned} \quad (5.3.6)$$

In the sum

$$\frac{d\sigma'}{dvdw} = \frac{d\sigma^{virt}}{dv} \delta(1-w) + \frac{d\sigma^{Brems}}{dvdw} + \frac{d\sigma^{fact}}{dvdw} \quad (5.3.7)$$

all the singular terms cancel, making $d\sigma'/dvdw$ finite. Then the dominant term, being proportional to this finite cross section, can be easily derived. This is presented in the next section.

5.4 The Dominant Part ($qg \rightarrow \gamma q$)

As in Ch. 4, we denote by σ_s^{HOC} the contribution of the dominant part f_s to the inclusive cross section Eq. (3.1.2). This can be written (see Eqs. (3.1.2) and (4.5.5)):

$$\sigma_s^{HOC} = \frac{\pi\alpha}{p_T^4} \left(\frac{\alpha_s(\mu)}{\pi}\right)^2 \frac{1}{2N_c} \left\{ \int_{v_1}^{v_2} dv \int_{w_1}^1 dw \bar{f}_s(v, w) F_{a/A}(x_a, M) F_{b/B}(x_b, M) \right. \\ \left. + (A \leftrightarrow B, \eta \leftrightarrow -\eta) \right\} \quad (5.4.1)$$

where η denotes the rapidity and v_1, v_2, w_1, x_a and x_b are given by Eqs. (4.5.4); in $F_{a/A}(x_a, M)$, a denotes a gluon. Note that the second term in (5.4.1) takes care of the asymmetry in \hat{t} and \hat{u} (discussed in Sect. 5.2) and involves the same function $\bar{f}_s(v, w)$ as the first term.

Writing $\bar{f}_s(v, w)$ in the form (4.5.6) we obtain:⁽⁷¹⁾

$$\bar{a}_1(v) = C_F \left\{ \left(\frac{2}{3}\pi^2 - \frac{7}{2} \right) B(v) - \pi^2 v(1-v)(2-v) + (1-v) \left[\frac{1}{2}(3-4v-3v^2) \ell n v + 4v \ell n(1-v) \right] \right. \\ \left. + (2-2v+3v^2) \ell n^2 v + 2(1-v)^2 \ell n^2(1-v) - 2(1-2v+2v^2) \ell n v \ell n(1-v) \right\} \\ + \frac{N_c}{2} \left\{ \pi^2 v(1-v)(2-v) + (1-v) [2v \ell n v - 4v \ell n(1-v) + v(2-v) \ell n^2 v + \right. \\ \left. - (1-4v+v^2) \ell n^2(1-v) - 2v(2-v) \ell n v \ell n(1-v)] \right\} + bB(v) \ell n \frac{\mu^2}{s} \\ \bar{b}_1(v) = \left\{ C_F (2 \ell n v - \frac{3}{2}) + 2N_c \ell n \frac{v}{1-v} \right\} B(v) \\ \bar{c}(v) = 2(C_F + 2N_c) B(v) \\ \bar{a}_2(v) = \left\{ b + C_F \left(\frac{3}{2} + 2 \ell n \frac{v}{1-v} \right) \right\} B(v) \\ \bar{b}_2(v) = 2(C_F + N_c) B(v) \quad (5.4.2)$$

Here, $B(v) = B_g(v) = (1-v)(1+v^2)$ (Eq. (5.3.2)).

The above results, are in agreement with corresponding results of computer outputs provided by P. Aurenche et al.^(59b) (to our knowledge, for $qg \rightarrow \gamma q$ there

exist no published complete HOC). We notice that these outputs contain two separate sets of HOC for $qg \rightarrow \gamma q$, corresponding to $\hat{t} \leftrightarrow \hat{u}$ interchanged contributions. We see no need for two sets (see Eq. (5.4.1)). In fact, regarding all the dominant part $\bar{f}_s(v, w)$, the results of the second set can be directly reproduced from those of the first; this is also true for the complete HOC $\bar{f}(v, w)$.

5.5 Conclusions and Remarks

As a first remark, we would like to establish some contact between this work and the K -factor approach of Ch. 2. As in most of our considerations, we take $\mu = M = p_T$. Returning to Ch. 3, we have seen that in $f_s(v, w)$ which dominates the HOC, the various terms contribute at $w = 1$ or mainly near $w = 1$. Thus, in a rough sense, all the involved distributions act as $\sim \delta(1 - w)$. Moreover, for either $q\bar{q} \rightarrow \gamma g$ or $qg \rightarrow \gamma q$, the functions $b_1(v)$, $c(v)$, $a_2(v)$, $b_2(v)$ and part of $a_1(v)$ are proportional to the corresponding Born term $\tilde{T}_0(v)$ ($\equiv B(v)/v(1 - v)$, see Eqs. (4.3.2) and (4.5.7) of Ch. 4, or Eqs. (5.3.2) and (5.4.2) of this chapter). Then, for any subprocess, we proceed as follows: we neglect $\tilde{f}(v, w)$ and approximately write^{(60),(61)}

$$f(v, w) = C_s \frac{\pi^2}{2} \tilde{T}_0(v) \delta(1 - w). \quad (5.5.1)$$

Regarding C_s , in view of the smoothness of $B(v)$ and of $\bar{a}_1(v)$ (Eqs. (4.5.7) or (5.4.2)), it is a smooth function of v ; also, to obtain the physical inclusive cross section σ , $f(v, w)$ should be integrated over v (and w) [Eq. (4.5.5) or (5.4.1)]. Thus as a first approximation we take $C_s \sim \text{constant}$. Then the total cross section (Born + HOC) becomes:

$$\frac{d\sigma}{dvdw} \sim \tilde{T}_0(v) \delta(1 - w) \left[1 + \frac{\alpha_s(p_T)}{2\pi} C_s \pi^2 \right] \quad (5.5.2)$$

This leads immediately to the K -factor (at the physical scale $\mu = M = p_T$)

$$K \simeq 1 + \frac{\alpha_s(p_T)}{2\pi} C_s \pi^2. \quad (5.5.3)$$

Clearly, this is exactly of the form of Eqs. (2.2.22) and (2.3.1) of Ch. 2, and offers significant insight into the reasons of the success of the approach of K -factors.^{(4)-(6),(55),(56)}

We would like also to point out that the simple form of the last equation arises from an approximation to the moments of certain of the terms of $f_s(v, w)$. As we have stated, the moments $M_1(k)$, $M_2(k)$ of $1/(1-w)_+$, $(\ln(1-w)/(1-w))_+$ are slowly (logarithmically) varying functions of k (see Table III). As a rough approximation, setting $M_1(k) \sim c_1$, $M_2(k) \sim c_2$ (with c_1 and c_2 constants) amounts to replacing $1/(1-w)_+$ and $(\ln(1-w)/(1-w))_+$ by δ -functions. One then arrives again to the expressions (5.5.1)–(5.5.3).

As a second remark we notice the efficiency and usefulness of our expressions in determining dominant parts of HOC to $2 \rightarrow 2$ subprocesses, as well as in providing a partial check of the results of existing complete HOC calculations (in fact of the dominant part of their HOC, as for example in Sects 4.5 and 5.4).

One may ask what is the accuracy of keeping only the dominant part without knowing in advance the complete HOC. As it is clear from Ch. 3, this depends on x_T and on the softness of the parton distributions. To estimate a bound on the contribution of the nondominant $\tilde{f}(v, w)$, e.g. for parton distributions inside a proton, we first consider the subprocess $q\bar{q} \rightarrow \gamma g$ which controls the difference $(p\bar{p} \rightarrow \gamma X) - (pp \rightarrow \gamma X)$ and involves quark valence distributions. Then Fig. 13(a) shows that for not too small x_T (≥ 0.1) the contribution of \tilde{f} is $\lesssim 20\%$ of the total inclusive cross section.^(f4) Now turning to $qg \rightarrow \gamma q$, since for such x_T the gluon distribution is softer than that of valence we may anticipate at most a comparable contribution.^(f5)

Now we briefly consider the possible usefulness of our work towards other directions.

We first mention the determination of HOC for inclusive reactions initiated by $2 \rightarrow 3$ particle subprocesses of the type $a + b \rightarrow c + d + e$, for which (due to their complexity) HOC are hitherto completely unknown. We believe that our procedures in Ch. 4 and in this chapter will be useful in determining the next-to-leading order terms comprising the dominant part of such subprocesses as well. So far, however, we have not carried any systematic study of such reactions

Furthermore, HOC beyond the next-to-leading order remain almost undeter-

mined. Recently Refs. 72 and 73, by taking into account terms arising from soft and collinear Brems, and virtual gluons, have been able to carry an approximate determination of the $O(\alpha_s^2)$ correction to the K -factor of the Drell-Yan process. One may hope that our approach will be useful in calculating next-to-next-to leading order terms for other processes as well. In fact, in going beyond the next-to-leading order, in addition to the terms of (3.1.7), there appear distributions of the form $(\ln^m(1-w)/(1-w))_+$ with $m \geq 2$.⁽⁷⁴⁾ For $k \rightarrow \infty$, the corresponding moments behave as $\sim \ln^{m+1} k$. Such terms further enhance the dominance of $f_s(v, w)$.

One may also ask whether our work is of any relevance to new physics. We believe that it is. In searches for new physics (e.g. Supersymmetry) it is very important to have at least some idea on the size and sign of corrections. For, if the corrections are large and negative, the signal will be much reduced.^(f6) Now even in conventional QCD which contains fewer partons than supersymmetric QCD (SQCD), complete calculations of corrections are, in general, very complicated and lengthy; in SQCD they are even more. On the other hand, the dominant part of HOC is easier to calculate. One may calculate this part to get an idea of the size and sign of corrections.

PART III

ADDITIONAL CONTRIBUTIONS AND APPLICATION

In this Part, in Ch. 6 and 7, we determine HOC for the nonsinglet contribution to $AB \rightarrow \gamma + X$ (i.e. contributions of the subprocess $q_v \bar{q}_v \rightarrow \gamma g$); we use published results on HOC for the nonsinglet contribution to $AB \rightarrow \ell^+ \ell^- + X$ (i.e. of $q_v \bar{q}_v \rightarrow \gamma^* g$).^(54b)

In particular, in Ch. 6 we determine the virtual contribution (loop graphs) to $q\bar{q} \rightarrow \gamma g$, which has been used in Ch. 4; also with crossing symmetry, it has been used in Ch. 5 to determine the virtual contributions to $qg \rightarrow \gamma q$. Our results will also provide a verification (check) of the correctness of our dominant contributions to $q\bar{q} \rightarrow \gamma g$, determined in Ch. 4.

In Ch. 7 we continue the calculation and determine the complete HOC to the nonsinglet part of $q\bar{q} \rightarrow \gamma g$. This was used in Ch. 3 (Fig. 13); in addition, it serves to provide an estimate of the accuracy of the dominant contribution of other subprocesses, as e.g. $qg \rightarrow \gamma q$ (see Sect. 5.4). In the same chapter we study graphs involving photon Brems and separate the collinear photon contribution.

The method we apply in Chs. 6 and 7 is also applicable to other QCD subprocesses involving photons at a tree level; therefore it is of rather general use.

Finally, in Ch. 8 we use all the results of this Part and of Part II for a phenomenological analysis of recent and old data on large p_T $pp \rightarrow \gamma + X$ and $p\bar{p} \rightarrow \gamma + X$. In this analysis we use complete HOC. The motivation of this analysis will be explained in Sect. 8.1.

CHAPTER 6

VIRTUAL CONTRIBUTIONS AND CHECK OF THE DOMINANT PART

In this chapter we begin by determining the virtual contribution (loop graphs) to the subprocess $q\bar{q} \rightarrow \gamma g$. For this, we use certain of the expressions of Ref. 54(b). This work determines HOC to the nonsinglet part of $A + B \rightarrow \ell^+ \ell^-$ (large p_T) $+ X$, which is dominated by the subprocess $q\bar{q} \rightarrow \gamma^* g$. Denoting by Q the 4-momentum of γ^* , we show by a proper procedure that for $Q^2 \rightarrow 0$, in spite of the presence of individually diverging terms, the limit of the aforementioned expressions is finite; moreover, as expected from physical considerations, it determines the virtual contribution to $q\bar{q} \rightarrow \gamma g$. In view of the success of the above procedure we then continue and evaluate in the same way contributions arising from $2 \rightarrow 3$ subprocesses. Our results provide a further check of the dominant contribution to $q\bar{q} \rightarrow \gamma g$, determined in Ch. 4. They also lead to the nondominant contributions which are determined in the next chapter.

6.1 HOC to $d\sigma/d\hat{t}(q\bar{q} \rightarrow \gamma g)$ from Loop Graphs

We present the derivation of the differential cross section $d\sigma^{vir}/d\hat{t}$ determining the contribution of virtual partons to the HOC of the subprocess $q\bar{q} \rightarrow \gamma g$.

First, we rewrite the relevant expressions (Eqs. (A2)–A(7) of App. A of Ref. 54(b)) in a slightly different form. With

$$\tilde{F} \equiv \frac{2\pi\alpha}{\hat{s}} \frac{C_F}{N_c} \frac{\alpha_s^2(\mu)}{2\pi} \left(\frac{4\pi\mu^2}{\hat{s}}\right)^{2\epsilon} \left(\frac{\hat{t}\hat{u}}{\hat{s}^2}\right)^{-\epsilon} \frac{1}{\Gamma(1-2\epsilon)} \quad (6.1.1)$$

and the Born matrix element denoted by

$$J_0(Q^2, \hat{t}, \hat{u}, \epsilon) \equiv (1-\epsilon) \left[(1-\epsilon) \frac{\hat{t}^2 + \hat{u}^2}{\hat{t}\hat{u}} + \frac{2Q^2(Q^2 - \hat{t} - \hat{u})}{\hat{t}\hat{u}} - 2\epsilon \right], \quad (6.1.2)$$

the differential cross section $d\sigma^{vir}/d\hat{t}$ for $q\bar{q} \rightarrow \gamma^* g$ to $O(\alpha_s^2)$ is written:

$$\hat{s} \frac{d\sigma^{vir}}{d\hat{t}} = \tilde{F} \left\{ J_0(Q^2, \hat{t}, \hat{u}, \epsilon) \left(\frac{\hat{s}}{Q^2}\right)^\epsilon \left[-\frac{2C_F + N_c}{\epsilon^2} - \frac{1}{\epsilon} (3C_F - 2C_F \ell n \frac{\hat{s}}{Q^2} + b + N_c \ell n \frac{\hat{s}Q^2}{\hat{t}\hat{u}}) \right] \right\}$$

$$\begin{aligned}
& + \tilde{J}_0(Q^2, \hat{s}, \hat{t}, \hat{u}) \left[\left(\frac{2}{3} C_F - \frac{N_c}{6} \right) \pi^2 - 8C_F - C_F \ell n^2 \frac{\hat{s}}{Q^2} + \frac{N_c}{2} \left(\ell n^2 \frac{\hat{s}}{Q^2} - \ell n^2 \frac{\hat{t}\hat{u}}{Q^4} \right) + b \ell n \frac{\mu^2}{Q^2} \right] \\
& + [F(Q^2, \hat{s}, \hat{t}, \hat{u}) + (\hat{t} \leftrightarrow \hat{u})]. \tag{6.1.3}
\end{aligned}$$

The function $F(Q^2, \hat{s}, \hat{t}, \hat{u})$ is given by:

$$\begin{aligned}
F(Q^2, \hat{s}, \hat{t}, \hat{u}) &= C_F \left(\frac{\hat{s}}{\hat{s} + \hat{t}} + \frac{\hat{s} + \hat{t}}{\hat{u}} \right) + \ell n \left| \frac{\hat{t}}{Q^2} \right| \left(C_F \frac{4\hat{s}^2 + 2\hat{s}\hat{t} + 4\hat{s}\hat{u} + \hat{t}\hat{u}}{(\hat{s} + \hat{u})^2} + N_c \frac{\hat{t}}{\hat{t} + \hat{u}} \right) \\
& + (2C_F - N_c) \left[\ell n \frac{\hat{s}}{Q^2} \left(\frac{\hat{s}^2}{(\hat{t} + \hat{u})^2} + \frac{2\hat{s}}{\hat{t} + \hat{u}} \right) - \frac{Q^2(\hat{t}^2 + \hat{u}^2)}{2\hat{t}\hat{u}(\hat{t} + \hat{u})} \right] \\
& - (2C_F - N_c) \frac{\hat{s}^2 + (\hat{s} + \hat{u})^2}{\hat{t}\hat{u}} R_1(Q^2, \hat{s}, \hat{t}) + N_c \tilde{J}_0(Q^2, \hat{t}, \hat{u}) R_2(Q^2, \hat{t}) \tag{6.1.4}
\end{aligned}$$

where

$$R_1(Q^2, \hat{s}, \hat{t}) = \ell n \frac{\hat{s}}{Q^2} \ell n \frac{\hat{t}}{Q^2 - \hat{s}} + \frac{1}{2} \ell n^2 \frac{Q^2}{\hat{s}} - \frac{1}{2} \ell n^2 \left(\frac{Q^2 - \hat{t}}{Q^2} \right) - \mathcal{L}_{i_2} \left(\frac{Q^2}{\hat{s}} \right) - \mathcal{L}_{i_2} \left(\frac{Q^2}{Q^2 - \hat{t}} \right) \tag{6.1.5}$$

and

$$R_2(Q^2, \hat{t}) = \frac{1}{2} \ell n^2 \left(\frac{Q^2 - \hat{t}}{Q^2} \right) + \mathcal{L}_{i_2} \left(\frac{Q^2}{Q^2 - \hat{t}} \right). \tag{6.1.6}$$

In (6.1.3) and (6.1.4), \tilde{J}_0 is the function J_0 of (6.1.2) at $\epsilon = 0$. $\mathcal{L}_{i_2}(x)$, in (6.1.5) and (6.1.6), is the Spence function introduced in Eq. (C.23) of App. C.

In the above forms we cannot set directly $Q^2 = 0$ because individual terms diverge. We notice, however, that the photon, which is emitted by initial quark legs, is produced at fixed angle relative to the beam direction and collinear photon emission cannot occur; no photon mass singularity should appear in the differential cross-section $d\sigma^{\text{vir}}/d\hat{t}$. Thus singularities arising in the individual terms, are expected to cancel.

Therefore, we apply the following reduction procedure. We first set $Q^2 = 0$, only in places where singularities do not arise. Then we combine terms to eliminate the residual Q^2 -dependence. This procedure is presented below.

Applying the first step and using $\hat{s} + \hat{t} + \hat{u} = 0$, we obtain the following reduced forms of (6.1.3)–(6.1.6):

$$\hat{s} \frac{d\sigma^{\text{vir}}}{d\hat{t}} = \tilde{F} \left\{ I_0(\hat{t}, \hat{u}, \epsilon) \left(\frac{\hat{s}}{Q^2} \right)^\epsilon \left[-\frac{2C_F + N_c}{\epsilon^2} - \frac{1}{\epsilon} (3C_F - 2C_F \ell n \frac{\hat{s}}{Q^2} + b + N_c \ell n \frac{\hat{s}Q^2}{\hat{t}\hat{u}}) \right] \right\}$$

$$\begin{aligned}
& +\bar{I}_0(\hat{t}, \hat{u})\left[\left(\frac{2}{3}C_F - \frac{N_c}{6}\right)\pi^2 - 8C_F - C_F\ell n^2\frac{\hat{s}}{Q^2} + \frac{N_c}{2}\left(\ell n^2\frac{\hat{s}}{Q^2} - \ell n^2\frac{\hat{t}\hat{u}}{Q^4}\right) + b\ell n\frac{\mu^2}{Q^2}\right] \\
& +[\bar{F}(Q^2, \hat{s}, \hat{t}, \hat{u}) + (\hat{t} \leftrightarrow \hat{u})] \}. \tag{6.1.7}
\end{aligned}$$

The function $\bar{F}(Q^2, \hat{s}, \hat{t}, \hat{u})$ is given by:

$$\begin{aligned}
\bar{F}(Q^2, \hat{s}, \hat{t}, \hat{u}) &= C_F\frac{\hat{t}}{\hat{u}} + \ell n\left(-\frac{\hat{t}}{Q^2}\right)[C_F\left(3\frac{\hat{u}}{\hat{t}} + 2\right) - N_c] - (2C_F - N_c)\ell n\frac{\hat{s}}{Q^2} \\
& - (2C_F - N_c)[\bar{I}_0(\hat{t}, \hat{u}) + \frac{\hat{t}}{\hat{u}} + 2]\bar{R}_1(Q^2, \hat{s}, \hat{t}) + N_c\bar{I}_0(\hat{t}, \hat{u})\bar{R}_2(Q^2, \hat{t}) \tag{6.1.8}
\end{aligned}$$

with

$$\bar{R}_1(Q^2, \hat{s}, \hat{t}) = \ell n\frac{\hat{s}}{Q^2}\ell n\left(-\frac{\hat{t}}{\hat{s}}\right) + \frac{1}{2}\ell n^2\frac{Q^2}{\hat{s}} - \frac{1}{2}\ell n^2\left(-\frac{\hat{t}}{Q^2}\right) \tag{6.1.9}$$

and

$$\bar{R}_2(Q^2, \hat{t}) = \frac{1}{2}\ell n^2\left(-\frac{\hat{t}}{Q^2}\right). \tag{6.1.10}$$

In writing the above equations we have introduced

$$I_0 \equiv J_0|_{Q^2=0} = (1 - \epsilon)\left[(1 - \epsilon)\frac{\hat{t}^2 + \hat{u}^2}{\hat{t}\hat{u}} - 2\epsilon\right] \tag{6.1.11}$$

and

$$\bar{I}_0 \equiv I_0|_{\epsilon=0} = \frac{\hat{t}^2 + \hat{u}^2}{\hat{t}\hat{u}}. \tag{6.1.12}$$

Now we proceed to the second step. We expand the factor $(\hat{s}/Q^2)^\epsilon$ in powers of ϵ , we recollect terms and after some algebra we find that the final expression of $d\sigma/d\hat{t}$ is manifestly Q^2 -independent. Clearly in (6.1.7)–(6.1.10), Q^2 plays the role of a subsidiary scale. Our final cross section is:

$$\begin{aligned}
\hat{s}\frac{d\sigma^{vir}}{d\hat{t}} &= \tilde{F}\{I_0(\hat{t}, \hat{u}, \epsilon)\left[-\frac{2C_F + N_c}{\epsilon^2} - \frac{1}{\epsilon}\left(3C_F + b - N_c\ell n\frac{\hat{t}\hat{u}}{\hat{s}^2}\right) + b\ell n\frac{\mu^2}{\hat{s}}\right] \\
& +\bar{I}_0(\hat{t}, \hat{u})\left[\left(\frac{2}{3}C_F - \frac{N_c}{6}\right)\pi^2 - 7C_F + C_F\left(\ell n^2\left(-\frac{\hat{t}}{\hat{s}}\right) + \ell n^2\left(-\frac{\hat{u}}{\hat{s}}\right)\right) - \frac{N_c}{2}\ell n^2\frac{\hat{t}\hat{u}}{\hat{s}^2}\right] \\
& + 3C_F\left[\frac{\hat{u}}{\hat{t}}\ell n\left(-\frac{\hat{t}}{\hat{s}}\right) + \frac{\hat{t}}{\hat{u}}\ell n\left(-\frac{\hat{u}}{\hat{s}}\right)\right] + 2\left(C_F - \frac{N_c}{2}\right)\ell n\frac{\hat{t}\hat{u}}{\hat{s}^2} \\
& + \left(C_F - \frac{N_c}{2}\right)\left[\left(\frac{\hat{t}}{\hat{u}} + 2\right)\ell n^2\left(-\frac{\hat{t}}{\hat{s}}\right) + \left(\frac{\hat{u}}{\hat{t}} + 2\right)\ell n^2\left(-\frac{\hat{u}}{\hat{s}}\right)\right] \}. \tag{6.1.13}
\end{aligned}$$

We remark that, since the final $d\sigma/d\hat{t}$ is Q^2 -independent, the expressions (6.1.7)–(6.1.10) must reduce to (6.1.13) for any particular choice of the subsidiary variable Q^2 . A very convenient choice is $Q^2 = \hat{s}$; then the factor $(\hat{s}/Q^2)^\epsilon$ and many terms in Eqs. (6.1.7)–(6.1.10) are immediately eliminated and with a simple rearrangement, Eq. (6.1.13) easily follows.

We have checked that the part of (6.1.13) proportional to C_F is in accord with Ref. 77.

Expression (6.1.13) can also be obtained from Eq. (2.28) of Ref. 66 by interchanging $\hat{s} \leftrightarrow \hat{t}$ and multiplying by $-1/N_c$.

6.2 Gluon Brems Contributions to the HOC

Here we apply the method of the previous section to obtain the HOC arising from the graphs Figs. 20(a)–(e). For this we use the expressions of App. B of Ref. 54(b), giving corresponding contributions for $q\bar{q} \rightarrow \gamma^* + \tau$. We denote by $d\sigma'/d\hat{t}d\hat{u}$ the contribution of these graphs to the differential cross section. The prime in $d\sigma'$ is to denote that the mass singularities, associated with collinear gluon emission from initial quark legs, have been factored out of the perturbative cross section $d\sigma/d\hat{t}d\hat{u}$, and absorbed in the (bar) parton distribution functions.

To simplify the presentation we split Eq. (B.10) of Ref. 54(b) as follows:

$$\frac{\hat{s}d\sigma'}{d\hat{t}d\hat{u}} = \sigma_\delta + \sigma_{A^+} + \sigma \quad (6.2.1)$$

where σ_δ contains all the terms proportional to $\delta(s_2)$ (here, $s_2 \equiv \hat{s} + \hat{t} + \hat{u} + Q^2$), and σ_{A^+} contains all the terms involving the distributions $1/(s_2)_{A^+}$ and $(\ell n(s_2/a)/s_2)_{A^+}$ which are defined by:

$$\int_0^A ds_2 f(s_2) \frac{1}{(s_2)_{A^+}} \equiv \int_0^A ds_2 [f(s_2) - f(0)] \frac{1}{s_2} \quad (6.2.2a)$$

and

$$\int_0^A ds_2 f(s_2) \left(\frac{\ell n(s_2/a)}{s_2} \right)_{A^+} \equiv \int_0^A ds_2 [f(s_2) - f(0)] \frac{\ell n(s_2/a)}{s_2} \quad (6.2.2b)$$

for any regular function $f(s_2)$ and any scale a . Finally in (6.2.1), σ contains all the other terms (not included in σ_δ or σ_{A^+}). We remark that, in the expressions of Ref. 54(b), each of the terms σ_δ , σ_{A^+} and σ is a function of Q^2 (with Q the 4-momentum of the virtual photon).

Now, as in Sect. 6.1, we observe that in the relevant graphs (Figs. 20(a)-(e)), the photon is emitted only by initial quark legs and collinear photon emission cannot occur. As before, no photon mass singularity should appear in the differential cross section $d\sigma'/d\hat{t}d\hat{u}$.

Again, as in Sect. 6.1, we first take the limit $Q^2 \rightarrow 0$ everywhere that this limit exists. In this way we obtain:

$$\begin{aligned} \sigma_\delta = & \tilde{F}\{I_0(\hat{t}, \hat{u}, \epsilon)\left(\frac{\hat{s}}{Q^2}\right)^\epsilon \left[\frac{2C_F + N_c}{\epsilon^2} + \frac{1}{\epsilon}(3C_F + b + 2C_F \ln \frac{Q^2}{\hat{s}} + N_c \ln \frac{Q^2 \hat{s}}{\hat{t}\hat{u}})\right] \\ & + \bar{I}_0(\hat{t}, \hat{u})\left[(C_F - \frac{N_c}{2})\frac{\pi^2}{3} + \rho + b \ln \frac{Q^2}{A} + N_c \ln^2 \frac{Q^2}{A} + 2C_F \ln \frac{\hat{t}\hat{u}}{A^2} \ln \frac{M^2}{Q^2} \right. \\ & \left. - 3C_F \ln \frac{M^2}{Q^2} + (C_F - \frac{N_c}{2}) \ln^2 \left(\frac{A^2 \hat{s}}{\hat{t}\hat{u} Q^2}\right)\right\} \delta(s_2) \end{aligned} \quad (6.2.3)$$

and

$$\begin{aligned} \sigma_{A^+} = & \tilde{F} \bar{I}_0(\hat{t}, \hat{u}) \left\{ \left[-b + 4\left(C_F - \frac{N_c}{2}\right) \ln \frac{\hat{s}A}{\hat{t}\hat{u}} \right] \frac{1}{(s_2)_{A^+}} \right. \\ & \left. + 4\left[C_F \left(\frac{\ln(s_2/M^2)}{s_2}\right)_{A^+} + \left(C_F - \frac{N_c}{2}\right) \left(\frac{\ln(s_2/A)}{s_2}\right)_{A^+} \right] \right\} \end{aligned} \quad (6.2.4)$$

Here, as in Part II, M stands for the factorization scale. In (6.2.4) we have not included terms $\sim 1/(s_2)_{A^+}$ having a vanishing coefficient as $s_2 \rightarrow 0$. In such terms the A^+ prescription can be removed from the relevant distribution; therefore these terms naturally belong to σ . With these terms transferred into σ , we obtain for $Q^2 = 0$:

$$\begin{aligned} \sigma = & \tilde{F}\{C_F \left[\frac{\hat{s}}{(\hat{s} + \hat{u})^2} + \frac{2}{\hat{s} + \hat{u}} + \frac{2}{\hat{u}}\right] + N_c \frac{\hat{s}}{\hat{t}\hat{u}} \left[\frac{\hat{s}(3s_2 - 4\hat{t})}{2(\hat{s} + \hat{u})^2} + \frac{2\hat{t}}{\hat{s} + \hat{u}}\right] - b \frac{\hat{s}}{\hat{t}\hat{u}} \\ & - 2\left(C_F - \frac{N_c}{2}\right) \frac{\hat{s}\hat{u}}{\hat{t}(\hat{t} - s_2)(\hat{u} - s_2)} \ln\left(\frac{\hat{s}s_2}{\hat{t}\hat{u}}\right) + 2\left(C_F - \frac{N_c}{2}\right) \frac{\hat{s}}{\hat{t}\hat{u}} \ln \frac{\hat{s}s_2}{(\hat{t} - s_2)(\hat{u} - s_2)} \\ & + C_F \left[\frac{4\hat{u} - s_2}{\hat{t}\hat{u}} - \frac{\hat{u}}{(\hat{s} + \hat{u})^2} + \frac{\hat{u}}{\hat{t}(\hat{s} + \hat{u})} - \frac{2}{\hat{t}}\right] \ln\left(\frac{M^2}{s_2}\right) \end{aligned}$$

$$+(2C_F - \frac{N_c}{2})\bar{I}_0(\hat{t}, \hat{u})\frac{1}{s_2}\ell n\frac{\hat{t}\hat{u}}{(\hat{t}-s_2)(\hat{u}-s_2)} + (\hat{t} \leftrightarrow \hat{u})\}. \quad (6.2.5)$$

In the above equations, \bar{F} , I_0 and \bar{I}_0 are given by (6.1.1), (6.1.11) and (6.1.12) respectively. A is the upper integration limit appearing in the definitions (6.2.2). b is introduced in (1.2.4), and we have set for convenience

$$\rho = \frac{1}{18}(67N_c - 10N_f).$$

Now, only in the term σ_δ (Eq. (6.2.3)) there is a residual Q^2 -dependence. This can be completely eliminated by expanding the factor $(\hat{s}/Q^2)^\epsilon$ in powers of ϵ and recollecting terms, or by taking the convenient choice $Q^2 = \hat{s}$, as in the virtual contribution. Either way we obtain the Q^2 -independent expression:

$$\begin{aligned} \sigma_\delta = & \bar{F}\{I_0(\hat{t}, \hat{u}, \epsilon)\left[\frac{2C_F + N_c}{\epsilon^2} + \frac{1}{\epsilon}(3C_F + b + N_c\ell n\frac{\hat{s}^2}{\hat{t}\hat{u}})\right] \\ & + \bar{I}_0(\hat{t}, \hat{u})\left[(C_F - \frac{N_c}{2})\frac{\pi^2}{3} + \rho + b\ell n\frac{A}{\hat{s}} + N_c\ell n^2\frac{A}{\hat{s}} + 2C_F\ell n\frac{\hat{t}\hat{u}}{A^2}\ell n\frac{M^2}{\hat{s}} \right. \\ & \left. - 3C_F\ell n\frac{M^2}{\hat{s}} + (C_F - \frac{N_c}{2})\ell n^2\frac{\hat{t}\hat{u}}{A^2}\right]\}\delta(s_2) \end{aligned} \quad (6.2.6)$$

In the last expression the singular terms $\sim 1/\epsilon^2$ and $\sim 1/\epsilon$ are cancelled by corresponding terms in $(\hat{s}d\sigma^{vir}/d\hat{t})\delta(s_2)$, Eq. (6.1.13). Thus, from now on, we shall consider only the finite contribution of (6.2.6), to be denoted by σ_δ^{finite} .

We observe that both σ_δ^{finite} and σ_{A+} depend on the variable A . This dependence is introduced by the distributions in (6.2.2), which are convenient in the evaluation of the physical cross section Eq. (3.1.2), when the integration over either parton's momentum fraction x_a or x_b is transformed into an integration over s_2 . A is precisely the upper limit of this integration and depends on the external variables of the process. However, the perturbative result of the subprocess cross section can be expressed always as a function of the invariants \hat{s} , \hat{t} and \hat{u} only. Therefore, A is another subsidiary variable and can be eliminated in the sum $\sigma_\delta^{finite} + \sigma_{A+}$, by introducing distributions with the standard $+$ prescription.

We proceed to show that this is indeed the case, and find the A independent expression. We need such an expression in order to compare with our results of Ch.

4. To this end we introduce the dimensionless variable

$$\bar{s}_2 \equiv \frac{s_2}{\hat{s}} = v(1 - w) \quad (6.2.7)$$

and using Eqs. (E.11) and (E.12) of App. E, we deduce the identities:

$$\frac{1}{(s_2)_{A+}} = \frac{1}{\hat{s}} \left[\frac{1}{(\bar{s}_2)_+} - \ell n \frac{A}{\hat{s}} \delta(\bar{s}_2) \right] \quad (6.2.8a)$$

$$\left(\frac{\ell n(s_2/a)}{s_2} \right)_{A+} = \frac{1}{\hat{s}} \left[\left(\frac{\ell n \bar{s}_2}{\bar{s}_2} \right)_+ - \ell n \left(\frac{a}{\hat{s}} \right) \frac{1}{(\bar{s}_2)_+} + \left(\ell n \frac{a}{\hat{s}} \ell n \frac{A}{\hat{s}} - \frac{1}{2} \ell n^2 \frac{A}{\hat{s}} \right) \delta(\bar{s}_2) \right] \quad (6.2.8b)$$

Notice that, by introducing (6.2.7), the argument of any logarithmic function in (6.2.8b) is dimensionless.

Now, using (6.2.8a) and (6.2.8b) with $a = M^2$ and $a = A$, the sum

$$\sigma_D \equiv \sigma_{\hat{s}}^{finite} + \sigma_{A+} \quad (6.2.9)$$

becomes:

$$\begin{aligned} \sigma_D \equiv & \frac{\tilde{F}}{\hat{s}} \bar{I}_0(\hat{t}, \hat{u}) \left\{ \left[\left(C_F - \frac{N_c}{2} \right) \frac{\pi^2}{3} + \rho + \left(C_F - \frac{N_c}{2} \right) \ell n^2 \frac{\hat{s}^2}{\hat{t}\hat{u}} + C_F \left(3 + 2 \ell n \frac{\hat{s}^2}{\hat{t}\hat{u}} \right) \ell n \frac{\hat{s}}{M^2} \right] \delta(\bar{s}_2) \right. \\ & \left. + \left[-b + 4 \left(C_F - \frac{N_c}{2} \right) \ell n \frac{\hat{s}^2}{\hat{t}\hat{u}} + 4 C_F \ell n \frac{\hat{s}}{M^2} \right] \frac{1}{(\bar{s}_2)_+} + (8 C_F - 2 N_c) \left(\frac{\ell n \bar{s}_2}{\bar{s}_2} \right)_+ \right\} \quad (6.2.10) \end{aligned}$$

This expression is manifestly A independent. It can also be obtained directly from (6.2.6) and (6.2.4) by setting $A = \hat{s}$ and changing integration variable $s_2 \rightarrow \bar{s}_2$.

6.3 Verification of the Dominant Part

We have reduced the expressions of Ref. 54(b) to corresponding forms for large p_T real photon production. Our final expressions Eqs. (6.1.13), (6.2.6) and (6.2.10) are functions of the subprocess invariants (and of the scales μ and M) only; consequently, in view of Eqs. (3.1.4), they can be expressed in terms of v and w .

The differential cross section $d\sigma^{vir}/dv$, obtained from (6.1.13) was presented in Sect. 4.3; its finite part has determined the virtual parton contribution to the coefficient $a_1(v)$. In the following, we shall consider the (finite) part σ_D , Eq. (6.2.10),

which involves distributions of the variable \bar{s}_2 and arises from $2 \rightarrow 3$ subprocesses. This part mainly contributes to the dominant part $f_s(v, w)$ of the HOC.

We denote by $(d\sigma/dv dw)_D$ the cross section differential in v and w that arises from (6.2.10). Using Eqs. (E.12) with $\lambda = v$ and $x = 1 - w$ we obtain after some calculations:

$$\begin{aligned} \left(\frac{d\sigma}{dv dw}\right)_D = & \frac{F}{wv(1-v)} \left\{ B(v) \left[\left(C_F - \frac{N_c}{2} \right) \frac{\pi^2}{3} + \frac{67}{18} N_c - \frac{5}{9} N_f - b \ln v + C_F \ln^2 \frac{v}{1-v} \right. \right. \\ & \left. \left. + \frac{N_c}{2} (\ln^2 v - \ln^2(1-v) + 2 \ln v \ln(1-v)) \right] \delta(1-w) + \right. \\ B'(v, w) & \left[(-b + 4C_F \ln \frac{v}{1-v} + 2N_c \ln(1-v)) \frac{1}{(1-w)_+} + 2(4C_F - N_c) \left(\frac{\ln(1-w)}{1-w} \right)_+ \right. \\ & \left. + C_F \left(\left(3 + 2 \ln \frac{v}{1-v} \right) \delta(1-w) + \frac{4}{(1-w)_+} \right) \ln \frac{\hat{s}}{M^2} \right. \\ & \left. \left. + N_c \frac{\ln w}{1-w} \right] \right\} \end{aligned} \quad (6.3.1)$$

where F and $B(v)$ are given by Eqs. (4.1.16) and (4.3.2) respectively. $B'(v, w)$ arises from the numerator of $\bar{I}_0(\hat{t}, \hat{u})$ and it is

$$B'(v, w) = v^2 w^2 + (1-v)^2. \quad (6.3.2)$$

This can be split as

$$B'(v, w) = B(v) + \Delta B; \quad \Delta B = -v^2(1-w^2). \quad (6.3.3)$$

Now, contributions to the HOC $\bar{f}(v, w)$, introduced in Sect. 4.5, are obtained by using the relation (see also Eqs. (4.5.2) and (4.5.3))

$$\bar{f}(v, w) = wv(1-v) \left(\frac{1}{F} \frac{d\sigma'}{dv dw} \right) \quad (6.3.4)$$

Regarding such contributions we make the following remarks:

- (a) The first and second lines of Eq. (6.3.1) exactly reproduce the Brems contribution (and more generally contributions arising from $2 \rightarrow 3$ subprocesses) to the coefficient $\bar{a}_1(v)$.

- (b) The part $\Delta B = -v^2(1 - w^2)$ of $B'(v, w)$ removes the $1 - w$ pole of the distributions involved in the third and fourth lines of Eq. (6.3.1), and provides contributions to the nondominant part \tilde{f} of the HOC. The last term of (6.3.1) also contributes to \tilde{f} .
- (c) The rest of the terms, i.e. those $\sim B(v)$, exactly reproduce the other coefficients $\bar{b}_1(v)$, $c(v)$, $\bar{a}_2(v)$ and $\bar{b}_2(v)$ of the dominant part.

CHAPTER 7

NONDOMINANT CONTRIBUTIONS AND COLLINEAR PHOTON BREMS

In this chapter we first consider the nondominant contributions to $q\bar{q} \rightarrow \gamma g$ continuing the calculation of Ch. 6. We then proceed to determine other contributions to the nonsinglet part, which arise from graphs involving photon Brems. Terms corresponding to collinear photon emission are present in the final expressions and are separated. The rest of the terms contribute to the nondominant part.

With these additional contributions the $O(\alpha_s^2)$ correction to the nonsinglet cross section is completely determined. As we mentioned these results serve to provide an estimate of the accuracy of the dominant contribution of other subprocesses, like $qg \rightarrow \gamma q$ and $\gamma q \rightarrow \gamma q$, considered in Part II. Moreover we will use these results in the analysis of the next chapter.

7.1 Nondominant Contributions

We proceed to determine the nondominant contributions arising from the set of graphs considered in Sect. 6.2 of Ch. 6, namely the graphs Figs. 20(a)–(e). These contributions are obtained from Eq. (6.2.5) and certain terms of Eq. (6.3.1) which do not contribute to the dominant part $f_s(v, w)$.

We denote the nondominant part of $\bar{f}(v, w)$ (Eq. (6.3.4)) by $\tilde{\bar{f}}(v, w)$ and write it in the general form:

$$\begin{aligned} \tilde{\bar{f}}(v, w) = & \bar{d} \ln \frac{\hat{s}}{M^2} + \bar{e} \ln v + \bar{f} \ln(1 - vw) + \bar{g} \ln(1 - v + vw) + \bar{h} \ln(1 - v) + \bar{i} \ln w \\ & + \bar{j} \ln(1 - w) + \bar{k} + \bar{\ell} \frac{\ln(1 - v + vw)}{1 - w} + \bar{m} \frac{\ln w}{1 - w} + \bar{n} \frac{\ln(\frac{1-vw}{1-w})}{1 - w} \end{aligned} \quad (7.1.1)$$

where the coefficients $\bar{d}, \bar{e}, \dots, \bar{n}$ are, in general, functions of v and w .

Now, we denote by \tilde{f}_1 contributions to \tilde{f} arising from (6.3.1). Using (6.3.3) we obtain after a straightforward calculation,

$$\begin{aligned} \tilde{f}_1(v, w) = & -v^2(1+w)[4C_F \ell n \frac{\hat{s}}{M^2} + 4C_F \ell n v - 2(2C_F - N_c) \ell n(1-v) + N_c \ell n w \\ & + 2(4C_F - N_c) \ell n(1-w) - b] + N_c B(v) \frac{\ell n w}{1-w}. \end{aligned} \quad (7.1.2)$$

Likewise, we denote by \tilde{f}_2 contributions arising from (6.2.5). After a lengthy calculation we obtain:

$$\begin{aligned} \tilde{f}_2(v, w) = & C_F[-1 + 4v - (1 - 2v)w - \frac{v(1-v)}{X^2} + \frac{v(1-2v)}{X}](\ell n \frac{\hat{s}}{M^2} + \ell n v) \\ & - 2(2C_F - N_c)v \ell n(1-vw) + (2C_F - N_c)[-1 - vw + \frac{1 + (1-v)^2}{X}][\ell n(1-v) + \ell n w] \\ & + \{C_F[1 + 8v + (-1 + 4v)w - \frac{v(1-v)}{X^2} - \frac{4-5v+4v^2}{X}] \\ & + N_c[-1 - 2v - vw + \frac{1 + (1-v)^2}{X}]\} \ell n(1-w) \\ & + C_F[-4v(1-v) + (1+v-4v^2)w + \frac{v(1-v)}{X}(\frac{1}{X} + 1)] - 2bv \\ & + \frac{N_c}{2}[3 + (1-4v)w + \frac{v(1-v)}{X^2} - \frac{v(1-4v)}{X}] \end{aligned} \quad (7.1.3)$$

where

$$X = 1 - vw \quad (7.1.4)$$

Eqs. (7.1.2) and (7.1.3) have been written in accord with the decomposition of Eq. (7.1.1). The coefficient functions \bar{d}, \dots, \bar{n} , specifying the nondominant part $\tilde{f}(v, w)$ are obtained by adding corresponding terms of (7.1.2) and (7.1.3). These functions are presented in App. F.

We remark that the term $-2bv$ in (7.1.3) can be obtained from the contribution $(\frac{2}{3}N_f v)$ of the curly bracket in (4.2.27) and a similar contribution $(-2\frac{11}{8}N_c v)$ arising from the $q\bar{q} \rightarrow \gamma gg$ subprocess. Also, the term $bv^2(1+w)$ in (7.1.2) can be obtained from the dominant term $-bB(v)/(1-w)_+$ (see $\bar{b}_1(v)$ in Eq. (4.5.7)) and the replacement $B(v) \rightarrow B'(v, w)$ (Eq. (6.3.2)). Several other terms can be similarly obtained. The above terms provide a test of the results of this section.

7.2 Classification of the Remaining Nonsinglet Contributions

To make clear the type of contributions we consider in this section, we begin with a brief discussion of the class of subprocesses contributing to the nonsinglet cross section. Here it is convenient to express the inclusive cross section for $AB \rightarrow \gamma + X$ in the following form:

$$\sigma^{AB} \equiv \sum_{a,b} \int dx_a dx_b f_{a/A}(x_a, M) f_{b/B}(x_b, M) \hat{\sigma}^{ab} \quad (7.2.1)$$

where $\hat{\sigma}^{ab}$ denotes the corresponding subprocess cross section for $a+b \rightarrow \gamma+x$. Then it is a simple matter to show that, assuming only charge conjugation invariance, the nonsinglet cross section can be written:

$$\sigma^{NS} \equiv \sigma^{\bar{A}B} - \sigma^{AB} = \sum_{i,j} \int dx_a dx_b q_{i/A}^v(x_a, M) q_{j/B}^v(x_b, M) \Delta \hat{\sigma}^{(ij)}(x_a, x_b) \quad (7.2.2)$$

where the summation runs over quark flavors, and $q_{i/H}^v$ denotes the valence distribution of quarks of flavor i within the hadron H ; it is

$$q_{i/H}^v(x, M) = f_{q_i/H}(x, M) - f_{\bar{q}_i/H}(x, M) \quad (7.2.3)$$

In (7.2.2), $\Delta \hat{\sigma}^{(ij)}$ is the difference of parton cross sections

$$\Delta \hat{\sigma}^{(ij)}(x_a, x_b) = \hat{\sigma}^{\bar{q}_i, q_j} - \hat{\sigma}^{q_i, q_j} \quad (7.2.4)$$

considered as a function of the momentum fractions x_a and x_b . We notice that to any order in α_s , only subprocesses of the type

$$\text{a) } \bar{q}_i, q_j \rightarrow \gamma + x \quad \text{b) } q_i, q_j \rightarrow \gamma + x \quad (7.2.5)$$

contribute to (7.2.2); contributions from gluon initiated subprocesses cancel out.

Of course, loop contributions refer to the subprocess

$$\text{(a) } q\bar{q} \rightarrow \gamma g;$$

the $2 \rightarrow 3$ subprocesses are of the type

$$\text{(b) } q\bar{q} \rightarrow \gamma g g \quad q\bar{q} \rightarrow \gamma q\bar{q}$$

or

$$(c) \quad qq \rightarrow \gamma qq \quad (7.2.6)$$

Among these subprocesses, (7.2.6), only (a) and (b) with q and \bar{q} of the same flavor contribute to the dominant part. Subprocesses $q_i \bar{q}_j \rightarrow \gamma q_i \bar{q}_j$, with $i \neq j$ or of the type (c) do not contribute because they proceed via gluon exchange; thus they involve neither collinear gluon Brems configurations nor a $q\bar{q}$ pair in the final state with q, \bar{q} collinear.

Now, we briefly discuss and classify the remaining contributions to the nonsinglet cross section Eq. (7.2.2). These contributions arise from graphs contributing to (7.2.2), but not to its dominant part. Such graphs are those of Figs. 20(f), (g), (h) for the subprocess $q\bar{q} \rightarrow \gamma q\bar{q}$ and of Figs. 21(a), (b) for $qq \rightarrow \gamma qq$.

We denote by M_f the sum of the amplitudes associated with the graph Fig. 20(f) (i.e. of the graph itself and the one with the photon emitted by the other final quark leg). Similarly, for the graph (e) (sum of amplitudes: M_e), graph (g) (sum: M_g) and graph (h) (sum: M_h). Then, regarding $q\bar{q} \rightarrow \gamma q\bar{q}$, contributions will arise from $|M_f|^2$ and $(M_e + M_f)(M_g + M_h)$.*

Now, we denote by $M_a(p_3, p_4)$ the sum of the amplitudes associated with the graph Fig. 21(a) (i.e. of the graph itself and the one with the photon emitted by the other initial quark leg). Similarly for the graph (b) (sum of amplitudes: $M_b(p_3, p_4)$) Then, regarding $qq \rightarrow \gamma qq$, contributions will arise only for identical incoming quarks from $[M_a(p_3, p_4) + M_b(p_3, p_4)][M_a(p_4, p_3) + M_b(p_4, p_3)]$.*

We note that contributions from $M_e \cdot M_f^*$ vanish because of charge conjugation. Also contribution from $|M_g + M_h|^2$ cancel in the nonsinglet cross section Eq. (7.2.2), with contributions either from $|M_a(p_3, p_4) + M_b(p_3, p_4)|^2$ for nonidentical quarks, or from $\frac{1}{2}[|M_a(p_3, p_4) + M_b(p_3, p_4)|^2 + (p_3 \leftrightarrow p_4)]$ for identical quarks.

A point to remark, is that contributions to the nonsinglet cross section arise only when the incoming q and \bar{q} or two quarks have the same flavor. As a result, in Eq. (7.2.2), the double summation is reduced to a single one, and we may write:

$$\sigma^{NS} = \sum_a \int dx_a dx_b q_{a/A}^v(x_a, M) q_{a/B}^v(x_b, M) \Delta \hat{\sigma}^{(aa)} \quad (7.2.7)$$

with $q_{a/A}^\nu$, and $\Delta\hat{\sigma}^{(aa)}$ given by (7.2.3) and (7.2.4) respectively.

Finally, we notice that the graphs providing the additional contributions considered above, contain kinematic configurations with the photon emitted collinearly with a final quark. Such configurations lead to factorized contributions of the form (2.1.14) discussed in Subsect. 2.1.3. The next section treats them in more detail.

7.3 Collinear Photon Brems and its Separation

Here we discuss collinear photon Brems. We show how the corresponding contributions arise and how they are separated. Such contributions are of $O(\alpha_s)$, and after separation they leave a nondominant contribution of $O(\alpha_s^2)$.

We take as example the squared amplitude $|M_f|^2$ and denote by $d\sigma_A/d\hat{t}d\hat{u}$ its contribution to the differential cross section. We use Eq. (C.1) of Ref. 54(b) and set $Q^2 = 0$ in places where a singularity does not arise. We write:

$$\frac{\hat{s}d\sigma_A}{d\hat{t}d\hat{u}} = \left(\frac{\hat{s}d\sigma_A}{d\hat{t}d\hat{u}}\right)_{sing} + \left(\frac{\hat{s}d\sigma_A}{d\hat{t}d\hat{u}}\right)_{fin} \quad (7.3.1)$$

where the first part contains all the terms which are singular for $Q^2 \rightarrow 0$, while the second those which are finite. We obtain:

$$\begin{aligned} \left(\frac{\hat{s}d\sigma_A}{d\hat{t}d\hat{u}}\right)_{sing} = & F_A \frac{1}{\lambda} \ln f(Q^2) \left\{ \frac{1}{\hat{s} - s_2} \left(\frac{2\hat{u}^2}{\hat{s}} + \frac{5}{2}\hat{u} + \frac{3}{2}\hat{s} \right) + \frac{1}{\hat{s}} \left(\frac{3}{4}\hat{s} + \hat{u} - \frac{s_2}{2} \right) \right. \\ & + \frac{1}{\lambda^2} \left[\frac{\hat{u}^2}{\hat{s} - s_2} \left(3\hat{u} - \hat{t} - \frac{\hat{u}^2}{\hat{s}} + \frac{\hat{t}^2}{\hat{s}} - 2\hat{s} \right) + \frac{\hat{u}}{\hat{s}} \left(2s_2\hat{t} - \hat{u}\hat{t} - 2s_2^2 + 4\hat{u}s_2 - 3\hat{u}^2 + 2\hat{s}s_2 - \hat{u}\hat{s} \right) \right. \\ & \left. \left. + \frac{1}{\lambda^4} \frac{3\hat{s}\hat{u}^2(\hat{u}^2 - \hat{t}^2)}{\hat{s} - s_2} \right\} + (\hat{t} \leftrightarrow \hat{u}) \end{aligned} \quad (7.3.2)$$

and

$$\begin{aligned} \left(\frac{\hat{s}d\sigma_A}{d\hat{t}d\hat{u}}\right)_{fin} = & F_A \left\{ \frac{1}{2(\hat{s} - s_2)} \left(\frac{\hat{u}}{\hat{s}} - 1 \right) - \frac{5}{4\hat{s}} + \frac{1}{\lambda^2} \left[\frac{\hat{u}}{\hat{s} - s_2} \left(-2\hat{s} + \frac{3}{2}\frac{\hat{u}}{\hat{s}}(\hat{t} - \hat{u}) + 4\hat{u} - 2\hat{t} \right) \right. \right. \\ & \left. \left. + \frac{\hat{u}}{2\hat{s}}(2(\hat{s} + s_2) + \hat{t} - \hat{u}) \right] + \frac{3\hat{u}^2(\hat{u} - \hat{t})}{\lambda^4} \left[\frac{2\hat{s} - \hat{u} - \hat{t}}{\hat{s} - s_2} - \frac{\hat{s} + s_2}{\hat{s}} \right] \right\} \\ & + (\hat{t} \leftrightarrow \hat{u}). \end{aligned} \quad (7.3.3)$$

where in (7.3.2) and (7.3.3) the overall factor F_A is given by^(f7)

$$F_A = \frac{2\pi a}{\hat{s}} \frac{C_F}{N_c} \left[\sum_k e_k^2 \right] \frac{\alpha_s}{2\pi} T(R) \quad (7.3.4)$$

and λ is:

$$\lambda = [(\hat{u} + \hat{t})^2 - 4Q^2 s_2]^{\frac{1}{2}} \xrightarrow{Q^2 \rightarrow 0} |\hat{u} + \hat{t}| = -(\hat{t} + \hat{u}) \quad (7.3.5)$$

We have set

$$f(Q^2) \equiv \frac{\hat{s} + Q^2 - s_2 + \lambda}{\hat{s} + Q^2 - s_2 - \lambda} \xrightarrow{Q^2 \rightarrow 0} \frac{-(\hat{u} + \hat{t})}{Q^2} \quad (7.3.6)$$

We notice that $\ln f(Q^2)$ diverges for $Q^2 \rightarrow 0$, and this is the reason we separated in (7.3.1) the terms $\sim \ln f(Q^2)$.

Now we introduce the variable

$$z \equiv -\frac{\hat{t} + \hat{u}}{\hat{s}}, \quad (7.3.7)$$

in terms of which we write for $Q^2 \rightarrow 0$:

$$\hat{t} + \hat{u} = -z\hat{s}, \quad \lambda = z\hat{s}, \quad s_2 = (1-z)\hat{s}, \quad f(Q^2) = \frac{z\hat{s}}{Q^2} \quad (7.3.8)$$

We also introduce

$$B_A(\hat{s}, \hat{t}, \hat{u}) \equiv \frac{\hat{t}^2 + \hat{u}^2}{\hat{s}^2} \quad (7.3.9)$$

which corresponds to the squared Born matrix element of the $2 \rightarrow 2$ parton graphs arising from the graph Fig. 20(f) when the photon is removed.

Since (7.3.2) and (7.3.3) are symmetric with respect to $\hat{t} \leftrightarrow \hat{u}$, they can be expressed in terms of the symmetric variables z and B_A , introduced in (7.3.7) and (7.3.9). After a lengthy but straightforward calculation we find the following expressions:

$$\left(\frac{\hat{s} d\sigma_A}{\hat{t} \hat{u}} \right)_{\text{sing}} = \frac{2F_A}{\hat{s} z^3} \ln\left(\frac{z\hat{s}}{Q^2}\right) \frac{1 + (1-z)^2}{z} B_A(\hat{s}, \hat{t}, \hat{u}) \quad (7.3.10)$$

and

$$\left(\frac{\hat{s} d\sigma_A}{\hat{t} \hat{u}} \right)_{\text{fin}} = \frac{4F_A}{\hat{s} z^2} [2(1-z) - (3-3z+z^2) B_A(\hat{s}, \hat{t}, \hat{u})] \quad (7.3.11)$$

We note that Eq. (7.3.10) includes contributions arising from configurations with the photon emitted collinearly with the final quark. It is known (see Ch. 2 Subsect.

2.1.3) that such contributions factorize in accord with (2.1.14); here Q acts as a regularization scale.

In (7.3.10) we separate the term $\sim \ell n z$ and define the rest as the collinear photon Brems. Thus, we write:

$$\frac{\hat{s} d\sigma_A^{coll}}{d\hat{t} d\hat{u}} = \frac{2F_A}{\hat{s} z} \ell n \left(\frac{\hat{s}}{Q^2} \right) P_{\gamma q}(z) B_A(\hat{s}, \frac{\hat{t}}{z}, \frac{\hat{u}}{z}) \quad (7.3.12)$$

Then Eq. (7.3.11), together with the term $\sim \ell n z$ from (7.3.10), gives the nondominant contribution to the HOC:

$$\frac{\hat{s} d\tilde{\sigma}_A}{d\hat{t} d\hat{u}} = \left(\frac{\hat{s} d\sigma_A}{d\hat{t} d\hat{u}} \right)_{fin} + \frac{2F_A}{\hat{s} z^3} \ell n z P_{\gamma q}(z) B_A(\hat{s}, \hat{t}, \hat{u}) \quad (7.3.13)$$

In Eqs. (7.3.12) and (7.3.13) $P_{\gamma q}(z)$ is the split function for $q \rightarrow \gamma$ introduced in Ch. 2, Eq. (2.1.18).

To obtain the final form of Eq. (7.3.12) we denote the regularization scale Q by $\tilde{\Lambda}$ and recall Eqs. (2.1.17) and (2.1.18):

$$\frac{1}{z} D_{\gamma/c}(z, \hat{s}) = \frac{\alpha}{2\pi} \left[\sum_k e_k^2 \right] P_{\gamma q}(z) \ell n \frac{\hat{s}}{\tilde{\Lambda}^2} \quad (7.3.14)$$

Then Eq. (7.3.12) becomes:

$$\frac{\hat{s} d\sigma_A^{coll}}{d\hat{t} d\hat{u}} = \frac{1}{z^2} D_{\gamma/q}(z, \hat{s}) \frac{d\sigma_A}{d\hat{t}} \left(\hat{s}, \frac{\hat{t}}{z}, \frac{\hat{u}}{z} \right) \quad (7.3.15)$$

where

$$\frac{d\sigma_A}{d\hat{t}}(\hat{s}, \hat{t}, \hat{u}) = \frac{\pi \alpha_s^2 C_F}{\hat{s}^2 N_c} 2 \frac{\hat{t}^2 + \hat{u}^2}{\hat{s}^2} \quad (7.3.16)$$

is the differential cross section for the $2 \rightarrow 2$ subprocess $q, \bar{q}_1 \rightarrow q_k \bar{q}_k$ (the factor of 2 accounts for $\hat{t} \leftrightarrow \hat{u}$).

Similar results follow for the other contributions to the nonsinglet cross section; each contains a collinear photon term and a leftover contribution to the nondominant part $\tilde{f}(v, w)$. Denoting by $d\sigma_B/d\hat{t} d\hat{u}$ and $d\sigma_C/d\hat{t} d\hat{u}$ the contributions arising from the amplitudes $(M_c + M_f)(M_g + M_h)^*$ and $[M_a(p_3, p_4) + M_b(p_3, p_4)][p_3 \leftrightarrow p_4]^*$ respectively (Sect. 7.2), collinear photon Brems gives:

$$\frac{\hat{s} d\sigma_{B(C)}^{coll}}{d\hat{t} d\hat{u}} = \frac{1}{z^2} D_{\gamma/q}(z, \hat{s}) \frac{d\sigma_{B(C)}}{d\hat{t}} \left(\hat{s}, \frac{\hat{t}}{z}, \frac{\hat{u}}{z} \right) \quad (7.3.17)$$

with

$$\frac{d\sigma_B}{d\hat{t}}(\hat{s}, \hat{t}, \hat{u}) = \frac{\pi\alpha_s^2}{\hat{s}^2} 4 \frac{C_F}{N_c} (C_F - \frac{N_c}{2}) \left[\frac{\hat{t}^2}{\hat{s}\hat{u}} + \frac{\hat{u}^2}{\hat{s}\hat{t}} \right] \quad (7.3.18a)$$

and

$$\frac{d\sigma_C}{d\hat{t}}(\hat{s}, \hat{t}, \hat{u}) = \frac{\pi\alpha_s^2}{\hat{s}^2} 4 \frac{C_F}{N_c} (C_F - \frac{N_c}{2}) \frac{\hat{s}^2}{\hat{t}\hat{u}} \quad (7.3.18b)$$

The last two differential cross sections correspond to Born contributions of $2 \rightarrow 2$ subprocesses. In (7.3.17) the photon fragmentation function is given by (7.3.14) with $\sum_k e_k^2$ replaced by e_k^2 (charge of the fixed final quark - see also Eq. (2.1.17)).

The contributions to the physical process $AB \rightarrow \gamma + X$ of the above collinear γ Brems terms, are of the same form as Eq. (2.1.14) of Ch. 2.

7.4 Leftover Contributions from Photon Brems

Now we present the contributions which are left after extracting collinear Brems (leftover contributions).

First, as we have seen the contribution arising from the squared amplitude $|M_f|^2$ is determined by Eqs. (7.3.11) and (7.3.13); these lead to the following expression:

$$\frac{\hat{s}d\tilde{\sigma}_A}{d\hat{t}d\hat{u}} = F \left[\sum_k e_k^2 \right] \frac{1}{\hat{s}^2 z^2} \left\{ 2(1-z) - \left[3 - 3z + z^2 - \frac{1}{2z} \ell n z P_{\gamma q}(z) \right] \frac{\hat{t}^2 + \hat{u}^2}{\hat{s}^2} \right\} \quad (7.4.1)$$

with

$$F \equiv 2\alpha\alpha_s^2 \frac{C_F}{N_c}. \quad (7.4.2)$$

The leftover contributions, arising from the other combinations of amplitudes, are obtained by applying the same procedures. The results are:

$$\begin{aligned} \frac{\hat{s}d\tilde{\sigma}_B}{d\hat{t}d\hat{u}} = & F \frac{e_k^2}{\hat{s}^2} (C_F - \frac{N_c}{2}) \left\{ -\frac{1}{z} \left(1 + \frac{4}{z} \right) - \frac{1}{z} \left(1 - z - \frac{1}{z} \ell n z P_{\gamma q}(z) \right) \left(\frac{\hat{t}^2}{\hat{s}\hat{u}} + \frac{\hat{u}^2}{\hat{s}\hat{t}} \right) \right. \\ & + \hat{s} \left[\frac{s_2^2 + (\hat{u} - s_2)^2}{\hat{s}\hat{u}(\hat{s} - s_2)} \ell n \left(\frac{\hat{s}\hat{u}}{s_2\hat{t}} \right) + \frac{1}{2} \left(\frac{s_2 + \hat{s}}{\hat{s}\hat{u}} + \frac{\hat{s}^2 + (\hat{u} - s_2)^2}{\hat{t}\hat{u}s_2} \right) \ell n \frac{\hat{u}^2}{z(\hat{u} - s_2)^2} - \left(\frac{3}{2} \frac{\hat{s}^2}{\hat{t}\hat{u}} + 1 \right) \frac{1}{\hat{u} - s_2} \right] \\ & \left. + \hat{s}[\hat{t} \leftrightarrow \hat{u}] \right\}. \quad (7.4.3) \end{aligned}$$

and

$$\frac{\hat{s}d\tilde{\sigma}_C}{d\hat{t}d\hat{u}} = F \frac{e_k^2}{\hat{t}\hat{u}} \left(C_F - \frac{N_c}{2} \right) \left\{ -z^2 + P_{\gamma q}(z) \left[z \ln \frac{\hat{t}\hat{u}}{\hat{s}s_2} - \frac{\hat{t}}{\hat{s} + \hat{t}} \ln \frac{s_2\hat{t}}{\hat{s}\hat{u}} - \frac{\hat{u}}{\hat{s} + \hat{u}} \ln \frac{s_2\hat{u}}{\hat{s}\hat{t}} \right] \right\} \quad (7.4.4)$$

where F is given by (7.4.2).

Eqs. (7.4.1), (7.4.3) and (7.4.4) can be expressed in terms of \hat{s} and the dimensionless variables v and w introduced in (3.1.4). The procedure is straightforward.

Clearly, the leftover contributions have the same form as the nondominant contribution $\tilde{f}(v, w)$. Hence, in the presence of structure functions they are suppressed (Sect. 3.2), and give a contribution to the physical cross section comparable to that of the nondominant term considered in Sect. 7.1.

As a final remark, the leftover contributions are much smaller than the corresponding collinear photon Brems. This is known since some time (see Ch. 2, Subsect. 2.1.3).^{(8),(10)}

CHAPTER 8

THE GLUON DISTRIBUTION AND PHYSICAL VERSUS OPTIMAL SCALES IN DIRECT PHOTON PRODUCTION

In various calculations of the previous chapters (e.g. in the phenomenological analyses of Ch. 2) we worked with scales μ, M such that

$$\mu^2 = M^2 = \alpha p_T^2$$

with $\alpha = 0(1)$. Other choices, like $\mu^2 = M^2 = -\hat{t}, \hat{s}$ or $2\hat{s}\hat{t}\hat{u}/(\hat{s}^2 + \hat{t}^2 + \hat{u}^2)$, lead to very similar results. We have called physical scale the choice $\mu = M = p_T$; and we shall call near-physical the other of the above scales. Most of the large- p_T physics has been developed with physical or near-physical scales.

Yet a different class of scales, called optimal, has been proposed.^{(68),(69)} Use of such scales in analysis of large- p_T data has been advocated in Refs. 59 and 78 and extensively applied to $AB \rightarrow \gamma + X$.

However, as we discuss (Sect. 8.1), there are certain problems with optimal scales. On the other hand, the answer to important questions affecting QCD phenomenology like the shape of the gluon distribution depends on whether one uses physical or optimal scales. Therefore, in this chapter, we carry an analysis of recent data using physical scales and compare with the results of optimal ones; our basic conclusion is that some ambiguity in the shape of the gluon distribution still remains.

8.1 Problems of Optimal Scales

As a way out of the uncertainty in the choice of the scales, the procedures of optimization have been proposed. According to these procedures the scales are fixed by imposing extra conditions on the correction term.

Two of the most prominent optimization procedures are the Principle of Minimal Sensitivity (PMS)⁽⁶⁸⁾ and the criterion of Fastest Apparent Convergence (FAC);⁽⁶⁹⁾ we briefly discuss them in the following.

The FAC criterion amounts to determining a scale $\mu = M = \mu_G$ such that:

$$\sigma_{HOC}(\mu_G) = 0 \quad \text{or} \quad \sigma(\mu_G) = \sigma_{Born}(\mu_G) \quad (8.1.1)$$

In imposing this condition the idea is that with $\mu = \mu_G$ one may hope that the perturbation expansion converge fast.

According to the PMS convention one determines scales $\mu = \mu_S$ and $M = M_S$ such that:

$$\frac{\partial}{\partial \mu} \sigma(\mu, M)|_{\mu_S, M_S} = \frac{\partial}{\partial M} \sigma(\mu, M)|_{\mu_S, M_S} = 0 \quad (8.1.2)$$

The argument for this convention goes as follows: Take, for simplicity, $\mu = M$; then the cross section is a function of M/p_T . Suppose that the exact cross section σ_{exact} , i.e. to all orders of α_s , is finite; suppose also that it is known. Then σ_{exact} is independent of M (a straight line), and

$$\frac{\partial \sigma_{exact}}{\partial M}(M) = 0 \quad (8.1.3)$$

However in reality σ is known only up to a finite order of α_s (for $AB \rightarrow \gamma X$ up to $0(\alpha_s^2)$), call it $\sigma^{(2)}$, and it is not independent of M (not a straight line, Fig. 22). Then PMS fixes M by choosing the point $M = M_S$ at which $\sigma^{(2)}$ satisfies the condition (8.1.3) (where $\sigma^{(2)}$ shows "minimal sensitivity", i.e. roughly speaking, looks more like a straight line).

The weakness of the argument is evident: First it is highly questionable that to all orders of α_s the cross section is finite; in fact it has been argued that perturbation series are asymptotic series.⁽⁷⁹⁾ Second, even if σ_{exact} is finite, it is completely unknown. If it corresponds to the dashed line of Fig. 22 the choice $M = M_S$ is good. But if it corresponds to the dash-dotted line of Fig. 22 the choice $M = M_S$ is poor, the best choice being $M = M_1$ or $M = M_2$, where $\sigma^{(2)}$ does not satisfy Eq (8.1.3).

Also, regarding the FAC criterion, suppose that $\mu = M = \mu_G$ has been determined so that, to $0(\alpha_s^2)$, $\sigma_{HOC}^{(2)}(\mu_G) = 0$. Nothing guarantees that, if σ_{HOC} is calculated to $0(\alpha_s^3)$, for the same $\mu = M = \mu_G$ one will obtain $\sigma_{HOC}^{(3)}(\mu_G) \simeq 0$ (i.e. $\sigma_{HOC}^{(3)}(\mu_G) \ll \sigma_{Born}(\mu_G)$).

In relation with this point as a nice feature of PMS optimization has been considered the fact that in many cases it leads to cross sections

$$\sigma(\mu_S, M_S) \simeq \sigma_{Born}(\mu_S, M_S) \simeq \sigma(\mu_G); \quad (8.1.4)$$

again the hope is that this indicates rapid convergence. Clearly the same objection as for the FAC solution can be raised.

Anyway, optimization is a possibility, and some test of it is very desirable. The opportunity for a test has been offered by a recent calculation up to $O(\alpha_s^3)$ (three loops) of the ratio⁽⁸⁰⁾

$$R = \frac{\sigma_{tot}(e^-e^+ \rightarrow hadrons)}{\sigma(e^-e^+ \rightarrow \mu^-\mu^+)} \quad (8.1.5)$$

In the \overline{MS} renormalization scheme the result is:

$$R = R_0 \left(1 + \frac{\alpha_s}{\pi} + 1.41 \left(\frac{\alpha_s}{\pi} \right)^2 + 64.8 \left(\frac{\alpha_s}{\pi} \right)^3 \right) \quad (8.1.6)$$

where $R_0 = 3 \sum_q e_q^2$, the value in the parton model. This calculation extends by one order of α_s , the existing ones⁽⁸¹⁾ and makes possible a test of the convergence in the PMS and FAC procedures.

The test is as follows:⁽⁸²⁾ Determine the optimal R using first the old ($O(\alpha_s^2)$) calculations⁽⁸¹⁾ and second the new calculation;⁽⁸⁰⁾ call $R^{(2)}$ and $R^{(3)}$ the corresponding ratios; then for each of PMS and FAC procedures consider the fractional difference

$$\delta \equiv \frac{R^{(3)} - R^{(2)}}{R^{(2)}} \quad (8.1.7)$$

If indeed PMS and FAC achieve rapid convergence, this difference should be small, at least smaller than of usual renormalization procedures, like MS or \overline{MS} (with the physical scale $\mu^2 = s$).

This test led to a negative result.⁽⁸²⁾ At $\sqrt{s} = 34$ Gev (and 5 flavors) it was found for FAC: $\delta = 0.27$ and for PMS: $\delta = 0.215$, in contrast to the MS renormalization scheme for which $\delta = 0.144$ and to \overline{MS} : $\delta = 0.156$. In view of the large contribution of the last term in (8.1.6), optimization remains powerless; anyway, the hope that it leads to rapid convergence is unsupported. (See also Refs. 83 and

84, and the argument of Ref. 85 that the FAC and PMS procedures will inevitably result in a zero limit of the perturbation series, if a limit exists.)

There are additional problems with optimization procedures as applied to large- p_T processes. In certain cases, values of the scales significantly smaller than $\mu = M = p_T$ are obtained; then it is unclear that the result is physically sensible.⁽⁸⁶⁾ In other cases, in certain kinematic domains (e.g. relatively low p_T ($p_T \leq 3$ Gev)), optimization is impossible; yet, in the same domains, the choice $\mu = M = p_T$ gives very reasonable results. To all these one should add the complexity of the optimal scales, i.e. the fact that their relation with p_T is not explicit, but varies from one point of phase space to another.

In recent comparisons of data with theory the scales μ , M have been fixed using PMS optimization.⁽⁵⁹⁾ Usually, very similar results are obtained using the FAC criterion. However, as we stated, various important conclusions, as e.g. the softness of the gluon distribution, significantly depend on the choice of the scales.

In view of all this, in this chapter⁽⁸⁷⁾ we present an analysis of recent (and some old) data on $pp \rightarrow \gamma + X$ and $\bar{p}p \rightarrow \gamma + X$ with the choice of physical scales ($\mu = M = p_T$), and compare with that of Ref. 59. Ref. 59 uses complete HOC, and a meaningful comparison requires that we also use complete HOC. In addition we study the variation of the predictions for a change of the scales in the reasonable interval $p_T/2 \leq \mu = M \leq 2p_T$.⁽⁸⁷⁾

8.2 Higher Order Corrections

As we have stated the reaction $A + B \rightarrow \gamma$ (large p_T) $+X$ is dominated by the subprocesses $qg \rightarrow \gamma + x$ and $q\bar{q} \rightarrow \gamma + x$, subsequently referred to as qg and $q\bar{q}$ respectively. The Feynman graphs determining the leading order and the next-to-leading order (HOC) terms for the above subprocesses are presented in Figs. 19 and 20. Graphs with self-energy loops on the initial or final partons are not presented. Fig. 21 presents the remaining graphs contributing to large- p_T $AB \rightarrow \gamma + X$ up to $O(\alpha_s^2)$; they correspond to $qg \rightarrow qq\gamma$ and $gq \rightarrow q\bar{q}\gamma$. As we indicate, in Figs. 20 and 21 graphs obtained by interchanging $p_1 \leftrightarrow p_2$, (i.e. $\hat{t} \leftrightarrow \hat{u}$) and/or $p_3 \leftrightarrow p_4$ are

not shown.

The contribution of either of the subprocesses qg and $q\bar{q}$ to the inclusive cross section of $AB \rightarrow \gamma + X$ is written in the general form of Eq. (3.1.2), in which the HOC f is decomposed as in Eqs. (3.1.6) and (3.1.7)

Regarding qg (Fig. 19), notice that the graphs 19(a), (b) and (c) contain kinematic configurations in which the final quark is produced collinearly with the photon (collinear γ Brems). These configurations, as we discussed, lead to a contribution which is of $O(\alpha_s)$; they will be further discussed in Sect. 8.3 together with related points. Then in Eq. (3.1.2) $f(v, w)$ contains all the HOC arising from the graphs of Fig. 19 (i.e. it contains no collinear γ Brems).

Regarding $q\bar{q}$ (Fig. 20), the graphs 20(f) and (h) also lead to collinear γ Brems; again the corresponding contributions are of $O(\alpha_s)$. Then $f(v, w)$ contains all the HOC arising from Fig. 20.

For $qq \rightarrow qq\gamma$, the graph Fig. 21(b) contains a collinear γ Brems configuration leading, as before, to an $O(\alpha_s)$ contribution. The remaining part that contributes to the HOC (of $O(\alpha_s^2)$) is of the same nature as the nondominant parts \tilde{f} (i.e. it contains no distributions $\delta(1-w)$, $1/(1-w)_+$ or $(\ln(1-w))/(1-w)_+$). As we stated in Sects. 2.1.3 and 7.3, compared with the corresponding collinear γ Brems, it is known since long ago^{(8),(10)} to be much less important.

Now we specify our procedures for obtaining the various contributions.

First, in Chs. 4 and 5 we have determined in all detail the dominant parts of both $q\bar{q}$ and qg , and have provided explicit expressions of them in Eqs. (4.5.7) and (5.4.2).

For the nondominant part of $q\bar{q}$ we have proceeded as follows: First we remind that this part contains a nonsinglet piece (contributing to the difference of cross sections e.g. for $\bar{p}p \rightarrow \gamma + X$ and $pp \rightarrow \gamma + X$) and a singlet piece (contributing to either $\bar{p}p \rightarrow \gamma + X$ or $pp \rightarrow \gamma + X$). Regarding the nonsinglet piece we have made use of the results of Ch. 7; (Sects. 7.1 and 7.4). Regarding the singlet piece we have determined it by using the matrix elements of previous work of our group,^{(8),(10)} and extending that work.

For the nondominant part \tilde{f} of $qq \rightarrow \gamma q$, we have used the results of the computer outputs of Ref. 59(b). We have checked several of these results by various direct and indirect procedures.^(f8)

Regarding $qq \rightarrow qq\gamma$ (Figs. 21(a),(b)), we have determined the HOC (of $0(\alpha_s^2)$) by extending previous work^{(8),(10)} and, for identical quarks, by including the contribution of Eq. (7.4.4). As stated before, compared with the corresponding collinear γ Brems, they are much less important; they are also less important compared with several uncertainties discussed in the next section.

Similar remarks hold for the HOC of $gg \rightarrow q\bar{q}\gamma$ (Figs. 21(c), (d), (e)); see also Ref. 88. We have taken them into account using computer outputs of Ref. 59(b).

8.3 Photon Brems, Related and Other Uncertainties

In this section we discuss collinear γ Brems and the uncertainties related with it, as well as certain other uncertainties which necessarily beset any present theoretical calculation. We also specify certain points of our calculational procedures in relation with these uncertainties.

As we discussed in Subsect. 2.1.3 collinear γ Brems configurations arise from subprocesses of the type $ab \rightarrow cd\gamma$, with γ emitted by one of the partons c, d ; in all this work we consider γ emitted by a quark. Denoting by p_1, p_2 and q the 4-momenta of a, b and γ , we again define the subprocess invariants $\hat{s}, \hat{t}, \hat{u}$ as in Eq. (2.1.8a). Then the result of the perturbative calculation includes certain terms of the following factorized form (see Sects. 2.1.3 and 7.3):

$$\frac{d\sigma_{coll}}{d\hat{t}d\hat{u}} \sim \frac{\alpha e_q^2}{2\pi} P_{\gamma q}(z) \ell n \frac{\hat{s}}{m^2} \hat{\sigma}'_B \quad (8.3.1)$$

where $\hat{\sigma}'_B$ the leading order (Born, of $0(\alpha_s^2)$) differential cross-section for the parton-parton subprocess $ab \rightarrow cd$, m a regularization mass, $z = -(\hat{t} + \hat{u})/\hat{s}$ and $P_{\gamma q}(z)$ the split function $q \rightarrow \gamma$, specified in Eq. (2.1.18).

A commonly accepted change in (8.3.1) is to replace m by a scale $\tilde{\Lambda}$. In fact, a usual choice is $\tilde{\Lambda} = \Lambda$, the QCD parameter, but this choice is not compelling; anyway, we work with this choice. Another usual change is to use for $P_{\gamma q}(z)$ forms other

than (2.1.18); as we stated, such forms have been derived on the basis of leading logarithm summations.^(f9) Regarding $P_{\gamma q}(z)$, detailed studies using three different forms have been carried, and show significantly different size of contribution.⁽⁵¹⁾ Subsequently, as in Ref. 88, we proceed with $P_{\gamma q}(z)$ corresponding to Ref. 49, (see Eq. (2.1.21)) which leads to intermediate results.⁽⁵¹⁾ Refs. 51 and 88 also show that collinear γ Brems, although generally less important than the qg and $q\bar{q}$ subprocesses (Sect. 8.2), gives a relatively large contribution at collider energies (small x_T) and a rather small at fixed-target energies (larger x_T).

It should be clear by now that photon Brems involves significant uncertainty. Yet, another serious uncertainty exists in relation with the isolation of the photon. Experimentally, an inclusive cross section for $AB \rightarrow \gamma + X$ can be determined only if the photon is in some way isolated from accompanying hadrons. The isolation criteria vary for different experiments. E.g. certain experiments employ the following acceptance criterion: Consider a hadron in the same hemisphere with the photon (accompanying hadron), let $\Delta\eta$ and $\Delta\phi$ be the difference in rapidity and azimuthal angle between this hadron and the photon, and define the quantity

$$R = [(\Delta\eta)^2 + (\Delta\phi)^2]^{1/2} \quad (8.3.2)$$

Then the criterion is that for $R < R_0$, the hadronic energy E be less than E_0 , where R_0 and E_0 fixed quantities.

To our knowledge, so far, no theoretical calculation satisfies exactly this criterion (see also Ref. 86); this holds for the present calculation, as well. To simulate the situation we proceed like Ref. 59(a), but in a somewhat modified way.⁽⁸⁷⁾ Let p be the 4-momentum of the final quark emitting the photon. As $p^2 \rightarrow 0$, the leading squared matrix element is $\sim 1/p^2$; thus with a regularization cutoff at $p^2 = m^2$ one obtains $\int_{m^2}^{\hat{s}} dp^2/p^2 = \ln(\hat{s}/m^2)$. Next, assuming that the final quark produces a collinear hadron jet, to exclude hadrons inside $R < R_0$ we require $p^2 \geq \hat{s}R_0^2/4 \cosh^2 \eta$. Thus in Eq. (8.3.1) we replace⁽⁸⁷⁾

$$\ln \frac{\hat{s}}{m^2} \rightarrow 2 \ln \frac{2 \cosh \eta}{R_0}; \quad (8.3.3)$$

clearly the singularity for $m \rightarrow 0$ becomes a singularity for $R_0 \rightarrow 0$.^(f10)

In the subsequent calculation, when we compare with data of experiments imposing acceptance criteria similar to the above (collider and ISR data), we use the replacement (8.3.3) with the experimental R_0 ; we repeat that we are well aware that we do not exactly reproduce the experimental cuts. When we compare with fixed-target data, we use (8.3.1) with the replacement $m \rightarrow \Lambda$.

Another source of uncertainty is the following: Since $\hat{\sigma}'_B$ in (8.3.1) is of $O(\alpha_s^2)$, with the factor $\ell n(\hat{s}/m^2)$ present, the overall contribution of (8.3.1) is of $O(\alpha_s)$. Then a next-to-leading logarithm calculation should include next-to-leading logarithm corrections (HOC) to the subprocess $ab \rightarrow cd$. Such HOC have been recently determined,⁽⁸⁹⁾ and they involve additional uncertainties (e.g. definition of HOC in relation with the gluon distribution); their complete expressions can be available only as computer outputs. Although such HOC can be incorporated, in view of the above discussion, the value of such an effort is highly questionable. Therefore, we neglect HOC to $ab \rightarrow cd$.

Finally we consider the effect of parton's intrinsic (primordial) transverse momentum k_T . This is somewhat important at the lower p_T ($\lesssim 5$ GeV) and at fixed-target energies where the cross sections are relatively steep; it is a further source of uncertainty. As in Subsect. 2.1.3, we take into account this effect using a Gaussian k_T distribution^{(1),(3),(10)} (Eq. (2.1.23)). Here we take $\langle k_T \rangle = 0.7$ GeV.^{(88),(87)}

We discuss the uncertainty in the scales μ , M in the next section.

8.4 Results and Discussion

We present results with three sets of parton distributions; EHLQ1 (dash-dotted lines),⁽⁹⁰⁾ DO1 (dashed) and DO2 (solid).⁽⁶²⁾ Between them, DO2 contains the hardest gluon distribution (biggest at large x) and QCD parameter $\Lambda = 0.4$ GeV. DO1 and EHLQ1 contain softer gluon distributions (EHLQ1 the softest) and $\Lambda = 0.2$.

For the running coupling we use the 2-loop form, Eq. (1.2.10):

$$\alpha_s(\mu) = \frac{\pi}{b \ell n(\mu/\Lambda)} \left(1 - \frac{c \ell n \ell n(\mu^2/\Lambda^2)}{b \ell n(\mu/\Lambda)} \right)$$

where

$$b = \frac{33 - 2N_f}{6} \quad c = \frac{153 - 10N_f}{2(33 - 2N_f)} \quad (8.4.1)$$

(see Eqs. (1.2.4) and (1.2.9)) and work with $N_f = 4$ flavors.

Most of the experiments present data averaged over a range of rapidities η ; we denote by $E\tilde{d}\sigma/d^3p$ the averaged inclusive cross sections:

$$E \frac{\tilde{d}\sigma}{d^3p}(p_T, s) = \frac{1}{\eta_2 - \eta_1} \int_{\eta_1}^{\eta_2} d\eta E \frac{d\sigma}{d^3p}(p_T, s, \eta) \quad (8.4.2)$$

Most of our results correspond to the physical scale $\mu = M = p_T$.

Figs. 23–25 present results at $\bar{p}p$ collider energies. The point to remark is the closeness of the predictions for the three sets; for the corresponding p_T and x_T the gluon distributions differ little. Essentially the same holds at the ISR energy, Fig. 26. Figs. 27–29 present results at fixed-target energies; now the predictions (corresponding to the same $\mu = M = p_T$) differ, with the set DO2 giving the largest.

Fig. 29(c) shows at $\sqrt{s} = 24.3$ GeV (UA6 experiment) the ratio of the cross-sections $E\tilde{d}\sigma/d^3p$ for $\bar{p}p \rightarrow \gamma + X$ and $pp \rightarrow \gamma + X$. As for $\pi^\pm p \rightarrow \gamma + X$,⁽⁸⁸⁾ this ratio is predicted to increase with p_T .

Finally Fig. 30 shows at two different energies ($\sqrt{s} = 1.8$ TeV and 23.75 GeV) the effect of changing the scales; it presents the ratio of the cross sections calculated with $\mu = M = p_T/2$ and with $\mu = M = 2p_T$, using DO1. The point to remark is that at collider energies the predictions are very stable against changes of the scale, but at fixed target energies they are rather unstable (see also Fig. 27). The reason is the difference in the range of x_T : At both energies, as the scale μ increases, $\alpha_s(\mu)$ decreases. However, at collider energies x_T is very small (Fig. 30), and as $M = \mu$ increases, the parton distributions (in particular the gluon) increase; this almost compensates the decrease of α_s . At fixed target energies x_T is large, and as $M = \mu$ increases the parton distributions decrease, thus adding to the decrease of α_s . The presence of the stabilizing terms,⁽⁵⁹⁾ included in our HOC (e.g. Eqs. (4.5.7) and (5.4.2)), does not prevent a significant variation.

A comparison of our results for the physical scale p_T to those obtained via PMS⁽⁵⁹⁾ optimization is in order. For the same set of parton distributions optimization generally predicts larger cross sections. This is particularly clear at ISR and fixed target energies, as indicated for example in Figs. 26–28 by the dotted line, which shows for DO2, results of Ref. 59 with optimal scales.

This effect is understood as follows: Take, for simplicity, $\mu = M$ and write the inclusive cross section calculated with the physical scale as follows:

$$\sigma(p_T) = \sigma_B(p_T)(1 + C(p_T)) \quad (8.4.3)$$

where $\sigma_B(p_T)$ ($C(p_T)$) stands for the Born term (HOC) calculated with $M = p_T$. It can be shown that the inclusive cross section calculated with the optimal $M = M_{opt}$ is, roughly:^{(67)(68b)}

$$\sigma(M_{opt}) \approx \sigma_B(p_T)e^{C(p_T)} \quad (8.4.4)$$

i.e. optimization amounts to exponentiating the HOC calculated at the physical scale. At fixed-target and ISR energies this HOC is fairly large (comparable to the Born contribution, see Subsect. 2.2.3), and exponentiation makes a considerable difference. Also, we saw that at fixed-target energies, DO2 gives an appreciably larger cross section; it also gives an appreciably larger HOC. Then, for DO2, optimization predicts a very large cross section, well above all the data (Figs. 26–28, dotted line).^{(59),(102)–(104)}

Using PMS optimization a recent detailed analysis of $pp \rightarrow \gamma + X$ data⁽⁷⁸⁾ has concluded that the gluon distribution $F_{g/p}$ should be very soft (softer than DO1). It should be clear that use of the physical scale invalidates this conclusion.

To conclude we would like to remark that, within the above uncertainties, with physical or near physical scales, the simple K -factors of Ch. 2^{(4)–(6),(55),(56)} still give a good account of the data. E.g. the A^2BC data of Fig. 26 are well accounted for with Eq. (2.3.1):

$$K = 1 + \frac{\alpha_s}{2\pi} C \pi^2 \quad (8.4.3)$$

(see Figs. 9 and 10). Also comparisons with data of predictions for $\pi^\pm p \rightarrow \gamma + X$,

were accounted for with (8.4.3) in Ref. 88, as well as UA2 data ($\bar{p}p \rightarrow \gamma X$) in Ref. 57.

8.5 Conclusions

First we consider our results for a fixed scale $\mu = M = p_T$. Then the existing collider data cannot distinguish between gluon distributions. On the whole, the fixed-target data, can be said to favor a distribution between DO1 and DO2. Certainly a distribution softer than DO1 is disfavored.

Now we consider variations of the scale in the reasonable range $p_T/2 \leq \mu = M \leq 2p_T$. Then we can see that with the proper choice of scale(s) any of the sets EHLQ1, DO1 or DO2 can give reasonable fits to the data.

We conclude that recent collider and fixed-target data on large- p_T direct photon production have nicely confirmed the success of perturbative QCD. However, because of inherent uncertainties in the theory, some ambiguity in the form of the gluon distribution still remains.

OVERALL CONCLUSIONS

In this work we have studied several aspects of higher order corrections (HOC) in perturbative QCD; we have also compared theoretical predictions with experimental data, in particular for large p_T direct photon production.

Our first conclusion is that, for several reactions and with the choice of physical or near-physical scales, there are certain well defined sources of large correction terms; such terms are indeed required by the data. These terms lead to simple expressions called K -factors.

Our second conclusion is that, as suggested by the above terms, for processes involving structure functions and/or fragmentation functions there is indeed a well defined part, that dominates the cross section over a sizable kinematic domain, i.e. not too small $x_T = 2p_T/\sqrt{s}$ (dominant part). This part is gauge invariant and its dominance increases with the softness of the structure and/or fragmentation functions. For processes initiated by $2 \rightarrow 2$ particle subprocesses, this part arises from collinear and soft gluon Brems configurations and, more generally such configurations of $2 \rightarrow 3$ subprocesses, as well as from virtual gluons. In addition we have shown that the Brems contributions to this part (which comprises its most complicated portion) can be efficiently determined from expressions remarkably simple and general. Under certain approximations, the form of this part reduces to that of the above simple K -factors. In this way we also offer significant insight into the reasons of their success.

We hope that this work will be useful towards several other directions.

One direction is the calculation of HOC beyond the next to leading order. In fact, recently Refs. 72 and 73, using similar procedures have been able to carry an approximate determination of the $O(\alpha_s^2)$ correction to the Drell-Yan process. One may hope that our approach will be useful in calculating next to next to leading order terms for other subprocesses as well.

Another direction is the determination of HOC for inclusive reactions initiated by $2 \rightarrow 3$ particle subprocesses of the type $a + b \rightarrow c + d + e$; for such subprocesses,

due to their complexity, HOC are hitherto completely unknown. In this respect our procedures of Part II may prove particularly useful.

A third possible direction is the calculation of HOC for reactions involving polarized particles and partons, a subject of great current interest in relation with the spin of the proton and the way it is shared between proton's constituents. In fact, relevant experiments (on polarized beams and targets) are generally fixed target experiments, at relatively low C.M. energies \sqrt{s} . Thus the corresponding x_T 's are not too small, and use of the dominant part has been shown to offer a good approximation.

Our final conclusion is in relation with the ambiguity of the gluon distribution in the nucleon. Using complete HOC we have carried a detailed analysis of recent and old data on large- p_T $pp \rightarrow \gamma + X$ and $p\bar{p} \rightarrow \gamma + X$ and we have investigated the dependence of the form of the gluon distribution on the choice of the scales (physical vs optimal). Our conclusion is that significant ambiguity in this distribution still remains.

APPENDIX A

The one particle inclusive cross section $E d\sigma/d^3p$ for the process

$$A(P_A) + B(P_B) \rightarrow C(P) + X \quad (\text{A.1})$$

due to the $2 \rightarrow 2$ subprocess

$$a(p_a) + b(p_b) \rightarrow c(p) + d \quad (\text{A.2})$$

is written⁽¹⁾:

$$E \frac{d\sigma}{d^3p} = \int \frac{dx_a}{x_a} \frac{dx_b}{x_b} \frac{dz}{z^3} F_{a/A}(x_a, Q^2) F_{b/B}(x_b, Q^2) D_{C/c}(z, Q^2) \frac{\hat{s}}{\pi} \frac{d\sigma^{(ab \rightarrow cd)}}{d\hat{t}} \delta(\hat{s} + \hat{t} + \hat{u}) \\ + (A \leftrightarrow B, \eta \leftrightarrow -\eta) \quad (\text{A.3})$$

Here,

$$p_a = x_a P_A, \quad p_b = x_b P_B, \quad p = \frac{P}{z} \quad (\text{A.4})$$

so that

$$\hat{s} = x_a x_b s, \quad \hat{t} = \frac{x_a}{z} t, \quad \hat{u} = \frac{x_b}{z} u \quad (\text{A.5})$$

where

$$t = -\frac{1}{2} x_T e^{-\eta} s, \quad u = -\frac{1}{2} x_T e^{\eta} s; \quad x_T \equiv \frac{2p_T}{\sqrt{s}} \quad (\text{A.6})$$

and η the pseudo-rapidity of the produced particle C ; this is related to the angle θ at which C emerges relative to the beam direction, in the C.M. frame of A and B , by:

$$\eta = \ln \cot \frac{\theta}{2} \quad (\text{A.7})$$

In (A.3) $F(x, Q^2)$ [$D(x, Q^2)$] denotes momentum distribution [fragmentation] function.

Eliminating the z integration with the δ -function, we obtain:

$$E \frac{d\sigma}{d^3p} = \frac{1}{\pi} \int_{x_1}^1 \frac{dx_a}{x_a} \int_{x_2}^1 \frac{dx_b}{x_b} F_{a/A}(x_a, Q^2) F_{b/B}(x_b, Q^2) \frac{1}{z^2} D_{C/c}(z, Q^2) \frac{d\sigma^{(ab \rightarrow cd)}}{d\hat{t}}$$

$$+(A \leftrightarrow B, \eta \leftrightarrow -\eta) \quad (\text{A.8})$$

with

$$z = \frac{x_T}{2} \left[\frac{e^\eta}{x_a} + \frac{e^{-\eta}}{x_b} \right] \quad (\text{A.9})$$

The restriction $z \leq 1$ determines the lower limit of the x_b integration,

$$x_2 \equiv x_{b,\min} = \frac{x_a x_T e^{-\eta}}{2x_a - x_T e^\eta} \quad (\text{A.10})$$

and then $x_2 \leq 1$ determines the lower limit of the x_a integration:

$$x_1 \equiv x_{a,\min} = \frac{x_T e^\eta}{2 - x_T e^{-\eta}}. \quad (\text{A.11})$$

Now, if the produced particle C (and c) is a photon, we take

$$D_{C/c}(z, Q^2) = D_{\gamma/\gamma}(z, Q^2) = \delta(1 - z) \quad (\text{A.12})$$

and (A.8) leads to

$$E \frac{d\sigma}{d^3p}(A + B \rightarrow \gamma + X) = \frac{2}{\pi} \int_{x_1}^1 \frac{dx_a}{2x_a - x_T e^\eta} F_{a/A}(x_a, Q^2) F_{b/B}(x_b, Q^2) \frac{d\sigma_{ab}}{d\hat{t}} \\ +(A \leftrightarrow B, \eta \leftrightarrow -\eta) \quad (\text{A.13})$$

where x_1 is given by (A.11) and

$$x_b = \frac{x_a x_T e^{-\eta}}{2x_a - x_T e^\eta}. \quad (\text{A.14})$$

For $\theta = 90^\circ$ ($\eta = 0$) and $A = B$, Eq. (A.13) is reduced into Eq. (2.1.2). Also if $C = \gamma \neq c$, then Eq. (A.8) leads to the (collinear) photon Brems contribution Eq. (2.1.14).

APPENDIX B

Here we present some details on the evaluation of certain integrals. We work in $n = 4 - 2\epsilon$ dimensions and refer to external momenta p_i, p_j such that:

$$p_i^2 = p_j^2 = 0 \quad , \quad s_{ij} \equiv (p_i + p_j)^2 = 2p_i \cdot p_j \quad (B.1)$$

B. 1 The Loop Integral

In the soft gluon limit the following integral appears:

$$L(p_i, p_j) = \mu^{2\epsilon} \int \frac{d^n k}{(2\pi)^n} \frac{1}{k^2(k-p_i)^2(k-p_j)^2} \quad (B.2)$$

where the imaginary part of the propagators has been suppressed. Introducing Feynman parameters and shifting the origin of the k integration, we obtain:

$$L(p_i, p_j) = \mu^{2\epsilon} \Gamma(3) \int_0^1 y dy \int_0^1 dx \int \frac{d^n k}{(2\pi)^n} \frac{1}{(k^2 - C)^3} \quad (B.3)$$

where

$$C = y(1-y)(1-x)s_{ij} \quad (B.4)$$

Performing the integration over $k^{(91)}$ we obtain the (UV finite) value:

$$\int \frac{d^n k}{(2\pi)^n} \frac{1}{(k^2 - c)^3} = \frac{-i}{(4\pi)^{2-\epsilon}} \frac{\Gamma(1+\epsilon)}{\Gamma(3)} \frac{1}{C^{1+\epsilon}} \quad (B.5)$$

Then, in view of (B.4) and (B.5), Eq. (B.3) easily leads to the $1/\epsilon^2$ IR divergent result:

$$L(p_i, p_j) = \frac{-i}{(4\pi)^2} \frac{\Gamma(1+\epsilon)\Gamma^2(1-\epsilon)}{\Gamma(1-2\epsilon)} \frac{1}{s_{ij}} \frac{1}{\epsilon^2} \left(\frac{s_{ij}}{4\pi\mu^2}\right)^{-\epsilon}. \quad (B.6)$$

B.2 The Brems Integral

The following integral appears in Brems contributions:

$$B(p_i, p_j) = \mu^{2\epsilon} \int^{k_0=k_{max}} \frac{d^n k}{(2\pi)^n} \frac{2\pi\delta_+(k^2)}{(k+p_i)^2(k+p_j)^2} \quad (B.7)$$

where the upper limit of the k_0 integration is determined from the kinematics of the subprocess.

To carry the integrations in (B.7), we introduce spherical coordinates in $n-1$ dimensions, and write in the C.M. frame of p_i and p_j :

$$k = k_0(1, \dots, \cos \theta) \quad (B.8)$$

Here, θ is the angle between \vec{p}_i and \vec{k} and the dots denote $n-2$ unspecified momenta. Then the denominators in (B.7) are written:

$$(k + p_i)^2 = 2\sqrt{s_{ij}}k_0y \quad , \quad (k + p_j)^2 = 2\sqrt{s_{ij}}k_0(1-y) \quad (B.9)$$

with

$$y = \frac{1 - \cos \theta}{2}. \quad (B.10)$$

In view of (B.9) the integral in (B.7) depends only on k_0 and θ (or y). Therefore, integrating over the other angles, we obtain with standard procedures⁽⁹¹⁾:

$$\int d^{n-1}k = \frac{(4\pi)^{1-\epsilon}}{\Gamma(1-\epsilon)} \int dk_0 k_0^{2-2\epsilon} \int_0^1 dy y^{-\epsilon} (1-y)^{-\epsilon} \quad (B.11)$$

Then the integral in (B.7) becomes

$$B(p_i, p_j) = \frac{1}{(4\pi)^2} \frac{(\pi\mu^2)^\epsilon}{\Gamma(1-\epsilon)} \frac{1}{s_{ij}} \int_0^{k_{max}} dk_0 k_0^{-1-2\epsilon} \int_0^1 dy y^{-1-\epsilon} (1-y)^{-1-\epsilon} \quad (B.12)$$

so that:

$$B(p_i, p_j) = \frac{1}{(4\pi)^2} \frac{\Gamma(1-\epsilon)}{\Gamma(1-2\epsilon)} \frac{1}{s_{ij}} \frac{1}{\epsilon^2} \left(\frac{4k_{max}^2}{4\pi\mu^2} \right)^{-\epsilon} \quad (B.13)$$

APPENDIX C

In much of the work presented in Ch. 4, (and particularly in Sect. 4.2) we used the C.M. frame of the two final partons.⁽⁵⁸⁾ We present here some details of the related kinematics, the three particle phase space (for $2 \rightarrow 3$ subprocesses) and some basic integrals encountered in our calculations.

C.1 Kinematics

Consider the $2 \rightarrow 3$ subprocess $a + b \rightarrow \gamma + c + d$ with particles a, b, γ, c, d having momenta in a n space-time dimensions, p_1, p_2, q, r and k respectively. These momenta satisfy the energy momentum equation:

$$p_1 + p_2 = q + r + k \quad (C.1)$$

Now consider the C.M. frame of particles c and d . Clearly in this frame particles c and d have no net spacial momentum, and consequently in view of (C.1) the spacial momenta of the other particles must satisfy the relation

$$\vec{p}_1 + \vec{p}_2 = \vec{q} \quad (C.2)$$

This relation implies that the three vectors \vec{p}_1, \vec{p}_2 and \vec{q} are coplanar. Hence we can choose a coordinate system so that the above vectors lie in the plane formed by the $(n-2)^{th}$ and $(n-1)^{th}$ axes (yz plane).

In addition, we choose the $(n-1)^{th}$ (z) axis to point along the direction of \vec{p}_1 and denote the resulting system by S_1 (Fig. 17). Referring to this system we write

$$r = \frac{\sqrt{s_2}}{2}(1, \dots, \cos \theta_2 \sin \theta_1, \cos \theta_1), \quad k = \frac{\sqrt{s_2}}{2}(1, \dots, -\cos \theta_2 \sin \theta_1, -\cos \theta_1) \quad (C.3)$$

where s_2 is the invariant mass of the c, d particle system recoiling against particle γ (here a photon). The dots in (C.3) indicate $n-3$ unspecified momenta exactly cancelling in the sum $k + r$.

Now we write the momenta p_1 , p_2 and q in the S_1 system (Fig. 17) as follows:

$$p_1 = p_{10}(1, 0, \dots, 1)$$

$$p_2 = p_{20}(1, 0, \dots, \sin \psi, \cos \psi), \quad q = q_0(1, 0, \dots, \sin \delta, \cos \delta) \quad (C.4)$$

and by taking the scalar product of each of (C.4) with (C.1) we obtain

$$\hat{s} + \hat{t} = 2p_{10}\sqrt{s_2}, \quad \hat{s} + \hat{u} = 2p_{20}\sqrt{s_2}, \quad -(\hat{t} + \hat{u}) = 2q_0\sqrt{s_2} \quad (C.5)$$

Then, in view of (3.1.4), relations (C.5) yield:

$$p_{10} = \frac{\hat{s}v}{2\sqrt{s_2}}, \quad p_{20} = \frac{\hat{s}(1-vw)}{2\sqrt{s_2}}, \quad q_0 = \frac{\hat{s}(1-v+vw)}{2\sqrt{s_2}} \quad (C.6)$$

and

$$\sin^2 \frac{\psi}{2} = \frac{1-w}{1-vw}, \quad \sin^2 \frac{\delta}{2} = \frac{(1-v)(1-w)}{1-v+vw}. \quad (C.7)$$

Similar expressions are obtained if we choose a coordinate system, denoted by S_2 , with the $(n-1)^{th}$ (z) axis pointing along the direction of \vec{p}_2 . In Table IV we present, in a summary form, the momenta parametrized according to S_1 (left part) or S_2 (right).

C.2 Three Particle Phase Space Differential in v and w

The three particle phase space integral for $a(p_1) + b(p_2) \rightarrow \gamma(q) + c(r) + d(k)$ is defined by:

$$(PS)_3 = \int \frac{d^n q}{(2\pi)^{n-1}} \frac{d^n k}{(2\pi)^{n-1}} \frac{d^n r}{(2\pi)^{n-1}} \delta_+(q^2) \delta_+(k^2) \delta_+(r^2) (2\pi)^n \delta^n(p_1 + p_2 - q - k - r) \quad (C.8)$$

The Lorentz invariant integral $\int d^n q \delta_+(q^2)$ can be calculated in any frame; it is most easily computed in the C.M. frame of the incoming particles. Working in this frame we find:

$$\int d^n q \delta_+(q^2) = \frac{\pi^{1-\epsilon}}{\Gamma(1-\epsilon)} \frac{1}{2\hat{s}} \int d\hat{t} d\hat{u} \left(\frac{\hat{t}\hat{u}}{\hat{s}}\right)^{-\epsilon} \quad (C.9)$$

Using (C.9) and performing the integration over r with the help of the n -dimensional δ -function in (C.8) we obtain:

$$(PS)_3 = \frac{\pi^{1-\epsilon}}{(2\pi)^{5-4\epsilon}} \frac{1}{2\hat{s}} \frac{1}{\Gamma(1-\epsilon)} \int d\hat{t} d\hat{u} \left(\frac{\hat{t}\hat{u}}{\hat{s}}\right)^{-\epsilon} d^n k \delta_+(k^2) \delta_+[(p_1 + p_2 - q - k)^2] \quad (C.10)$$

The integration over k can be easily worked out in the rest frame of $k+r$ introduced in the first part of this Appendix. To this end, we write:

$$\delta(p_1 + p_2 - q - k)^2 = \delta(s_2 - 2\sqrt{s_2}k_0) = \frac{\delta(k_0 - \frac{\sqrt{s_2}}{2})}{2\sqrt{s_2}} \quad (C.11)$$

which is used to perform the integration of k_0 . Introducing spherical coordinates in $n-1$ dimensions, and integrating over irrelevant angles, we find with standard procedures⁽⁹¹⁾:

$$\int \frac{d^{n-1}k}{2k_0} \delta_+[(p_1 + p_2 - q - k)^2] = \frac{\pi^{-\epsilon}}{4} \frac{\Gamma(1-\epsilon)}{\Gamma(1-2\epsilon)} s_2^{-\epsilon} \int_0^\pi d\theta_1 \int_0^\pi d\theta_2 \sin^{1-2\epsilon} \theta_1 \sin^{-2\epsilon} \theta_2. \quad (C.12)$$

Finally, using Eqs. (C.10), (C.12) and relations (3.1.4) and (4.2.1), with

$$d\hat{t}d\hat{u} = \hat{s}^2 v dv dw, \quad (C.13)$$

we find for the 3-particle phase space differential with respect to v and w :

$$\frac{d(P\mathcal{S})_3}{dv dw} = N \frac{\hat{s}}{4\pi} [vw(1-w)]^{-\epsilon} \int_0^\pi d\theta_1 \int_0^\pi d\theta_2 \sin^{1-2\epsilon} \theta_1 \sin^{-2\epsilon} \theta_2 \quad (C.14)$$

where N is given by Eq.(4.1.12) with $\mu = 1$.

C.3 The Differential Cross Section

To find the contribution of the squared Matrix element $|M|^2$ to the differential cross section we first introduce the average value of $|M|^2$ over the angular variable θ_2 , that is,

$$|\tilde{M}|^2 \equiv \frac{1}{N_{\theta_2}} \int_0^\pi d\theta_2 \sin^{-2\epsilon} \theta_2 |M|^2 \quad (C.15)$$

with the normalization factor N_{θ_2} defined by

$$N_{\theta_2} \equiv \int_0^\pi d\theta_2 \sin^{-2\epsilon} \theta_2 = 2^{2\epsilon} \pi \frac{\Gamma(1-2\epsilon)}{\Gamma^2(1-\epsilon)}, \quad (C.16)$$

so that $|\tilde{M}|^2$ coincides with $|M|^2$ when the latter is independent of θ_2 .

Finally, we introduce the variable

$$y = \frac{1}{2}(1 - \cos \theta_1) \quad (C.17)$$

and using (C.14)–(C.16) we obtain for the differential cross section $d\sigma/dv dw$:

$$\frac{d\sigma}{dv dw} = \frac{N}{4} [vw(1-w)]^{-\epsilon} \frac{\Gamma(1-2\epsilon)}{\Gamma^2(1-\epsilon)} \int_0^1 dy y^{-\epsilon} (1-y)^{-\epsilon} |\tilde{M}|^2 \quad (C.18)$$

where N is again given by (4.1.12) with $\mu = 1$.

C.4 Integrals Encountered in the Calculations

We make use of the integral over phase space of the invariant quantity:

$$\Pi^a \equiv \frac{1}{(p_1 - k)^2 (p_2 - k)^2} = \frac{1}{2p_1 \cdot k \ 2p_2 \cdot k} \quad (C.19)$$

which is needed for the evaluation of the contribution of Fig. 15(a) to the differential cross section.

Using (C.3)–(C.6), we obtain:

$$\frac{d[(PS)_3 \Pi^a]}{dv dw} = \frac{N}{\pi \hat{s} v (1 - vw)} [vw(1-w)]^{-\epsilon} J^a(\psi) \quad (C.20)$$

where

$$J^a(\psi) \equiv \int_0^\pi d\theta_2 \int_0^\pi d\theta_1 \frac{\sin^{-2\epsilon} \theta_2 \sin^{1-2\epsilon} \theta_1}{(1 + \cos \theta_1)(1 + \cos \theta_2 \sin \theta_1 \sin \psi + \cos \theta_1 \cos \psi)} \quad (C.21)$$

This double integral is given in Ref. 58 its App. B. The result is :

$$J^a(\psi) = -\frac{\pi}{\epsilon} \left(\sin^2 \frac{\psi}{2}\right)^{-1-\epsilon} \left[1 + \epsilon^2 \mathcal{L}_{12}(\cos^2 \frac{\psi}{2})\right] \quad (C.22)$$

where $\mathcal{L}_{12}(x)$ denotes the Spence function

$$\mathcal{L}_{12}(x) \equiv -\int_0^x \frac{dt}{t} \ln(1-t). \quad (C.23)$$

For $w \rightarrow 1$ in view of (C.7) we find

$$J^a(\psi) \rightarrow -\frac{\pi}{\epsilon} \left(\frac{1-w}{1-v} \right)^{-1-\epsilon} \left(1 + \epsilon^2 \frac{\pi^2}{6} \right) \quad (C.24)$$

so that Eq. (C.20) becomes in this limit ($w \rightarrow 1$):

$$\frac{d[(PS)_3 \Pi^a]}{dv dw} \rightarrow \frac{N}{\hat{s}v} \left(\frac{v}{1-v} \right)^{-\epsilon} (1-w)^{-1-2\epsilon} \left(1 + \epsilon^2 \frac{\pi^2}{6} \right). \quad (C.25)$$

We notice that (C.21) is the only integral, among those appearing in initial state Brems contributions, which provides a factor $(1-w)^{-1-\epsilon}$ and hence a pole at $w = 1$ in $n = 4$ dimensions ($\epsilon = 0$).

For example consider the integral over phase space of the invariant quantity

$$\Pi^b \equiv \frac{1}{(p_1 - r)^2 (p_2 - k)^2} = \frac{1}{2p_1 \cdot r \ 2p_2 \cdot k} \quad (C.26)$$

encountered in the contribution of Fig. 15(b) to the differential cross section.

Using (C.3)–(C.6) we find that $d[(PS)_3 \Pi^b]/dv dw$ is given by Eq. (C.20) with $J^a(\psi)$ replaced by:

$$J^b(\psi) \equiv \int_0^\pi d\theta_2 \int_0^\pi d\theta_1 \frac{\sin^{-2\epsilon} \theta_2 \sin^{1-2\epsilon} \theta_1}{(1 - \cos \theta_1)(1 + \cos \theta_2 \sin \theta_1 \sin \psi + \cos \theta_1 \cos \psi)} \quad (C.27)$$

Changing in (C.27) integration variable,

$$\theta_1 \rightarrow \theta'_1 = \pi - \theta_1 \quad (C.28)$$

and introducing

$$\tilde{\psi} = \pi - \psi, \quad (C.29)$$

we find

$$J^b(\psi) = J^a(\tilde{\psi}) \quad (C.30)$$

where J^a is given by (C.22). Hence in view of (C.29) we immediately obtain:

$$J^b(\psi) = -\frac{\pi}{\epsilon} \left(\cos^2 \frac{\tilde{\psi}}{2} \right)^{-1-\epsilon} \left[1 + \epsilon^2 \mathcal{L}_{12}(\sin^2 \frac{\tilde{\psi}}{2}) \right] \xrightarrow{w \rightarrow 1} \left(-\frac{\pi}{\epsilon} \right) \quad (C.31)$$

Consequently this integral introduces no term $\sim (1-w)^{-1-2\epsilon}$ or $\sim (1-w)^{-1-\epsilon}$ to the associated differential cross section.

APPENDIX D

In this Appendix we present some details on the kinematics, the three particle phase space and related integrations expressed in terms of Sudakov variables. These variables were introduced in Eqs. (4.1.1)–(4.1.3) and used in Sect. 4.1.

D.1 Kinematics

As in App. C, we refer to the general $2 \rightarrow 3$ subprocess $a(p_1) + b(p_2) \rightarrow \gamma(q) + c(r) + d(k)$. In the C.M. of the two initial partons we set

$$p_1 = \frac{\sqrt{\hat{s}}}{2}(1; 0, \dots, 0, 1) \quad , \quad p_2 = \frac{\sqrt{\hat{s}}}{2}(1; 0, \dots, 0, -1) \quad (D.1)$$

and we specify the vectors ℓ (introduced in (4.1.1)) and q as follows:

$$\ell = (0; \dots, |\vec{\ell}| \cos \phi, |\vec{\ell}| \sin \phi, 0) \quad (D.2)$$

$$q = q_0(1; 0, \dots, \sin \gamma, 0, \cos \gamma) \quad (D.3)$$

where the dots in (D.1) denote $n - 4$ unspecified momentum components and q_0 and γ in (D.3) are determined so that (4.1.2) are satisfied. It is

$$q_0 = \frac{\sqrt{\hat{s}}}{2}(1 - v + vw) \quad , \quad \tan^2 \frac{\gamma}{2} = \frac{1 - v}{vw}. \quad (D.4)$$

Using $r = p_1 + p_2 - q - k = (1 - \alpha)p_1 + (1 - \beta)p_2 - q - \ell$, Eqs. (D.1)–(D.4) imply:

$$r^2 = \hat{s}\{v(1 - w) - \alpha v - \beta(1 - vw) - 2[\alpha\beta(1 - v)vw]^{\frac{1}{2}} \cos \phi\}. \quad (D.5)$$

We set:

$$A = (\alpha v)^{\frac{1}{2}} \quad , \quad B = (\beta(1 - v))^{\frac{1}{2}}; \quad (D.6)$$

then for $w \rightarrow 1$:

$$r^2 \rightarrow -\hat{s}(A^2 + B^2 + 2AB \cos \phi) \quad (D.7)$$

so that

$$-(A + B)^2 \leq r^2 / \hat{s} \leq -(A - B)^2. \quad (D.8)$$

Hence for general v , the on-shell condition $r^2 = 0$, for $w \rightarrow 1$ implies

$$\alpha \rightarrow 0, \beta \rightarrow 0 \quad (D.9)$$

and consequently in view of (4.1.1) and (4.1.3), $k \rightarrow 0$. We conclude that for $w \rightarrow 1$ nonzero contributions to the cross section $d\sigma/dv dw$ arise only from soft gluons.

D.2 Three Particle Phase Space Differential in v and w

We proceed to express the phase space integral, Eq. (C.10), in terms of integrations over the Sudakov parameters. To this end, we find

$$\int \frac{d^{n-1}k}{2k_0} \theta(r_0) = \frac{\hat{s}^{1-\epsilon}}{4} \int_0^1 d\beta \beta^{-\epsilon} \int_0^{1-\beta'} d\alpha \alpha^{-\epsilon} \int d\Omega_T \quad (D.10)$$

where $\int d\Omega_T$ denotes integration over a proper set of $n - 3$ angles, and β' , in the upper limit of the α integration, is determined from the condition $r_0 \geq 0$, which gives:

$$\beta' = \beta + (1 - w) \xrightarrow{w \rightarrow 1} \beta. \quad (D.11)$$

Then using (D.10), (C.13) and (C.10), we find for the three particle phase space differential in v and w :

$$\frac{d(P S)_3}{dvdw} = \frac{\hat{s}^2 \Gamma(1 - 2\epsilon)}{2\pi^{1-\epsilon} \Gamma(1 - \epsilon)} N w^{-\epsilon} \int_0^1 d\beta \beta^{-\epsilon} \int_0^{1-\beta'} d\alpha \alpha^{-\epsilon} \int d\Omega_T \delta(r^2) \quad (D.12)$$

where the factor N is given by Eq. (4.1.12) with $\mu = 1$, and $r = p_1 + p_2 - q - k$.

D.3 Certain Integrals

Now we consider the integral over phase space of the invariant

$$\Pi^a \equiv \frac{1}{(p_1 - k)^2 (p_2 - k)^2} = \frac{1}{\hat{s}^2 \alpha \beta} \quad (D.13)$$

where the second equality in (D.13) is due to relations (4.1.1) and (4.1.2). Then we obtain:

$$\frac{d[(PS)_3 \Pi^a]}{dvdw} = \frac{\Gamma(1 - 2\epsilon)}{2\pi^{1-\epsilon} \Gamma(1 - \epsilon)} N w^{-\epsilon} \int_0^1 d\beta \beta^{-1-\epsilon} \int_0^{1-\beta'} d\alpha \alpha^{-1-\epsilon} \int d\Omega_T \delta(r^2). \quad (D.14)$$

We are interested in the leading term as $w \rightarrow 1$; we have seen that in this case $\alpha \rightarrow 0$ and $\beta \rightarrow 0$. We proceed by first taking $\alpha \rightarrow 0$; then in view of (D.5) the argument of the δ -function in (D.14) becomes ϕ independent and all the angular integrations are easily carried out. Also the α integration is performed with β' in the upper limit replaced by β . Finally, the δ function is used to perform the β integration; this amounts to setting

$$\beta = \frac{v(1-w)}{1-vw}, \quad (D.15)$$

and dividing by $\hat{s}(1-vw)$. The final result (for $w \rightarrow 1$) is proportional to $(\Gamma(1-2\epsilon)/\Gamma^2(1-\epsilon))(v/(1-v))^{-\epsilon}(1-w)^{-1-\epsilon}(-1/\epsilon)$. For a more proper treatment we write:

$$\frac{d[(PS)_3 \Pi^a]}{dv dw} = \frac{N \Gamma(1-2\epsilon)}{\hat{s}v \Gamma^2(1-\epsilon)} \left(\frac{v}{1-v}\right)^{-\epsilon} (1-w)^{-1-\epsilon} \left(-\frac{1}{\epsilon}\right) g(v, w) \quad (D.16)$$

where $g(v, w)$ a function to be determined. Using

$$\frac{\Gamma(1-2\epsilon)}{\Gamma^2(1-\epsilon)} \simeq 1 + \epsilon^2 \frac{\pi^2}{8} + \dots \quad (D.17)$$

and comparing with Eq. (C.25) we obtain $g(v, w) = (1-w)^{-\epsilon}$.

Finally, instead of (D.13), consider

$$\tilde{\Pi}^a = \frac{F(\beta)}{(p_1 - k)^2 (p_2 - k)^2} = \frac{F(\beta)}{\hat{s}^2 \alpha \beta}. \quad (D.18)$$

where $F(\beta)$ a function smooth at $\beta = 0$ ($w = 1$). The same treatment easily leads to the following leading term for $w \rightarrow 1$:

$$\frac{d[(PS)_3 \tilde{\Pi}^a]}{dv dw} = \frac{N}{\hat{s}v} \left(\frac{v}{1-v}\right)^{-\epsilon} (1-w)^{-1-2\epsilon} \left(-\frac{1}{\epsilon}\right) \left(1 + \epsilon^2 \frac{\pi^2}{6}\right) F(0). \quad (D.19)$$

This result is easily understood by observing that the smooth function $F(\beta)$ can be expanded in powers of β :

$$F(\beta) = F(0) + \beta F'(0) + O(\beta^2); \quad (D.20)$$

then we notice that terms of order β and higher cancel the β in the denominator of (D.18) and hence the corresponding integrals do not contain terms proportional to $\beta^{-1-\epsilon}$ of $(1-w)^{-1-\epsilon}$. Consequently, the leading contribution arises from $F(0)$.

APPENDIX E

In this Appendix we present the basic relations by which results for the dominant part referred to the nonuniversal definition of corrections^(52a) are reduced to corresponding results referred to the universal definition⁽⁵³⁾ and vice versa. We also consider some related and other properties of distributions.

We consider the subprocess $q\bar{q} \rightarrow \gamma g$. Our expressions [Eq. (4.5.7)], for the coefficient functions of the dominant part $f_s(v, w)$, correspond to the universal definition of corrections,⁽⁵³⁾ specified by $u_{qq} = 0$ (Sect. 4.4). However, if corrections are defined as in Ref. 52(a) then $u_{qq}(x)$ is determined from (corrections to) DIS and is given by^(52a):

$$u_{qq}(x) = f_{qq}(x) = C_F \left[-\left(\frac{9}{2} + \frac{\pi^2}{3}\right) \delta(1-x) - \frac{3}{2} \frac{1}{(1-x)_+} + (1+x^2) \left(\frac{\ell n(1-x)}{1-x} \right)_+ - \frac{1+x^2}{1-x} \ell n x + 3 - 2x \right] \quad (E.1)$$

Then in view of Eq. (4.4.4) an additional term in $d\sigma^{fact}/dvdw$ is included and, for $w \rightarrow 1$, given by:

$$\frac{d\tilde{\sigma}^{fact}}{dvdw} = -F\tilde{T}_0(v) \left[f_{qq}(w) + \frac{v}{1-v} f_{qq}\left(\frac{1-v}{1-vw}\right) \right] \quad (E.2)$$

We are interested in contributions to the dominant part. Omitting terms regular at $w \rightarrow 1$ the first term in (E.2) gives

$$f_{qq}(w) \rightarrow C_F \left[-\left(\frac{9}{2} + \frac{\pi^2}{3}\right) \delta(1-w) - \frac{3}{2} \frac{1}{(1-w)_+} + 2 \left(\frac{\ell n(1-w)}{1-w} \right)_+ \right]. \quad (E.3)$$

To treat the second term in (E.2) we need the expressions of the distributions $1/(1-x)_+$ and $(\ell n(1-x)/(1-x))_+$ with $x = (1-v)/(1-vw)$. To this end, we use the expansion

$$(1-x)^{-1-\epsilon} = -\frac{1}{\epsilon} \delta(1-x) + \frac{1}{(1-x)_+} - \epsilon \left(\frac{\ell n(1-x)}{1-x} \right)_+ + 0(\epsilon^2) \quad (E.4)$$

and since for $x = (1-v)/(1-vw)$

$$(1-x)^{-1-\epsilon} = \left(\frac{v(1-w)}{1-vw} \right)^{-1-\epsilon} = \left(\frac{v}{1-vw} \right)^{-1-\epsilon} (1-w)^{-1-\epsilon} \quad (E.5)$$

we obtain by expanding $(1-w)^{-1-\epsilon}$ and $(v/(1-vw))^{-\epsilon}$ in powers of ϵ :

$$(1-x)^{-1-\epsilon} = \frac{1-vw}{v} \left\{ -\frac{1}{\epsilon} \delta(1-w) + \left[\frac{1}{(1-w)_+} + \ell n \frac{v}{1-v} \delta(1-w) \right] \right. \\ \left. -\epsilon \left[\left(\frac{\ell n(1-w)}{1-w} \right)_+ + \ell n \left(\frac{v}{1-vw} \right) \frac{1}{(1-w)_+} + \frac{1}{2} \ell n^2 \left(\frac{v}{1-v} \right) \delta(1-w) \right] \right\}. \quad (E.5)$$

Comparing similar powers of ϵ in (E.4) and (E.6), we obtain the identities (see also Ref. 58):

$$\delta(1-x) = \frac{1-v}{v} \delta(1-w) \quad (E.6a)$$

$$\frac{1}{(1-x)_+} = \frac{1-vw}{v} \left[\frac{1}{(1-w)_+} + \ell n \left(\frac{v}{1-v} \right) \delta(1-w) \right] \quad (E.6b)$$

$$\left(\frac{\ell n(1-x)}{1-x} \right)_+ = \frac{1-vw}{v} \left[\left(\frac{\ell n(1-w)}{1-w} \right)_+ + \ell n \left(\frac{v}{1-vw} \right) \frac{1}{(1-w)_+} + \frac{1}{2} \ell n^2 \frac{v}{1-v} \delta(1-w) \right]. \quad (E.6c)$$

Now, using (E.6) we find for $w \rightarrow 1$:

$$\frac{v}{1-v} f_{qq} \left(\frac{1-v}{1-vw} \right) = C_F \left\{ \left[\left(-\frac{9}{2} + \frac{\pi^2}{3} \right) - \frac{3}{2} \ell n \left(\frac{v}{1-v} \right) + \ell n^2 \left(\frac{v}{1-v} \right) \right] \delta(1-w) \right. \\ \left. + \left[-\frac{3}{2} + 2 \ell n \left(\frac{v}{1-v} \right) \right] \frac{1}{(1-w)_+} + 2 \left(\frac{\ell n(1-w)}{1-w} \right)_+ \right\} \quad (E.7)$$

Then, denoting by $\bar{f}^{NU}(v, w)$ the HOC corresponding to the definition of corrections in accord with Ref. 52(a) (Eq. (E.1)), and decomposing $\bar{f}_s^{NU}(v, w)$ as in Eq. (4.5.6) with $\bar{a}_1(v)$ replaced by $\bar{a}_1^{NU}(v)$ etc., we find:

$$\bar{a}_1^{NU}(v) = \bar{a}_1(v) + C_F \left[\left(9 + \frac{2\pi^2}{3} \right) + \frac{3}{2} \ell n \left(\frac{v}{1-v} \right) - \ell n^2 \left(\frac{v}{1-v} \right) \right] E(v) \\ \bar{b}_1^{NU}(v) = \bar{b}_1(v) + C_F \left[3 - 2 \ell n \left(\frac{v}{1-v} \right) \right] B(v) \\ \bar{c}^{NU}(v) = \bar{c}(v) - 4 C_F B(v). \quad (E.8)$$

Here, $\bar{a}_1(v)$, $\bar{b}_1(v)$, $\bar{c}(v)$ and $B(v)$ refer to $q\bar{q} \rightarrow \gamma g$ and are given by Eqs. (4.5.7) and (4.3.2).

Similarly for $qg \rightarrow \gamma q$ (Ch. 5) with the definition of corrections corresponding to the nonuniversal choice:

$$u_{qq}(x) = f_{qq}(x), \quad u_{gg}(x) = 0 \quad (E.9)$$

we find:

$$\begin{aligned}
 \bar{a}_1^{NU}(v) &= \bar{a}_1(v) + C_F \left[\frac{9}{2} + \frac{\pi^2}{3} + \frac{3}{2} \ell n \left(\frac{v}{1-v} \right) - \ell n^2 \left(\frac{v}{1-v} \right) \right] B_g(v) \\
 \bar{b}_1^{NU}(v) &= \bar{b}_1(v) + C_F \left[\frac{3}{2} - 2 \ell n \left(\frac{v}{1-v} \right) \right] B_g(v) \\
 \bar{c}^{NU}(v) &= \bar{c}(v) - 2 C_F B_g(v).
 \end{aligned} \tag{E.10}$$

In (E.10), $\bar{a}_1(v)$, $\bar{b}_1(v)$, $\bar{c}(v)$ and $B_g(v)$ refer to $qg \rightarrow \gamma q$ and are given by Eqs. (5.4.2) and (5.3.2).

Finally, we provide some other relations among distributions which are helpful in Ch. 6. First, for the distributions $(\ell n^k x/x)_{A+}$ $k = 0, 1, \dots$ defined in the interval $(0, A)$ as in Eqs. (6.2.2), we easily find the transformation

$$\left(\frac{\ell n^k x}{x} \right)_{A+} = \left(\frac{\ell n^k x}{x} \right)_+ - \frac{1}{k+1} \ell n^{k+1} A \delta(x) \tag{E.11}$$

which reduces them to the standard distributions defined in the interval $(0, 1)$. Second, following a procedure similar to that leading to (E.6), we find for any constant λ :

$$\frac{1}{(\lambda x)_+} = \frac{1}{\lambda} \left[\frac{1}{x_+} + \ell n \lambda \delta(x) \right]$$

and,

$$\left(\frac{\ell n(\lambda x)}{\lambda x} \right)_+ = \frac{1}{\lambda} \left[\left(\frac{\ell n x}{x} \right)_+ + \ell n \lambda \frac{1}{x_+} + \frac{1}{2} \ell n^2 \lambda \delta(x) \right]. \tag{E.12}$$

Very similar relations are obtained under $x \leftrightarrow 1-x$.

APPENDIX F

Here we present the coefficient functions of the terms comprising, as in Eq. (7.1.1), the nondominant part \tilde{f} of the HOC. In accord with Sect. 7.1 we find:

$$\begin{aligned}
 \bar{d}(v, w) &= C_F[-(1-2v)^2 - (1-2v+4v^2)w - \frac{v(1-v)}{X^2} + \frac{v(1-2v)}{X}] \\
 \bar{e}(v, w) &= \bar{d}(v, w) \\
 \bar{f}(v, w) &= 2C_F v(-1+v+vw) + N_c v(2-v-vw) \\
 \bar{g}(v, w) &= 0 \\
 \bar{h}(v, w) &= 2C_F[-1-vw + \frac{1+(1-v)^2}{X}] + N_c[1-v^2 + v(1-v)w - \frac{1+(1-v)^2}{X}] \\
 \bar{i}(v, w) &= \bar{h}(v, w) \\
 \bar{j}(v, w) &= C_F[1+8v(1-v) - w(1-4v+8v^2) - \frac{v(1-v)}{X^2} - \frac{4-5v+4v^2}{X}] \\
 &\quad + N_c[-1-2v(1-v) - v(1-2v)w + \frac{1+(1-v)^2}{X}] \\
 \bar{k}(v, w) &= C_F[-4v(1-v) + (1+v-4v^2)w + \frac{v(1-v)}{X}(\frac{1}{X}+1)] \\
 &\quad + \frac{N_c}{2}[3+(1-4v)w + \frac{v(1-v)}{X^2} - \frac{v(1-4v)}{X}] + bv(v-2+vw) \\
 \bar{l}(v, w) &= 0 \\
 \bar{m}(v, w) &= N_c B(v) \\
 \bar{n}(v, w) &= (-4C_F + N_c)B(v) \tag{F.1}
 \end{aligned}$$

with $X = 1 - vw$ and $B(v) = v^2 + (1 - v)^2$. (Cf. Eqs. (7.1.4) and (4.3.2)).

TABLE I. Soft gluon factors for graphs in Fig. 6. The entries give the factors for *A* type (Figs. 6(a)–6(f)) and *B* type (Figs. 6(g)–6(l)) Born terms. Here $M(P)^{\alpha\mu} \equiv \overline{M}(P)^{\alpha\mu} t_a$ and $\Gamma_L(\epsilon) = \Gamma(1 + \epsilon)\Gamma^2(1 - \epsilon)/\Gamma(1 - 2\epsilon)$.

Graph	Factor	Dirac and Color Structure
<i>a</i> (<i>g</i>)	$\frac{\alpha_s N_c}{4\pi} \frac{N_c}{2} \Gamma_L(\epsilon) \left(\frac{-2}{\epsilon^2}\right) \left(\frac{-2p_1 \cdot p_2}{4\pi\mu^2}\right)^{-\epsilon}$	
<i>b</i> (<i>h</i>)	$\frac{\alpha_s}{4\pi} \left(C_F - \frac{N_c}{2}\right) \Gamma_L(\epsilon) \left(\frac{-2}{\epsilon^2}\right) \left(\frac{2p_2 \cdot r}{4\pi\mu^2}\right)^{-\epsilon}$	$\overline{M}_{A(B)}^{(1)}(P)^{\alpha\mu} t_a$
<i>c</i> (<i>i</i>)	$\frac{\alpha_s N_c}{4\pi} \frac{N_c}{2} \Gamma_L(\epsilon) \left(\frac{-2}{\epsilon^2}\right) \left(\frac{2p_1 \cdot r}{4\pi\mu^2}\right)^{-\epsilon}$	
<i>d</i> (<i>j</i>)	$g \frac{2p_1^\rho}{-2p_1 \cdot k}$	$i f_{acb} \overline{M}_{A(B)}^{(1)}(P)^{\alpha\mu} t_b$
<i>e</i> (<i>k</i>)	$g \frac{2r^\rho}{-2r \cdot k}$	$\overline{M}_{A(B)}^{(1)}(P)^{\alpha\mu} t_c t_a$
<i>f</i> (<i>l</i>)	$g \frac{2p_2^\rho}{2p_2 \cdot k}$	$\overline{M}_{A(B)}^{(1)}(P)^{\alpha\mu} t_a t_c$

TABLE II. Soft gluon factors for $q^0 d\sigma^{(2)}/d^3q$ as multiples of the Born cross section. Unitarity graphs in horizontal rows of Fig. 7 have identical factors multiplying the Born term at the top of each column. To find the contribution of e.g. the set $(BB'FF')$ in Fig. 7, replace $(CC'GG')$ respectively and c with b in Table II. Here $\Gamma_B(\epsilon) = \Gamma(1 - \epsilon)/\Gamma(1 - 2\epsilon)$ and $\Gamma_L(\epsilon) = \Gamma(1 + \epsilon)\Gamma^2(1 - \epsilon)/\Gamma(1 - 2\epsilon)$

Graph	Factor	Born Term
C	$\frac{\alpha_s}{2\pi} \frac{N_c}{2} \frac{2}{\epsilon^2} \Gamma_B(\epsilon) \left \frac{\hat{s}}{4\pi\mu^2} \right ^{-\epsilon}$	$q^0 d\sigma_c^{(1)}/d^3q$
C'	$\frac{\alpha_s}{2\pi} \frac{N_c}{2} \left(\frac{-2}{\epsilon^2} + \theta(p_1 \cdot p_2) \pi^2 \right) \Gamma_L(\epsilon) \left \frac{\hat{s}}{4\pi\mu^2} \right ^{-\epsilon}$	
G	$\frac{\alpha_s}{2\pi} \left(C_F - \frac{N_c}{2} \right) \frac{2}{\epsilon^2} \Gamma_B(\epsilon) \left \frac{2p_1 \cdot r}{4\pi\mu^2} \right ^{-\epsilon}$	
G'	$\frac{\alpha_s}{2\pi} \left(C_F - \frac{N_c}{2} \right) \left(-\frac{2}{\epsilon^2} + \theta(-p_1 \cdot r) \pi^2 \right) \Gamma_L(\epsilon) \left \frac{2p_1 \cdot r}{4\pi\mu^2} \right ^{-\epsilon}$	

TABLE III. Moments of some functions in $f(v, w)$, Eq. (3.1.6).

$\phi(w)$	$M(k)$	$M(k)$ for large k
$\delta(1-w)$	1	1
$\frac{1}{(1-w)_+}$	$-(\gamma + \psi(k))$	$-\ell n k$
$(\frac{\ell n(1-w)}{1-w})_+$	$\frac{1}{2}[(\gamma + \psi(k))^2 - \psi'(k) + \frac{\pi^2}{6}]$	$\frac{1}{2} \ell n^2 k$
1	$\frac{1}{k}$	$\frac{1}{k}$
$\ell n w$	$-\frac{1}{k^2}$	$-\frac{1}{k}$
$\ell n(1-w)$	$-(\psi(k) + \gamma + \frac{1}{k}) \frac{1}{k}$	$-\frac{\ell n k}{k}$
$\ell n w / (1-w)$	$-\psi'(k)$	$\frac{1}{k}$
w^ℓ	$\frac{1}{k+\ell}$	$\frac{1}{k}$
$w^\ell \ell n w$	$-\frac{1}{(k+\ell)^2}$	$-\frac{1}{k^2}$
.	.	.
.	.	.
.	.	.
$w^\ell \phi(w)$	$M(\ell + k)$	$M(k)$

TABLE IV. Parametrization of the momenta p_1, p_2, q, r and k of the subprocess $a(p_1) + b(p_2) \rightarrow \gamma(q) + c(r) + d(k)$ in the C.M. frame of c and d . In this frame, system $S_i (i = 1, 2)$ is defined by choosing \vec{p}_i along the z axis. See also App. C and Fig. 17. The variables v, w and s_2 are defined in Eqs. (3.1.3) and (4.2.1).

	$r = \frac{\sqrt{s_2}}{2}(1, \dots, \cos \theta_2 \sin \theta_1, \cos \theta_1)$ $k = \frac{\sqrt{s_2}}{2}(1, \dots, -\cos \theta_2 \sin \theta_1, -\cos \theta_1)$	
	SYSTEM S_1	SYSTEM S_2
$p_1 =$	$\frac{\hat{s}v}{2\sqrt{s_2}}(1, 0, \dots, 0, 1)$	$\frac{\hat{s}v}{2\sqrt{s_2}}(1, 0, \dots, \sin \psi, \cos \psi)$
$p_2 =$	$\frac{\hat{s}(1-vw)}{2\sqrt{s_2}}(1, 0, \dots, \sin \psi, \cos \psi)$	$\frac{\hat{s}(1-vw)}{2\sqrt{s_2}}(1, 0, \dots, 0, 1)$
$q =$	$\frac{\hat{s}(1-v+vw)}{2\sqrt{s_2}}(1, 0, \dots, \sin \delta, \cos \delta)$	$\frac{\hat{s}(1-v+vw)}{2\sqrt{s_2}}(1, 0, \dots, \sin \delta', \cos \delta')$
	$\sin^2 \frac{\delta}{2} = \frac{(1-v)(1-w)}{1-v+vw}, \cos^2 \frac{\delta}{2} = \frac{w}{1-v+vw}$	$\sin^2 \frac{\delta'}{2} = \frac{v^2w(1-w)}{(1-vw)(1-v+vw)}, \cos^2 \frac{\delta'}{2} = \frac{1-v}{(1-vw)(1-v+vw)}$
	$\sin^2 \frac{\psi}{2} = \frac{1-w}{1-vw}, \cos^2 \frac{\psi}{2} = \frac{w(1-v)}{1-vw}$	

TABLE V. Upper part: Scalar products of the momenta listed in TABLE IV. Lower part: Symmetric under $k \leftrightarrow r$ (or $y \leftrightarrow (1 - y)$) combinations of these products used in Sect. 4.2 case (ii). Each combination is listed under the proper system S_1 or S_2 in which it is θ_2 independent. Of course, the integrated over phase space result is the same in any system.

SYSTEM S_1	SYSTEM S_2
$2p_1 \cdot r = \hat{s}vy$ $2p_1 \cdot k = \hat{s}v(1 - y)$ $2p_2 \cdot r = \hat{s}[w(1 - v)y + (1 - w)(1 - y) - A_1 \cos \theta_2]$ $2p_2 \cdot k = \hat{s}[w(1 - v)(1 - y) + (1 - w)y + A_1 \cos \theta_2]$ $2q \cdot r = \hat{s}[wy + (1 - v)(1 - w)(1 - y) - A_1 \cos \theta_2]$ $2q \cdot k = \hat{s}[w(1 - y) + (1 - v)(1 - w)y + A_1 \cos \theta_2]$ $A_1 = 2[y(1 - y)(1 - v)w(1 - w)]^{\frac{1}{2}}$	$2p_2 \cdot r = \hat{s}(1 - vw)y$ $2p_2 \cdot k = \hat{s}(1 - vw)(1 - y)$ $2p_1 \cdot r = \frac{\hat{s}}{1 - vw}[v(1 - v)wy + v(1 - w)(1 - y) - A_2 \cos \theta_2]$ $2p_1 \cdot k = \frac{\hat{s}}{1 - vw}[v(1 - v)w(1 - y) + v(1 - w)y + A_2 \cos \theta_2]$ $2q \cdot r = \frac{\hat{s}}{1 - vw}[v^2w(1 - w)(1 - y) + (1 - v)y - A_2 \cos \theta_2]$ $2q \cdot k = \frac{\hat{s}}{1 - vw}[v^2w(1 - w)y + (1 - v)(1 - y) + A_2 \cos \theta_2]$ $A_2 = 2v[y(1 - y)(1 - v)w(1 - w)]^{\frac{1}{2}}$
$4(p_1 \cdot r)(p_1 \cdot k) = (\hat{s} + \hat{t})^2 Y$ $4[(p_1 \cdot r)(q \cdot r) + (p_1 \cdot k)(q \cdot k)] = -\hat{s}\hat{u}Y_s - 2\hat{t}s_2 Y$ $4[(p_1 \cdot r)(q \cdot k) + (p_1 \cdot k)(q \cdot r)] = -\hat{t}s_2 Y_s - 2\hat{s}\hat{u}Y$	$4(p_2 \cdot r)(p_2 \cdot k) = (\hat{s} + \hat{u})^2 Y$ $4[(p_2 \cdot r)(q \cdot r) + (p_2 \cdot k)(q \cdot k)] = -\hat{s}\hat{t}Y_s - 2\hat{u}s_2 Y$ $4[(p_2 \cdot r)(q \cdot k) + (p_2 \cdot k)(q \cdot r)] = -\hat{u}s_2 Y_s - 2\hat{s}\hat{t}Y$
$4[(p_1 \cdot r)(p_2 \cdot r) + (p_1 \cdot k)(p_2 \cdot k)] = \hat{t}\hat{u}Y_s + 2\hat{s}s_2 Y$ $4[(p_1 \cdot r)(p_2 \cdot k) + (p_1 \cdot k)(p_2 \cdot r)] = \hat{s}s_2 Y_s + 2\hat{t}\hat{u}Y$ $4(q \cdot r)(q \cdot k) = (\hat{t} + \hat{u})^2 Y$	

TABLE VI. Contributions to the squared amplitude of $q\bar{q} \rightarrow \gamma gg$, from final Brems Figs. 16(a)–16(g). Terms with simple and double poles at $w = 1$ ($s_2 = 0$) are presented. The latter cancel in pairs of graphs, while the former sum up to a contribution proportional to the Born squared amplitude times the split function $P_{gg}(y) = \frac{1}{Y} - 2 + Y$ ($Y = y(1 - y)$). For the expressions defining $Ag, \tilde{T}_0(v), T_0(v, \epsilon), s_2$ etc. see Sect. 4.2.

Graph of Fig. 16	$Ag\tilde{T}_0(v)$						$2Ag$						$2Ag\hat{s}/s_2$					
	1			ϵ			1			ϵ			1			ϵ		
	$\frac{1}{Y}$	1	Y	$\frac{1}{Y}$	1	Y	$\frac{1}{Y}$	1	Y	$\frac{1}{Y}$	1	Y	$\frac{1}{Y}$	1	Y	$\frac{1}{Y}$	1	Y
(a)	2	-2		-2	2													
(b)	3			-2	2		1	2		-2	2							
(c)	-1	-2					-1	-2		-2	2							
(d)		-4	5		4	-4							-1	-5			-1	4
(e)										4	-5		1	5			1	-4
(f)			-1										$-\frac{1}{4}$	1				
(g)											1		$\frac{1}{4}$	-1				
Total	4	-8	4	-4	8	-4	0	0	0	-4	8	-4	0	0	0	0	0	0
(a)–(g)	$4(1 - \epsilon)P_{gg}(y)$						$-4\epsilon P_{gg}(y)$						0					
$T_{a-g} = 4AgP_{gg}(y)[(1 - \epsilon)\tilde{T}_0(v) - 2\epsilon] = C\frac{1}{s_2}N_cP_{gg}(y)T_0(v, \epsilon)$																		

FOOTNOTES

- (f0) Subsequent more accurate determinations of the experimental $E d\sigma/d^3p$ for $pp \rightarrow \pi^0 + X$ led to lower cross sections. Use of them results in γ/π^0 ratios higher than those shown in Figs. 4(a), (b). (see Fig. 10).
- (f1) For $w \rightarrow 1$, the replacement (4.2.4) is equivalent with the replacements: $k \rightarrow (1-y)p_3$, $r \rightarrow yp_3$, where $p_3 \equiv k+r$ and $p_3^2 \rightarrow 0$. These are equally effective in reducing the number of terms. Also they dictate that in any other frame, for $w \rightarrow 1$, the partons with 4-momenta k and r become collinear to the parton with 4-momentum p_3 .
- (f2) We thank P. Aurenche et al. for providing us with their computer outputs.
- (f3) One may equally well use the split function $P_{gq}(y, \epsilon)$; then in view of $P_{gq}(y, \epsilon) = P_{gq}(1-y, \epsilon)$ the integral in Eq. (5.2.8) leads to the same results.
- (f4) For $x_T \gtrsim 0.1$ the contribution of \tilde{f} to the HOC is $\lesssim 45\%$, and decreases with x_T with the same rate as the contribution of \tilde{f} to the total inclusive cross section (cf. Fig. 12(b)). We have verified many of the results of Ch. 3 and of Ref. 11, using the complete HOC which we have determined in Ch. 7 and used in Ch. 8.
- (f5) This is indeed found to be the case in our subsequent calculations (Ch. 8). For smaller x_T , \tilde{f} contributes more, in particular since $qg \rightarrow \gamma q$ involves a gluon distribution which is large at small x_T .
- (f6) An example of large and negative HOC is provided by the decay $Y \rightarrow H + \gamma$.^{(75),(76)}
- (f7) Referring to Eq. (7.3.4), the corresponding expression of Ref. 54(b) involves a color factor C_F instead of $T(R)$. We have checked, however, that (7.3.4) leads to the correct results for the collinear photon Brems contributions.
- (f8) Several nondominant terms, arising from the implementation of factorization, can be directly tested. An example of such a term is the coefficient $\bar{d}(v, w)$ of $\ln(\hat{s}/M^2)$ (see Eq. (7.1.1)).
- (f9) Use of leading logarithm summation leads also to a contribution from $g \rightarrow \gamma$.

As we stated in Subsect. 2.1.3 contributions of this type are known to be small;^{(50),(51)} here they are neglected.

- (f10) For not too large $\Delta\eta$, $\Delta\phi$ one finds $R \simeq 2 \cosh \eta \sin(\delta/4)$, where δ is the angle opening of a cone with the photon as its axis.
- (f11) By some misunderstanding, in this publication the presented predictions of their Ref. 10 correspond to a different rapidity range.

REFERENCES

1. a) A.P. Contogouris, R. Gaskell and S. Papadopoulos, *Phys. Rev. D* **17** (1978) 2314.
b) A.P. Contogouris, R. Gaskell and S. Papadopoulos, *Nuovo Cim.* **51A** (1979) 263.
c) A.P. Contogouris, R. Gaskell and S. Papadopoulos, in *Proceedings of the IX International Symposium on H.E. Multiparticle Dynamics (Tabor, Czechoslovakia, 1978)* p. D-61.
d) S. Papadopoulos, "Quantum Chromodynamics and the Production of Hadrons at Large Transverse Momentum", M.Sc. Thesis, McGill University, Montreal (1979).
2. A.P. Contogouris, S. Papadopoulos and M. Hongoh, *Phys. Rev. D* **19** (1979) 2607.
3. I.J.R. Aitchison, A.P. Contogouris, S. Papadopoulos et al., *Phys. Lett.* **B91** (1980) 275.
4. A.P. Contogouris, S. Papadopoulos and J. Ralston, *Phys. Lett.* **B104** (1981) 70.
5. A.P. Contogouris, S. Papadopoulos and J. Ralston, *Phys. Rev. D* **25** (1982) 1280.
6. a) A.P. Contogouris, S. Papadopoulos and J. Ralston, in *Proceedings of the XII International Symposium on Multiparticle Dynamics, Notre Dame, Indiana, 1981 (World Scientific)* p. 639.
b) A.P. Contogouris, S. Papadopoulos and J. Ralston, in "Perturbative Quantum Chromodynamics", *Proceedings of Florida State University Workshop, Tallahassee, 1981 (Am. Institute of Physics)* p. 410.
7. A.P. Contogouris, S. Papadopoulos and J. Ralston, *Phys. Rev. D* **25** (1982) 2218.
8. A.P. Contogouris, J. Kripfganz, L. Marleau and S. Papadopoulos, in *Proceedings of 15th Rencontre de Moriond, Les Arcs, France, March 1980, (Editions Frontières)* p. 477.

9. A.P. Contogouris, L. Marleau and S. Papadopoulos, *Phys. Rev. D* 22 (1980) 1629.
10. a) A.P. Contogouris, S. Papadopoulos and C. Papavassiliou, *Nucl. Phys. B* 179 (1981) 461.
 b) A.P. Contogouris, S. Papadopoulos, C. Papavassiliou and E.N. Argyres, in *Proceedings of the XI International Symposium on H.E. Multiparticle Dynamics, Bruges, Belgium (1980)* p. 497.
11. A.P. Contogouris, N. Mebarki and H. Tanaka, in "Progress of Theoretical Physics", *Proceedings of the Tenth Annual Montreal-Rochester-Syracuse-Toronto Meeting, May 1988*, (World Scientific) p. 103.
12. N. Mebarki, Ph.D. Thesis, McGill University, Montreal (1988).
13. H.D. Politzer, *Phys. Reports* 14C (1974) 129.
14. J. Ellis, in *Proceedings of "Les Houches" Summer School, 1976* (North Holland 1977), p. 1.
15. W.J. Marciano and H. Pagels, *Phys. Reports* 36C (1978) 137.
16. M. Jacob and P. Landshoff, *Phys. Reports* 48C (1978) 285.
17. A.J. Buras, *Rev. Mod. Phys.* 52 (1980) 199.
18. E. Reya, *Phys. Reports* 69 (1981) 195.
19. G. Altarelli, *Phys. Reports* 81 (1982) 1.
20. A.P. Contogouris, in *Proceedings of the 1st International School of Elementary Particle Physics, Corfu, Greece, September 1982* (World Scientific) p. 173.
21. W.J. Stirling, in *Proceedings of the 3rd International School of Elementary Particle Physics, Corfu, Greece, September 1989*, (World Scientific) to be published.
22. C. Itzykson and J.-B. Zuber, "Quantum Field Theory" (McGraw-Hill 1980).
23. T. Muta, "Foundations of Quantum Chromodynamics – An Introduction to Perturbative Methods in Gauge Theories" (World Scientific 1987).
24. T.-P. Cheng and L.-F. Li, "Gauge Theory of Elementary Particle Physics" (Oxford University Press 1986).
25. I.J.R. Aitchison and A.J.G. Hey, "Gauge Theories in Particle Physics", 2nd edition (Hilger, Bristol 1989).

26. D.J. Gross and F. Wilczek, *Phys. Rev. Lett.* 30 (1973) 1343; H.D. Politzer, *Phys. Rev. Lett.* 30 (1973) 1346.
27. D.W. Duke and R.G. Roberts, *Phys. Reports* 120 (1985) 275.
28. a) R.P. Feynman, *Phys. Rev. Lett.* 23 (1969) 1415; "Photon-Hadron Interactions" (Benjamin, New York 1972).
 b) J.D. Bjorken, *Phys. Rev.* 179 (1969) 1547.
 c) S.M. Berman, J.D. Bjorken and J. Kogut, *Phys. Rev.* D4 (1971) 3388.
29. a) H.D. Politzer, *Nucl. Phys.* B129 (1977) 301.
 b) C.T. Sachrajda, *Phys. Lett.* B73 (1978) 185; *Phys. Lett.* B76 (1978) 100.
30. A.H. Mueller, *Phys. Rev.* D18 (1978) 3705; *Phys. Reports* 73 (1981) 237.
31. a) S.B. Libby and G. Sterman, *Phys. Rev.* D19 (1979) 2468.
 b) Yu. L. Dokshitzer, D.I. Dyakonov and S.I. Troyan, *Phys. Lett.* B78 (1978) 290; *Phys. Reports* 58 (1980) 269.
 c) R.K. Ellis et al., *Phys. Lett.* B78 (1978) 281; *Nucl. Phys.* B152 (1979) 285.
 d) D. Amati, R. Petronzio and G. Veneziano, *Nucl. Phys.* B140 (1978) 54; *ibid* B146 (1978) 29.
32. G. Altarelli and G. Parisi, *Nucl. Phys.* B126 (1977) 298.
33. B. Cox, in "Proceedings of the 1979 International Symposium on Lepton and Photon interactions at High Energies, Fermilab" (Fermilab, Batavia, Illinois, 1980), p. 602.
34. M. Tannenbaum, in "Particles and Fields - 1979", Proceedings of the Annual Meeting of the Division of Particles and Fields of APS, Montreal, 1979 (Am. Institute of Physics, New York 1980) p. 263.
35. P. Darriulat, *Ann. Rev. Nucl. Part. Sci.* 30 (1980) 159.
36. W. Willis, in Proceedings of the 4th International Colloquium on Photon-Photon Interactions, Paris, 1981 (World Scientific, Singapore, 1981).
37. L. Resvanis, in Multiparticle Dynamics, 1981, proceedings of the XII International Symposium, Notre Dame, Indiana, (World Scientific, Singapore, 1982).
38. T. Ferbel and W. Molzon, *Rev. Mod. Phys.* 56 (1984) 181.
39. Proceedings of Advanced Research Workshop on QCD Hard Hadronic Processes, St. Croix, US Virgin Islands, October 1987, (Plenum Corp.).

40. T. Ferbel, presented at "Physics in Collision", Capri, Italy, October 1988, Rochester preprint UR-1097.
41. F. Halzen and D. Scott, Phys. Lett. 40 (1978) 1117; Phys. Rev. D18 (1978) 3378.
42. R. Ruckl, S. Brodsky and J. Gunion, Phys. Rev. D18 (1978) 2469.
43. M. Glück and E. Reya, Phys. Rev. D14 (1976) 3034.
44. J. Owens and E. Reya, Phys. Rev. D17 (1978) 3008.
45. A. Buras and K. Gaemers, Nucl. Phys. B132 (1978) 249.
46. G. Fox, Nucl. Phys. B131 (1977) 107; *ibid* B134 (1978) 269.
47. P. Aurenche and J. Lindfors, Nucl. Phys. B168 (1980) 296.
48. W. Frazer and J. Gunion, Phys. Rev. D20 (1979) 147.
49. A. Nicolaidis, Nucl. Phys. B163 (1980) 156.
50. E. Berger, E. Braaten and R. Field, Nucl. Phys. B239 (1984) 52.
51. E. Argyres et al., Phys. Rev. D29 (1984) 2527.
52. a) G. Altarelli, R.K. Ellis and G. Martinelli, Nucl. Phys. B143 (1978) 521; (E) B146 (1978) 544; *ibid* B157 (1979) 461.
b) J. Kubar-André and F.E. Paige, Phys. Rev. D19 (1979) 221.
c) B. Humpert and W.L. van Neerven, Nucl. Phys. B184 (1981) 225.
53. L. Beaulieu and C. Kounnas, Nucl. Phys. B141 (1978) 423; J. Kodaira and T. Uematsu, *ibid* B141 (1978) 497.
54. R. Ellis, G. Martinelli and R. Petronzio, a) Phys. Lett. B104 (1981) 45; b) Nucl. Phys. B211 (1983) 106.
55. A.P. Contogouris, Phys. Rev. D26 (1982) 1618.
56. A.P. Contogouris and H. Tanaka, Phys. Rev. D33 (1986) 1265; Proceedings of the Europhysics Conference on H.E. Physics, Bari, Italy, July 1985, p. 186.
57. A.P. Contogouris, N. Mebarki, H. Tanaka and S. Vlassopoulos, in Proceedings of the XXIII International Conference on H.E. Physics, Berkeley, California, July 1986, p. 1131.
58. R.K. Ellis, M.A. Furman, H.E. Haber and I. Hinchliffe, Nucl. Phys. B173 (1980) 397.
59. P. Aurenche et al., a) Nucl. Phys. B297 (1988) 661; b) computer outputs.^(f2)

60. A.P. Contogouris and S. Papadopoulos, Nucl. Phys. B (in press).
61. A.P. Contogouris, N. Mebarki and S. Papadopoulos, Int. J. Mod. Phys. A (in press).
62. D. Duke and J. Owens, Phys. Rev. D30 (1984) 49.
63. P. Aurenche et al., Z. Phys. C24 (1984) 309; *ibid* C29 (1985) 423.
64. P. Astbury et al. (NA14 Collab.), Phys. Lett. B152 (1985) 419.
65. P. Aurenche et al., a) Phys. Lett. B135 (1984) 164; b) *ibid* B140 (1984) 87.
66. P. Aurenche et al., Nucl. Phys. B286 (1987) 553.
67. A.P. Contogouris, N. Mebarki and H. Tanaka, Phys. Rev. D37 (1988) 2458.
68. a) P. Stevenson, Phys. Rev. D23 (1981) 2916.
b) H.D. Politzer, Nucl. Phys. B194 (1982) 493.
c) P. Stevenson and H.D. Politzer, *ibid*, B277 (1986) 758.
69. G. Grunberg, Phys. Lett. B95 (1980) 70; Phys. Rev. D29 (1984) 2315.
70. R.K. Ellis, D. Ross and A. Terrano, Nucl. Phys. B178 (1981) 421.
71. A.P. Contogouris and S. Papadopoulos, "The Dominant Part of Higher Order Corrections for the Subprocess $qg \rightarrow \gamma q$ ", McGill University preprint (1989), to be published.
72. W. van Neerven, in Proceedings of International Europhysics Conference on H.E. Physics, Uppsala, June 1987, p. 198.
73. T. Matsuura, S. van der Marck and W. van Neerven, Phys. Lett. B211 (1988) 171, Nucl. Phys. B319 (1989) 570.
74. T. Matsuura and W. van Neerven, Z. Phys. C38 (1988) 623.
75. M.I. Vysotsky, Phys. Lett. B97 (1980) 159.
76. P. Nason, Phys. Lett. B175 (1986) 223.
77. F.A. Berends, Z. Kunszt and R. Gastmans, Nucl. Phys. B182 (1981) 397.
78. P. Aurenche et al., Phys. Rev. D39 (1989) 3275.
79. a) L.N. Lipatov, Sov. Phys. JETP 45 (1977) 216; JETP Lett. 24 (1976) 157; *ibid* 25 (1977) 104.
b) A.H. Mueller, Plenary Talk at the EPS Conference on H.E. Physics, Madrid, September 1989.
80. S. Gorishny, A. Kataev and A. Larin, Phys. Lett. B212 (1988) 238.

81. a) K. Chetyrkin, A. Kataev and T. Tkatchov, *Phys. Lett.* B85 (1979) 227.
 b) M. Dine and J. Sapirstein, *Phys. Rev. Lett.* 43 (1979) 668.
 c) W. Celmaster and R. Gonsalves, *Phys. Rev. Lett.* 44 (198) 560, and *Phys. Rev. D*21 (1980) 3112.
82. A.P. Contogouris and N. Mebarki, *Phys. Rev. D*39 (1989) 1464.
83. C. Maxwell and J. Nicholls, *Phys. Lett.* B213 (1988) 217.
84. G. Altarelli, Lecture Series, CERN Academic Training Program 1977-78.
85. C. Maxwell, *Phys. Rev. D*28 (1983) 2037.
86. I. Hinchliffe and M. Shapiro, in Proceedings of 1988 Summer Study on H.E. Physics in the 1990's (World Scientific) to appear.
87. a) A.P. Contogouris, S. Papadopoulos and D. Atwood, "The Gluon Distribution and Physical Versus Optimal Scales", in Proceedings of the 3rd International School of Elementary Particle Physics, Corfu, Greece, September 1989, (World Scientific) to be published.
 b) D. Atwood, A.P. Contogouris and S. Papadopoulos, in Proceedings of the Eleventh Annual Montreal-Rochester-Syracuse-Toronto Meeting, May 1989, (ed. by C. Rosenzweig and K.C. Wali) p.8.
88. A.P. Contogouris, N. Mebarki, H. Tanaka and S. Vlassopoulos, *Phys. Rev. D*32 (1985) 1134.
89. F. Aversa, P. Chiappetta, J. Guillet and M. Greco, *Phys. Lett.* B210 (1988) 225 and Marseille preprint CPT-88/P. 2186.
90. E. Eichten, I. Hinchliffe, K. Lane and C. Quigg, *Rev. Mod. Phys.* 56 (1984) 579.
91. W.J. Marchiano, *Phys. Rev. D*12 (1975) 3861.
92. P. Darriulat et al., *Nucl. Phys.* B110 (1976) 365.
93. J.H. Cobb et al., CERN Report, 1978.
94. E. Amaldi et al., *Phys. Lett.* B77 (1978) 240.
95. Rome-Brookhaven-CERN Collaboration, work presented at the 19th International Conference on H.E. Physics, Tokyo, 1978.
96. M. Diakonou et al. (Athens²-Brookhaven-CERN Collab.), *Phys. Lett.* B87 (1979) 292 and B91 (1980) 296.

97. A. Angelis et al. (CERN-Columbia-Oxford-Rockefeller Collab.), Phys. Lett. B94 (1980) 106.
98. E. Amaldi et al. (Rome-Brookhaven-CERN-Adelphi Collab.), Nucl. Phys. B150 (1979) 326.
99. M. Sochet (CDF Collab.), in Proceedings of XXIV International Conference on H.E. Physics, Munich, August 1988, (Springer Verlag, 1988) p. 18.
100. C. Albajar et al. (UA1 Collab.), Phys. Lett. B209 (1988) 385.
101. J. Appel et al. (UA2 Collab.), Phys. Lett. B176 (1986) 239.
102. a) T. Akesson et al. (Axial Field Spectrometer Collab., experiment R807), in EPS Conf. on H.E. Physics, Bari, Italy, July 1985, and Z. Phys. C34 (1987) 293
b) E. Anassontzis et al. (Athens²-Brookhaven-CERN Collab., experiment R806), Z. Phys. C13 (1982) 277.
c) Ref. 97.
103. C. De Marzo et al. (NA24 Collab.), Phys. Rev. D36 (1987) 8.
104. M. Bonesini et al. (WA70 Collab.), Z. Phys. C38 (1988) 371.
105. A. Bernasconi et al. (UA6 Collab.), Phys. Lett. B206 (1988) 163.^(f11)

FIGURE CAPTIONS

- Fig. 1** (a) DIS in the original PM. The blob represents the fragmentation of the nucleon to a parton (here quark or antiquark), which interacts with the virtual photon. Parallel solid lines denote the other fragments of the nucleon (spectator partons). (b) Next to leading order Feynman graphs, considered in the QCD improved PM, and giving rise to scale violations and HOC. Solid lines: quarks or antiquarks; dashed: gluon; wavy: virtual photon.
- Fig. 2** (a) Large- p_T hadron production in hadronic collisions according to the PM. Blobs in the initial (final) state represent the fragmentation of a hadron (parton) to a parton (hadron). Here the subprocess $qq \rightarrow qq$ (or $q\bar{q} \rightarrow q\bar{q}$) is considered. (b) Typical Feynman graphs for other subprocesses (involving gluons in the initial and/or final state), considered in the QCD improved PM and contributing to leading order. (c) Certain next to leading order Feynman graphs, for the subprocess in (a), giving rise to scale violations and HOC. HO graphs for other subprocesses are not shown. Lines as in Fig. 1.
- Fig. 3** Certain Feynman graphs of QCD subprocesses contributing to $A + P \rightarrow \gamma + X$. (a), (b) Born terms. (c) Photon Brems. Solid lines: quarks; dashed: gluon; wavy: photon.
- Fig. 4** (a) Predicted $Ed\sigma/d^3p$ for $pp \rightarrow \gamma + X$ and ratios γ/π^0 using the parton distributions of set I.⁽⁴⁴⁾ - qg denotes the contribution of $q + g \rightarrow q + \gamma$ and $q\bar{q}$ of $q + \bar{q} \rightarrow g + \gamma$; γ/π correspond to the sum of these two contributions. Dashed lines: scaling parton distributions. Solid lines: nonscaling (Q^2 -dependent) distributions. Dash-dotted lines: the adopted experimental $Ed\sigma/d^3p$ for $pp \rightarrow \pi^0 + X$. Experimental data on γ/π : \sqcup Ref. 92, \triangle Ref. 93, \downarrow Ref. 94, \circ Ref. 95. (b) Same as in (a) using the parton distributions of set II.⁽⁴⁶⁾

Fig. 5 (a) Contributions of Born terms and of photon Brems to the inclusive cross section for $pp \rightarrow \gamma + X$ at $\theta_{cm} = 90^\circ$. Solid lines: total contribution of $O(\alpha_s)$ (i.e., $qg \rightarrow q\gamma$ and $q\bar{q} \rightarrow g\gamma$). Dashed lines: contribution of photon Brems (i.e. $qq \rightarrow qq\gamma$). For comparison at each energy we give the range of the experimental $pp \rightarrow \pi^0 + X$. (b) The effect of parton's intrinsic transverse momenta calculated with a Gaussian k_T distribution of $\langle k_T \rangle = 0.5$ GeV. We denote by $\sigma(k_T)$ the $p + p \rightarrow \gamma + X$ inclusive cross section with k_T effects and by $\sigma(0)$ the same cross section calculated without k_T effects ($\langle k_T \rangle = 0$).

Fig. 6 (A), (B) The Born graphs associated with subprocess (2.1a). Solid lines: quarks; dashed: gluons; wavy; photons. (a)-(1) Doubly logarithmic IR divergent graphs in Feynman gauge at $O(\alpha_s^2)$ shown below the corresponding Born graphs. Gluons in the soft approximation are shown by dotted lines. (u), (v) Some non IR divergent graphs at $O(\alpha_s^2)$.

Fig. 7 (a)-(d) Unitarity (transition probability) graphs at lowest order describing subprocess (2.1a). (A)-(H') IR divergent unitarity graphs giving π^2 at $O(\alpha_s^2)$, from Fig. 6, shown below the corresponding unitarity Born graphs.

Fig. 8 (a) One of the lowest order unitarity graphs describing $\gamma^* + g \rightarrow q + \bar{q}$. (b)-(c') Unitarity graphs illustrating crossing of soft gluon corrections to $\gamma^* + g \rightarrow q + \bar{q}$ discussed in Subsect. 2.2.2. Lines as in Fig. 6.

Fig. 9 Comparison of the differential cross section $q^0 d\sigma/d^3q = Ed\sigma/d^3p$ for real photon production in pp collisions at $\theta_{cm} = 90^\circ$ with data. Dashed lines are the QCD predictions with a strong gluon distribution from Ref. 46; solid lines include the correction (2.2.22). Circles are data of Ref. 96, squares of Ref. 97, triangles of Ref. 98.

Fig. 10 Predictions for the ratio of inclusive cross sections γ/π^0 ($\theta_{cm} = 90^\circ$) compared with data of Ref. 96. Dashed lines: lowest order prediction

with a strong gluon distribution.⁽⁴⁶⁾ Solid lines: including the correction of Eq. (2.2.22). In calculating γ/π^0 we use π^0 data of the same Collaboration.

Fig. 11 Inclusive cross sections for $\bar{p} + p \rightarrow \gamma + X$.⁽⁵⁶⁾ Solid and dashed lines: predictions using the K -factors of Eq. (2.3.1) and two sets of parton distributions (see caption of Fig. 5 of Ref. 56). Dash-dotted lines: predictions of the complete calculation of Ref. 65(b) with parton distributions as for solid line.⁽⁵⁶⁾ Everywhere $Q^2 = p_T^2$.⁽⁵⁶⁾

Fig. 12 The kinematic region of the $x_a - x_b$ integration in the expression (3.1.2). The boundary corresponds to $\hat{s} + \hat{t} + \hat{u} = 0$ (or $w = 1$), the hatched region to $\hat{s} + \hat{t} + \hat{u} > 0$ (or $w < 1$), and the cross-hatched region denotes the neighborhood of the boundary. (a) Corresponding to rapidity $\eta = 0$; (b), (c) for $|\eta| \simeq 0.7$.

Fig. 13 (a) The ratio $(\sigma_s - \sigma_{HO})/(\sigma_B + \sigma_{HO})$ for the contribution of $q\bar{q} \rightarrow \gamma q$ to the difference of cross sections for $\bar{p}p \rightarrow \gamma + X$ and $pp \rightarrow \gamma + X$ at rapidity $\eta = 0$ (in this case $\sigma_s > \sigma_{HO}$). Solid line: Results for the d -quark distribution (Duke-Owens set 1). Dash-dotted: Results for a fictitious distribution of the form (3.2.5) with $n = 20$. Dashed: the same with $n = 0.01$. (b) The ratio $(\sigma_s - \sigma_{HO})/\sigma_{HO}$ for the same contribution. Lines as in (a).

Fig. 14 (a) The ratio $(\sigma_{HO} - \sigma_s)/(\sigma_B + \sigma_{HO})$ for the contribution $\gamma q \rightarrow \gamma q$ to $\gamma p \rightarrow \gamma$ (large p_T) $+ X$ at $\eta = 0$ (here $\sigma_s < \sigma_{HO}$). Lines as in Fig. 13(a). (b) The ratio $(\sigma_{HO} - \sigma_s)/\sigma_{HO}$ for the same contribution. Lines as in Fig. 13(a).

Fig. 15 Unitarity graphs contributing to $(\bar{p}p \rightarrow pp) \rightarrow \gamma X$ and considered in Sect. 4.1 (Brems from initial partons). (o) Corresponding to a Born contribution. (a),(a') Contributing to the dominant part of

HOC. (b),(c) Giving nondominant contributions. Solid lines: quarks; dashed: gluons; wavy: photons.

Fig. 16 Unitarity graphs contributing to $(\bar{p}p - pp) \rightarrow \gamma X$ and considered in Sect. 4.2 (Brems from final partons). They contribute to the dominant part of HOC. (a)–(g) Associated with the subprocess $q\bar{q} \rightarrow \gamma gg$; (a'),(b') with the subprocess $q\bar{q} \rightarrow \gamma q\bar{q}$. Lines as in Fig. 15. In graphs (f) and (g) the dash-dotted line stands for a Faddeev-Popov ghost.

Fig. 17 Configuration of the 3-momenta of the $2 \rightarrow 3$ subprocess $a(p_1) + b(p_2) \rightarrow \gamma(q) + c(r) + d(k)$ in the center of momentum frame of the two final partons c and d , with the z axis chosen along \vec{p}_1 (system S_1).

Fig. 18 Unitarity graph determining the contribution to the dominant part $f_s(v, w)$, for the subprocess $qg \rightarrow \gamma q$, from initial parton Brems (Sect. 5.2). Solid lines: quarks; dashed: gluons; wavy: photon.

Fig. 19 Feynman graphs determining the contributions of the subprocess $qg \rightarrow \gamma + x$ up to $0(\alpha_s^2)$. Solid lines: quarks; dashed: gluons; wavy: photons.

Fig. 20 Feynman graphs determining the contributions of $q\bar{q} \rightarrow \gamma + x$ up to $0(\alpha_s^2)$. Solid, dashed and wavy lines as in Fig. 19. Dash-dotted line: Faddeev-Popov ghost.

Fig. 21 Feynman graphs determining the contributions of $qq \rightarrow qq\gamma$ and $gq \rightarrow q\bar{q}\gamma$. Lines as in Fig. 19.

Fig. 22 Example illustrating the variation of the cross section σ , of some physical process, with the scale $\mu = M$. The solid line represents the second order approximant $\sigma^{(2)}$ of σ . The dashed and dashed-dotted horizontal lines represent possible values of the (unknown) exact cross section.

Fig. 23 Predictions at $\sqrt{s} = 1.8$ TeV for $\bar{p}p \rightarrow \gamma + X$. Inclusive cross sections averaged in the rapidity range $0 < |\eta| < 0.8$,⁽⁹⁹⁾ acceptance cut (Eq.

(8.3.3) $R_0 = 0.7^{(99)}$. Dash-dotted line: with the parton distributions of EHLQ1.⁽⁹⁰⁾ Dashed: DO1. Solid: DO2.⁽⁶²⁾ All predictions for $\mu = M = p_T$.

Fig. 24 Inclusive cross sections at $\sqrt{s} = 630$ GeV for $\bar{p}p \rightarrow \gamma + X$, averaged in the rapidity range $0 < |\eta| < 0.8$; acceptance cut $R_0 = 0.7$. Lines as in Fig. 23. Data: open squares, Ref. 100; closed squares, Ref. 101.

Fig. 25 As in Fig. 24 for $1.0 < |\eta| < 1.8$ and $R_0 = 0.35$. Data: Ref. 101.

Fig. 26 Inclusive cross sections at $\sqrt{s} = 63$ GeV for $pp \rightarrow \gamma + X$ at $\eta = 0$. R_0 of Eq. (8.3.3) determined from the difference in the polar and azimuthal angles $\Delta\theta_0 = \pm 35^\circ$ and $\Delta\phi_0 = \pm 40^\circ$ (Ref. 102(a)). Dash-dotted, dashed and solid lines as in Fig. 23. Dotted: Results of Ref. 59 with DO2 and optimal scales. Data: closed circles, Ref. 102(a); open circles, Ref. 102(b); triangles, Ref. 102(c).

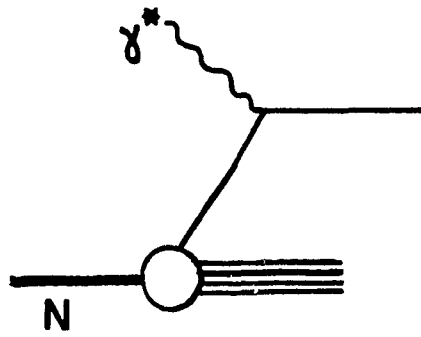
Fig. 27 Inclusive cross sections at $\sqrt{s} = 23.75$ GeV for $pp \rightarrow \gamma + X$ averaged over $-0.62 < \eta < 0.55$. Strong dash-dotted, dashed and solid lines: EHLQ1, DO1 and DO2, all with $\mu = M = p_T$. Dotted: as in Fig. 26.⁽¹⁰³⁾ Upper thin line: DO2 with $\mu = M = p_T/2$. Lower thin line: DO1 or EHLQ1 with $\mu = M = 2p_T$. Data: Ref. 103.

Fig. 28 Inclusive cross sections at $\sqrt{s} = 22.9$ GeV for $pp \rightarrow \gamma + X$. Lines as in Fig. 26. (a) Averaged over $-0.35 < x_F < -0.15$ (b) Over $-0.15 < x_F < 0.15$. Data from Ref. 104.

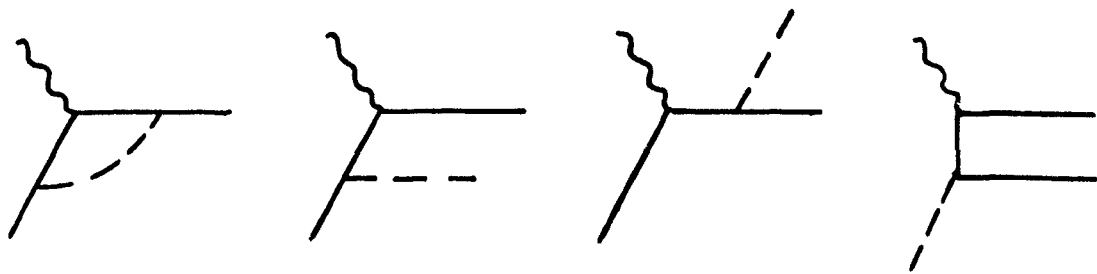
Fig. 29 Inclusive cross sections at $\sqrt{s} = 24.3$ GeV averaged over $-0.4 < \eta < 1.2$. Lines as in Fig. 23. (a) for $\bar{p}p \rightarrow \gamma + X$. (b) For $pp \rightarrow \gamma + X$. (c) The ratio of averaged cross sections for $\bar{p}p \rightarrow \gamma + X$ and $pp \rightarrow \gamma + X$. Data from Ref. 105.

Fig. 30 Variation of the predictions with the scale $\mu = M$. The ratio of the cross sections calculated with $\mu = M = p_T/2$ and with $\mu = M = 2p_T$,

for the distributions DO1. (a) At $\sqrt{s} = 1.8$ TeV for $\bar{p}p \rightarrow \gamma + X$, averaged over $0 < |\eta| < 0.8$; $R_0 = 0.7$. (b) At $\sqrt{s} = 23.75$ GeV for $pp \rightarrow \gamma + X$, averaged over $-0.62 < \eta < 0.55$.

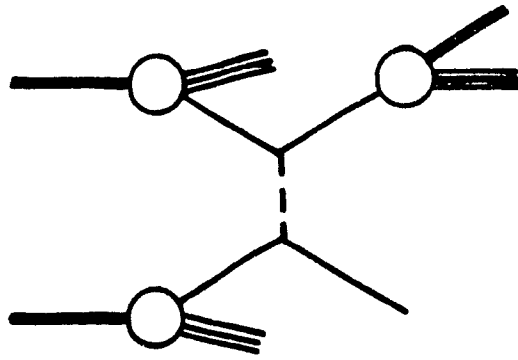


(a)

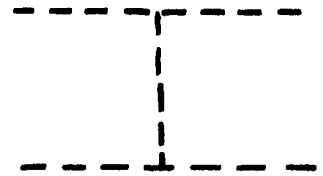
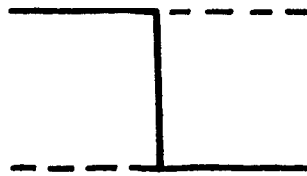
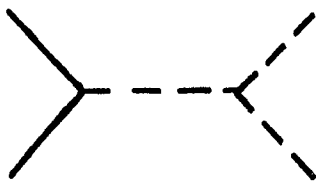


(b)

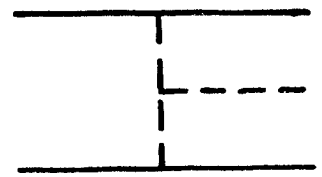
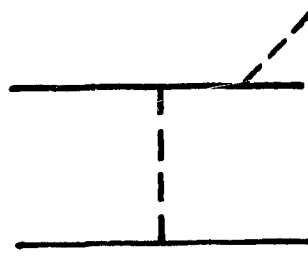
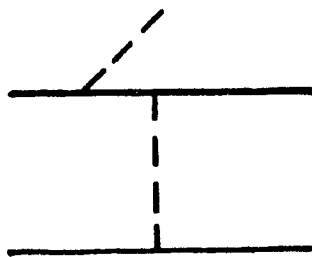
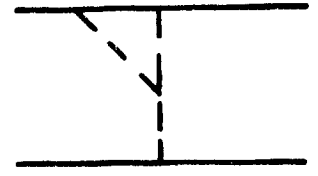
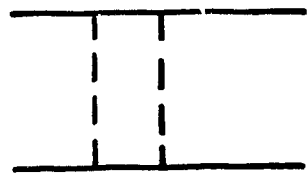
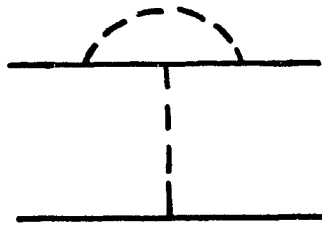
Fig. 1



(a)

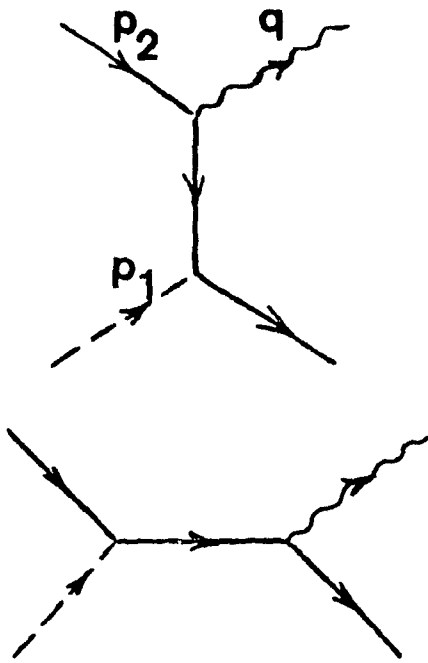


(b)

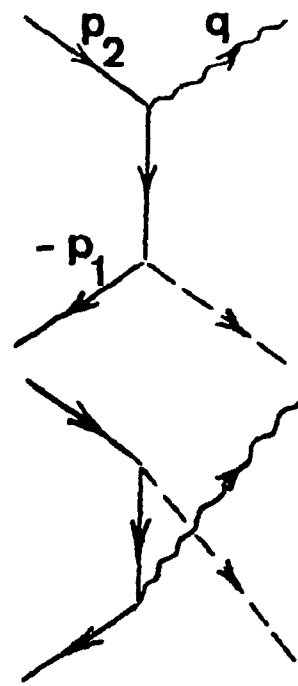


(c)

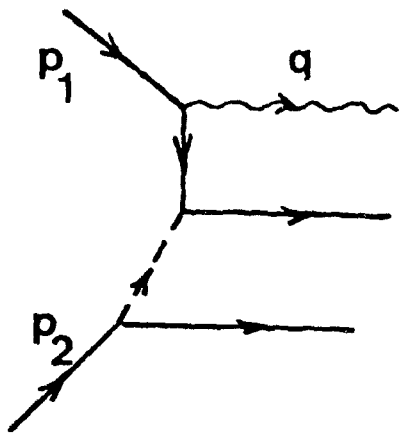
Fig. 2



(a)



(b)



(c)

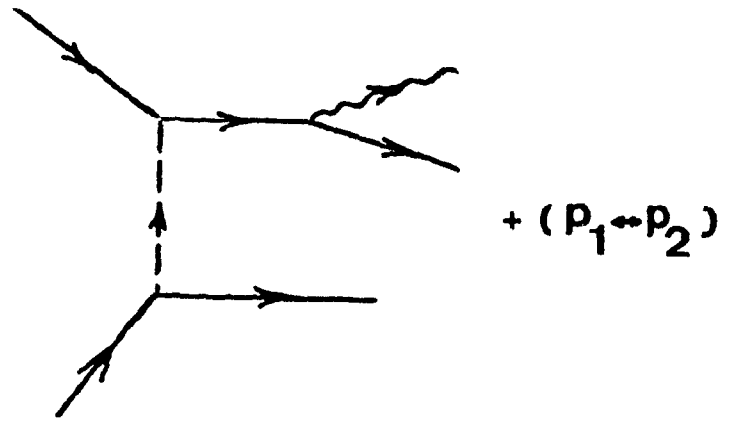


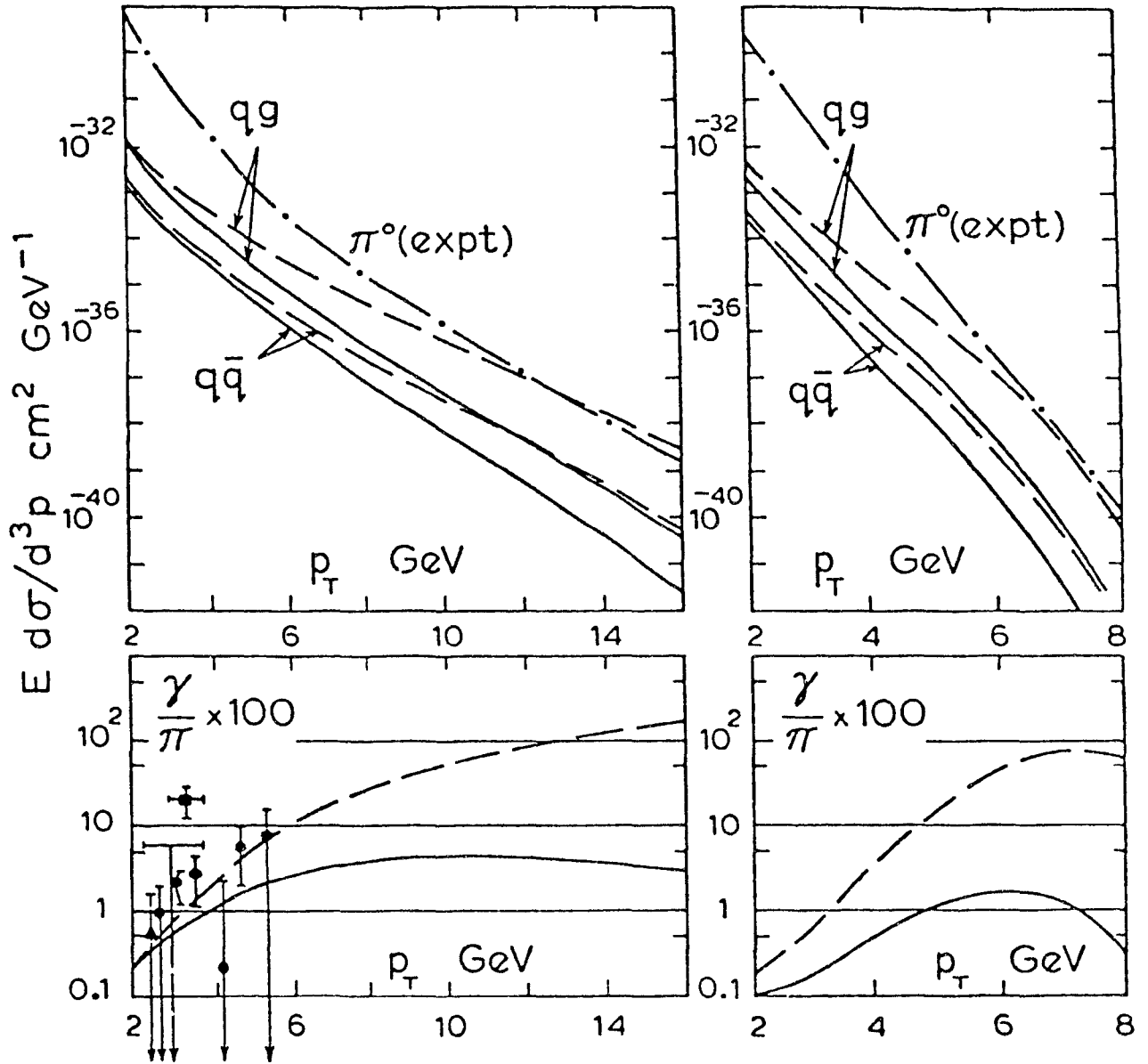
Fig. 3

QCD DISTRIBUTIONS SET I

--- scaling — nonscaling

$\sqrt{s} = 53$

$\sqrt{s} = 19.4$



(a)

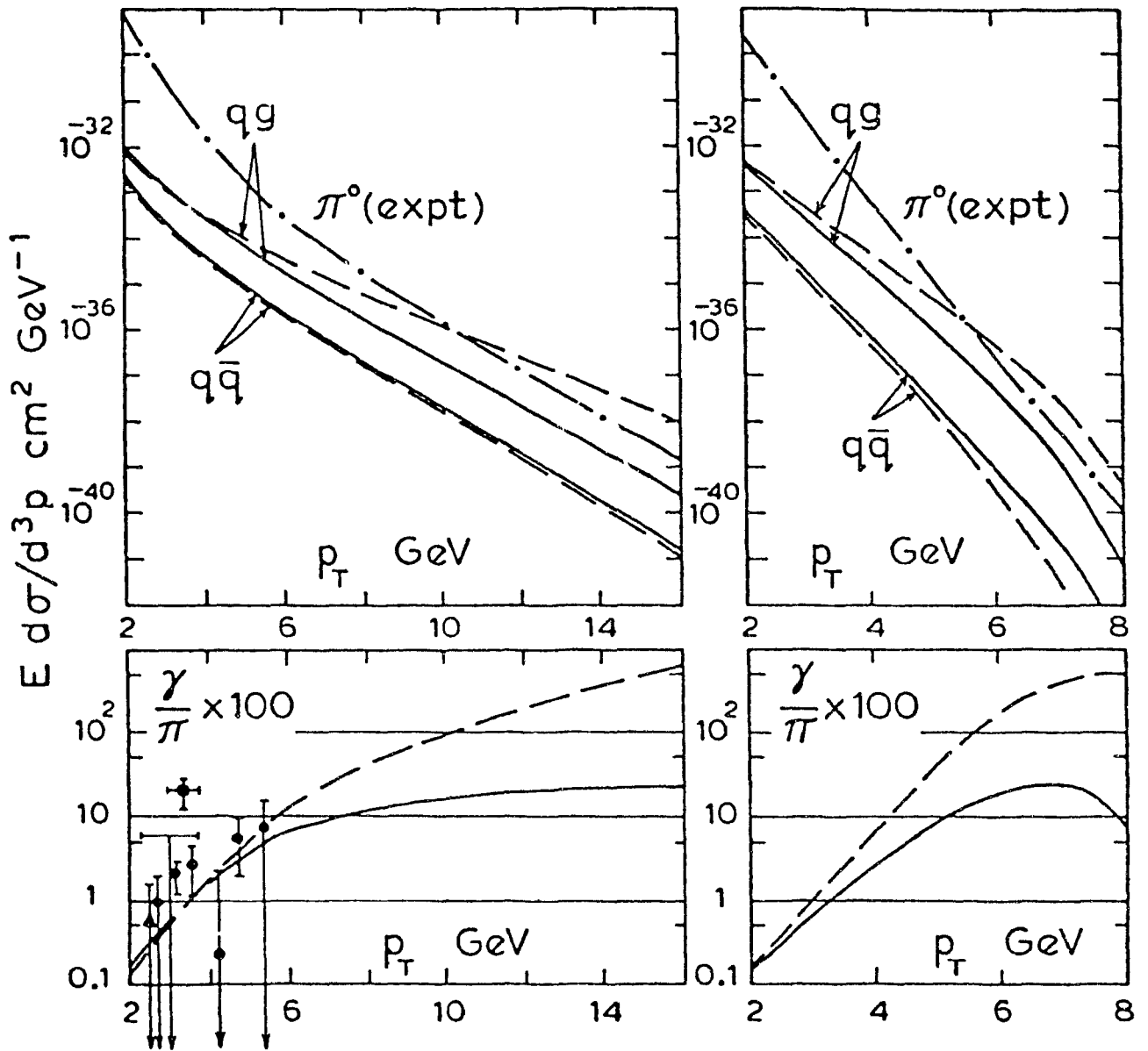
Fig. 4

QCD DISTRIBUTIONS SET II

--- scaling ——— nonscaling

$\sqrt{s} = 53$

$\sqrt{s} = 19.4$



(b)

Fig. 4

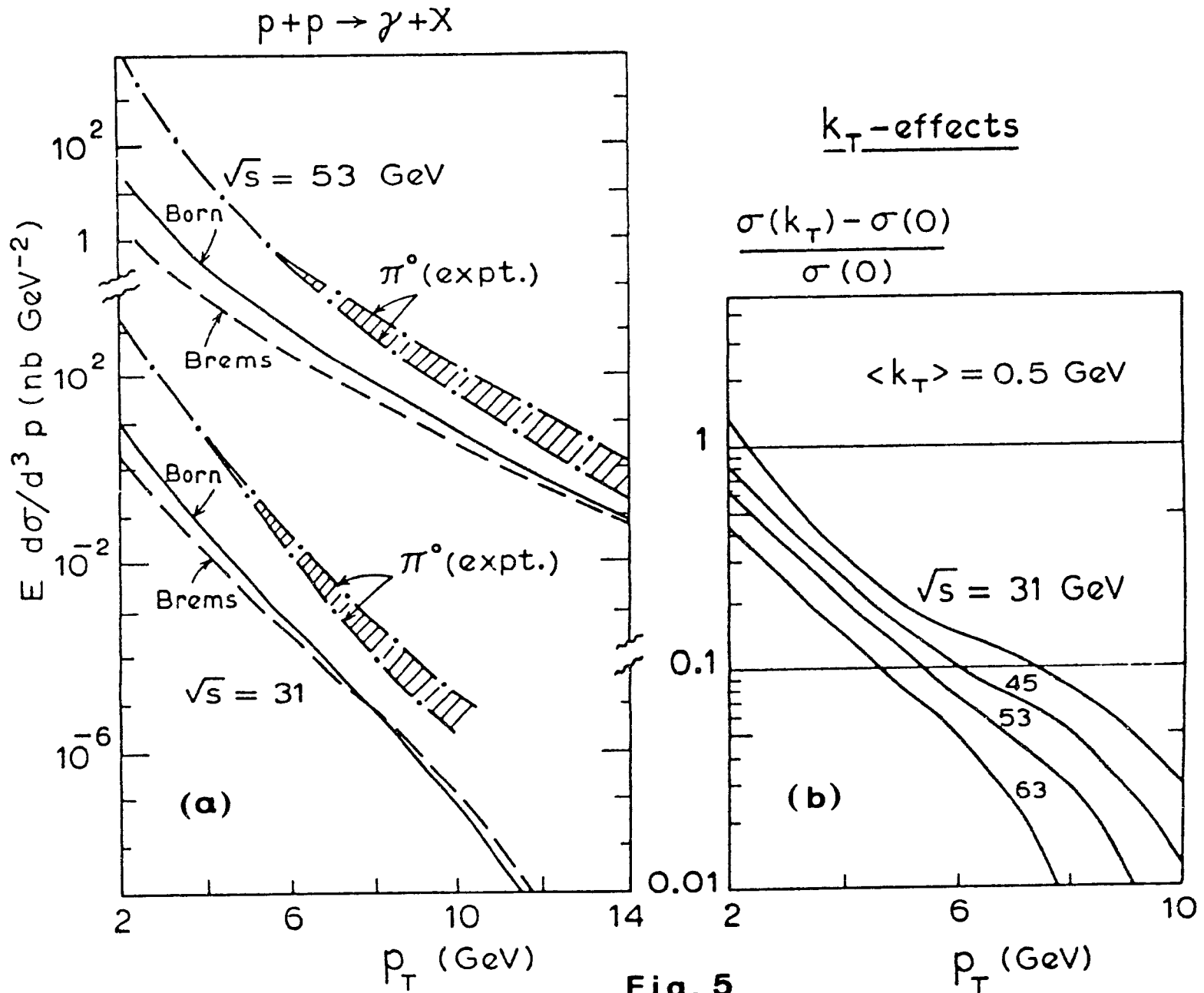


Fig. 5

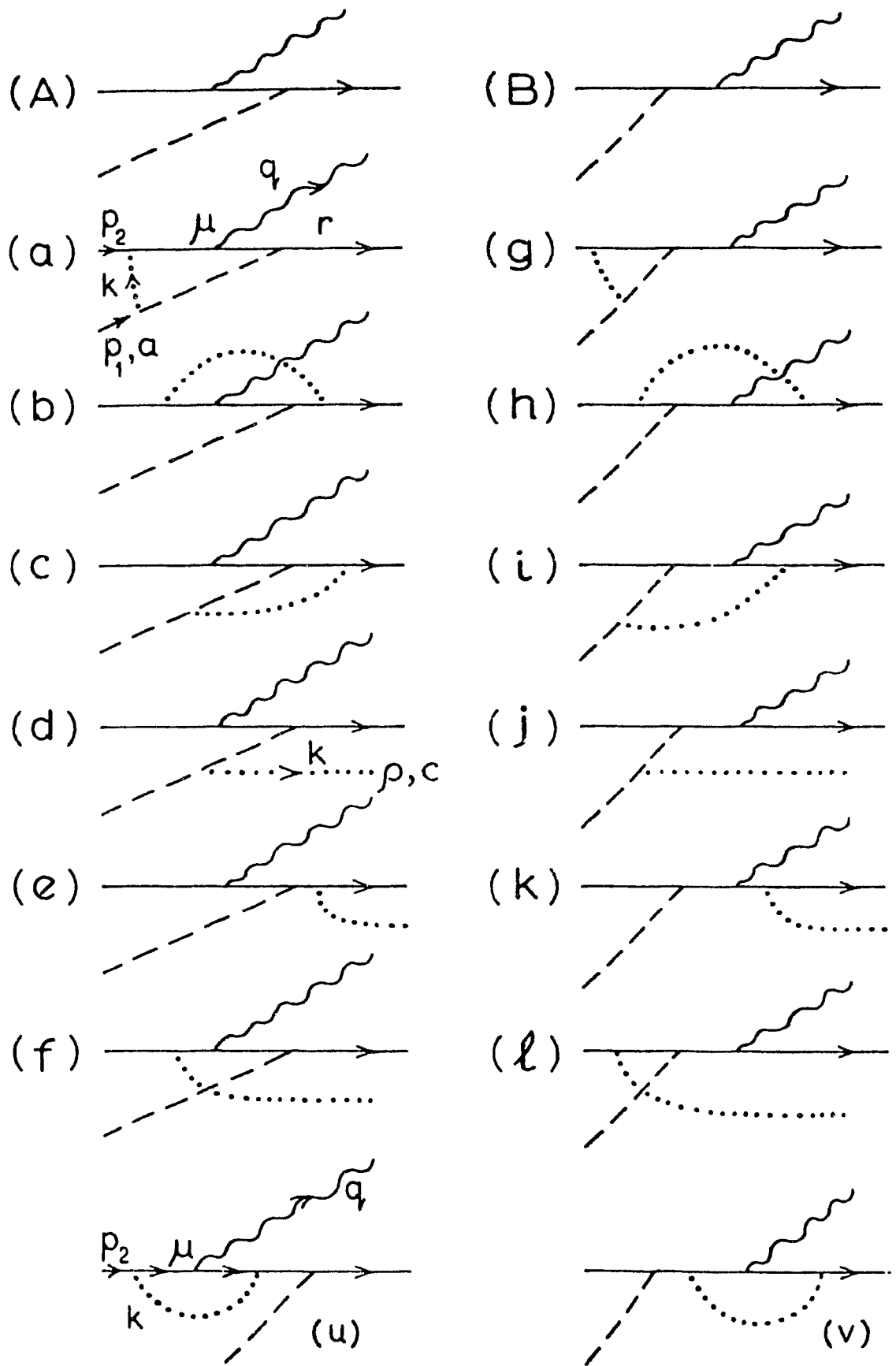


Fig. 6

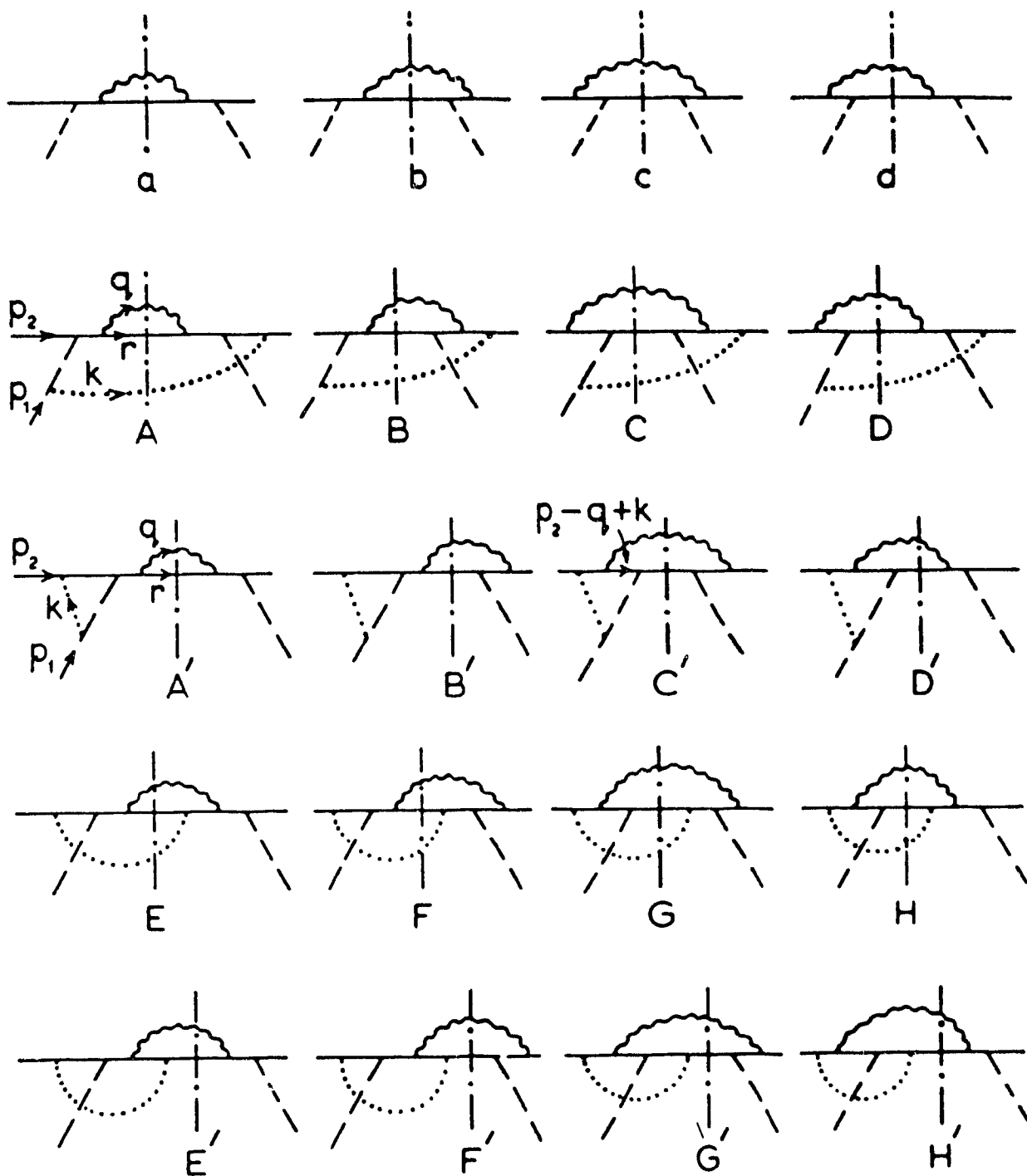


Fig. 7

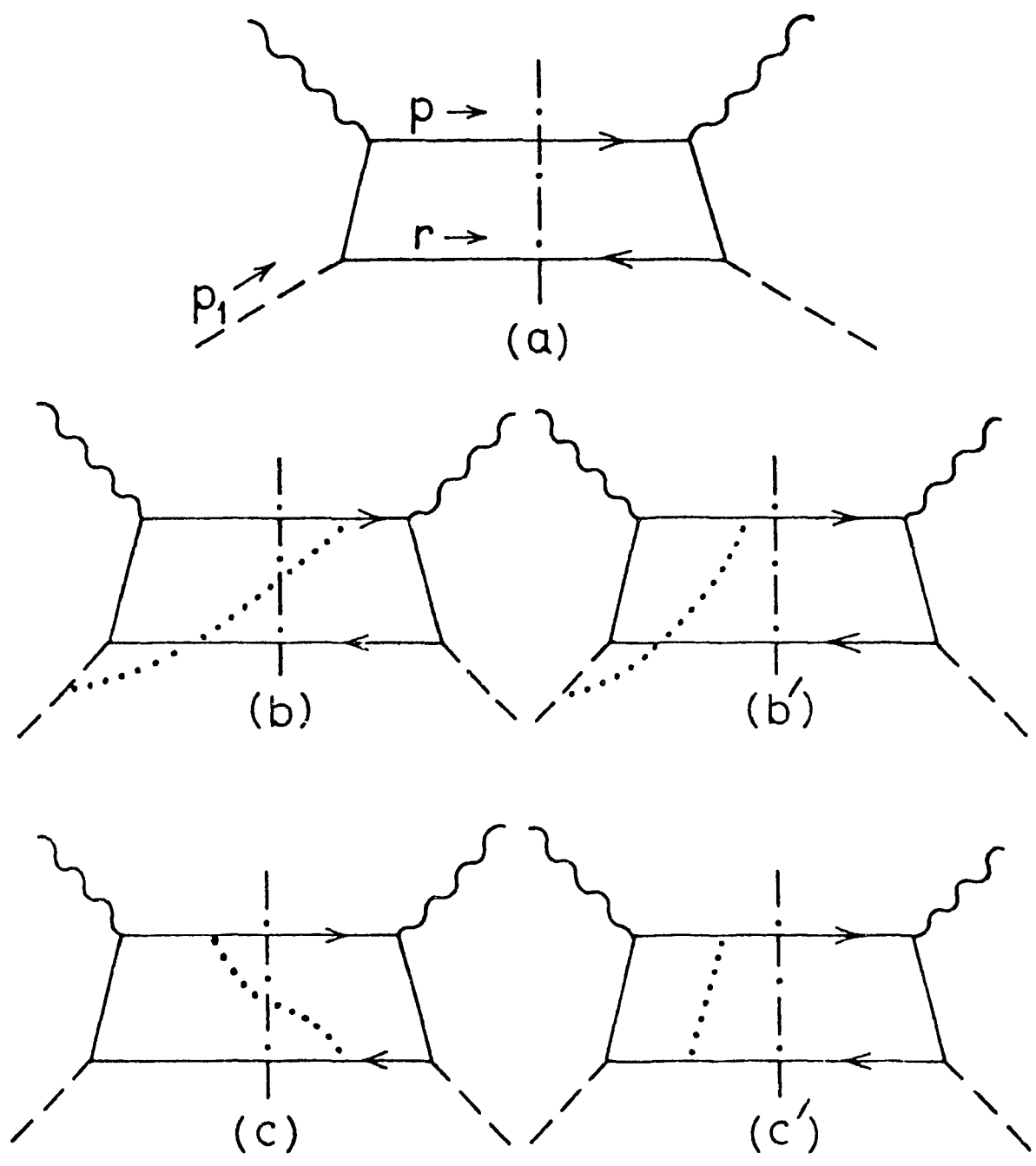


Fig. 8

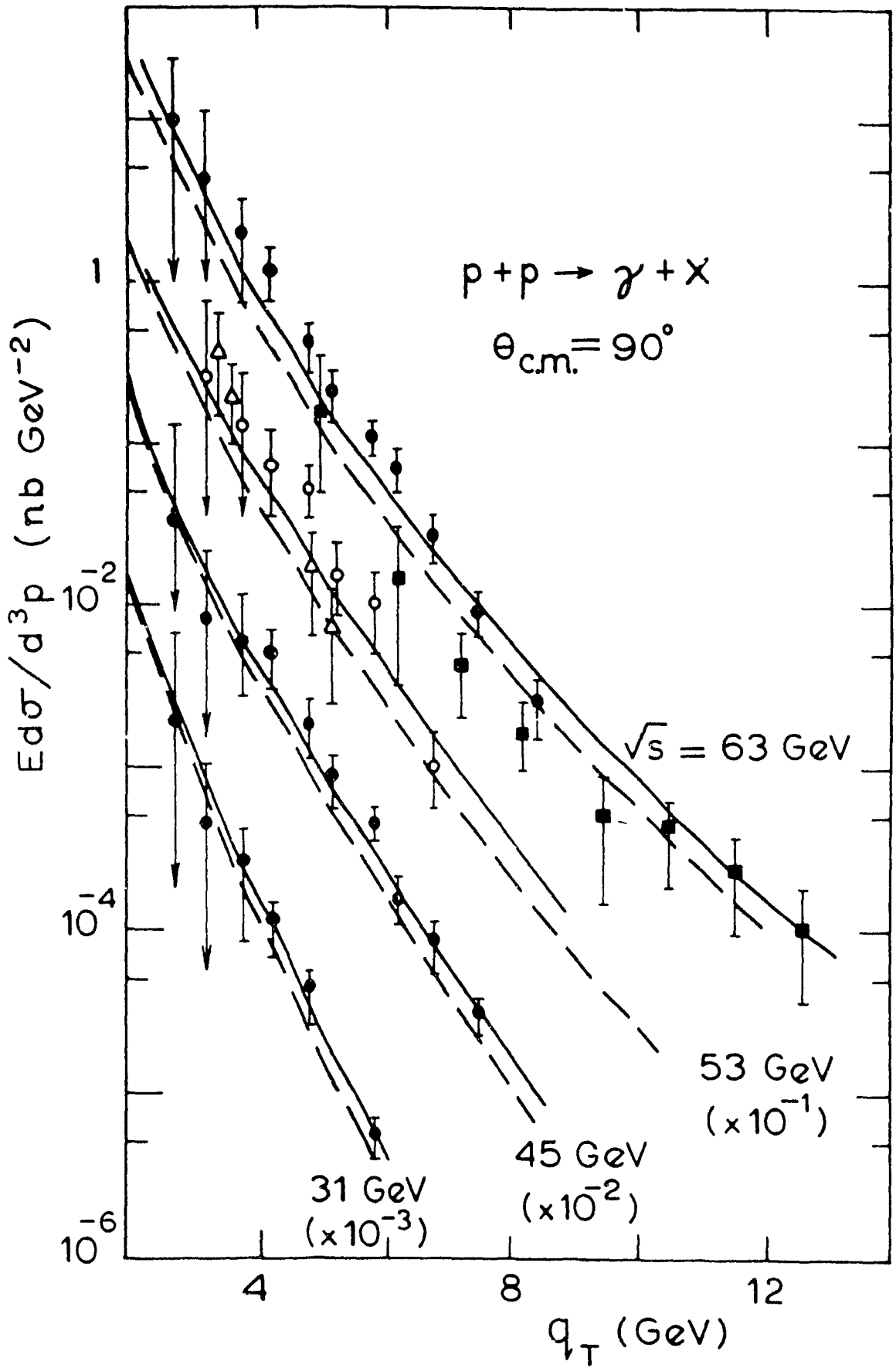


Fig. 9

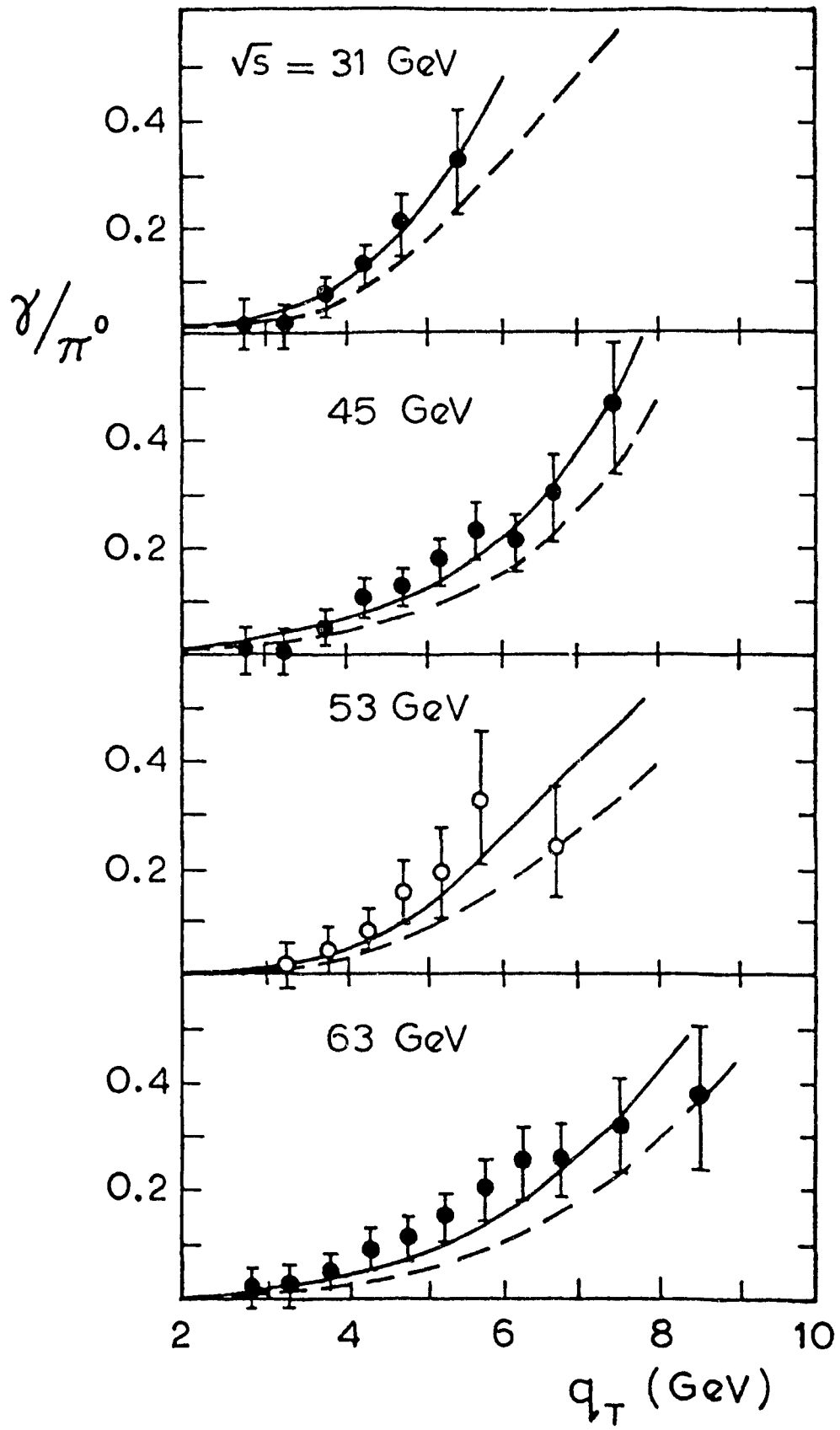


Fig.10

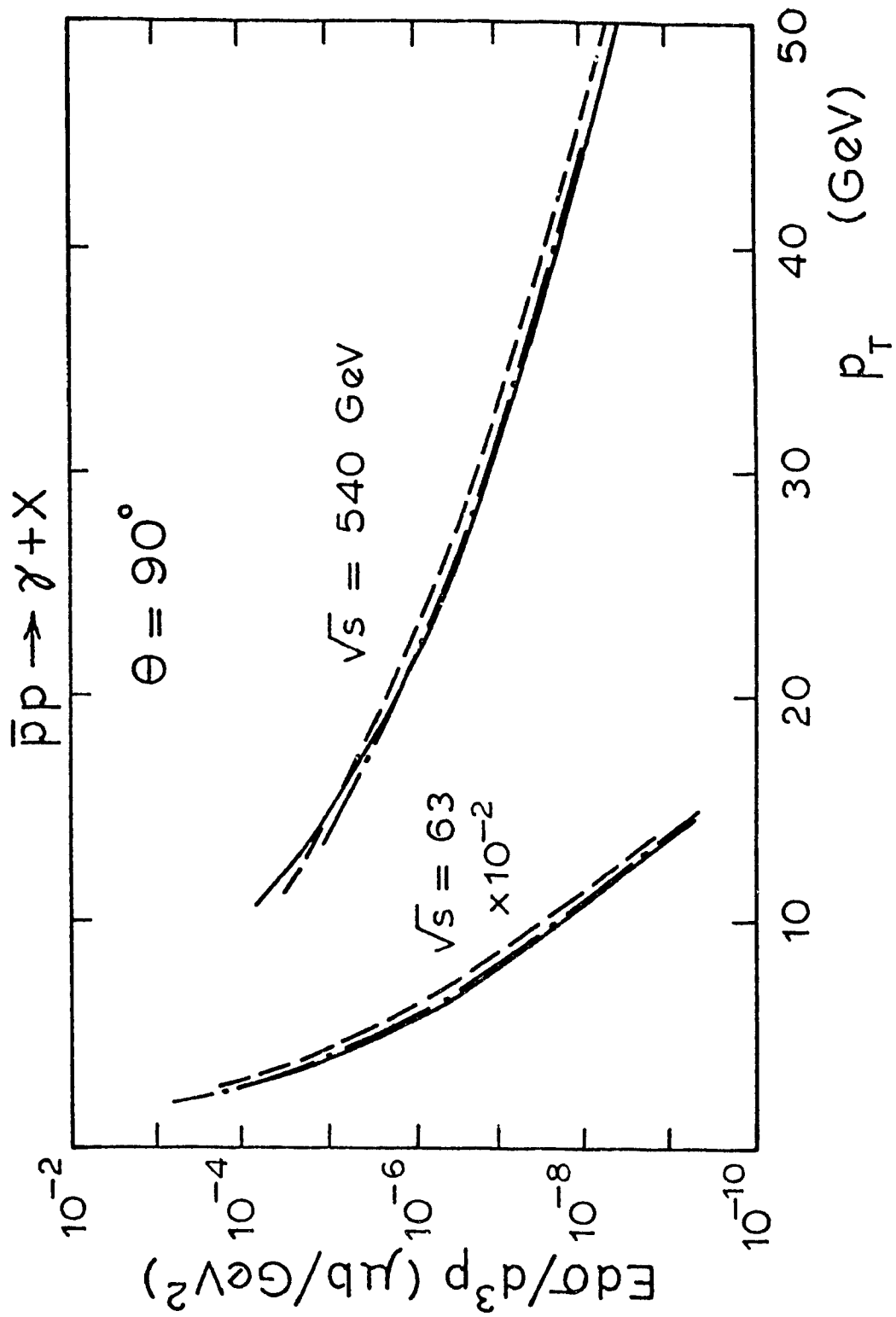
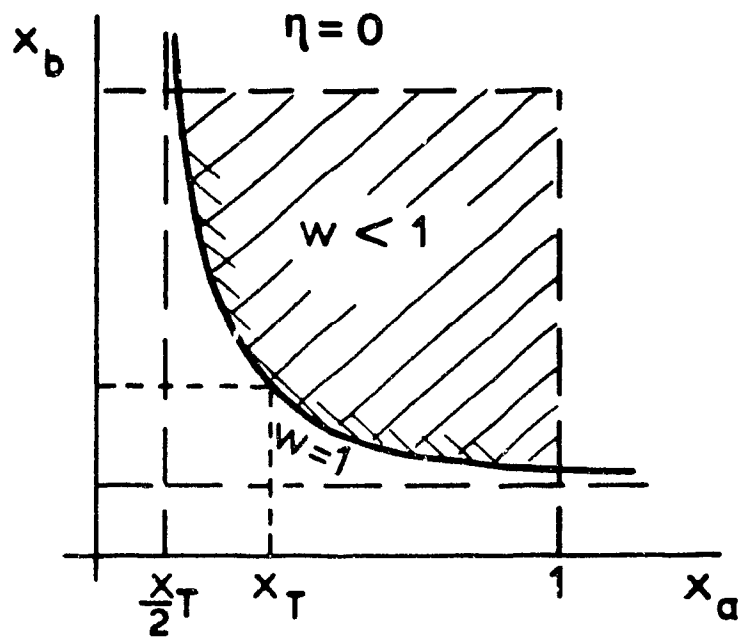
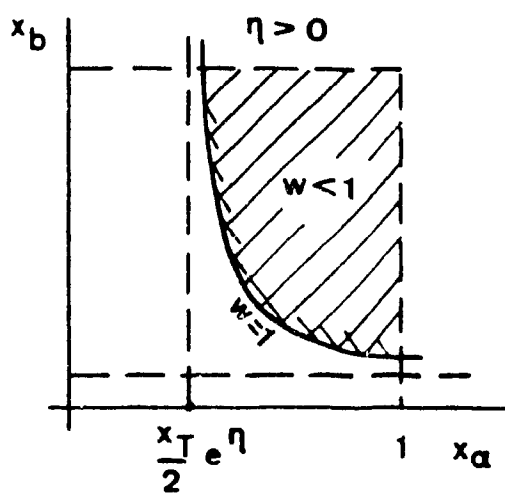


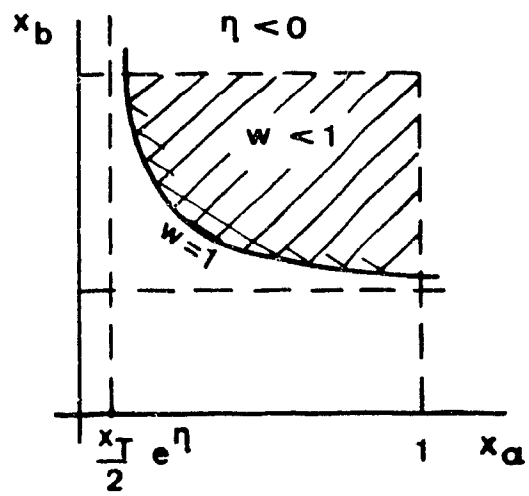
Fig.11



(a)



(b)



(c)

Fig.12

$$q\bar{q} \rightarrow \gamma g$$

$$\sqrt{s} = 63 \text{ GeV}$$

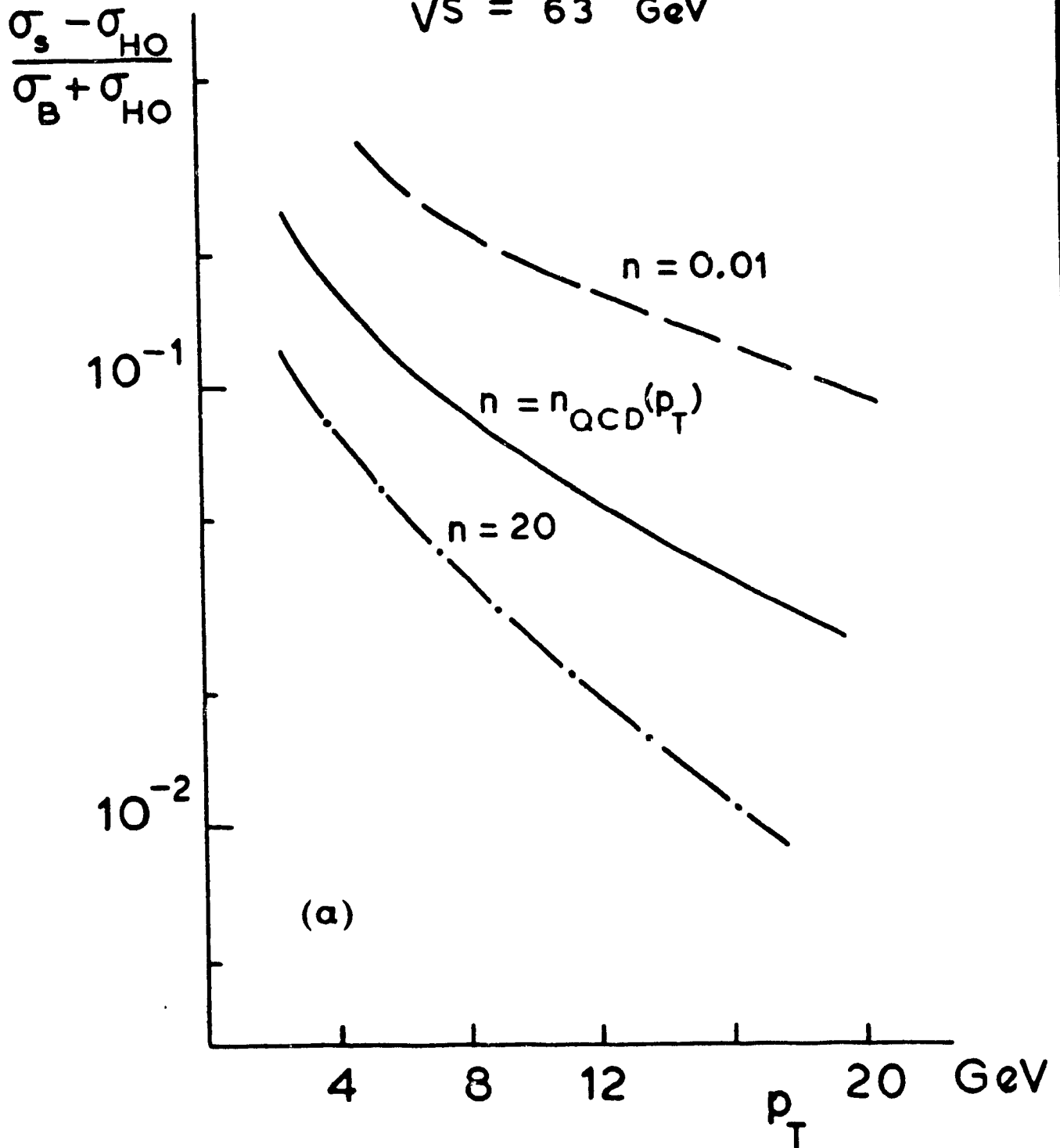


Fig.13

$q\bar{q} \rightarrow \gamma g$

$\sqrt{s} = 63 \text{ GeV}$

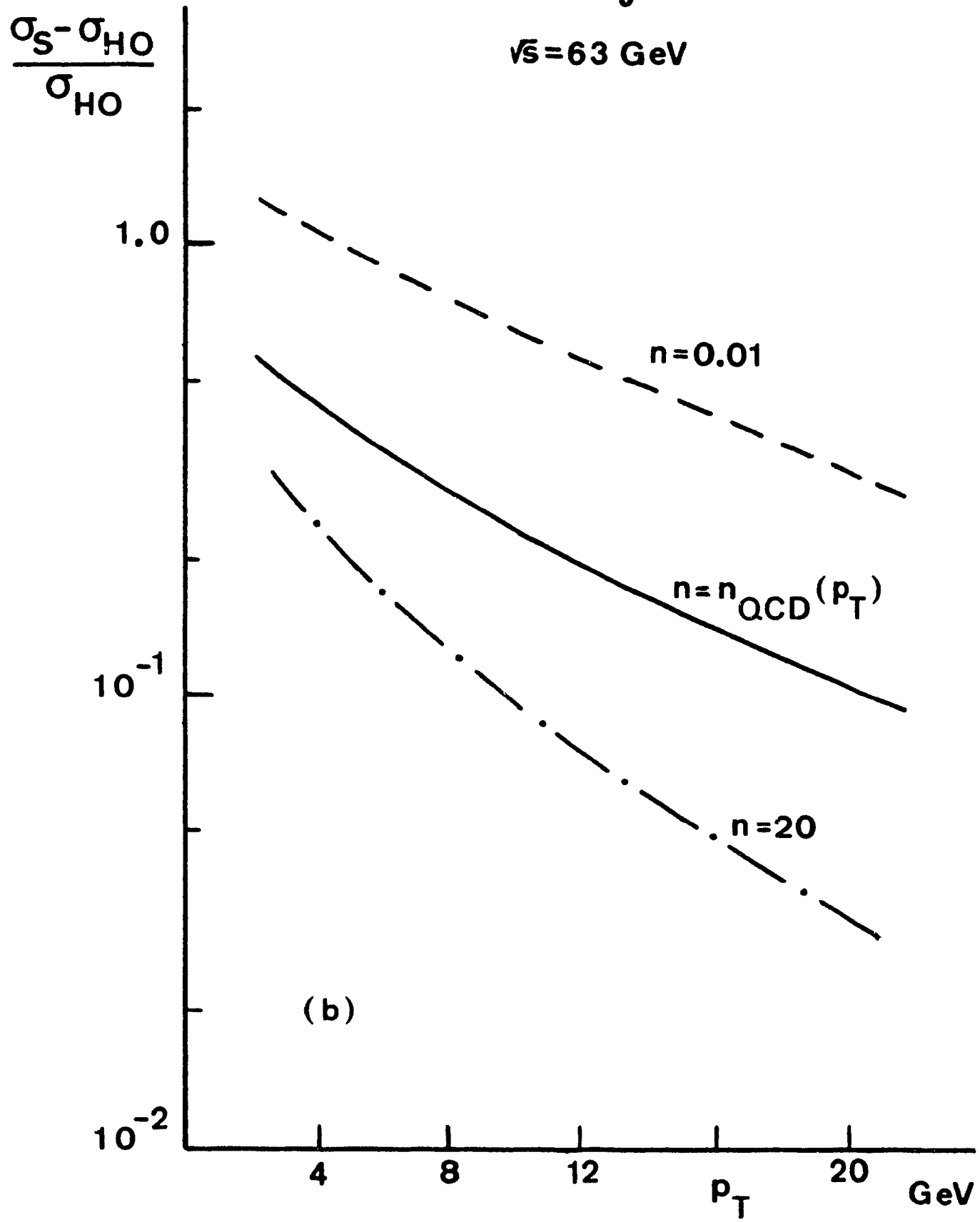


Fig.13

$$\gamma q \rightarrow \gamma q$$

$$E_\gamma = 100 \text{ GeV}$$

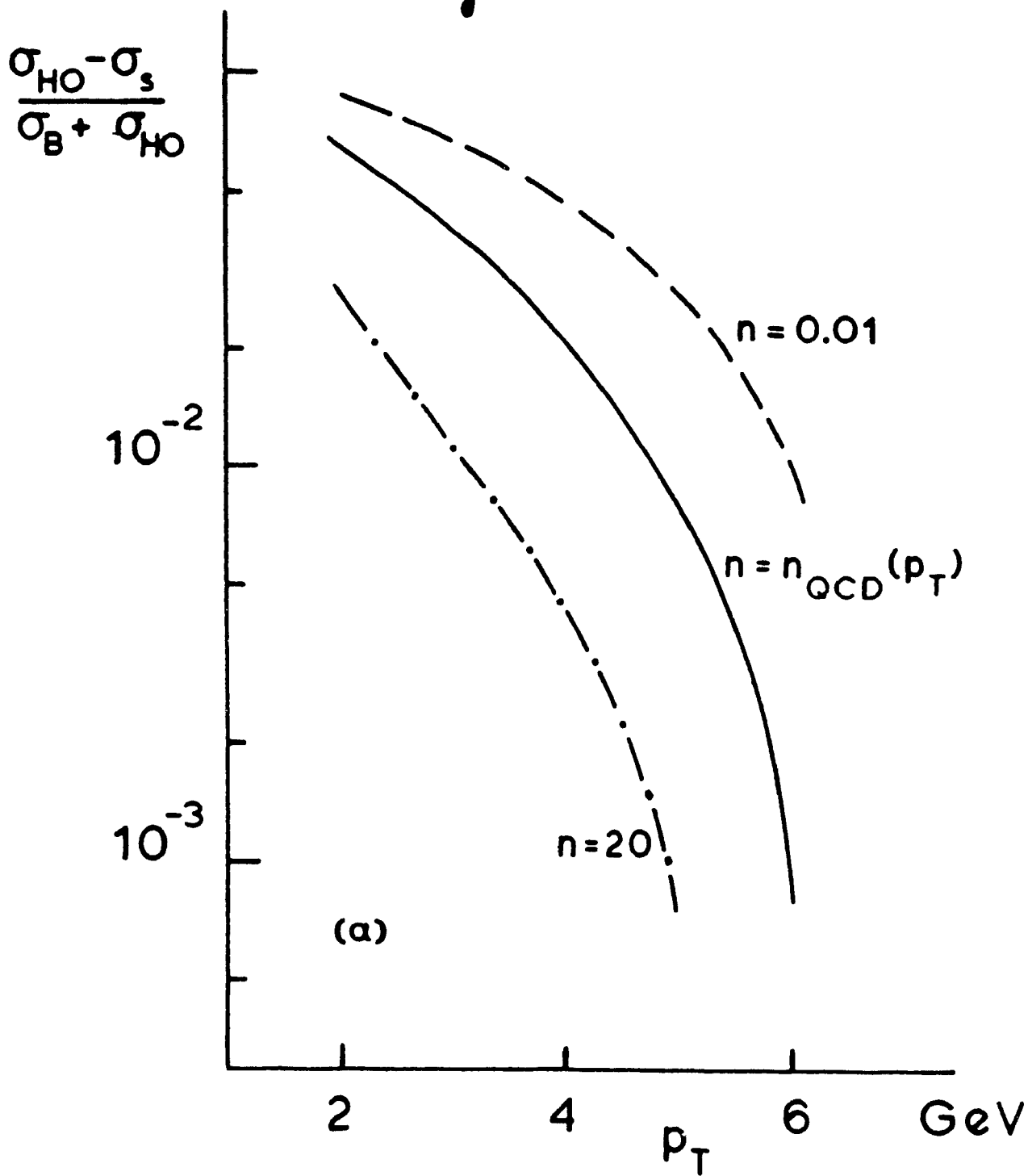


Fig.14

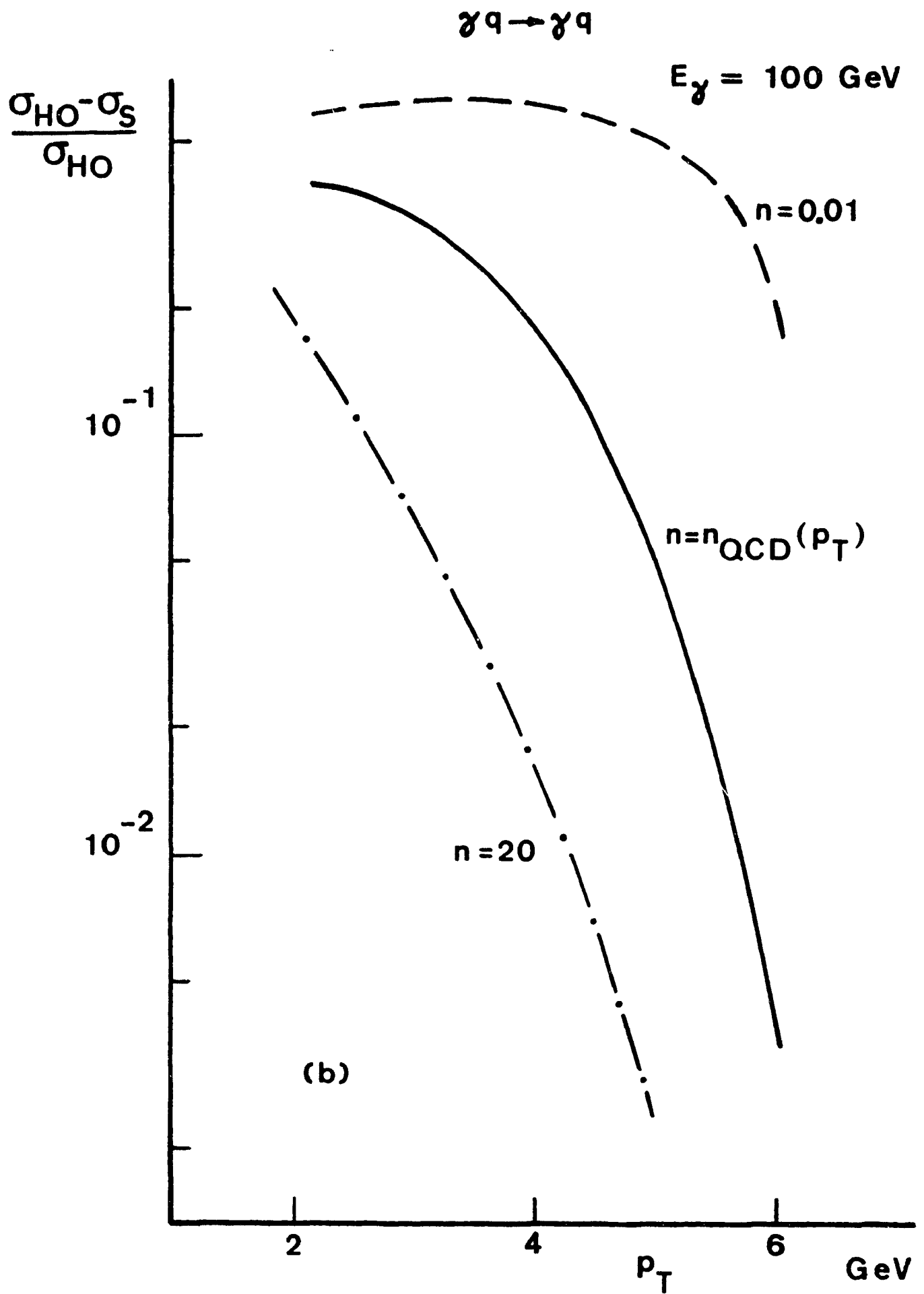


Fig.14

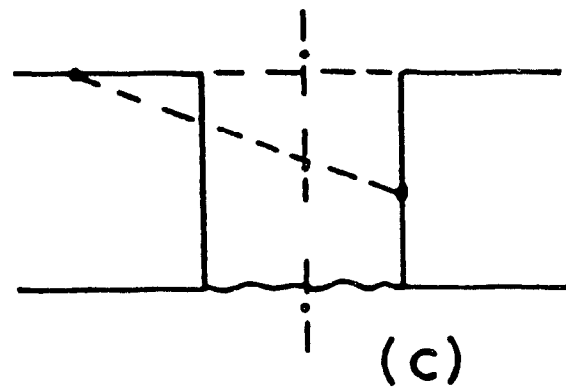
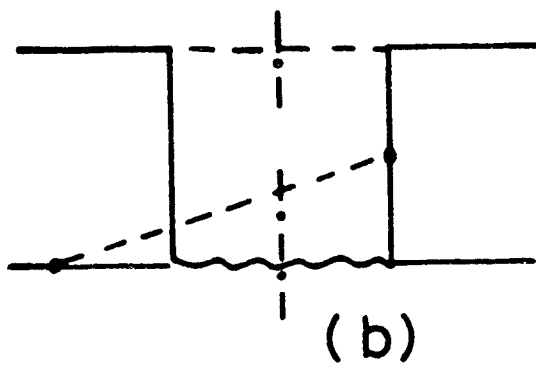
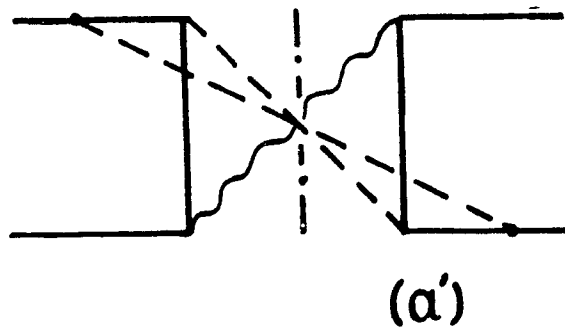
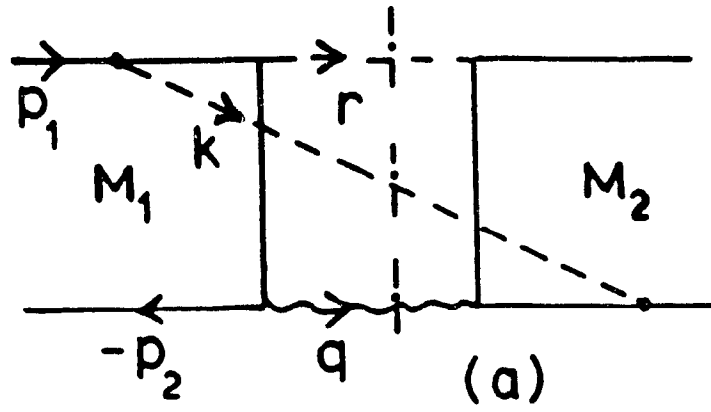
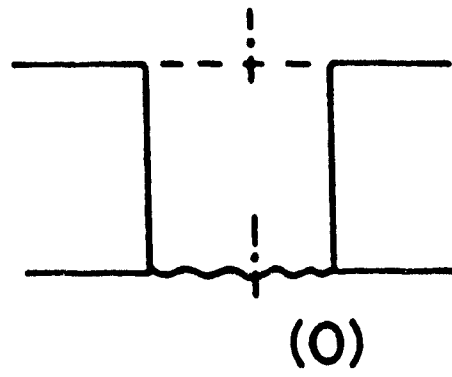


Fig.15

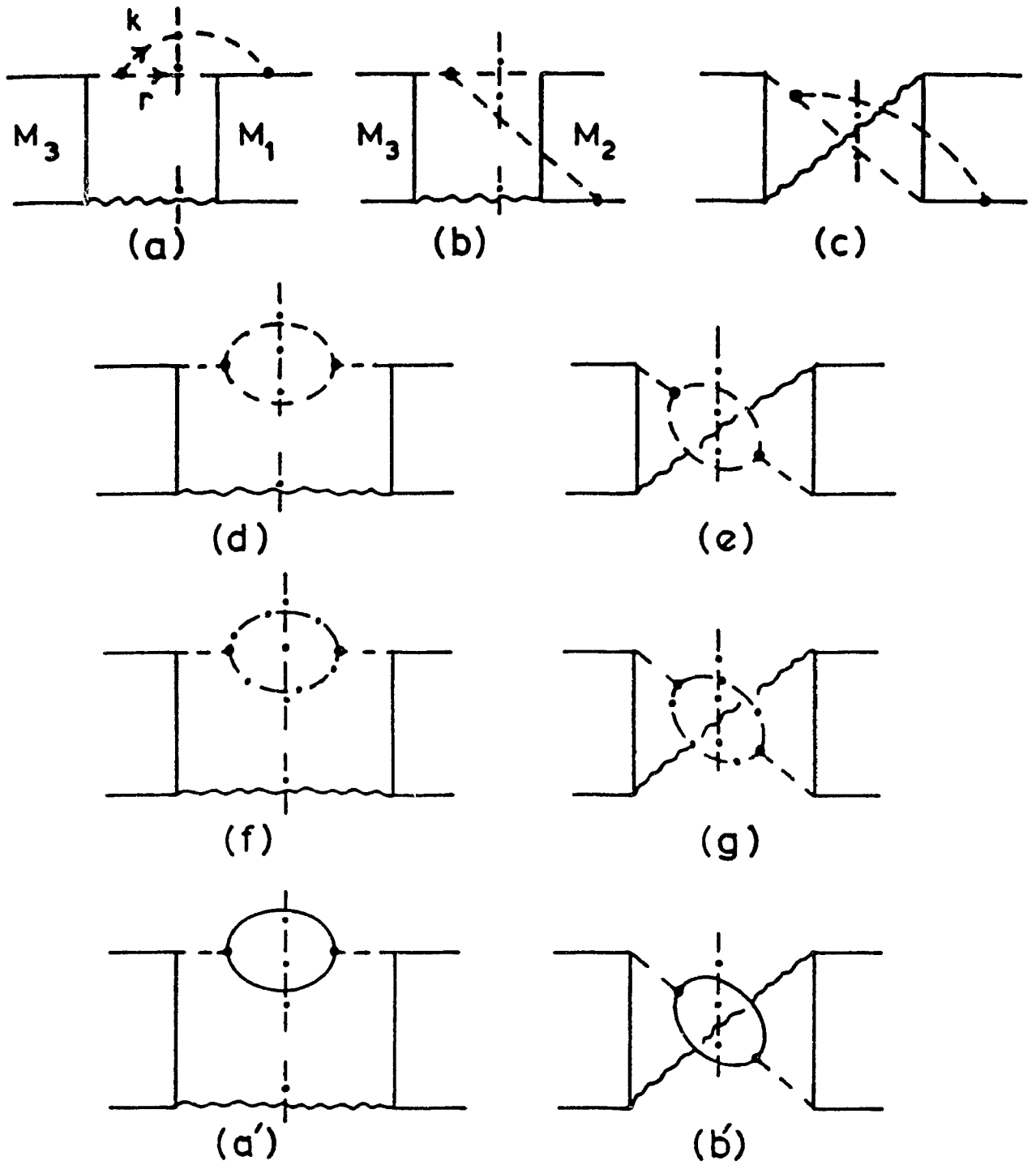


Fig.16

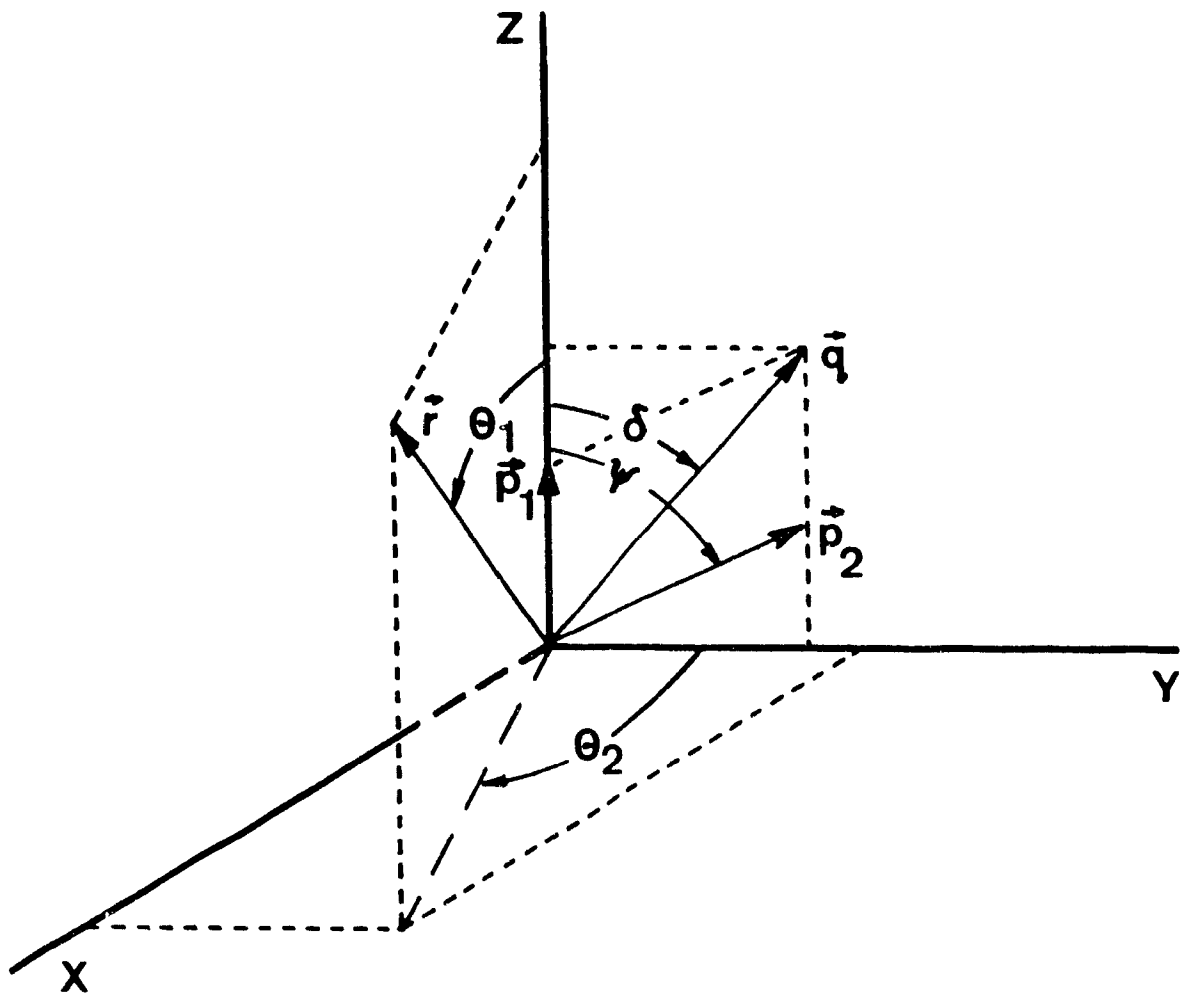


Fig.17

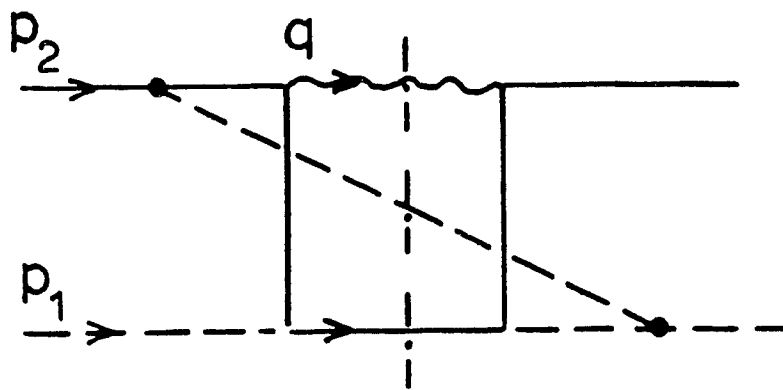


Fig.18

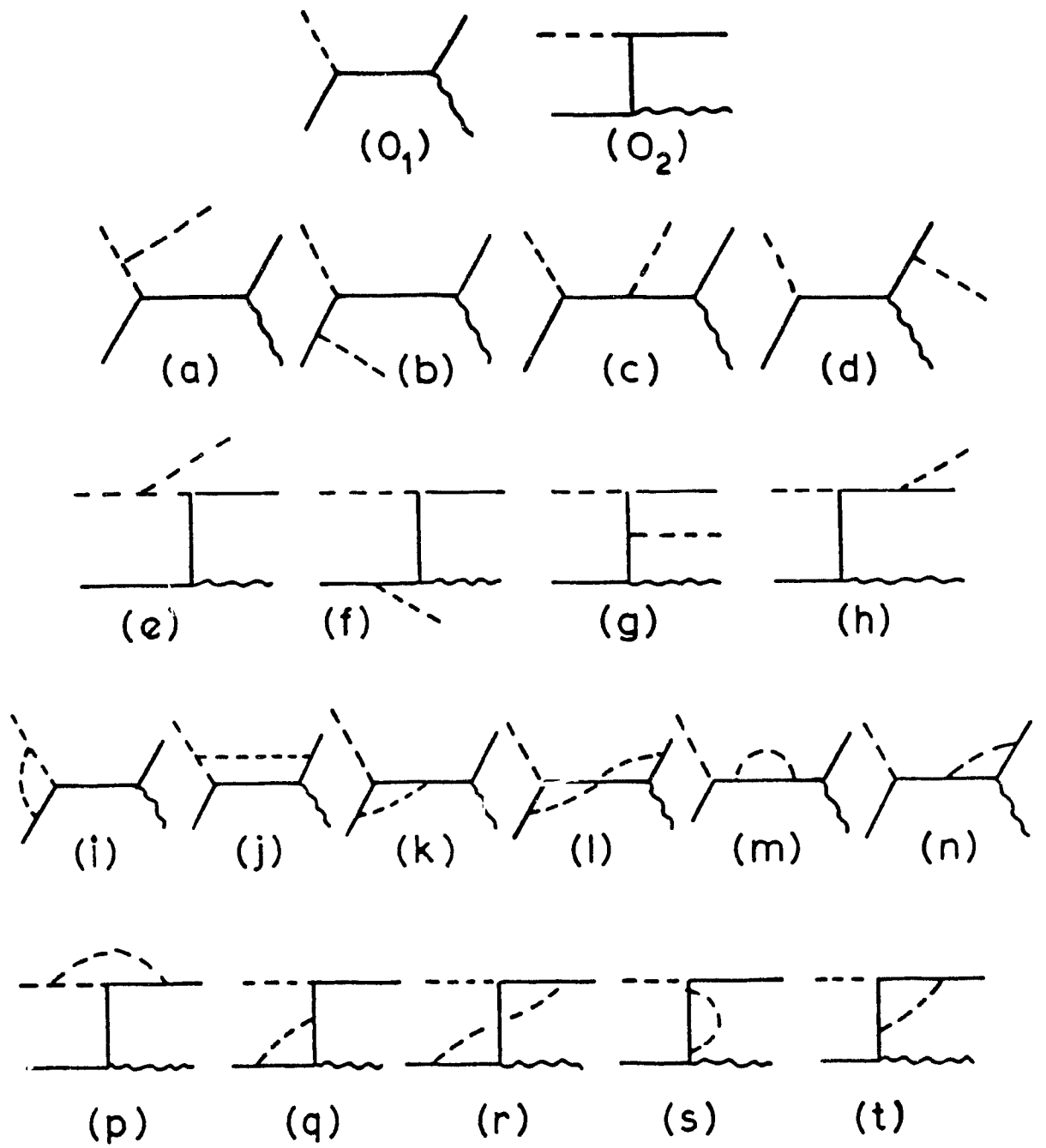


Fig. 19

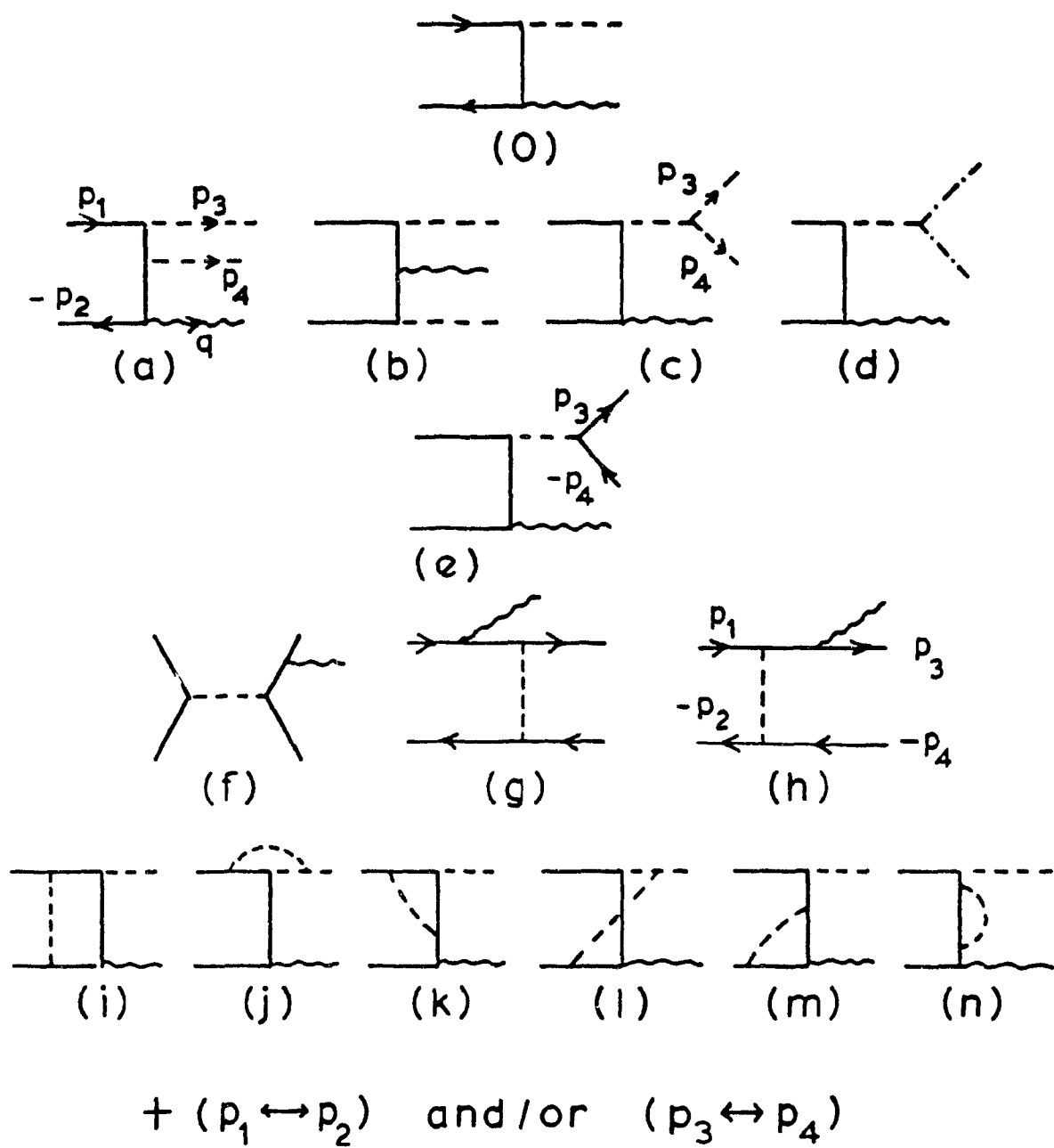
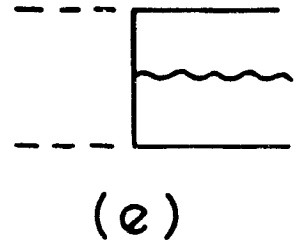
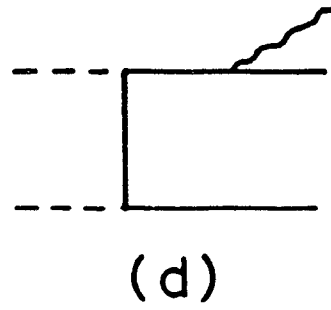
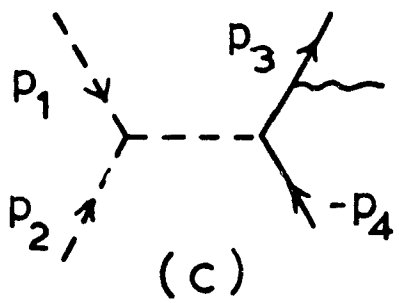
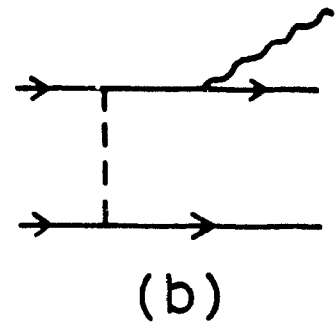
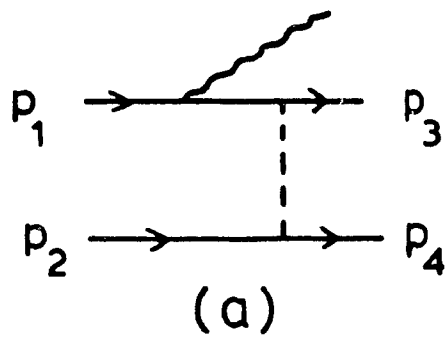


Fig.20



+ $(p_1 \leftrightarrow p_2)$ and/or $(p_3 \leftrightarrow p_4)$

Fig. 21

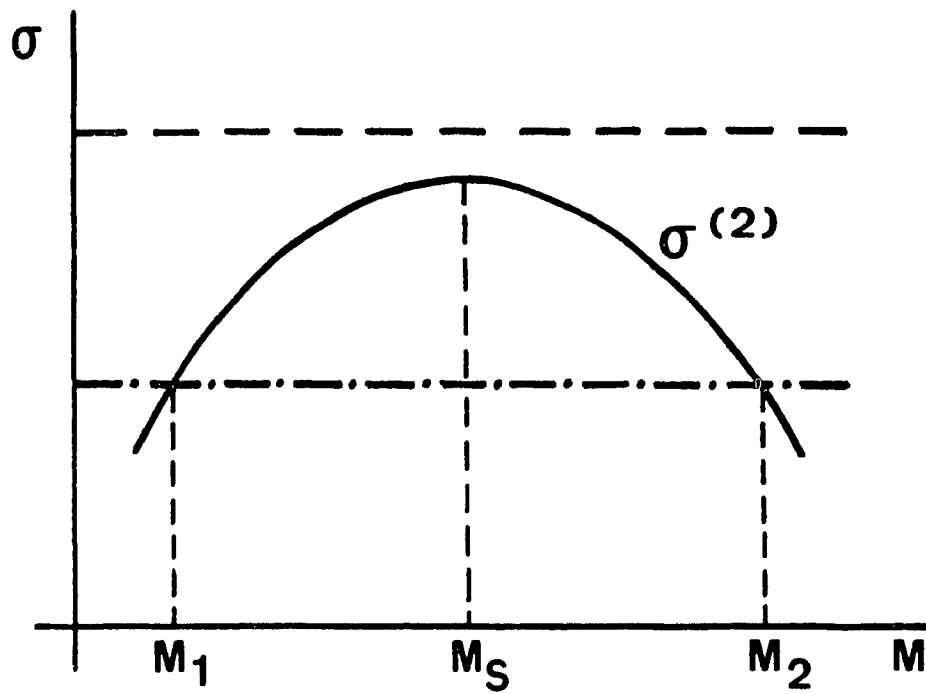


Fig.22

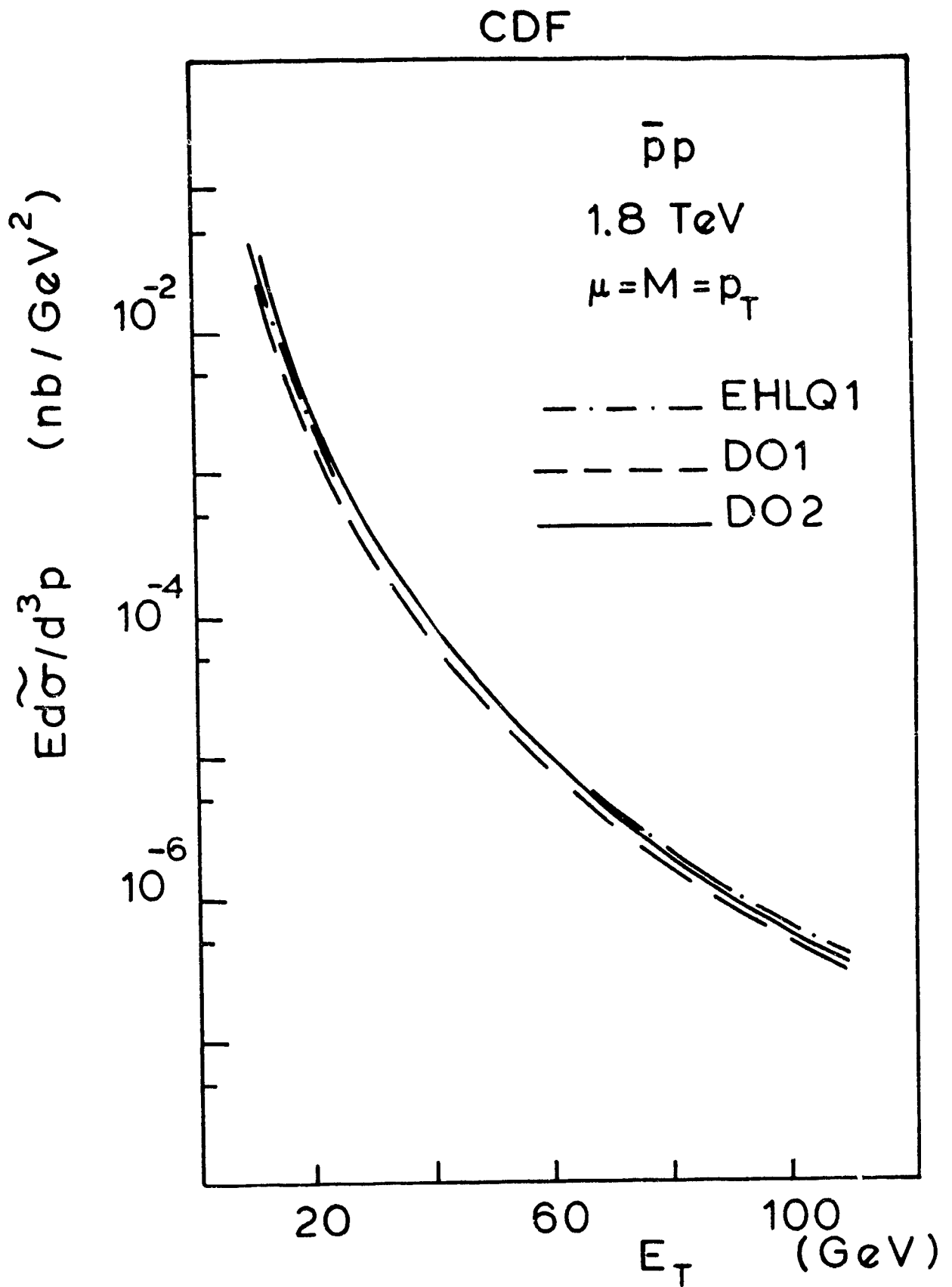


Fig. 23

UA1,UA2

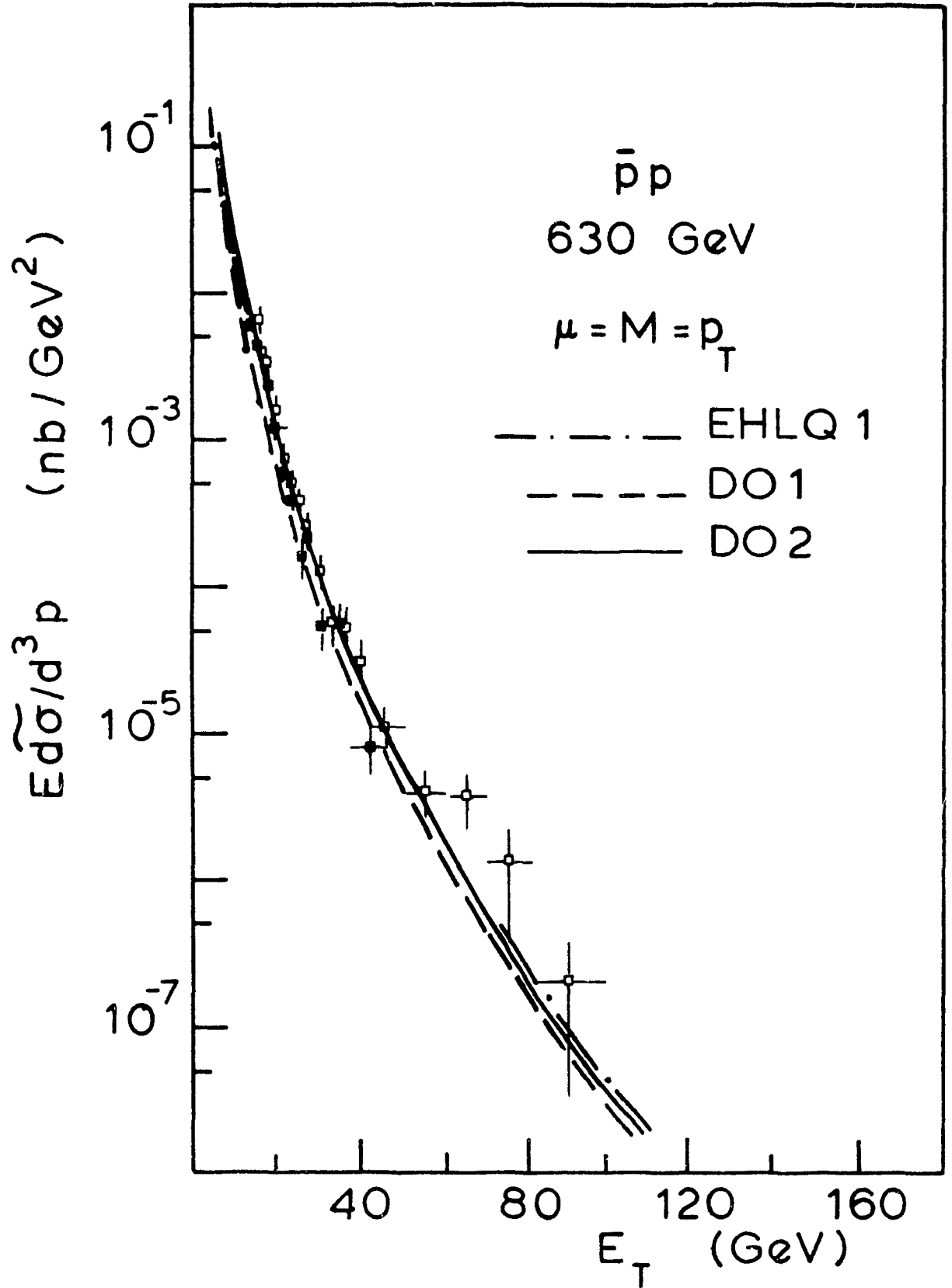


Fig.24

UA 2

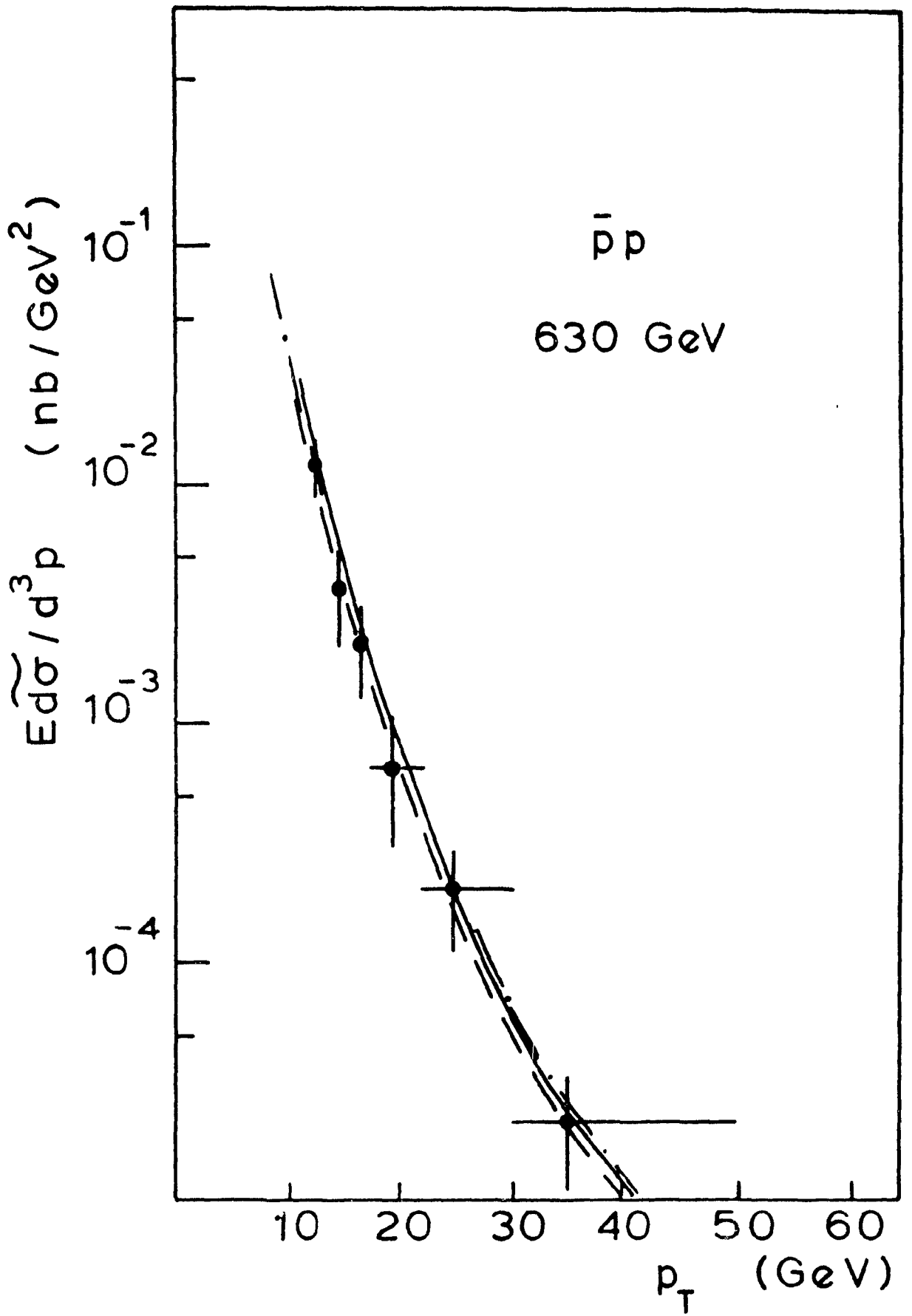


Fig. 25

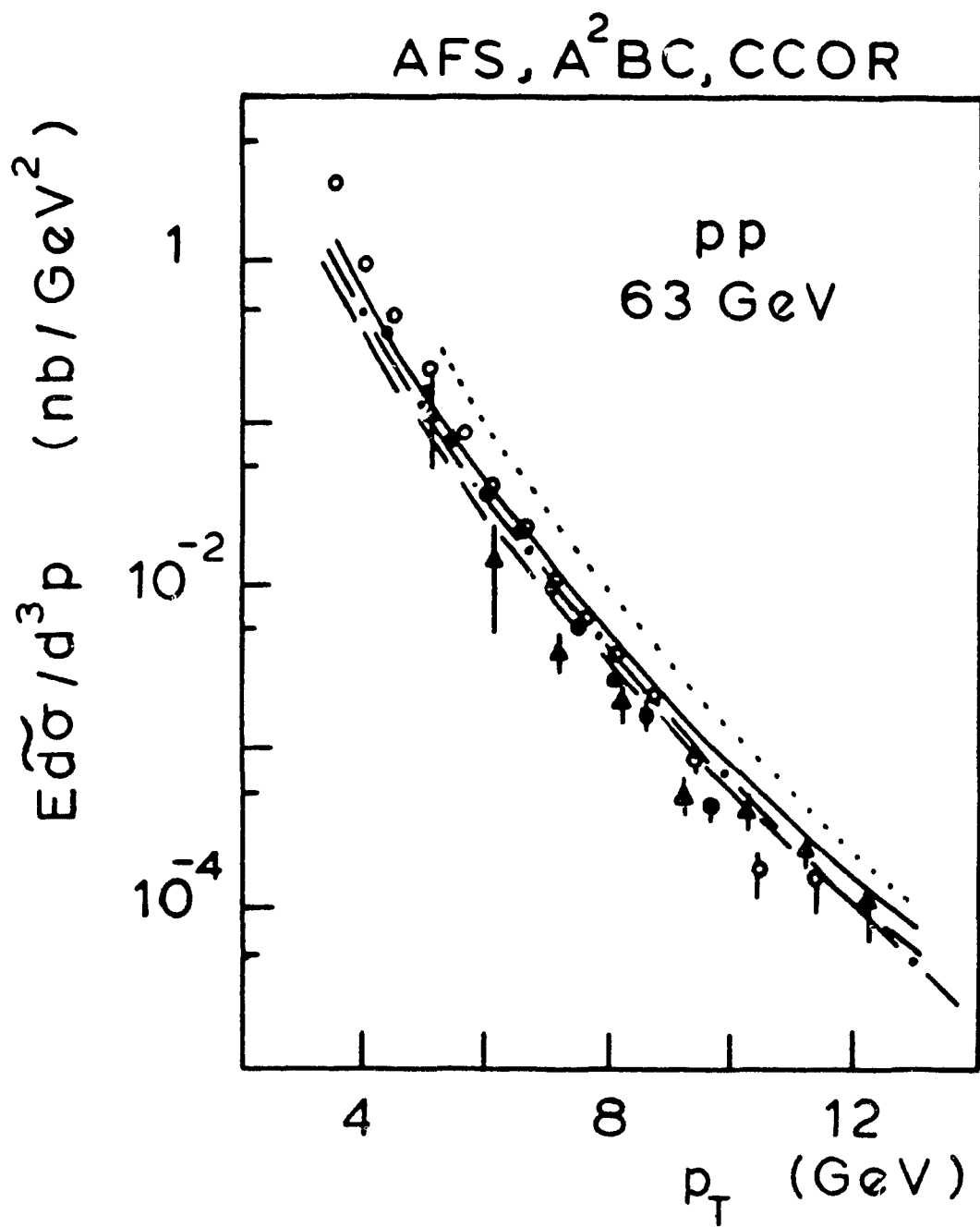


Fig.26

NA 24

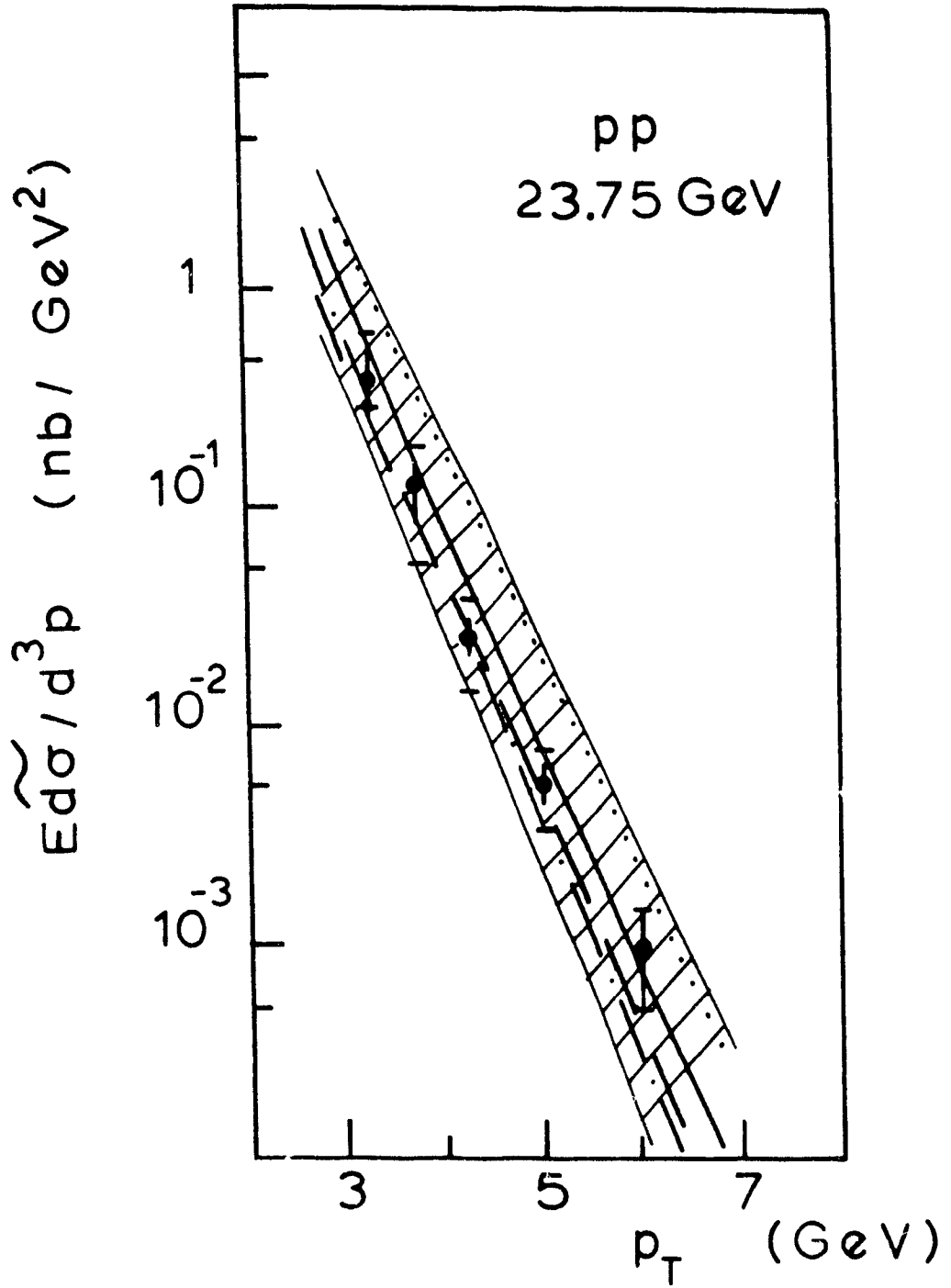


Fig. 27

WA 70

pp 22.9 GeV

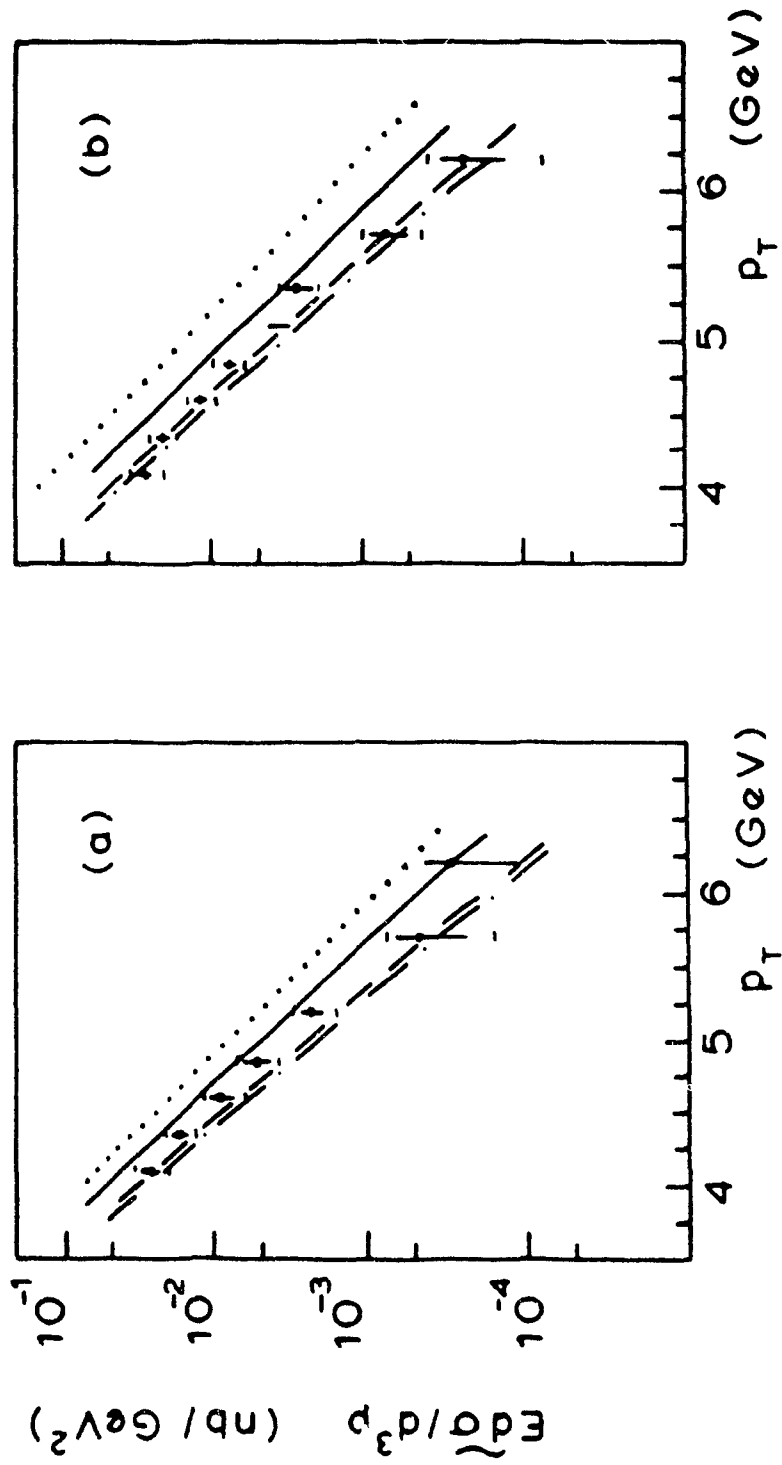


Fig. 28

UA6

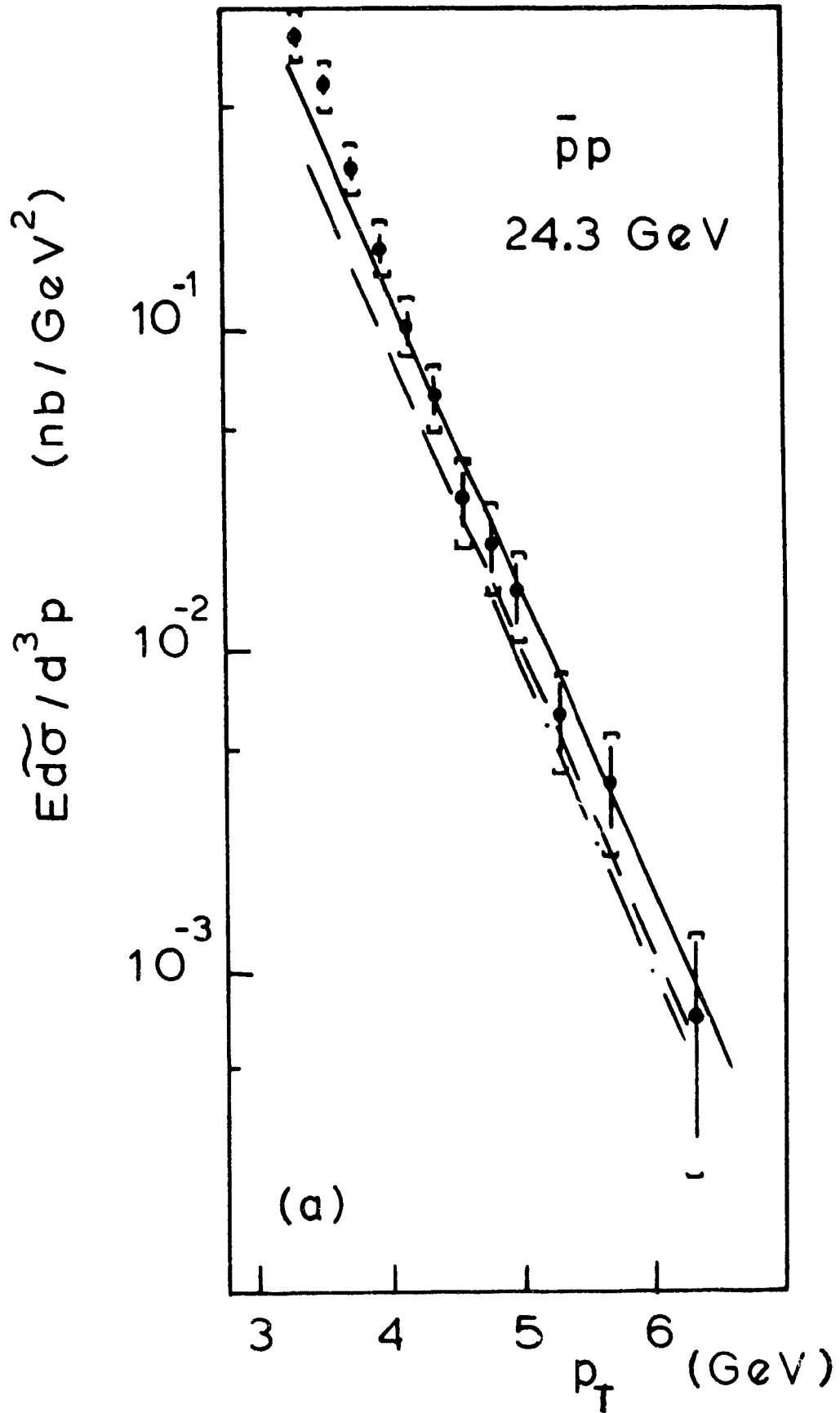


Fig. 29

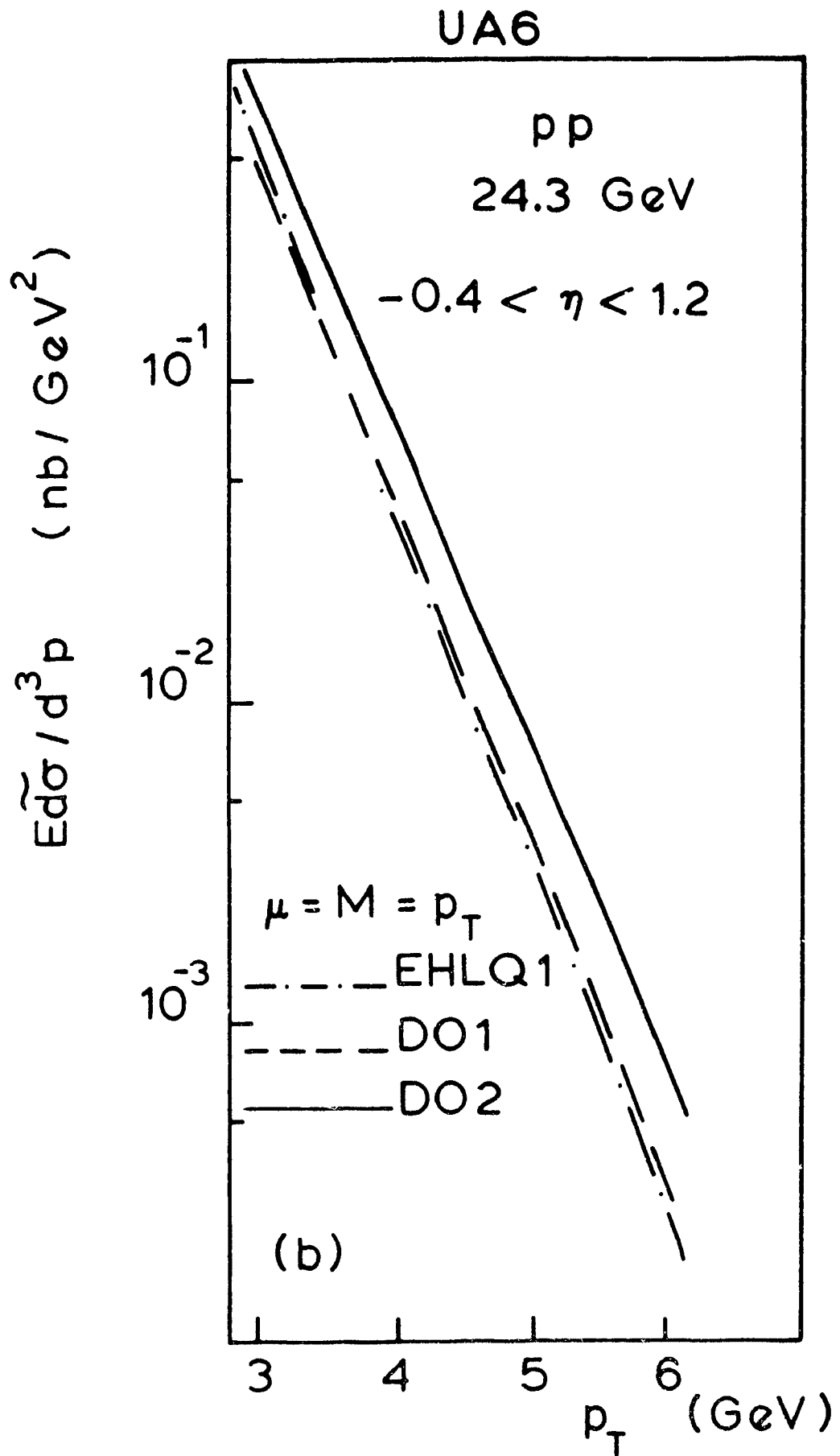


Fig. 29

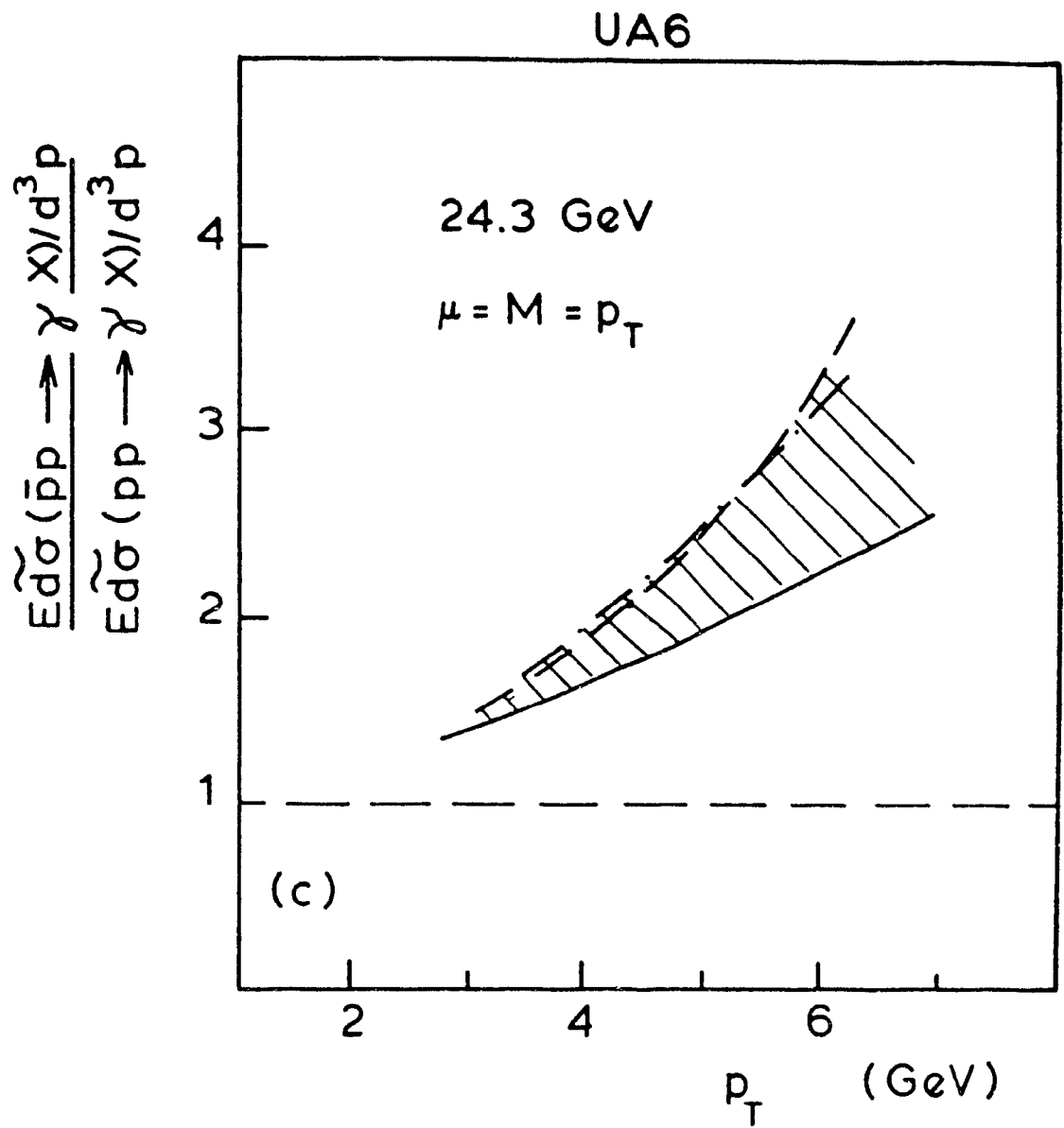


Fig. 29

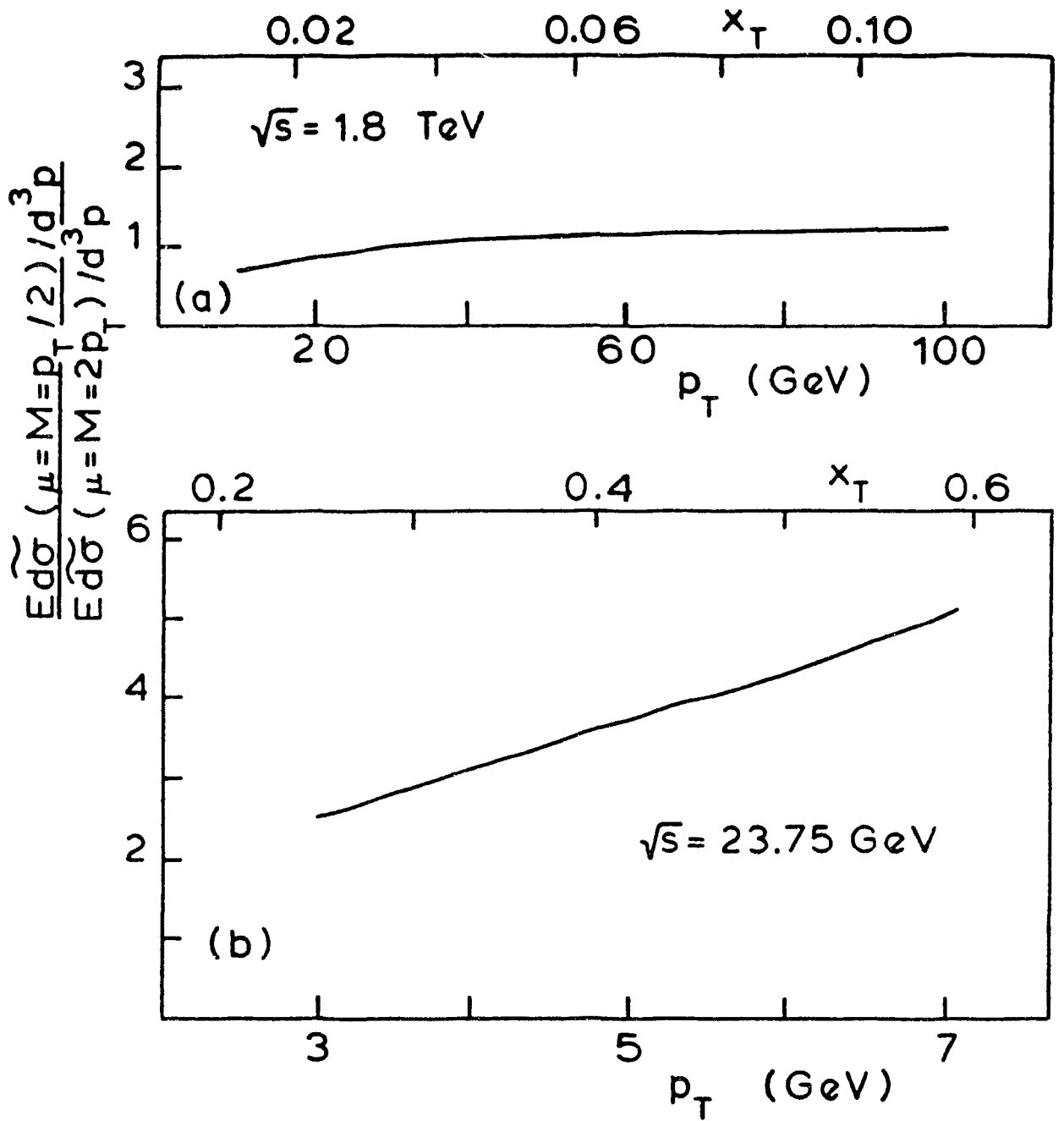


Fig. 30